EUROPEAN COMMISSION
European Research Area

CArbon-14 Source Term
CAST

D6.3 – Integration of CAST results to safety assessment

Henocq P., Robinet J.-C., Perraud D., Munier I., Wendling J., Treille E., Schumacher S. (ANDRA); Hart J., Dijkstra J.J., Meeussen J.C.L. (NRG); Capouet M., Meert K., Vandoorne T., Gaggiano R., Dorado E. (ONDRAF/NIRAS); Nummi O. (FORTUM); Diaconu D., Constantin A., Bucur C. (INR); Grigaliuniene D., Poskas P., Narkuniene A. (LEI); Vokál A., Vetešník A. (SURAO); Ferrucci B., Levizzari R., Luce A. (ENEA); Rübel A. (GRS); Gray L., Carter A. (RWM); Mibus J., Smith P., Kämpfer T. (NAGRA)

Date of issue of this report: 06/06/2018

The project has received funding form the European Union's European Atomic Energy Community's (Euratom) Seventh Framework Programme FP7/2207-2013 under grant agreement no. 604779, the CAST project.		
Dissemination Level		
PU	Public	**PU**
RE	Restricted to the partners of the CAST project	
CO	Confidential, only for specific distribution list defined on this document	

EURATOM

CAST – Project Overview

The CAST project (CArbon-14 Source Term) aims to develop understanding of the potential release mechanisms of carbon-14 from radioactive waste materials under conditions relevant to waste packaging and disposal to underground geological disposal facilities. The project focuses on the release of carbon-14 as dissolved and gaseous species from irradiated metals (steels, Zircaloys), irradiated graphite and from ion-exchange materials as dissolved and gaseous species.

The CAST consortium brings together 33 partners with a range of skills and competencies in the management of radioactive wastes containing carbon-14, geological disposal research, safety case development and experimental work on gas generation. The consortium consists of national waste management organisations, research institutes, universities and commercial organisations.

The objectives of the CAST project are to gain new scientific understanding of the rate of release of carbon-14 from the corrosion of irradiated steels and Zircaloys and from the leaching of ion-exchange resins and irradiated graphites under geological disposal conditions, its speciation and how these relate to carbon-14 inventory and aqueous conditions. These results will be evaluated in the context of national safety assessments and disseminated to interested stakeholders. The new understanding should be of relevance to national safety assessment stakeholders and will also provide an opportunity for training for early career researchers.

For more information, please visit the CAST website at:
http://www.projectcast.eu

CAST		
Work Package: WP6	CAST Document no. :	Document type: R
Task: 6.3	CAST-2018-D6.3	R = report, O = other
Issued by: Manuel Capouet (ONDRAF/NIRAS)		Document status:
Internal no. : *NA*		Final

Integration of CAST results to safety assessment

Executive Summary

Workpackage 6 regroups the Waste Management Organisations (WMOs and other national organisations involved in safety assessments) participating to CAST with the aim to consider the results from WP2 to WP5 at the scale of their disposal system, to analyse their impact in terms of long-term safety and how they fit in safety cases.

Deliverable D6.3 reports a preliminary integration exercise of the CAST technical outcomes. This study was conducted by WP6 organisations. Two activities of integration are covered by the organisations in function of their programme needs: 1/ Safety assessment modelling studies, and 2/ integration of the CAST results at the level of the safety case. The contributions from the organisations are sorted by host rock type: clay, crystalline, salt and generic.

With safety assessment calculations, WP6 explores the influence of CAST results (experimental studies as well as literature reviews) on the radiological impacts of C-14 released from a disposal system for the four categories of waste materials investigated in CAST. It was decided within WP6 to broaden the scope of these modelling studies to include also sensitivity analyses to identify and assess key-processes influencing C-14 release and transport. Generally, the features and processes explored are:

- the release rate (and the potential instant release fraction of C-14, abbreviated as IRF), function of the corrosion rates of Zircaloy, steel and graphite;
- the potential retention capacity of C-14 in the cementitious and clay environment, function of its speciation;

- the evolution of the hydraulic properties of the Engineered Barrier Sytem (EBS);
- the transport regimes (from diffusive to advective).

The expected evolution scenario is investigated in the first place, but some alternative scenarios are also studied such as early canister failure scenario and scenario in which the transport of C-14 towards the surface environment is accelerated (e.g., gas phase scenario in clay host rock, accelerated alteration of the EBS).

A project as CAST provides a diversity of results: experimental data, modelling studies, integrated and consensual understanding over process conceptualisation or over parameter value. Integration to safety case consists for WMOs (and organisations responsible for radioactive waste management) to scrutinise these results in order to identify the elements that increase the knowledge-base of their disposal programme and to set new uncertainties. This analysis implies to assess the quality of these elements in order to evaluate whether their form a robust line of demonstration for the long-term safety of the disposal system, a second rank evidence or a new uncertainty to be further investigated by RD&D. Some organisations carried out such a preliminary integration of the CAST products in the context of their programme.

The table hereafter synthetises the integration activities that were conducted in WP6.3, carried out at the level of national programmes. The table lists the themes addressed by each organisation.

Consideration of the CAST outcomes at a more general level, in function of the host rock (clay, crystalline and salt), by category of investigated materials (steel, Zircaloy, graphite and SIERs) and independently of national programme specificities will be discussed in the final deliverable D6.4.

Table: Contributors to the CAST D6.3 report, with their reported research themes

Organisation	Waste type - material(s) investigated	Themes
Part 1: Clay host rock		
ANDRA	IL-LLW	Mechanistic model of the inorganic C-14 uptake in cement and clay-rocks (key processes being C-14 solid diffusion in calcite, surface adsorption by C-S-H, carbonation of portlandite); sensitivity analysis over scenarios of C-14 in aqueous phase and in gaseous phase (speciation, retention, solubility, source term).
Nagra	L/ILW & HLW	Sensitivity analysis over C-14 source terms (corrosion rates and IRF), retention in clay and cementitious environments; investigation of the gas pathway scenario; Integration of CAST results to safety Case.
NRG	CSD-C (Zircaloy-4)	Full probabilistic uncertainty/sensitivity analysis on two scenarios: 'Reference case' and 'Enhanced C-14 Migration case'; Pearson Correlation Coefficient (*PCC*), Rank Correlation Coefficient (*RCC*), and conditional Cobweb plots; Key factors investigated are corrosion rates, IRF/congruent release, sorption coefficients; Integration of CAST results to safety Case.
ONDRAF / NIRAS	CSD-C (Zircaloy-4)	Update of the conceptualisation of the reference scenario based on CAST results; 100% IRF scenario; Sensitivity analysis on inventory, release rate/IRF, speciation, retention; Integration of CAST results to safety Case.
Part 2: Crystalline host rock		
Fortum	SIERs, steel	Sensitivity analysis (speciation, retention, backfill diffusion parameters, groundwater flow rate in different compartments, design geometry). Integration of CAST results to safety Case.
INR	UOx assemblies	Update of the reference case conceptualisation based on CAST; Sensitivity analysis (IRF, release rate, speciation, diffusion coefficients, retention); Integration of CAST results to safety Case.

Organisation	Waste type - material(s) investigated	Themes
LEI	Graphite	Update of the conceptualisation of the normal evolution scenario using more realistic hypothesis based on CAST results (inventory, release rate, speciation, sorption); Different cases assessed: best estimate and conservative hypothesis, containment options; Sensitivity analysis to evaluate the impact of key processes; Integration of CAST results to safety Case.
SURAO	Decomm. Waste	Sensitivity analysis (C-14 speciation, containment, leaching rate, backfill diffusion parameters, solubility, retention, geosphere flow rate, inventories). Free-gas phase and aqueous phase scenarios; Integration of CAST results to Safety Case.
Part 3: salt host rock		
ENEA	Graphite	Conservative and realistic scenarios of generation and migration of gaseous C-14 in a generic geological repository in salt rock; Full repository and single storage room modelling; Sensitivity analysis (retention in different compartments); Integration of CAST results to Safety Case.
GRS	UO2, MOX, CSD-V, CSD-C	Initial container defects scenario giving rise to gas transport; Sensitivity analysis (congruent release/IRF, release start time, backfill porosity and permeability).
Generic host rock		
RWM	Uranium, Magnox, steel, graphite	Integrated methodology to identify key conditions leading to critical C-14 impact; C-14 release scenarios during the operational period; Gas generation and migration post-closure scenarios for low and high heat generating waste in generic disposal system in higher strength rock (HSR), lower strength sedimentary rock (LSSR) and halite.

List of Contents

PART 1 – Clay host rock

CArbon-14 Source Term

CAST

Integration of CAST results to safety assessment: Contribution from Andra to D6.3

Henocq P., Robinet J.-C., Perraud D., Munier I., Wendling J., Treille E. and Schumacher S.

Date of issue of this report: 09/01/2018

List of Contents

1 Andra: Performance assessment studies of ^{14}C in a deep geological disposal in clay

1.1 *Design of Cigéo, the French deep geological repository*

Andra has studied the safety and feasibility of disposing of intermediate-level long-lived radioactive waste and vitrified high level radioactive waste in a deep geological repository in the framework of the Dossier 2005 [Andra, 2005a]. According to the 28th June 2006 Act, a reversible waste disposal in a deep geological formation and corresponding studies and investigations shall be conducted with a view to selecting a suitable site and to designing a repository. The application for the authorization will be reviewed in 2019, and subject to that authorization, the repository will be commissioned in 2025. The industrial center for disposal in geological medium (Cigéo) will be located in the Callovo-Oxfordian claystone layer at about 500 m depth. The host rock is an argillaceous layer of at least 150 m of thickness with good confining hydraulic and diffusive properties. The reference design for the surface installation and the disposal areas are illustrated in Figure 1.

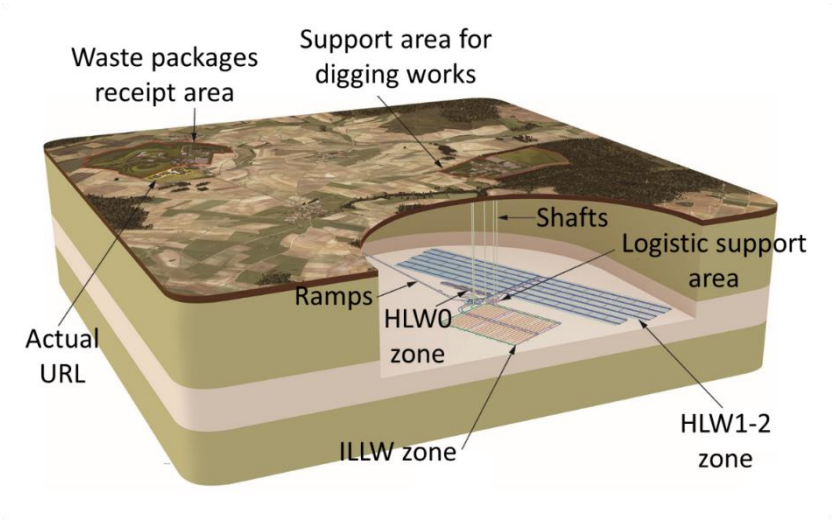

Figure 1: General scheme of Cigéo project in preliminary design phase (2014)

Separate disposal areas are envisaged for intermediate-level long-lived (IL-LL) waste and high-level (HL) waste to ensure phenomenological independence between them.

The HL waste will be disposed in small diameter (0.9 m) disposal cells, ranging from 80 m to 150 m length depending on the thermal power of the vitrified waste. The HL waste disposal area is subdivided into several modules for operational reasons as well as for separating less exothermal vitrified waste (HLW0) from more exothermal vitrified waste (HLW1-2). There are several thousand disposal cells deserved by a network of access galleries whose length can reach several kilometres. The cells are disposed horizontally on each side of these galleries and perpendicular to their axis with a variable centre distance depending on the thermal power of the vitrified waste (Figure 2).

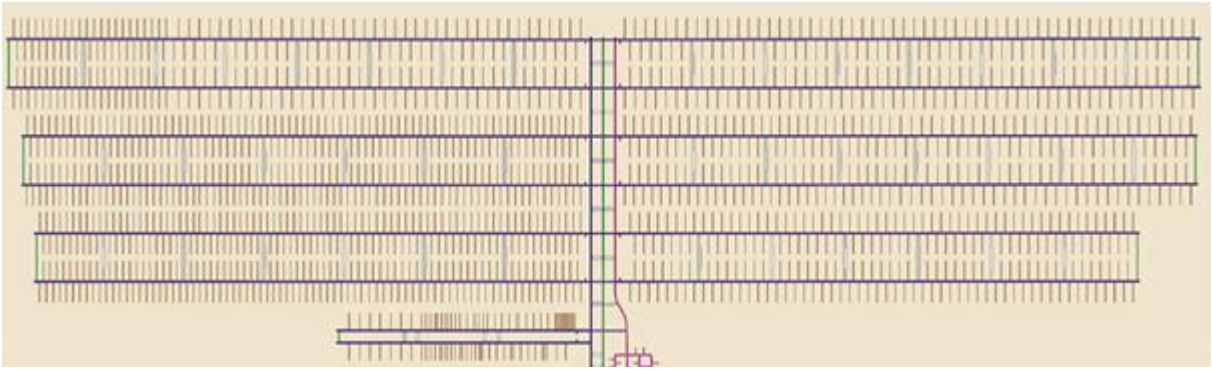

Figure 2: Global architecture of the HLW zone, preliminary design phase of Cigéo (2014)

The HL waste packages contains almost no ^{14}C but this zone plays an important role regarding transient two-phase flow behaviour as part of the hydrogen generated (by corrosion) in this zone will move toward the wells and ramps and can influence the migration of gaseous ^{14}C, generated in the IL-LL waste disposal cells.

Before being transferred to underground installations, IL-LL waste packages will be placed in concrete containers (disposal packages). In the repository, they will be juxtaposed and stacked in large diameter (8-10 m) and long (~600 m) disposal cells (Figure 3). There will be a few tens disposal cells in the IL-LL waste zone (Figure 4). All the wastes packages containing ^{14}C are disposed in this zone.

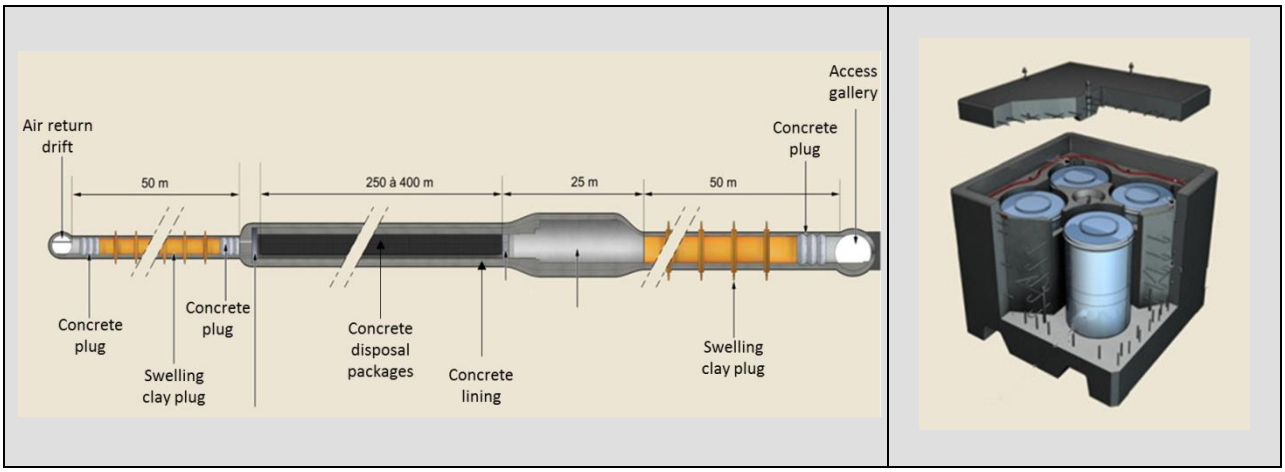

Figure 3: Schematic illustration for IL-LL waste disposal cell (left) and IL-LL waste disposal package (right)

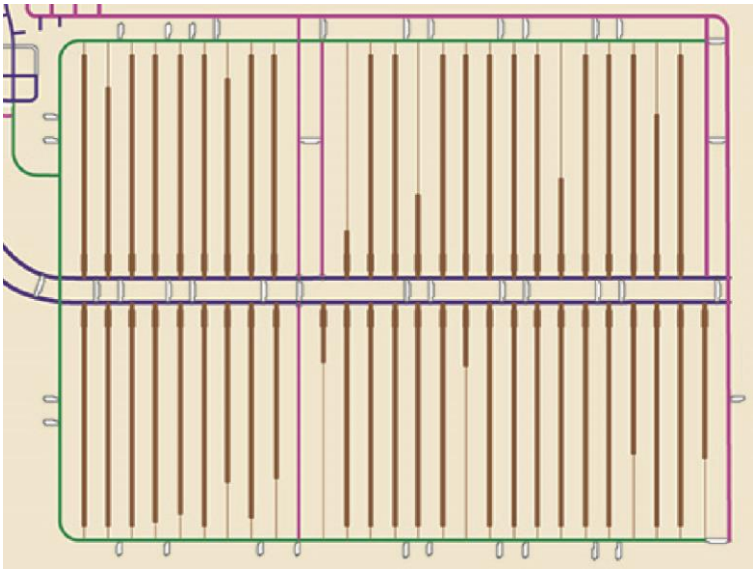

Figure 4: Global architecture of the ILLW zone, preliminary design phase of Cigéo (2014)

The central logistical support zone (ZSL) includes the arrivals of wells and ramps, as well as various sections of gallery (possibly blind) used for the management of the exploitation of the repository (zone of storage of cuttings before surface evacuation, computer area, garage for vehicles, emergency zone...).

Figure 5: Global architecture of the ZSL zone, preliminary design phase of Cigéo (2014)

1.2 *Inventory of ^{14}C*

^{14}C inventory is mainly divided between more than 80 different families of IL-LL waste packages. It corresponds to more than 14,000 moles. Among these families, seven of them represent more than 98.5% of the total amount of carbon-14 inventory. One of these families, corresponding to the irradiated vessels internals made of stainless steel, represents around 80% of the total amount of carbon 14 inventory.

1.2.1 Performance assessment studies of ^{14}C

The fate of ^{14}C in deep geological repository depends on its speciation:

- In gaseous phase, the solubility of the ^{14}C will be determined by its speciation (CH_4, CO_2, CO…). In that case, another important parameter will be the hydrogen source term which pilots the hydraulic-gas transient phase, together with the effective diffusion coefficient in the host rock.

- In aqueous phase, the retention of ^{14}C on cementitious materials and on clay host rock will be determined by its speciation (organic/inorganic). This is all the more true than

the period of ^{14}C is relatively small (~5,700 years) in comparison with the time needed for 14C to diffuse out of the cementitious/clay barrier.

The work carried out to assess ^{14}C transfer in deep geological repository is structured in three parts:

- The first part deals with the phenomenological behavior of ^{14}C in deep geological repository and, more precisely, with the interaction of ^{14}C with the cementitious and clay materials, as a function of its speciation, taking into account the isotopic exchange between ^{14}C and ^{12}C;
- The second part addresses the performance assessment of ^{14}C transfer in aqueous phase, released from a disposal cell of intermediate level waste within the Callovo-Oxfordian clay host rock. This study considers two different chemical forms of ^{14}C: (i) the inorganic anionic form (CO_3^{2-}), and (ii) the organic neutral form (CH_4);
- The third part addresses the performance assessment of ^{14}C transfer in gaseous phase, released from a deep geological repository.

2 Modelling ^{14}C in disposal systems

2.1 *Introduction*

The aim of this first study was to assess the transfer of aqueous ^{14}C in an Intermediate-Level Waste disposal cell taking into account the state-of-the art of the phenomenological behavior of ^{14}C in cements and clay-rocks. The fundamental processes ruling the migration of aqueous ^{14}C were first evaluated for clay-rocks and cement based materials. Inorganic ^{14}C is (i) weakly sorbed in clayrocks and (ii) strongly sorbed by cement-based materials. For both materials, solid carbonate minerals mainly contribute to the retention of inorganic ^{14}C. The retention of ^{14}C onto calcite is a time controlled processes related to the isotopic exchange between ^{14}C and ^{12}C constituting calcite. Kinetic exchange experiments of ^{12}C by ^{13}C performed on nanoparticles of calcite by [Andra, 2014] reveal that solid diffusion phenomena can explain the behavior of ^{14}C as regard to calcite. From this work, a solid diffusion model was applied

to estimate ^{14}C retention kinetics and associated Kd for the Callovo-Oxfordian clay-rock. This model takes into account carbonate content and the mean size of calcite grains. In concrete, the presence of calcareous aggregates will mainly contribute to fix inorganic ^{14}C. Experimental ^{14}C retention experiments on cement-based materials were also successfully interpreted by considering such a solid diffusion mechanism. For hydrated cement pastes, the calcite content is low, and then, a surface adsorption by C-S-H has to be considered likely combined with the carbonation of portlandite. The results of this study provide reliable Kd of inorganic ^{14}C in various materials considered for the ^{14}C bearing waste disposal with the objective of reducing the uncertainties of PA calculations. The retention of organic ^{14}C molecules was evaluated based on a literature review, notably [Rasamimanana, 2017] for clay-rocks and [Wieland, 2016] for cements.

2.2 *Model description*

The kinetic isotopic exchange of carbonate in ^{12}C nano-calcite with ^{12}C-^{13}C atmosphere ($\delta^{13}C \sim 0.8\%$; 98.898% ^{12}C and 1.102% ^{13}C) was measured [Andra, 2014]. The experimental results at 21°C are shown in Figure 6. These measurements confirm the kinetically slow mechanism of ^{14}C uptake by calcite and, furthermore, by cement-based materials for which diffusion processes have been supposed [Bayliss, 1998].

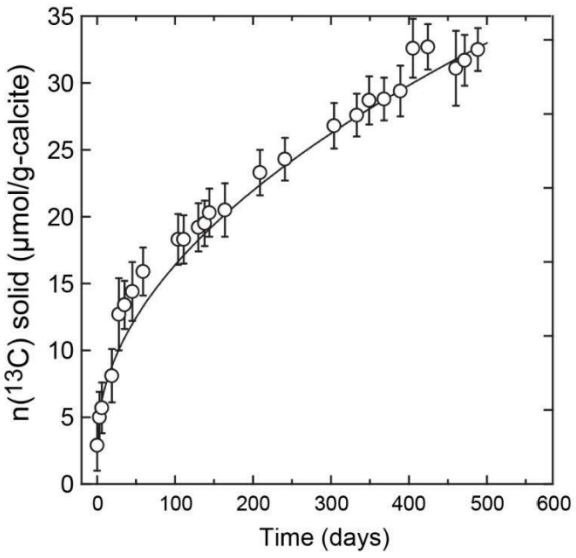

Figure 6: ^{13}C uptake by ^{12}C nano-calcite as function of time [Andra, 2014]

The kinetic data in Figure 1 were interpreted using a solid diffusion model. The model considers a cubic crystal of calcite with volume c^3. The penetration of ^{13}C into the crystal is characterized by a penetration depth a defining "contaminated" and "sound" volumes as depicted in Fig. 2. The depth a is defined according to a 1D diffusion process:

$$a = \sqrt{2Dt} \qquad \textbf{(Eq. 1)}$$

where D is the diffusion coefficient of ^{13}C into the nano-calcite grain (m^2/s) and t is the time (s).

The ^{13}C "contaminated" volume ΔV, as described in Figure 7, is written as follows:

$$\Delta V = c^3 - \left(c - 2\sqrt{2Dt}\right)^3 \qquad \textbf{(Eq. 2)}$$

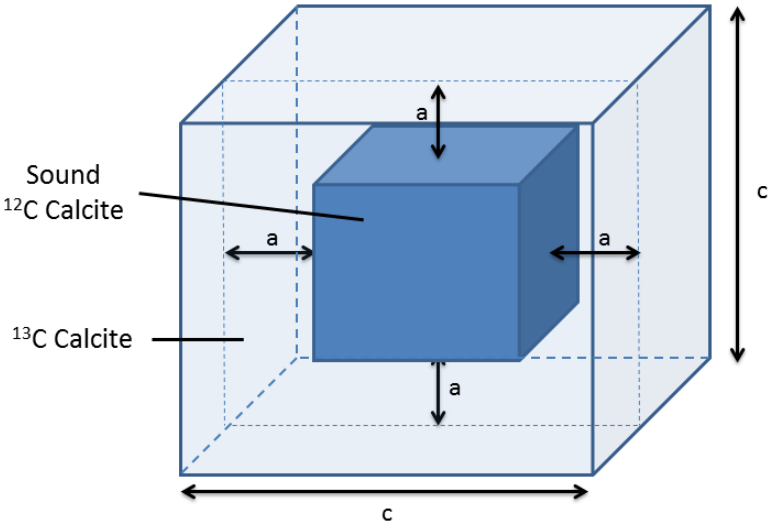

Figure 7: ^{13}C "contaminated" calcite and remaining sound ^{12}C calcite volumes in a calcite cubic crystal

The initial ^{13}C content in nano-calcite was $^{13}C/^{12}C$=0.0253% which was equivalent for 1g of calcite to $n^{13}C_{init}$ = 2.56.10^{-6} mol. The relationship between total carbon nC_{tot} and $n^{13}C$ for isotopically equilibrated calcite is [Andra, 2014]:

$$n^{12}C + n^{13}C = 89.7949 \times n^{13}C \qquad \textbf{(Eq. 3)}$$

For 1g of calcite, the maximum amount of ^{13}C in the solid would be:

$$n^{13}C = \frac{nC_{tot}}{89.7949} - n^{13}C_{init} \qquad \textbf{(Eq. 4)}$$
$$= 1.1\ 10^{-4}\ mol/g$$

The ^{13}C uptake value of 30 µmol/g at 400 days was considered. This amount corresponds to the contaminated volume ratio of 0.246 (= (3.10^{-5} – 2.56.10^{-6})/1.1.10^{-4}). Consequently, at 400 days, the contaminated volume of a calcite cubic particle with a volume c^3 is:

$$\Delta V = 0.246\ c^3 \qquad \textbf{(Eq. 5)}$$

On the other hand, the corresponding contaminated depth a_{400} is equal to:

$$a_{400} = \sqrt{2Dt_{400}} \quad \textbf{(Eq. 6)}$$

and the analytical expression of the contaminated volume is

$$\Delta V = c^3 - \left(c - 2\sqrt{2Dt_{400}}\right)^3 = 0.246\,c^3 \quad \textbf{(Eq. 7)}$$

The diffusion coefficient D is then the parameter to be defined. D was determined by solving Eq. 7. The value D = 6.6.10^{-25} m^2/s has been found. This value allows reproducing all the kinetic evolution of the ^{13}C uptake (Figure 8). This model was also applied to data acquired at 50°C with a D value of 2-3.10^{-24} m^2/s. These values can be compared to those obtained solid diffusion of Ca, Sr, Mg and C in calcite at high temperature (T > 550°C) [Fisler, 1999]. Diffusion coefficients are ranged between 10^{-17}-10^{-22} m²/s, these values are in a good agreement with the ones determined for ^{13}C taking into account the differences of temperature.

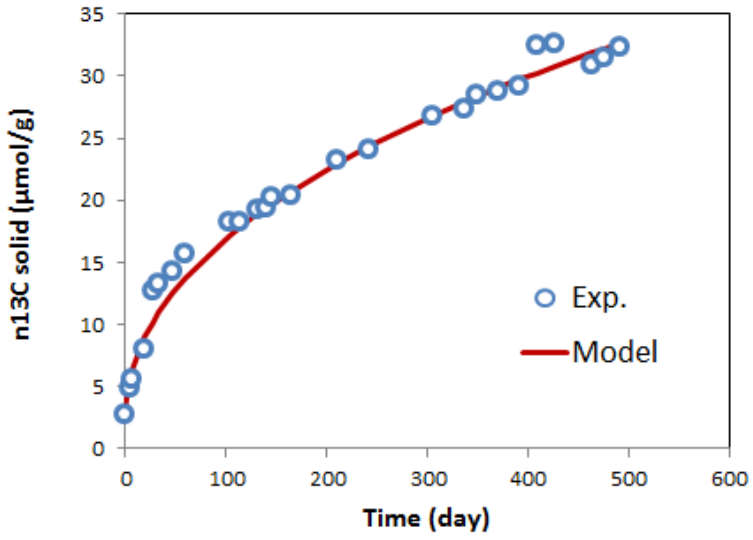

Figure 8: ^{13}C uptake on calcite. Simulation results with a 1D diffusion model (D = 6.6.10^{-25} m^2/s) and experimental data from [Andra, 2014]

As seen in Figure 8, the solid diffusion hypothesis for explaining the kinetic of ^{13}C uptake by ^{12}C calcite is relevant. A similar process is assumed for ^{14}C retention. The diffusion properties determined for ^{13}C are considered for ^{14}C. The total amount of $^{14}C/^{13}C$ diffusing into calcite by solid diffusion processes depends on (i) the size of calcite particles and (ii) the kinetic parameter i.e. the diffusion coefficient in solid phase (D) and will evolve with time.

The solid-to-liquid of ^{12}C in a system containing calcite is limited by the quantity of calcite and the solubility of calcite. The aqueous concentration of the ^{12}C in the liquid phase [^{12}C] depends on the solubility of the calcite which is strongly linked to the chemical environment (pH, pCO2). The mass of calcite gives the maximum amount of ^{12}C associated to the solid phase. The concentration of ^{12}C in the solid phase is equal to the molar mass of calcite (0.01 mol of ^{12}C/g of calcite) × mass of calcite. Assuming an isotopic equilibrium and the absence of fractionation, we can consider that the solid-to-liquid for ^{13}C and ^{14}C is the same than for ^{12}C.

The partition coefficients Rd of ^{14}C (or ^{13}C) can be then derived from the quantity of ^{14}C diffusing into calcite and the concentration of ^{14}C in the aqueous phase. When ^{14}C is introduced into the aqueous phase, the amount of ^{14}C into calcite is 0 leading to Rd=0. Then, due solid diffusion of ^{14}C into calcite, the amount of ^{14}C in the solid progressively increase leading to Rd > 0. When ^{14}C has completely diffused in calcite, the amount of ^{14}C in calcite remains constant and the Rd is equal to the solid-to-liquid ratio of C in the system (assuming no fractionation of ^{14}C between liquid and solid).

Regarding to the aforementioned experiment on nano-calcite [Andra, 2014], the evolution of the Rd of ^{13}C with time can be derived considered a simple diffusion model, a D value = 6.6×10^{-25} m^2/s, a particle size of 50 nm and atmospheric conditions. This model estimates a complete diffusion of ^{13}C in calcite after more than 10 years leading to a maximum Rd value of 10 $m^3.kg^{-1}$. A same exercise can be done for various calcite grain sizes leading to increase time to reach a complete diffusion of ^{13}C. Considering a grain size of 1 µm, the complete diffusion of ^{13}C into calcite will be reached after more than 1000 years.

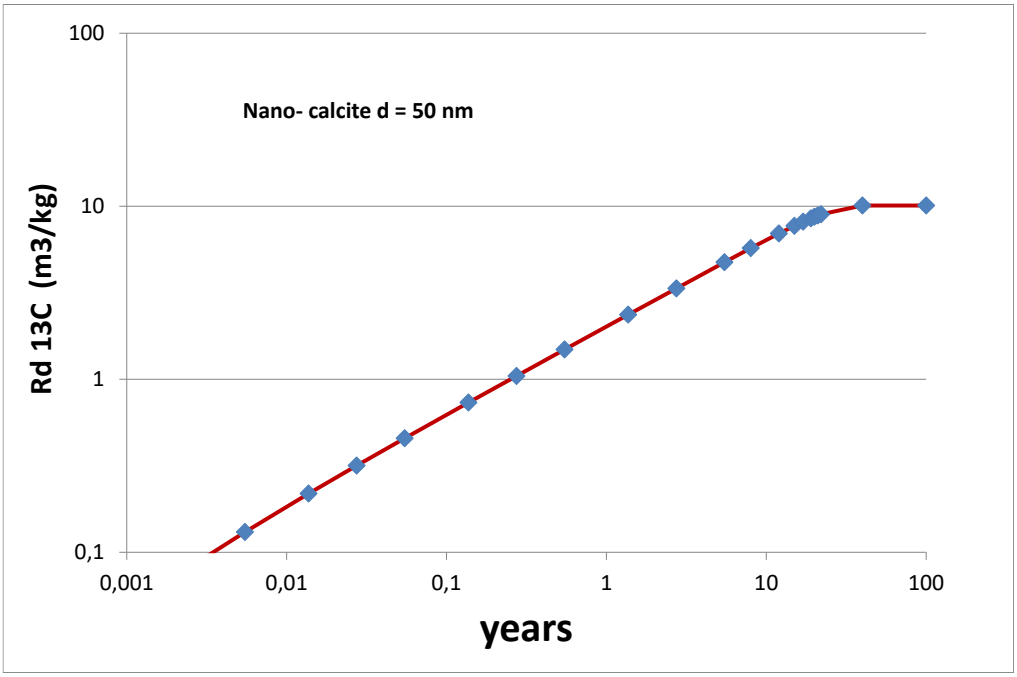

Figure 9: Predicted Rd(^{13}C) for the calcite system assuming a 1D solid diffusion model of ^{13}C into calcite, D(^{13}C) = 6.6×10^{-25} m^2/s, a size of calcite grains of 50 nm and atmospheric conditions.

2.3 *Results and discussions*

This section presents the results of the diffusion modelling as previously described. The model will be applied on the ^{14}C retention on calcite and cement-based materials.

2.3.1 Calcite

Several studies investigated ^{14}C sorption on calcite. Each work performed measurements in specific conditions. That explains the difficulty to compare the available data in Literature and the choice in this document to present each set of data.

2.3.1.1 [Pointeau, 2003]

Pointeau (2003) investigated ^{14}C sorption on calcite and calcareous aggregates in cementitious solutions (saturated portlandite (WCH), diluted saturated portlandite (DWCH),

and 0.1M sodium hydroxide (NaOH)). CO_3^{2-} concentration was calculated to 6.7×10^{-5} M, 3.3×10^{-5} M, and 2.1×10^{-5} M for the WCH, DWCH, and NaOH conditions respectively. The granulometry of calcite was 14 µm. Figure 10 presents the modelling results for ^{14}C sorption on calcite in WCH and NaOH solutions assuming D = 6.6×10^{-25} m^2/s as determined in section 1.2.

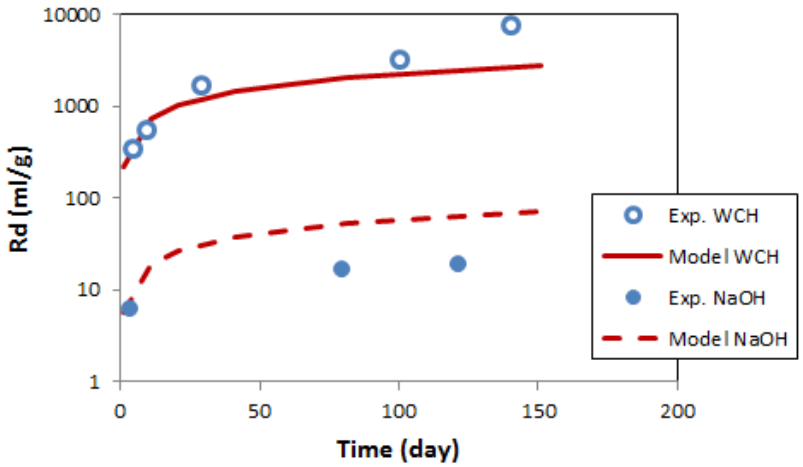

Figure 10: ^{14}C uptake on calcite in WCH and NaOH solutions [Pointeau, 2003]. Simulations with *D* = 6.6×10^{-25} m^2/s.

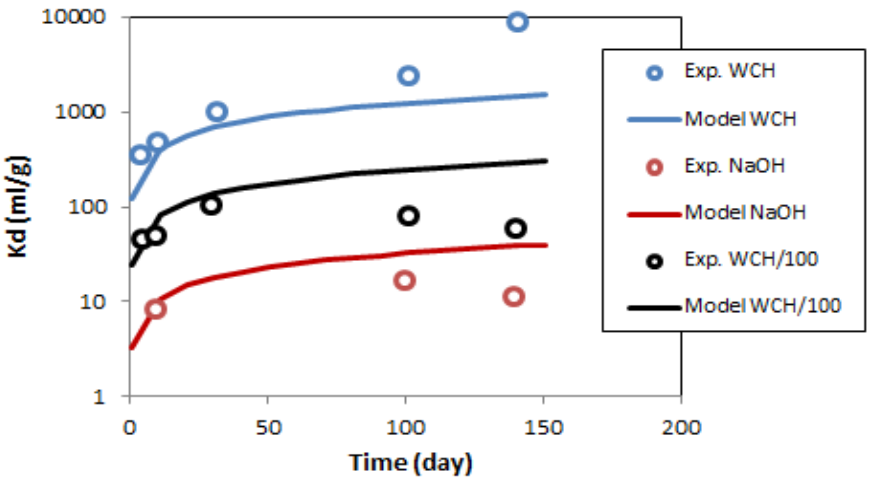

Figure 11: ^{14}C uptake on sand fines (< 50 µm) in various solutions [Pointeau, 2003]. Simulations with *D* = 6.6×10^{-25} m^2/s.

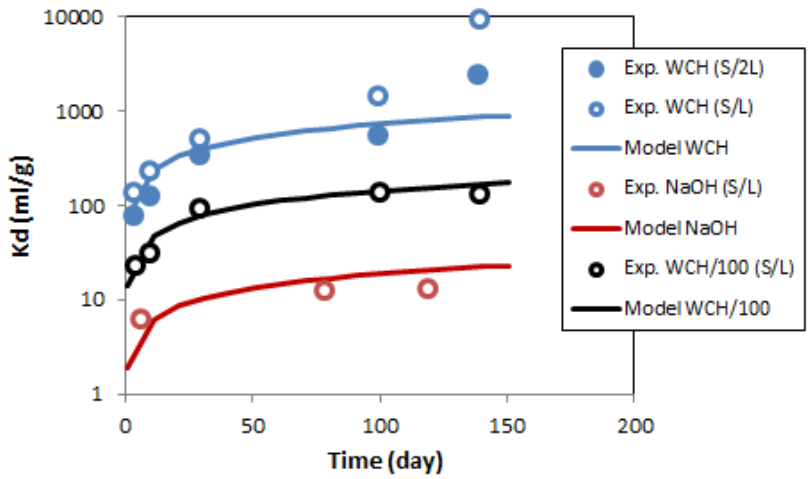

Figure 12: ^{14}C uptake on calcareous sand (average *c* at 0.075 mm) in various solutions [Pointeau, 2003]. Simulations with $D = 2\times10^{-24}$ m²/s.

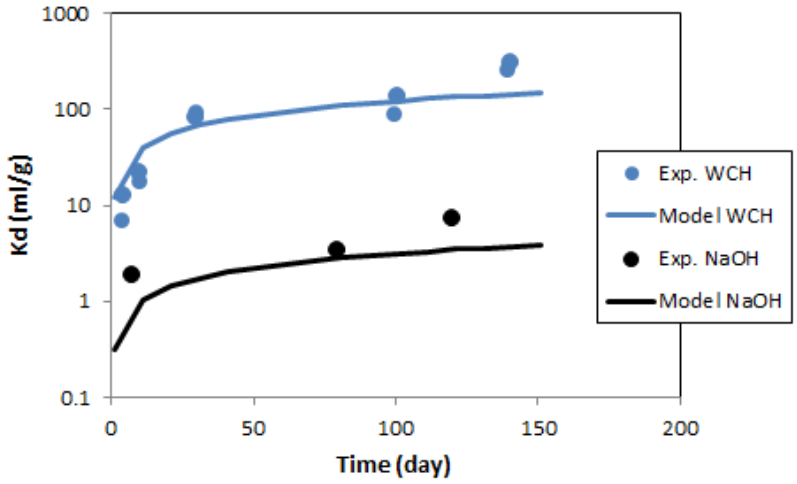

Figure 13: ^{14}C uptake on calcareous sand (average *c* at 10 mm) in various solutions [Pointeau, 2003]. Simulations with $D = 1\times10^{-21}$ m²/s.

The results on calcareous sands showed that it was necessary to adjust the diffusion coefficient for each granulometry. The diffusion coefficient is superior to this one of calcite and it increases as a function of the sand size that is consistent regarding the following points: (1)

calcareous sand aggregates are not pure calcite including defects, (2) for the small granulometry close to this one of calcite, the diffusion coefficients are quite similar (slightly higher) while (3) for large sands, the diffusion significantly increases with sand size.

2.3.1.2 [Tertre, 2011]

In this study, commercial calcite was used to evaluate ^{14}C retention on calcite. The size of the calcite particles can be estimated from the specific surface area (= 0.32 $m^2.g^{-1}$). Assuming cubic particles, the relationship between the particle size *c* and the specific surface area *S* is:

$$c = \frac{6}{\rho_{calcite} S} \quad \textbf{(Eq. 10)}$$

The calculation led to c = 6.9×10^{-6} m, in agreement with the previous studies.

The test conditions of this work were a carbonate concentration controlled by (i) calcite in equilibrium with $p_{CO2}=10^{-3.5}$ atm corresponding to $[HCO_3^-] = 1.1\times10^{-3}$ M, and (ii) a grain calcite size of 6.9×10^{-6} m (Eq. 10). The simulations were made with $D = 6.6\times10^{-25}$ m^2/s as evaluated on nano-calcite in section 1.2. The results are depicted in Figure 14.

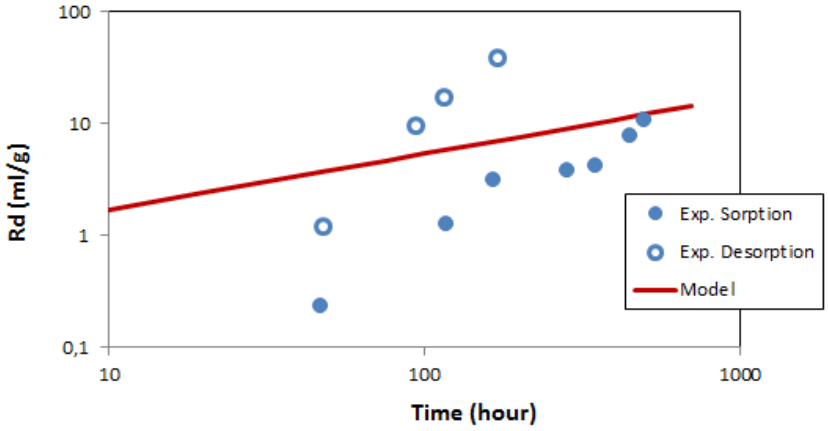

Figure 14: ^{14}C uptake on calcite in $[CO_3^{2-}] = 1.1.10^{-3}$ M solution [Tertre, 2011]. Simulations with $D = 6.6\times10^{-25}$ m^2/s.

2.3.1.3 [Allard, 1981]

This work presented ^{14}C sorption on calcite particles with a granulometry between 0.067 and 0.09 mm. A diffusion coefficient D = 1×10^{-22} m^2/s was found.

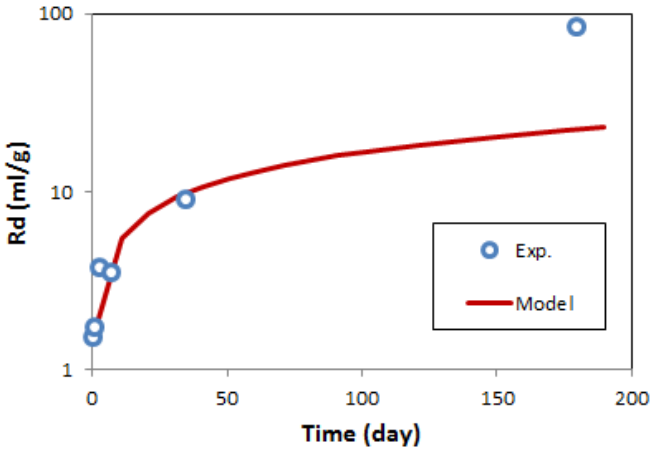

Figure 15: ^{14}C uptake on calcite in $[CO_3^{2-}] = 2\times10^{-3}$ M solution [Allard, 1981]. Simulations with $D = 1\times10^{-22}$ m^2/s.

2.3.1.4 Synthesis

On the basis of the isotopic exchange rate measurements by [Andra, 2014] and the ensuing diffusion coefficient in nano-calcite (D = 6.6×10^{-25} m^2/s), simulations of ^{14}C uptake on calcite have been performed comparatively to previous works. The same kinetic parameter, i.e. the diffusion coefficient, was found for similar systems composed by synthetized calcite or calcareous sand with a small granulometry except for [Allard, 1981] where the calcite type was not detailed. Nevertheless, these results would show that the solid diffusion coefficient of ^{14}C in calcite could be a fundamental parameter. For higher granulometry, it was found that the diffusion coefficient in calcareous sand increases with the expected particle size. The latter points out how to consider the crystallographic properties of calcite in terms of mono or poly crystals. This issue limits the application of the model for materials with a wide granulometry

of calcite particles or for large particles for which the crystallographic properties are unknown.

2.3.2 Cement-based materials

The assumption of solid diffusion of ^{14}C in calcite has been analysed a for cement-based materials. Generally, the calcite content in cement-based materials is low; it was fixed for the cement paste at 5% in mass. The size of calcite is expected to be small between 5×10^{-6} and 5×10^{-5} m. Consequently, retention of ^{14}C is related to calcite content taking into account the parameters defined on pure calcite systems as seen in section 1.3.1 while Rd values given in literature are expressed as regards to the total mass of tested cement-based materials. The ^{14}C uptake verifies the equivalence between the distribution factors $Rd(^{14}C)$ and $Rd(^{12}C)$ **in calcite** as expressed by Eq. 8:

$$Rd(^{12}C) = Rd(^{14}C) = \frac{[^{14}C]_{solid}}{[^{14}C]_{liquid}} \quad \textbf{(Eq. 11)}$$

Additionally, the total amount of ^{14}C ($n^{14}C_{tot}$) in the system is[1]:

$$[^{14}C]_{solid} \times m_{calcite} + [^{14}C]_{liquid} \times V = n^{14}C_{tot} \quad \textbf{(Eq. 12)}$$

Where $[^{14}C]_{solid}$ is the amount of ^{14}C in the calcite (mol/kg), $[^{14}C]_{liquid}$ is the concentration of ^{14}C in the solution (mol/l), m is the mass of calcite (Kg), and V is the volume of solution (l).

From Eqs. 11 and 12, at the equilibrium, the amount in the solid $n^{14}C_{solid}$ (given in moles) is

$$n^{14}C_{solid} = \frac{Kd(^{12}C) \times n^{14}C_{tot} \times m}{Kd(^{12}C) \times m + V} \quad \textbf{(Eq. 13)}$$

[1] If the ^{14}C concentration is not controlled by pCO_2 of the atmosphere

And, the concentration of ^{14}C in solution is

$$\left[{}^{14}C\right]_{liquid} = \frac{n^{14}C_{tot} - n^{14}C_{solid}}{V} \quad \textbf{(Eq. 14)}$$

And finally, $Kd(^{14}C)$ for the considered cement-based material is expressed as

$$Kd\left({}^{14}C\right) = \frac{n^{14}C_{solid}}{\left[{}^{14}C\right]_{liquid} \times m_{cem}} \quad \textbf{(Eq. 15)}$$

Where m_{cem} is the mass of the cement-based material.

2.3.2.1 [Matsumoto, 1994]

With respect to the test conditions used by [Matsumoto, 1994] and the previous assumptions given above (mortar contains 25% of cement paste), Rd evolution of ^{14}C uptake on mortar was calculated according to analytical approach described by Eq.11 to Eq. 15. The diffusion coefficient value D = 6.6×10^{-25} m^2/s was applied (Figure 16). The results show an agreement in terms of order of magnitude; it can be noticed that the trend is quite different than the experimental one (Figure 16(b)).

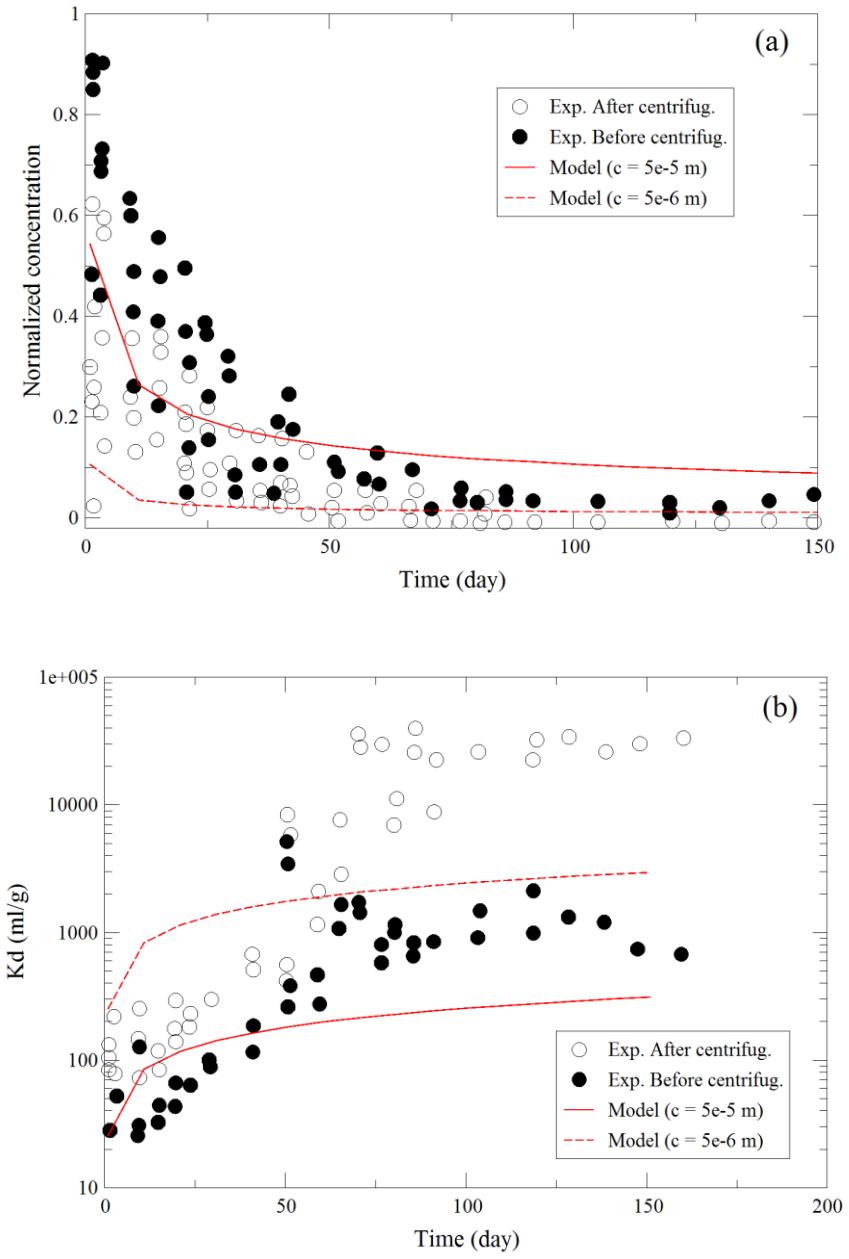

Figure 16: ^{14}C uptake on mortars by considering only calcite [Matsumoto, 1994]: Normalized concentration (a) and Kd (b). Simulations with $D = 6.6\times10^{-25}$ m^2/s and the particle size *c* as indicated.

For cement-based materials, ^{14}C can react by isotopic exchange with calcite as aforementioned. Calcite content is very low in sound cementitious materials but ^{14}C can also react with portlandite and C-S-H. For C-S-H, a fast adsorption mechanism is assumed with a fixed Kd = 40 ml/g related to cement paste. On the other hand, for portlandite, a kinetic carbonation process through the portlandite particle is supposed similarly to the isotopic exchange. The ^{14}C uptake in portlandite is associated to the carbonated layer which is evaluated according Eq. 2. The amount of calcium related to portlandite in the penetration depth is assumed to be equivalent to the amount of ^{14}C chemically fixed. The kinetic penetration of ^{14}C within the portlandite particle is characterized by the diffusion coefficient D_{CH}. Consequently, the available amount of ^{14}C for diffusing in calcite becomes ($n_{tot}{}^{14}C - n_{CH}{}^{14}C - n_{CSH}{}^{14}C$).

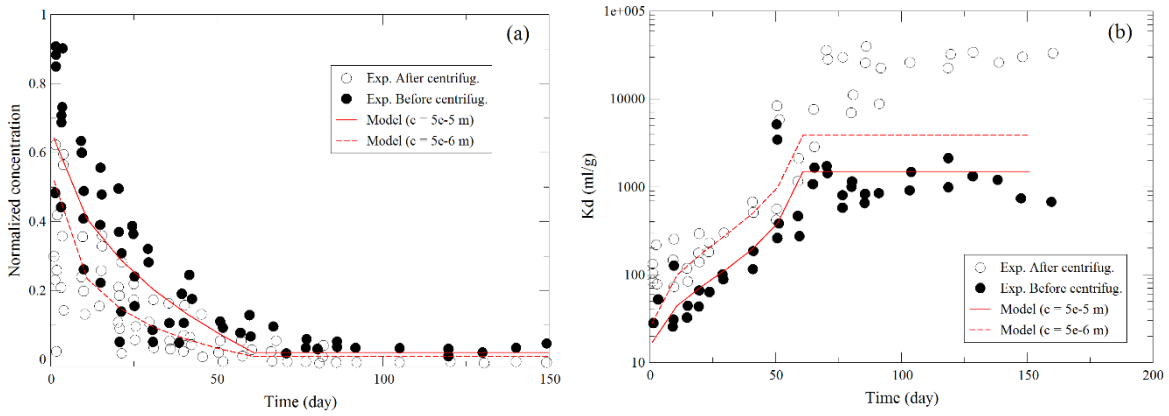

Figure 17: ^{14}C uptake on mortars by considering retention on calcite, portlandite and C-S-H [Matsumoto, 1994]: Normalized concentration (a) and Kd (b). Simulations with $D = 6.6\times10^{-25}$ m²/s and the particle size *c* as indicated.

2.3.2.2 [Bayliss, 1988]

The ^{14}C sorption experiments were performed on mortars including calcareous sand. Two sizes of calcite have to be considered for (i) pure calcite in HCP (estimated between 5 and 50 µm) and (ii) calcareous sand (0.4 mm). Consequently, Eq. 12 becomes:

$$\left[{}^{14}C\right]_{sand} \times \mathrm{m}_{\mathrm{sand}} + \left[{}^{14}C\right]_{calcite\_HCP} \times \mathrm{m}_{\mathrm{calcite\_HCP}} + \left[{}^{14}C\right]_{liquid} \times V = n^{14}C_{tot} \quad \textbf{(Eq. 16)}$$

The calculations take into account two contributions for the isotopic exchange in addition with the sorption on C-S-H and the carbonation of portlandite considered as a kinetic process similarly to the isotopic exchange. These results are shown in Figure 18.

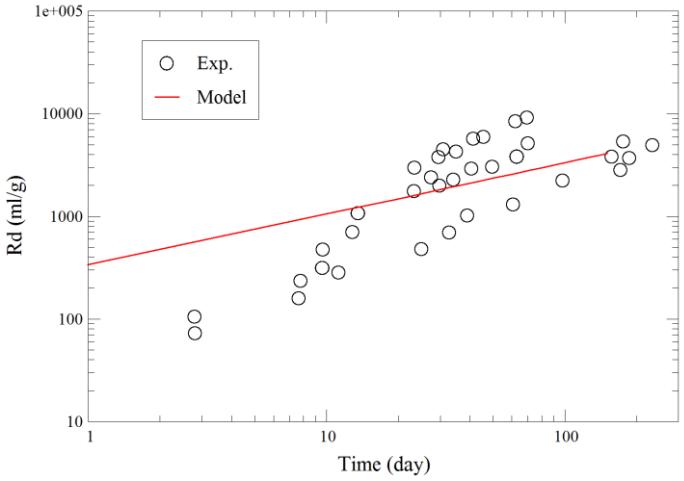

Figure 18: Simulations of ^{14}C uptake on mortars by considering retention on calcite, sand, portlandite and C-S-H [Bayliss, 1988]

The calculations are related in this last case to many parameters: (1) the size of calcite, sand, portlandite and (2) solid diffusion coefficient in these various solid phases. Additionally, a Kd of ^{14}C in C-S-H is also considered. Fig. 11 presents the results related to a given set of parameters; others sets can be also suitable. These calculations aims to show that the kinetic assumption associated to ^{14}C diffusion in solid phases can explain the measurements of ^{14}C in cement-based materials.

2.3.2.3 [Pointeau, 2008]

This study presents Rd of ^{14}C measurements in degraded hydrated cement pastes. This degradation induces various CO_3^{2-} concentrations as a function of calcium concentration and pH (Table 1).

Table 1: CO_3^{2-} concentration as a function of pH defined by the equilibrium with calcite

pH	13.3	13.2	12.9	12.5	12.2	11.4
CO_3^{2-} (mol/l)	2.1×10^{-4}	8.2×10^{-5}	2.1×10^{-5}	7.7×10^{-6}	6.8×10^{-6}	9.5×10^{-6}

The model considers the sorption of 14C on (1) C-S-H with a constant sorption, (2) portlandite with the parameters defined previously only for the systems with pH > 12.5, and (3) calcite with a content of 5% and a particle size of 0.5 µm. The diffusion coefficient in calcite is the one determined on nano-calcite in §1.2 (6.6×10^{-25} m^2/s). Figure 19 presents the results of the model in case of (1) the evolution of Kd with time for cement paste equilibrated at pH 12.2 and (2) the evolution of Kd on the range of pH corresponding to the degradation states I, II, and III. These results confirm the relevance of the hypothesis assuming a kinetic isotopic sorption hypothesis by solid diffusion.

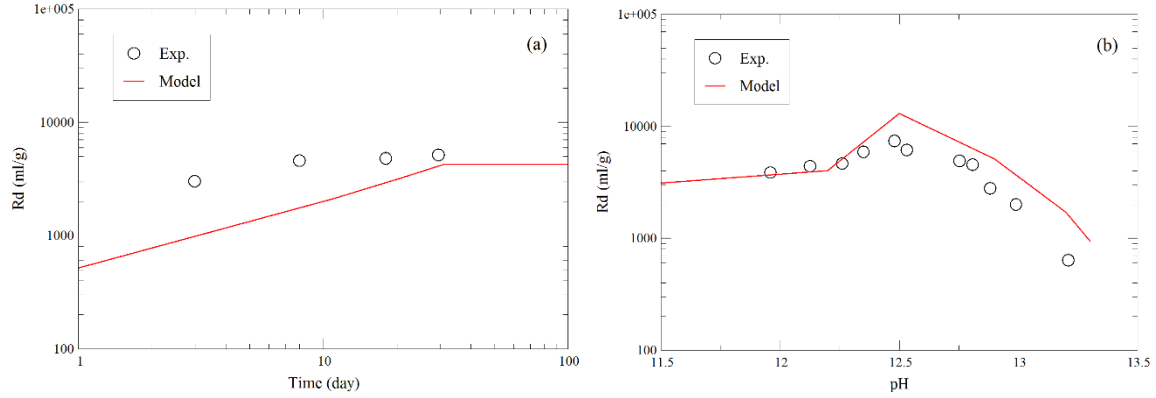

Figure 19: Simulations of ^{14}C uptake on degraded cement pastes [Pointeau, 2008]: as a function of time (a) and of pH (b). The size of calcite was fixed at 0.5 µm and the diffusion coefficient in calcite was 6.6×10^{-25} m^2/s.

2.3.3 Clay-rocks

The solid diffusion of ^{14}C into calcite can be assumed as the main phenomena for ^{14}C retention in clay-rocks. Consequently, the retention of ^{14}C in clay-rock depends on: (i) the calcite content, (ii) the solubility of calcite, (iii) the size of the calcite grains, (iv) the solid diffusion coefficient of ^{14}C into calcite and (v) time.

For the Callovo-Oxfordian clay-rock, we have assumed the following input parameters: (i) a calcite content of 20%, (ii) a solubility of calcite of 2.10^{-3} M in equilibrium with atmosphere and (iii) a solid diffusion coefficient of ^{14}C into calcite D = $6.6.10^{-25}$ m^2/s as determined in section 1.2. Figure 13 gives the evolution of the Rd(^{14}C) with time for various sizes of calcite grains. When ^{14}C will have completely diffuse through calcite a maximum Rd of 0.7 $m^3.kg^{-1}$ could expected for the Callovo-Oxfordian clay-rock. The size of calcite grains has a strong effect of the ^{14}C retention kinetic. In the Callovo-Oxfordian clay-rock, calcite sizes are mainly ranged between 0.1 and 10 µm [Robinet, 2008]. As regards to the low mobility of anion species in the Callovo-Oxfordian formation (De ~ 5.10^{-12} m^2/s), we can assumed a Rd value of 1.10^{-3} m^3/kg to be phenomenologically representative of ^{14}C up take.

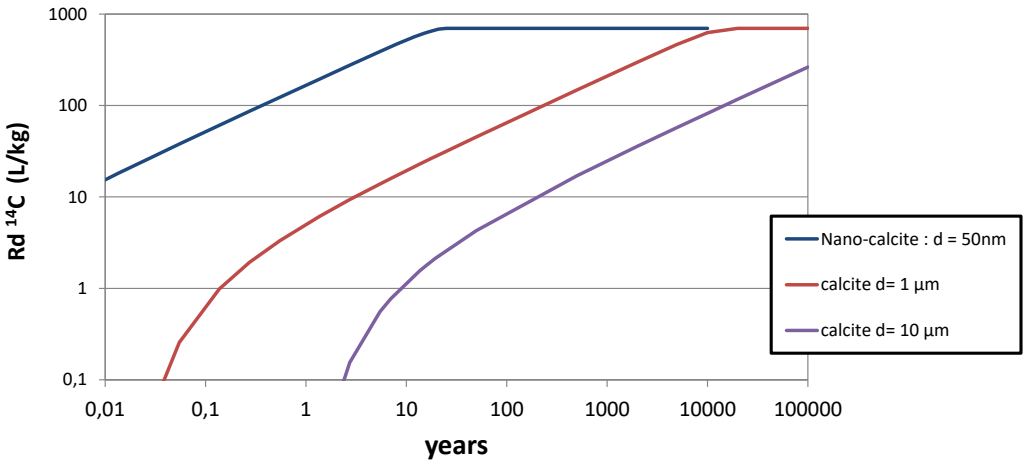

Figure 20: ^{14}C uptake on Callovo-Oxfordian clay-rock by considering retention on calcite for various sizes of calcite grains. Simulations were performed with $D = 6.6.10^{-25}$ m^2/s.

2.4 Organic ^{14}C

Organic ^{14}C can migrate in pore water as dissolved gas (CH_4) or as ^{14}C bearing molecules. In clay-rocks, the retention of alkanes is dominated by organic matter [Vinsot, 2017]. For dissolved CH_4, a low Rd value of 0.02 $L.kg^{-1}$ was found based on an in-situ gas injection experiment [Vinsot, 2017]. The retention behaviour of ^{14}C bearing molecules have been studied for cements and clay-rocks. For the Callovo-Oxfordian clay-rock, the Rd values resulting from batch sorption experiments have been summarized by a recent work [Rasamimanana, 2017] (Figure 21). Rd of organic molecules is mainly ranged between 0.1 and 10 $L.kg^{-1}$. These authors propose also a "sorption model" based on the organic matter content and the octanol/water partition coefficients. This model means that knowing the inventory of organic molecules a given Rd value can deduced and used as a mean Rd for the ^{14}C bearing molecules inventory. Today, it is not possible to propose a ^{14}C Rd value due to the lack of knowledge on the ^{14}C bearing molecules for the several waste forms.

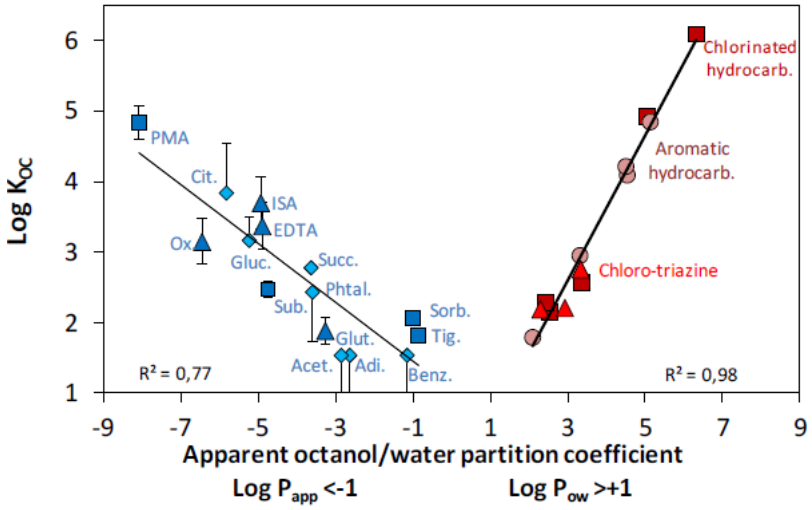

Figure 21: Correlation between adsorption data (normalised by organic content, KOC = Rd/fOC) and polarity of molecules [Rasamimanana, 2017].

2.5 *Discussion and perspectives*

This work presented a ^{14}C sorption model in cement-based materials based on a isotopic exchange evolving with time. The kinetics of the isotopic mechanism is associated to a solid diffusion process in calcite crystals. This approach was applied to several experimental data sets on calcite and on cementitious materials. The Kd evolutions of ^{14}C with time, systematically observed by experiments, were successfully reproduced. The model mainly depends on the size of calcite particles. The diffusion coefficient in solid was determined based on ^{13}C retention on ^{12}C calcite; this value appeared to be relevant in most cases.

Regarding the objectives and the aforementioned results of this task, Kd of ^{14}C in cement-based materials can be estimated at 10^4 L/kg. This value was obtained between 30 and 500 days. This assessment does not consider the coupling with pore diffusion. Consequently, further works should focus on coupling the solid diffusion of ^{14}C, as identified in the present work, with the ^{14}C diffusion in the porous network of cement-based materials. As the diffusion in the pore solution is much faster, an incomplete ^{14}C sorption by isotopic exchange could be expected.

3 ^{14}C transfer performance assessment in aqueous phase in the context of an Intermediate-Level Waste disposal cell

This part addresses the performance assessment of ^{14}C transfer in aqueous phase (no gas phase represented here), released from a disposal cell of intermediate level waste within the Callovo-Oxfordian clay host rock of the Cigéo project.

Two different chemical forms of ^{14}C have been successively considered: (i) the inorganic anionic form (CO_3^{2-}), and (ii) the organic neutral form (CH_4). In the aqueous phase, these two forms can be distinguished according to their diffusional transfer properties within the Callovo-Oxfordian clay host rock (effective diffusion coefficient, diffusional porosity), but also according to their geochemical reactivity within cementitious materials (higher level of sorption and possible role of the chemical precipitation for the carbonate form) and within

clay host rock (sorption only for the carbonate form). Within the modelling numeric tool used in this study, sorption is represented by a partition coefficient (Kd) between aqueous and solid phases, and precipitation is represented by a solubility limit (Csat).

3.1 *Conceptual model description*

The considered geometry is a 2D vertical cross-section of the disposal cell, involving the inventory of 6 disposal packages (3 packages on the horizontal axis, 2 packages on the vertical axis), each one of them containing one primary package. As shown on Figure 22, the 2D conceptual model comprises several materials, all represented as equivalent continuous porous media: (i) primary packages, (ii) disposal packages, (iii) technical gaps (empty space at top and around disposal packages stacks, and also between two stacks), (iv) disposal chamber (filling concrete surrounding the packages), (v) concrete liner, (vi) damaged zone of the host rock, (vii) over-damaged zone of the host rock, and (viii) pristine clay host rock. Due to symmetry conditions, only the half of the cross-section has been considered.

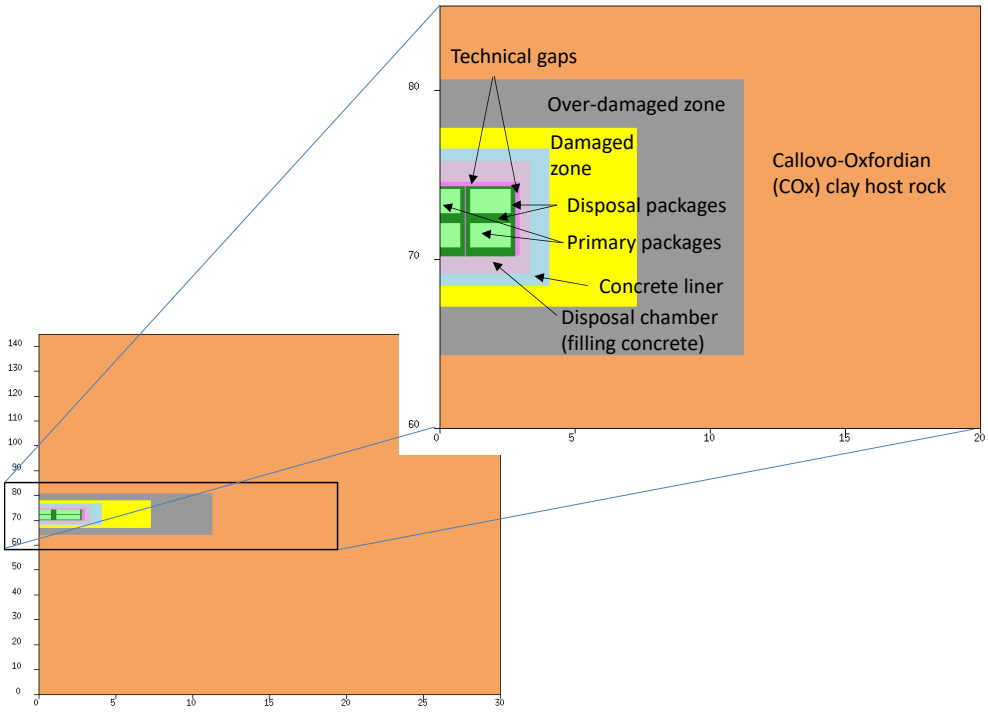

Figure 22: 2D geometry and represented components and materials

The main indicators are the ^{14}C instantaneous molar fluxes computed (i) at different interfaces between materials, (ii) at different surfaces defined within the clay host rock layer every 10 m starting from the central position, and (iii) at the limits of the clay layer (see Figure 23).

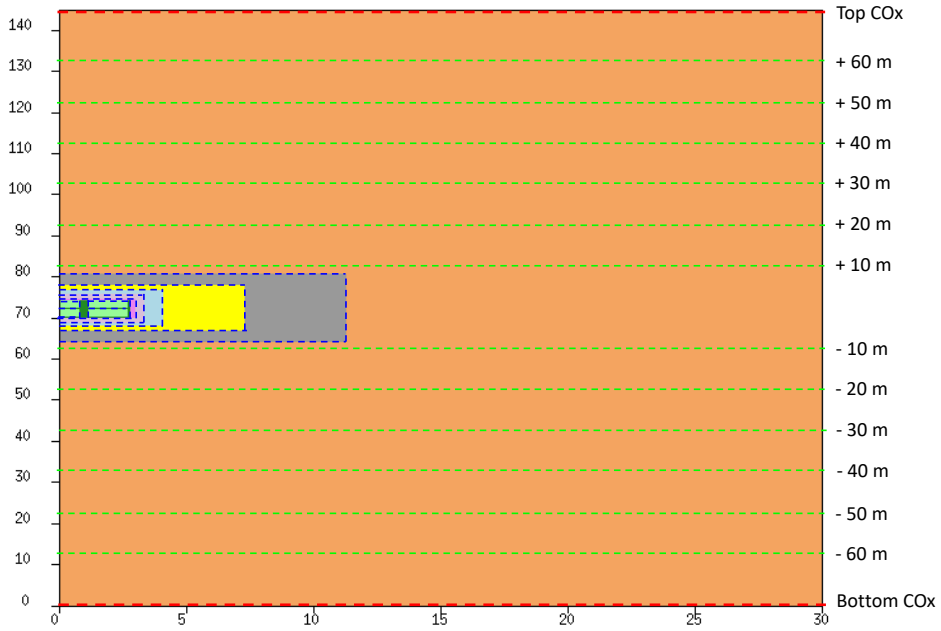

Figure 23: Localization of the different surfaces where molar fluxes are computed

3.2 *Types of calculations and parameter values*

Two sets of calculations have been performed: (i) a "phenomenological" case corresponding to a situation considering expected performances for reactivity and transfer properties of cementitious materials and clay host rock, and (ii) an "envelope" case corresponding to a more "conservative" situation for which transfer properties of cementitious materials are considered as "degraded" from initial time. The "phenomenological" case also considers unsaturated conditions at the beginning of the simulation and then an evolution of the effective diffusion coefficients with saturation (for all materials with the exception of gaps and Callovo-Oxfordian), up to saturated conditions reached after ~ 1.7×10^5 years.

These two sets of calculations are characterized by specific sets of transfer and chemical reactivity properties for the different cementitious and clayey media (hydraulic conductivity,

effective diffusion coefficient, diffusional porosity, sorption coefficient, solubility limit), as shown in following Table 2 and Table 3. Except during the transient unsaturated period, parameters values are considered as constant over the simulated time.

For each of the two previous "phenomenological" and "envelope" sets, different cases have been performed considering different constant Kd values either for cementitious components (disposal packages, disposal chamber and concrete liner): (i) 0 and 10^{-3} m^3/kg for organic ^{14}C (CH_4), and (ii) 10^{-1}, 1 and 10 m^3/kg for inorganic ^{14}C (CO_3^{2-}) (according to section 1) or within the clay host rock (Callovo-Oxfordian, damaged zones): (i) no sorption for organic ^{14}C (CH_4), and (ii) constant Kd values of 0, 10^{-3} and 10^{-2} m^3/kg for inorganic ^{14}C (CO_3^{2-}). No sorption is considered within primary packages and technical gaps. The solubility limit has only been considered for inorganic ^{14}C in the primary packages; the organic ^{14}C has no concentration limitation.

Table 2: Parameter values (hydraulic, transport, retention) for the "phenomenological" case

	Hydraulic conductivity K (m/s)		Effective diffusion coefficient De (m²/s)		Porosity ω (-)		Partition coefficient Kd (m^3/kg)		Dry density ρ_s (kg/m^3)		Retardation coefficient R (-)		Solubility limit C_{sat} (mol/m^3)	
	^{14}C org.	^{14}C inorg.	^{14}C org.	^{14}C inorg.	^{14}C org.	^{14}C inorg.	^{14}C org.	^{14}C inorg.	^{14}C org.	^{14}C inorg.	^{14}C org.	^{14}C inorg.	^{14}C org.	^{14}C inorg.
Disposal packages (concrete CEM V)	10^{-11}		10^{-12}		0,15		0 10^{-3}	10^{-1} 1 10	2 250		1 16	1 501 15 001 150 001	infinite	infinite
Disposal chamber (filling concrete) and concrete liner (concrete CEM V)	10^{-11}		10^{-11}		0,15		0 10^{-3}	10^{-1} 1 10	2 250		1 16	1 501 15 001 150 001	infinite	infinite
Primary packages	10^{-11}		10^{-12}		0,2		0		2 250		1		infinite	infinite or $9{,}5.10^{-3}$
Technical gaps (empty space)	10^{-15} (unsat.) then 10^{-6}		10^{-20} (unsat.) then $2{,}3.10^{-9}$		1		0		-		1		infinite	
Callovo-Oxfordian (COx)	4.10^{-14}		$2{,}3.10^{-11}$	3.10^{-12}	0,18	0,07	0	0 10^{-3} 10^{-2}	2 300		1	1 34 330	infinite	
Damaged and over-damaged zones	10^{-9}		$4{,}6.10^{-11}$	6.10^{-12}	0,18	0,07	0	0 10^{-3} 10^{-2}	2 300		1	1 34 330	infinite	

Table 3: Parameter values (hydraulic, transport, retention) for the "envelope" case (values in red colour highlight the differences with the "phenomenological" case)

	Hydraulic conductivity K (m/s)		Effective diffusion coefficient De (m²/s)		Porosity ω (-)		Partition coefficient Kd (m³/kg)		Dry density ρs (kg/m³)		Retardation coefficient R (-)		Solubility limit C_{sat} (mol/m³)	
	^{14}C org.	^{14}C inorg.	^{14}C org.	^{14}C inorg.	^{14}C org.	^{14}C inorg.	^{14}C org.	^{14}C inorg.	^{14}C org.	^{14}C inorg.	^{14}C org.	^{14}C inorg.	^{14}C org.	^{14}C inorg.
Disposal packages (concrete CEM V)	10^{-6}		$4{,}6.10^{-10}$		0,2		0 10^{-3}	10^{-1} 1 10	2 250		1 12,25	1 126 11 251 112 501	infinite	infinite
Disposal chamber (filling concrete) and concrete liner (concrete CEM V)	10^{-6}		$4{,}6.10^{-10}$		0,2		0 10^{-3}	10^{-1} 1 10	2 250		1 12,25	1 126 11 251 112 501	infinite	infinite
Primary packages	10^{-6}		$4{,}6.10^{-10}$		0,2		0		2 250		1		infinite	infinite or $9{,}5.10^{-3}$
Technical gaps (empty space)	10^{-6} (saturated at t=0)		$2{,}3.10^{-9}$ (saturated at t=0)		1		0		-		1		infinite	
Callovo-Oxfordian (COx)	4.10^{-14}		$2{,}3.10^{-11}$	3.10^{-12}	0,18	0,07	0	0 10^{-3} 10^{-2}	2 300		1	1 34 330	infinite	
Damaged and over-damaged zones	10^{-9}		$4{,}6.10^{-11}$	6.10^{-12}	0,18	0,07	0	0 10^{-3} 10^{-2}	2 300		1	1 34 330	infinite	

Two types of source terms have been also considered for the release of the ^{14}C inventory contained within the packages (4.31×10^{12} Bq (or 1.86 mol) per primary package): (i) a quasi-instantaneous (labile) release (over 1 year in practice), and (ii) a progressive kinetic release over about 50,000 years corresponding to corrosion of stainless steel (thickness of around 1mm) at a rate of 10nm/year (10^{-5}mm/year). The results described in § 3.3 (molar fluxes) are given for the whole disposal cell containing 1,590 primary packages (6.85×10^{15} Bq or 2,951 mol of ^{14}C).

In the whole modelled cases, the ^{14}C decay (5,700 years period) has been considered.

Table 4, Table 5 and Table 6 synthesize the list of calculation cases computed respectively for ^{14}C organic form, for ^{14}C inorganic form in "phenomenological" case and for ^{14}C inorganic form in "envelope" case.

Table 4: List of calculation cases computed for ^{14}C organic form

	Type of case	Sorption in cementitious components	Sorption in clay host rock	Solubility limit in primary packages	Type of ^{14}C source term (ST)
^{14}C organic form (CH_4)	"Phenomeno-logical" case	Kd=0 m^3/kg	Kd=0 m^3/kg	Not applicable (no solubility limit)	Instantaneous ST
					Kinetic ST
		Kd=10^{-3} m^3/kg			Instantaneous ST
					-
	"Envelope" case	Kd=0 m^3/kg			Instantaneous ST
					-
		Kd=10^{-3} m^3/kg			Instantaneous ST
					-

Table 5: List of calculation cases computed for ^{14}C inorganic form ("phenomenological" case)

	Type of case	Sorption in cementitious components	Sorption in clay host rock	Solubility limit in primary packages	Type of ^{14}C source term (ST)
^{14}C inorganic form (CO_3^{2-})	"Phenomeno-logical" case	Kd=10^{-1} m^3/kg	Kd=0 m^3/kg	Not considered	Instantaneous ST
					Kinetic ST
				Considered	Instantaneous ST
					-
			Kd=10^{-3} m^3/kg	Not considered	Instantaneous ST
					-
				Considered	-
					-
			Kd=10^{-2} m^3/kg	Not considered	Instantaneous ST
					-
				Considered	-
					-
		Kd=1 m^3/kg	Kd=0 m^3/kg	Not considered	Instantaneous ST
					-
				Considered	-
					-
		Kd=10 m^3/kg	Kd=0 m^3/kg	Not considered	Instantaneous ST
					-
				Considered	-
					-

Table 6: List of calculation cases computed for ^{14}C inorganic form ("envelope" case)

	Type of case	Sorption in cementitious components	Sorption in clay host rock	Solubility limit in primary packages	Type of ^{14}C source term (ST)
^{14}C inorganic form (CO_3^{2-})	"Envelope" case	$Kd=10^{-1}$ m^3/kg	$Kd=0$ m^3/kg	Not considered	Instantaneous ST
					-
				Considered	Instantaneous ST
					-
			$Kd=10^{-3}$ m^3/kg	Not considered	Instantaneous ST
					-
				Considered	-
					-
			$Kd=10^{-2}$ m^3/kg	Not considered	Instantaneous ST
					-
				Considered	-
					-
		$Kd=1$ m^3/kg	$Kd=0$ m^3/kg	Not considered	Instantaneous ST
					-
				Considered	-
					-
		$Kd=10$ m^3/kg	$Kd=0$ m^3/kg	Not considered	Instantaneous ST
					-
				Considered	-
					-

3.3 *Main results*

3.3.1 ^{14}C organic form (CH_4)

3.3.1.1 "Phenomenological" case

3.3.1.1.1 Initial case

Figure 24 illustrates the organic ^{14}C molar fluxes at different interfaces for the "**phenomenological" case**, for an instantaneous source term and no sorption in cementitious components (Kd=0 m^3/kg).

The top graph of Figure 24 shows a successive decrease (attenuation) of the ^{14}C maximum molar flux during the transfer within the different components:

(i) a reduction of more than 3 orders of magnitude brought by the primary packages (low diffusion),

(ii) an additional reduction of 2 orders of magnitude brought by the disposal packages (low diffusion),

(iii) an additional global reduction by a factor of 3 brought by the disposal chamber, the concrete liner and host rock damaged zones,

(iv) and an additional reduction of at least 5 orders of magnitude brought by the Callovo-Oxfordian clay layer (the molar flux coming out of the surface "Bottom COx" is higher than the one coming out of the surface "Top COx" because technical gaps at the top of the disposal packages stacks play the role of a "shield" during unsaturated conditions preventing ^{14}C from transferring, which is not the case under the disposal packages in direct contact with the filling concrete of the disposal chamber).

The bottom graph of Figure 24 showing the molar fluxes coming out of the surfaces defined within the COx clay layer, indicates that each tens of additional meters of clay thickness reduces the maximum molar flux by a factor of about 8, and delays the dates of occurrence of

the maximum molar flux due to the combined effect of increasing transfer distance and ^{14}C radioactive decay (5,700 years period).

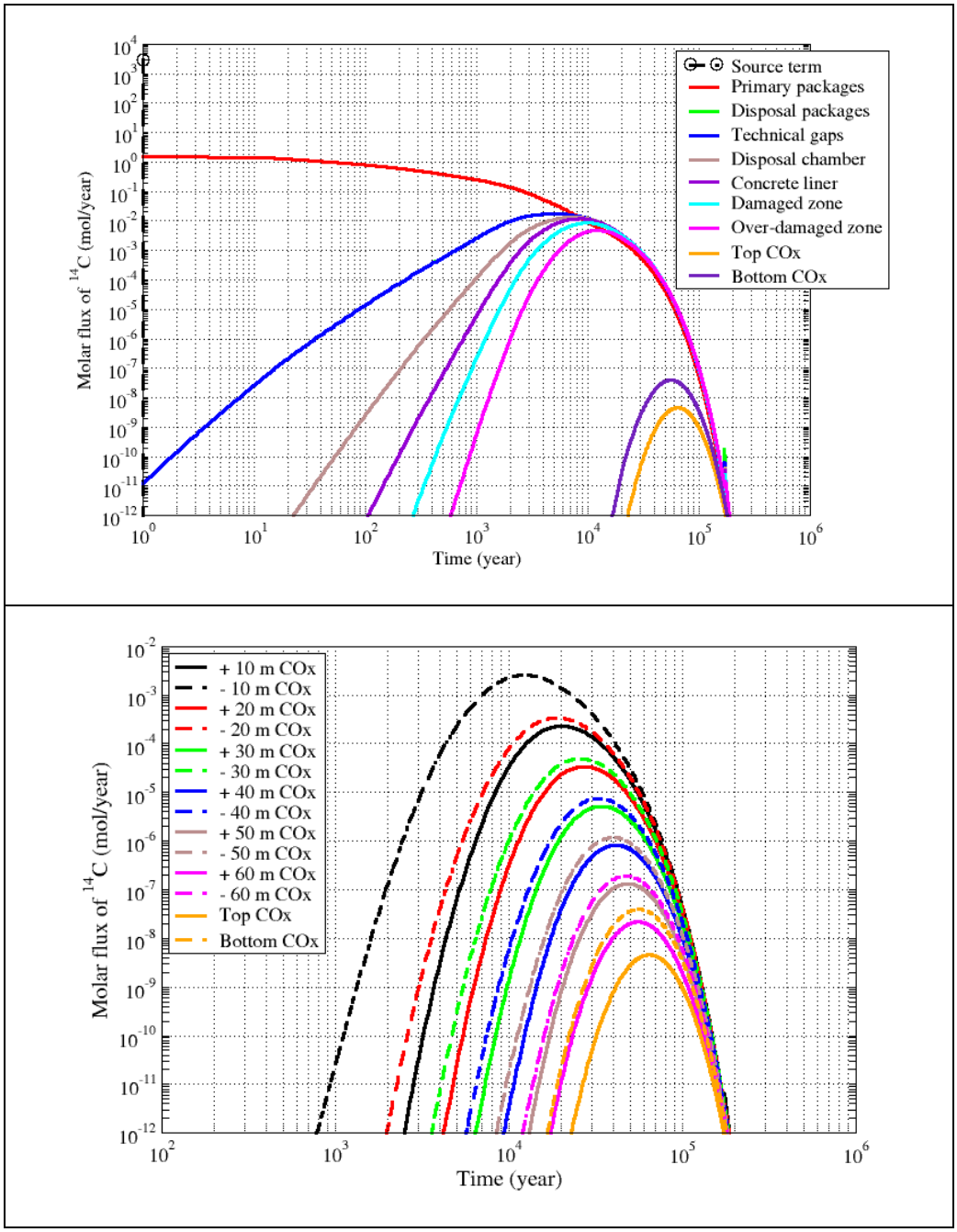

Figure 24: ^{14}C organic form (CH_4) – "Phenomenological" case: molar fluxes evolution with time at different interfaces between materials (top graph) and different interfaces within and at the limits of the COx clay layer (bottom graph) for an instantaneous source term and no sorption in cementitious components (Kd=0 m^3/kg)

3.3.1.1.2 Sensitivity to chemical reactivity (sorption) in cementitious components

Considering the effect of chemical reactivity (sorption) in cementitious components, Figure 25 illustrates the impact of a constant Kd value of 10^{-3} m^3/kg for organic ^{14}C in cementitious components (disposal packages, disposal chamber, concrete liner), in comparison with the initial case considering no sorption (Kd=0 m^3/kg), in the case of an instantaneous source term.

Figure 25 shows that sorption (Kd = 10^{-3} m^3/kg) in cementitious components:

- increases the reduction effect brought by the disposal packages, disposal chamber and concrete liner on the maximum molar flux (reduction of 1 order of magnitude for the disposal packages and disposal chamber, and reduction of 2 orders of magnitude for the concrete liner, compared to the initial case considering no sorption), and this has an effect up to the limits of the COx clay layer (reduction of the molar flux between 1 and 2 orders of magnitude),
- delays the dates of occurrence of the maximum molar flux for these cementitious components up to 15,000/20,000 years (these dates were less than 10,000 years for the initial case considering no sorption).

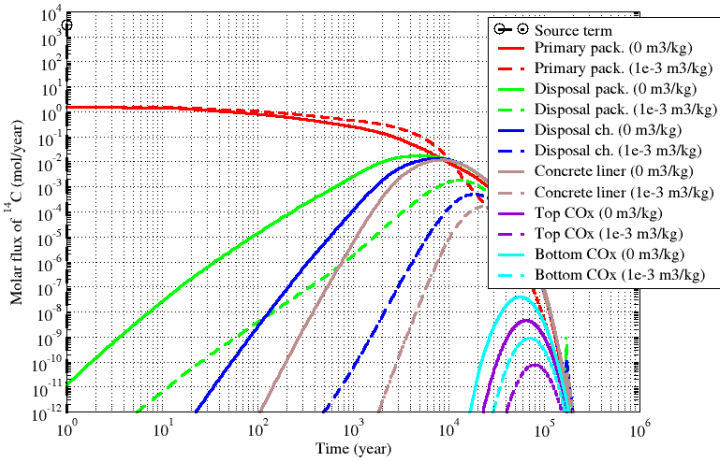

Figure 25: ^{14}C organic form (CH_4) – "Phenomenological" case: molar fluxes evolution with time at different interfaces between materials for an instantaneous source term and a constant Kd value in cementitious components of 10^{-3} m^3/kg (dashed lines), compared to those of the initial "phenomenological" case considering no sorption in cementitious components (Kd=0 m^3/kg) (solid lines)

3.3.1.1.3 Sensitivity to ^{14}C kinetic source term

With the same initial conditions ("phenomenological" case, no sorption in cementitious components), Figure 26 illustrates the effect of considering a kinetic ^{14}C source term over about 50,000 years, compared to an instantaneous source term.

Of course, the highest value of the source term has been reduced by 4 ½ orders of magnitude between both cases. In addition, Figure 26 shows (i) a reduction of 2 orders of magnitude of the ^{14}C maximum molar flux brought by primary packages (along with a "shift" of the date of occurrence of the maximum molar flux from 1 year to 5,000 years), and (ii) a reduction of 1 order of magnitude of the ^{14}C maximum molar flux brought by disposal packages, disposal chamber and concrete liner. The molar fluxes coming out "Bottom COx" and "Top COx" surfaces have decreased (by a factor of 4) compared to the initial case, but are still in the same order of magnitude (around 10^{-8} and 10^{-9} mol/year, respectively at the surfaces "Bottom COx" and "Top COx").

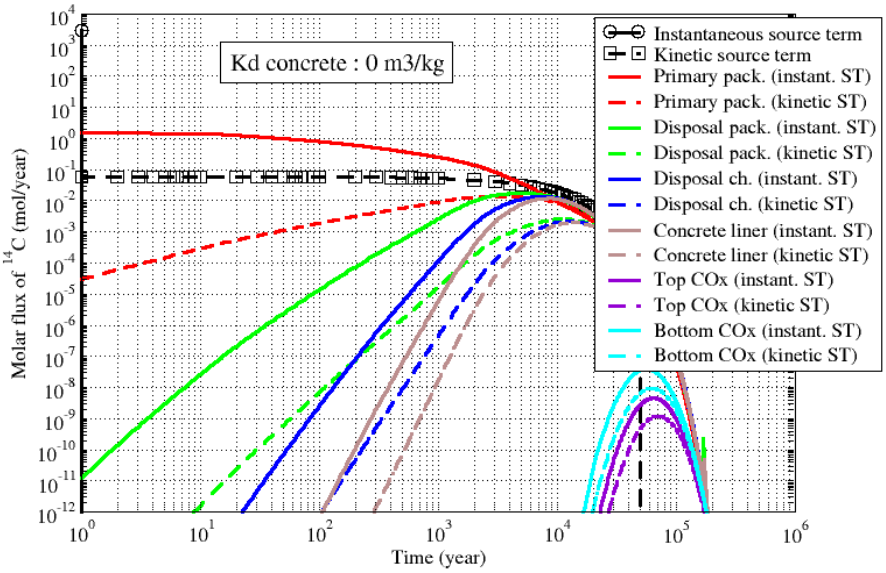

Figure 26: ^{14}C organic form (CH_4) – "Phenomenological" case: molar fluxes evolution with time at different interfaces between materials for a kinetic source term (over 50,000 years) (dashed lines), compared to those of the initial "phenomenological" case considering an instantaneous source term (solid lines)

Another computed case (not shown) considering the kinetic source term and the effect of a constant Kd value in cementitious components of 10^{-3} m^3/kg for organic ^{14}C, illustrates a similar behaviour as the one described in Figure 25: a significant reduction of the maximum molar fluxes coming out of the cementitious components and at the limits of the host rock clay layer.

3.3.1.2 "Envelope" case

3.3.1.2.1 Initial case

Figure 27 illustrates the organic ^{14}C molar fluxes at different interfaces for the **"envelope" case**, considering an instantaneous source term and no sorption in cementitious components (Kd=0 m^3/kg).

The top graph of Figure 27 shows a successive decrease (attenuation) of the ^{14}C maximum molar flux during the transfer within the different components:

(i) a reduction by a factor of 3 brought by the primary packages (high diffusion),

(ii) an additional reduction by a factor of 2 brought by the disposal packages (high diffusion),

(iii) an additional reduction of one order of magnitude brought by the disposal chamber,

(iv) an additional reduction by a factor of 3.5 brought by the concrete liner,

(v) an additional reduction by a factor of 6 brought by the host rock damaged zone,

(vi) an additional reduction by a factor of 3 brought by the host rock over-damaged zone,

(vii) and an additional reduction of 6 orders of magnitude brought by the clay host rock.

As for the "phenomenological" case, the bottom graph of Figure 27 showing the molar fluxes coming out of the surfaces defined within the COx clay layer, indicates that each tens of additional meters of clay thickness reduces the maximum molar flux by a factor of about 8 to

10, and delays the dates of occurrence of the maximum molar flux due to the combined effect of increasing transfer distance and ^{14}C radioactive decay (5,700 years period).

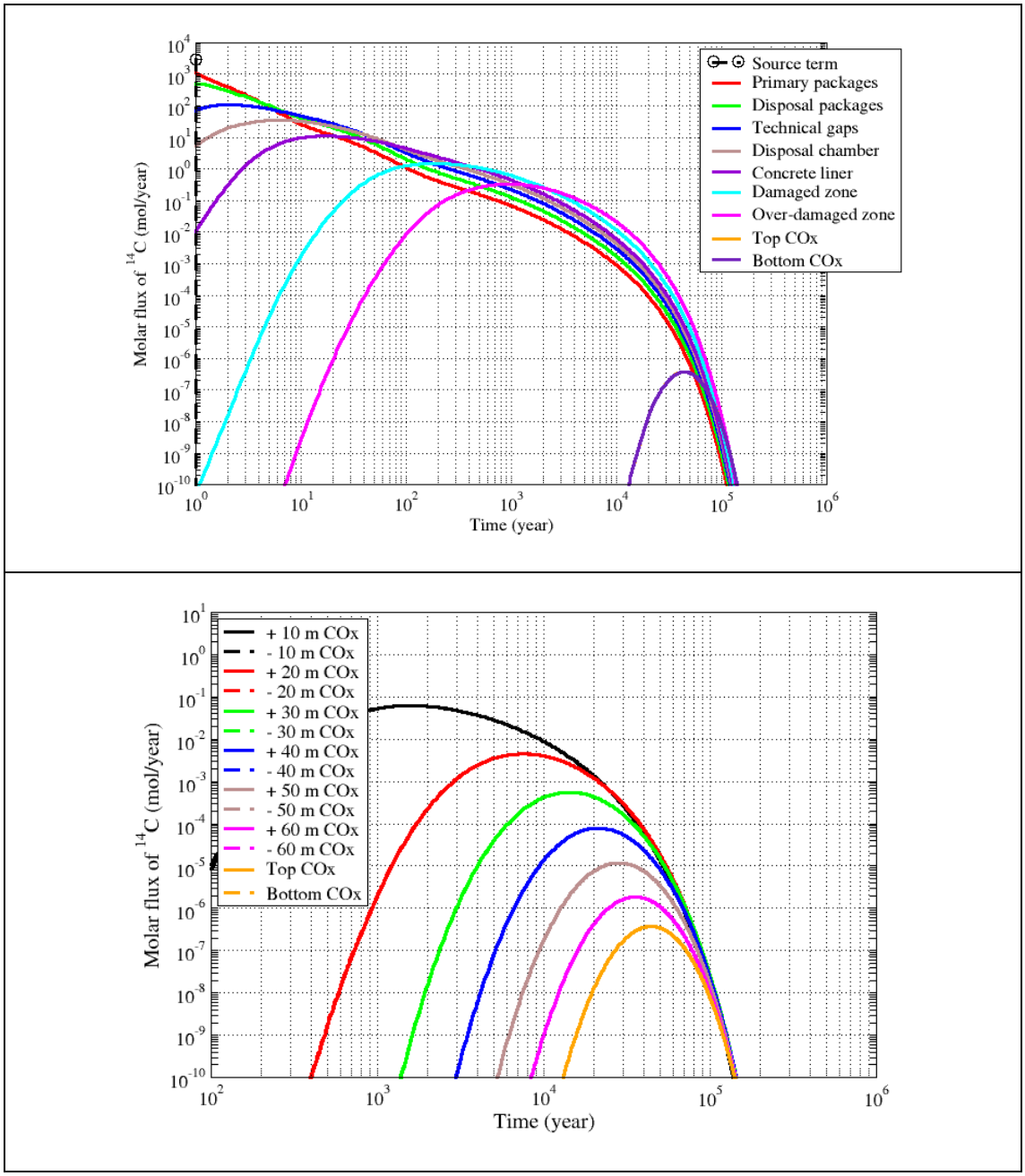

Figure 27: ^{14}C organic form (CH_4) – "Envelope" case: molar fluxes evolution with time at different interfaces between materials (top graph) and different interfaces within and at the limits of the COx clay layer (bottom graph) for an instantaneous source term and no sorption in cementitious components (Kd=0 m^3/kg)

3.3.1.2.2 Sensitivity to chemical reactivity (sorption) in cementitious components

Starting from this initial "envelope" case, considering a constant Kd value of 10^{-3} m^3/kg for organic ^{14}C in cementitious components has qualitatively the same effect as for the "phenomenological" case, but the reduction of maximum molar flux is quantitatively slightly lower (see Figure 28): sorption in cementitious components enhances the reduction effect on the maximum molar flux, brought by the disposal packages (reduction by a factor of 3), the disposal chamber (additional reduction by a factor of 4) and the concrete liner (additional reduction of one order of magnitude), compared to the initial "envelope" case considering no sorption, and this has a slight effect up to the limits of the COx clay layer.

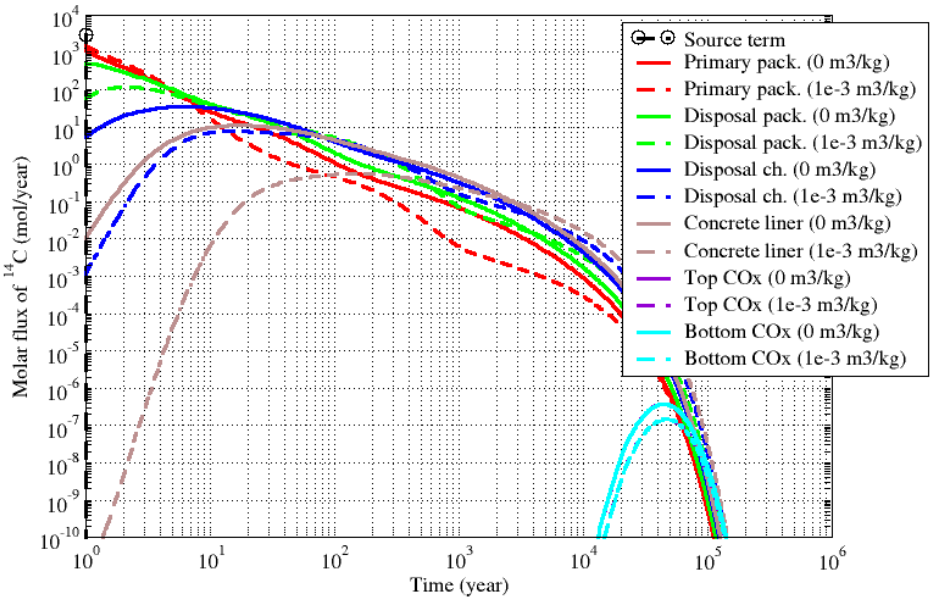

Figure 28: ^{14}C organic form (CH_4) – "Envelope" case: molar fluxes evolution with time at different interfaces between materials for an instantaneous source term and a constant Kd value in cementitious components of 10^{-3} m^3/kg (dashed lines), compared to those of the initial "envelope" case considering no sorption (Kd=0 m^3/kg) (solid lines)

3.3.1.3 Synthesis of maximum molar fluxes for ^{14}C organic form

Table 7 summarizes the ^{14}C organic maximum molar fluxes coming out of the disposal cell (surface "concrete liner"), obtained for the different computed cases.

The indicated results confirm that considering sorption of ^{14}C organic in cementitious components (constant Kd of 10^{-3} m^3/kg compared to no sorption) brings a reduction of the maximum molar flux coming out of the disposal cell of (i) almost 2 orders of magnitude for the "phenomenological" case, and (ii) at least 1 order of magnitude for the "envelope" case.

The effect of considering a kinetic source term instead of an instantaneous one reduces the maximum molar flux by a factor of 6, only for the "phenomenological" case.

Table 7: ^{14}C organic maximum molar fluxes coming out of the disposal cell

	Type of case	**Sorption in cementitious components**	**Sorption in clay host rock**	**Type of ^{14}C source term (ST)**	**^{14}C maximum molar flux (level and date of occurrence)**
^{14}C organic form (CH_4)	"Phenomeno-logical" case	Kd=0 m^3/kg	Kd=0 m^3/kg	Instantaneous ST	~ 1.2×10^{-2} mol/year (t ~ 9,000 years)
				Kinetic ST	~ 2×10^{-3} mol/year (t ~ 14,000 years)
		Kd=10^{-3} m^3/kg		Instantaneous ST	~ 1.7×10^{-4} mol/year (t ~ 23,000 years)
	"Envelope" case	Kd=0 m^3/kg		Instantaneous ST	~ 11 mol/year (t ~ 20 years)
		Kd=10^{-3} m^3/kg		Instantaneous ST	~ 0.56 mol/year (t ~ 150 years)

3.3.2 ^{14}C inorganic form (CO_3^{2-})

3.3.2.1 "Phenomenological" case

3.3.2.1.1 Initial case

Figure 29 illustrates the inorganic ^{14}C molar fluxes at different interfaces for the **"phenomenological" case** and for an instantaneous source term, a Kd value in cementitious components of 10^{-1} m^3/kg, and no sorption in clay host rock (Kd=0 m^3/kg).

The graph shows a successive decrease (attenuation) of the ^{14}C maximum molar flux during the transfer within the different materials:

(i) a reduction of more than 3 orders of magnitude brought by the primary packages (low diffusion), as for ^{14}C organic form,

(ii) an additional reduction of 7 orders of magnitude brought by the disposal packages (low diffusion and sorption), much more important than for ^{14}C organic form (due to higher sorption),

(iii) an additional reduction of almost 4 orders of magnitude brought by the disposal chamber,

(iv) an additional global reduction of at least 4 orders of magnitude brought by the concrete liner and host rock damaged zones, so that the molar fluxes at these interfaces are very small (~ 10^{-16} mol/year).

The molar fluxes coming out of the surfaces defined within the COx clay layer are very small, below 10^{-16} mol/year (graph not shown), so that the molar fluxes at the limits of the COx clay layer are totally negligible.

Obviously, an increased sorption in cementitious components (Kd=1 or 10 m^3/kg) and/or an increased sorption in clay host rock (Kd=10^{-3} or 10^{-2} m^3/kg) would further strengthen this last statement.

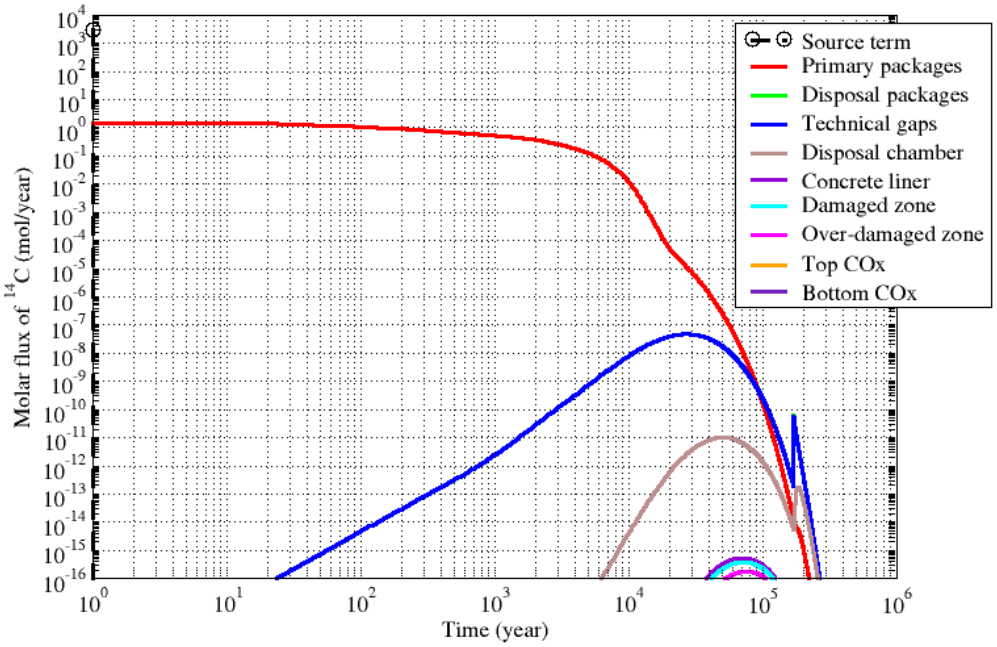

Figure 29: ^{14}C inorganic form (CO_3^{2-}) – "Phenomenological" case: molar fluxes evolution with time at different interfaces between materials for an instantaneous source term, a constant Kd value in cementitious components of 10^{-1} m^3/kg and no sorption in clay host rock (Kd=0 m^3/kg)

3.3.2.1.2 Sensitivity to chemical reactivity (sorption) in cementitious components

Considering the effect of chemical reactivity (sorption), Figure 30 illustrates the effect of two constant Kd values of 1 m^3/kg and 10 m^3/kg for inorganic ^{14}C in cementitious components (disposal packages, disposal chamber, concrete liner), in comparison with the initial "phenomenological" case considering a constant Kd value of 10^{-1} m^3/kg (and no sorption in clay host rock for the three cases).

Figure 30 shows that increasing sorption of inorganic ^{14}C in concrete components drastically enhances the reduction effect brought by the disposal packages, disposal chamber and concrete liner on the maximum molar flux (for instance, reduction of 3 orders of magnitude (respectively 6 orders of magnitude) brought by the Kd value of 1 m^3/kg (respectively 10 m^3/kg) in disposal packages, and reduction of more than 5 orders of magnitude brought by the Kd value of 1 m^3/kg in the disposal chamber).

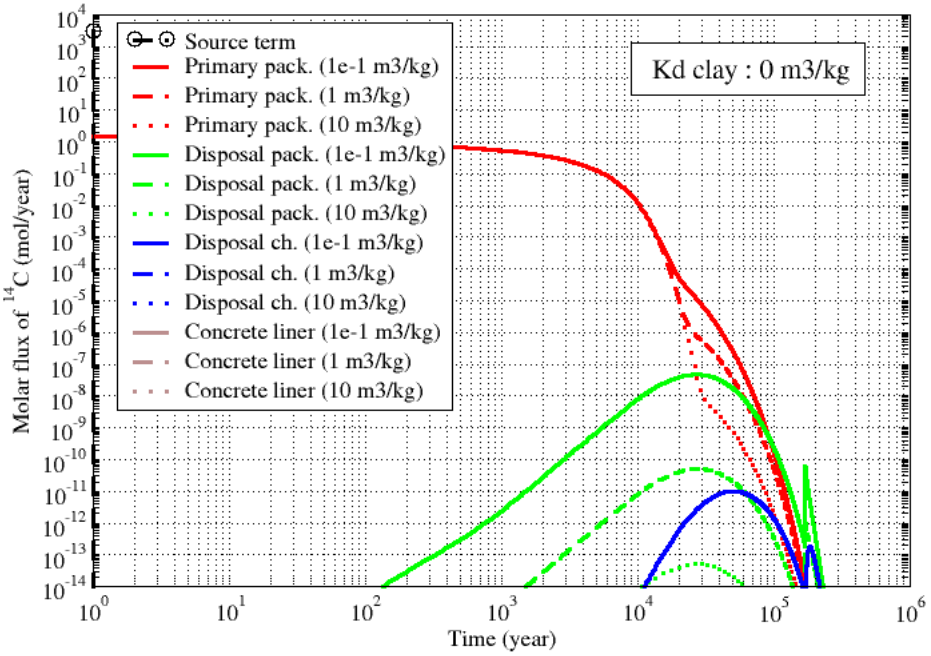

Figure 30: ^{14}C inorganic form (CO_3^{2-}) - "Phenomenological" case: molar fluxes evolution with time at different interfaces between materials for an instantaneous source term, no sorption in clay host rock and two constant Kd values in cementitious components of 1 m^3/kg (dashed lines) and 10m^3/kg (dotted lines), compared to those of the initial "phenomenological" case considering a constant Kd value of 10^{-1} m^3/kg (solid lines)

3.3.2.1.3 Sensitivity to chemical reactivity (precipitation) in primary packages

In addition to considering sorption processes in cementitious components (Kd=10^{-1} m^3/kg), Figure 31 illustrates the effect of inorganic ^{14}C solubility limit in primary packages (Csat=9.5×10^{-3} mol/m^3), in comparison with the initial "phenomenological" case considering no solubility limit (Csat=0 mol/m^3) (no sorption in clay host rock).

The graph shows that considering solubility limit of inorganic ^{14}C in primary packages has a reduction effect on the ^{14}C maximum molar flux: (i) reduction of 2 orders of magnitude for primary packages, (ii) reduction of almost 1 order of magnitude for disposal packages, and (iii) reduction of almost 1 order of magnitude for disposal chamber and concrete liner.

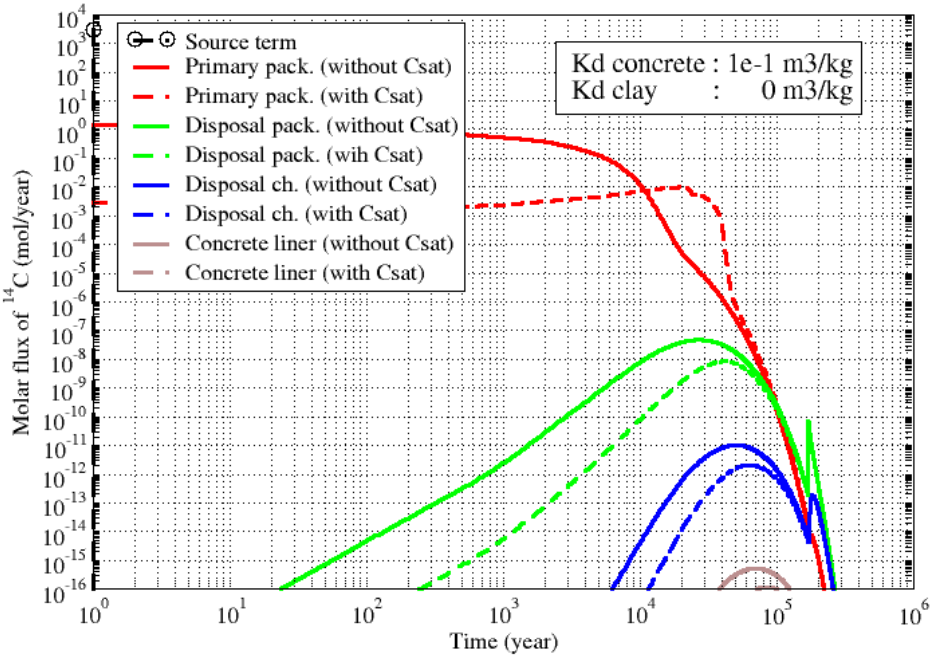

Figure 31: ^{14}C inorganic form (CO_3^{2-}) - "Phenomenological" case: molar fluxes evolution with time at different interfaces between materials for an instantaneous source term and a solubility limit in primary packages (Csat=9.5×10^{-3} mol/m^3) (dashed lines), compared to those of the initial "phenomenological" case considering no solubility limit (Csat=0 mol/m^3) (solid lines). Kd value in cementitious materials of 10^{-1}m^3/kg and no sorption in clay host rock

3.3.2.1.4 Sensitivity to of ^{14}C kinetic source term

With the same initial conditions ("phenomenological" case, a constant Kd value in cementitious components of 10^{-1}m^3/kg, no sorption in clay host rock, no solubility limit in primary packages), Figure 32 illustrates the effect of considering a kinetic ^{14}C source term over about 50,000 years, compared to an instantaneous source term.

As for ^{14}C organic form, the highest value of the source term has been reduced by 4 ½ orders of magnitude between both cases. In addition, the graph also shows a reduction of the ^{14}C maximum molar flux between the two cases: (i) of at least 1 order of magnitude brought by primary packages (along with a "shift" of the date of occurrence of the maximum molar flux from 1 year to 5,000 years), (ii) by a factor of 5 brought by disposal packages, and (iii) by a factor of 3 brought by the disposal chamber. In both cases, molar fluxes coming out of the

concrete liner are lower than 10^{-12} mol/year and molar fluxes through the surfaces defined within the clay layer and at the limits of the COx clay layer are (totally) negligible.

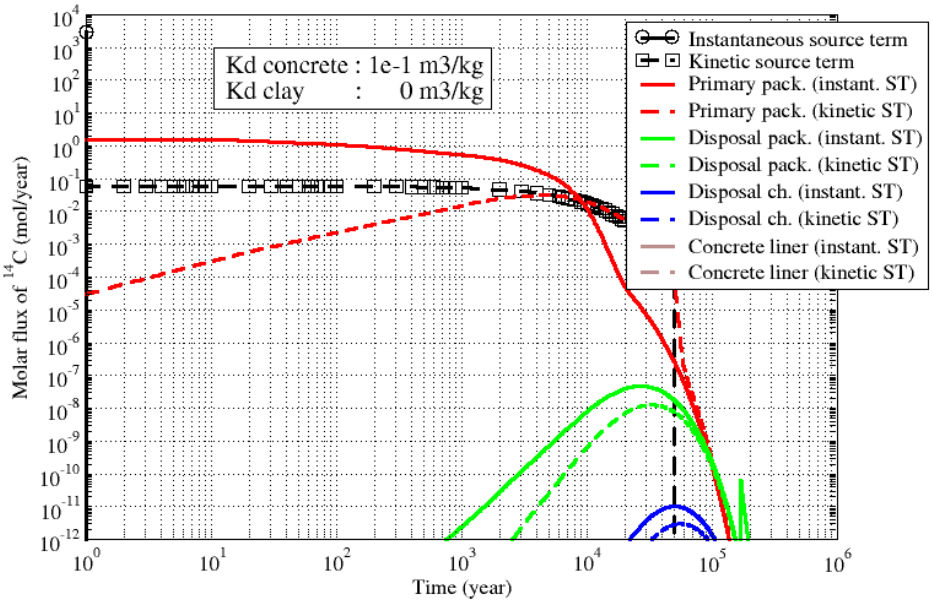

Figure 32: ^{14}C inorganic form (CO_3^{2-}) – "Phenomenological" case: molar fluxes evolution with time at different interfaces between materials for a kinetic source term (over 50,000 years) (dashed lines), compared to those of the initial "phenomenological" case considering an instantaneous source term (solid lines). Kd value in cementitious materials of 10^{-1} m^3/kg and no sorption in clay host rock

3.3.2.2 "Envelope" case

3.3.2.2.1 Initial case

Figure 33 illustrates the inorganic ^{14}C molar fluxes at different interfaces for the **"envelope" case**, for an instantaneous source term, a constant Kd value in cementitious components of 10^{-1} m^3/kg, and no sorption in clay host rock (Kd=0 m^3/kg).

The top graph of Figure 33 shows a successive decrease (attenuation) of the ^{14}C maximum molar flux during the transfer within the different components:

(i) a reduction by a factor of 2 brought by the primary packages (high diffusion),

(ii) an additional reduction of 3 orders of magnitude brought by the disposal packages (high diffusion),

(iii) an additional reduction of 1 order of magnitude brought by the disposal chamber,

(iv) an additional reduction of 3 orders of magnitude brought by the concrete liner,

(v) an additional reduction of 1 order of magnitude brought by the host rock damaged zones,

(vi) and an additional reduction of several orders of magnitude brought by the clay host rock.

The bottom graph of Figure 33 showing the molar fluxes coming out of the surfaces defined within the COx clay layer, indicates that each tens of additional meters of clay thickness reduces the maximum molar flux by more than one order of magnitude, and delays the dates of occurrence of the maximum molar flux due to the combined effect of increasing transfer distance and ^{14}C radioactive decay (5,700 years period), so that the molar fluxes at the limits of the COx layer are small (around 10^{-14} mol/year).

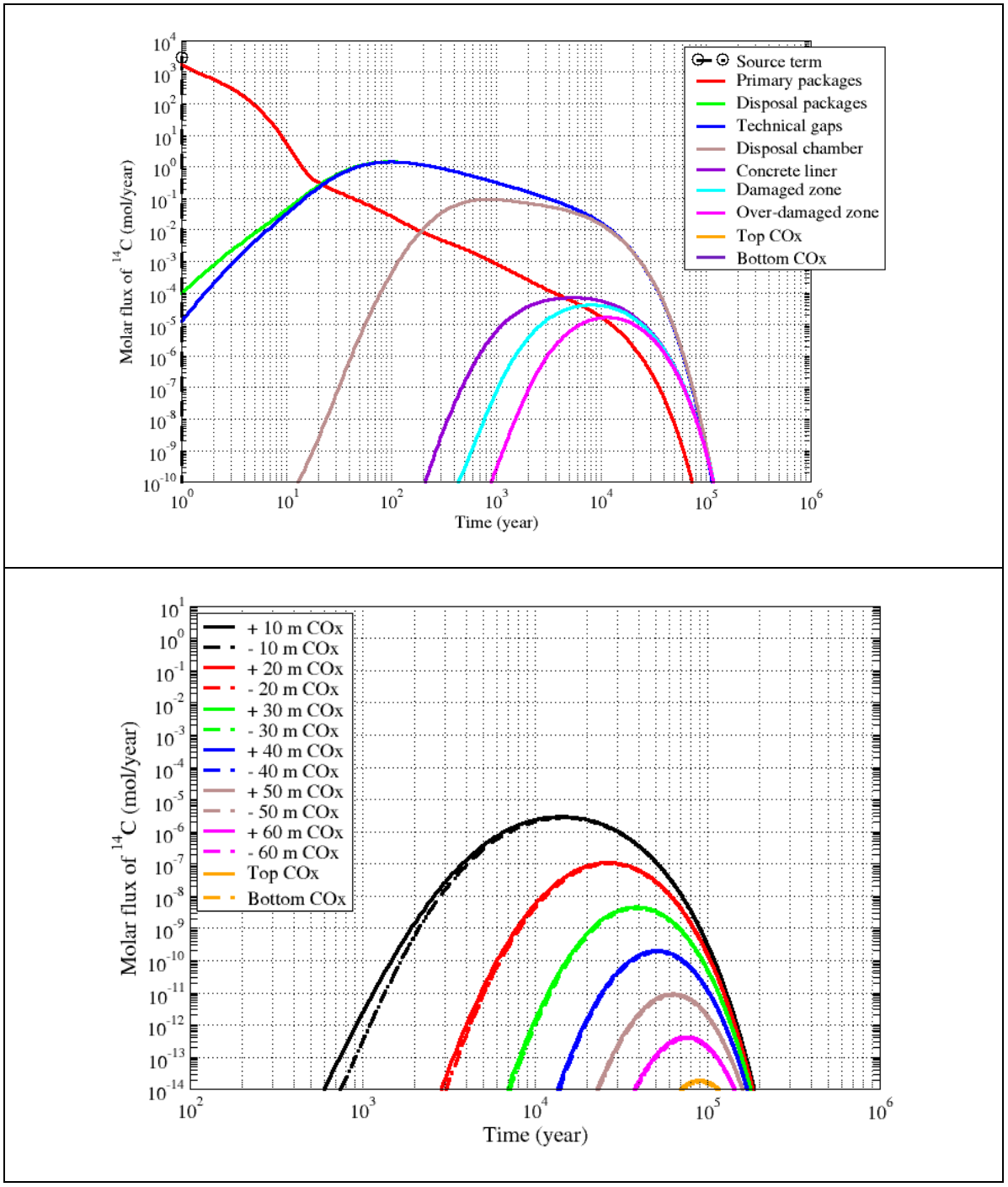

Figure 33: ^{14}C inorganic form (CO_3^{2-}) – "Envelope" case: molar fluxes evolution with time at different interfaces between materials (top graph) and different interfaces within and at the limits of the COx clay layer (bottom graph) for an instantaneous source term, a constant Kd value in cementitious components of 10^{-1} m^3/kg and no sorption in clay host rock (Kd=0 m^3/kg)

3.3.2.2.2 Sensitivity to chemical reactivity (sorption) in cementitious components

Starting from this initial "envelope" case (no sorption in clay host rock), considering two constant Kd values of 1 m^3/kg and 10 m^3/kg for inorganic ^{14}C in cementitious components, has qualitatively the same effect as for the "phenomenological" case, but the reduction of maximum molar flux is quantitatively slightly lower (Figure 34) compared to the initial "envelope" case considering a constant Kd value of 10^{-1} m^3/kg (Figure 33): sorption in cementitious components enhances the reduction effect on the maximum molar flux brought (i) by the disposal packages (reduction of 1 and 2 orders of magnitude respectively for the Kd values of 1 m^3/kg and 10 m^3/kg), (ii) by the disposal chamber (additional reduction of 1 and 2 orders of magnitude respectively for the Kd values of 1 m^3/kg and 10 m^3/kg), (iii) and by the concrete liner (additional reduction of 3 and 8 orders of magnitude respectively for the Kd values of 1 m^3/kg and 10 m^3/kg).

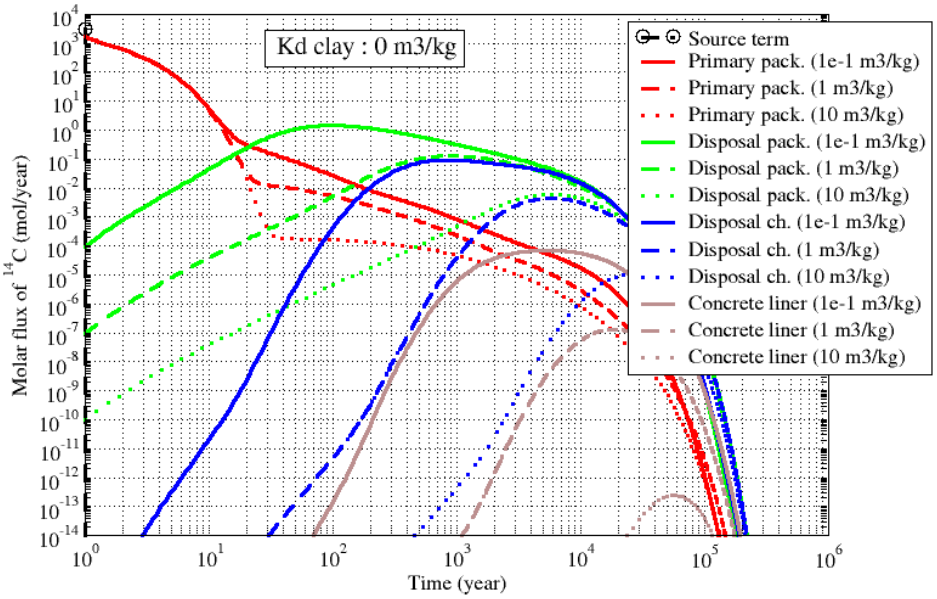

Figure 34: 14C inorganic form (CO_3^{2-}) – "Envelope" case: molar fluxes evolution with time at different interfaces between materials for an instantaneous source term, no sorption in clay host rock and two constant Kd values in cementitious components of 1 m^3/kg (dashed lines) and 10 m^3/kg (dotted lines), compared to those of the initial "envelope" case considering a constant Kd value of 10^{-1} m^3/kg (solid lines)

3.3.2.2.3 Sensitivity to chemical reactivity (precipitation) in primary packages

In addition to considering sorption processes in cementitious components, Figure 35 illustrates the effect of inorganic ^{14}C solubility limit in primary packages ($Csat=9.5\times10^{-3}mol/m^3$), in comparison with the initial "envelope" case considering no solubility limit ($Csat=0mol/m^3$), a constant Kd value in cementitious components of $10^{-1}m^3/kg$ and no sorption in clay host rock.

The graph shows that considering solubility limit of inorganic ^{14}C in primary packages has a reduction effect on the ^{14}C maximum molar flux: (i) reduction of 2 orders of magnitude for primary packages, (ii) and reduction by a factor of 3 for disposal packages. Then, the effect of solubility limit slowly decreases (disposal chamber) and becomes negligible (concrete liner) at distance from primary packages (domain in which solubility limit is applied).

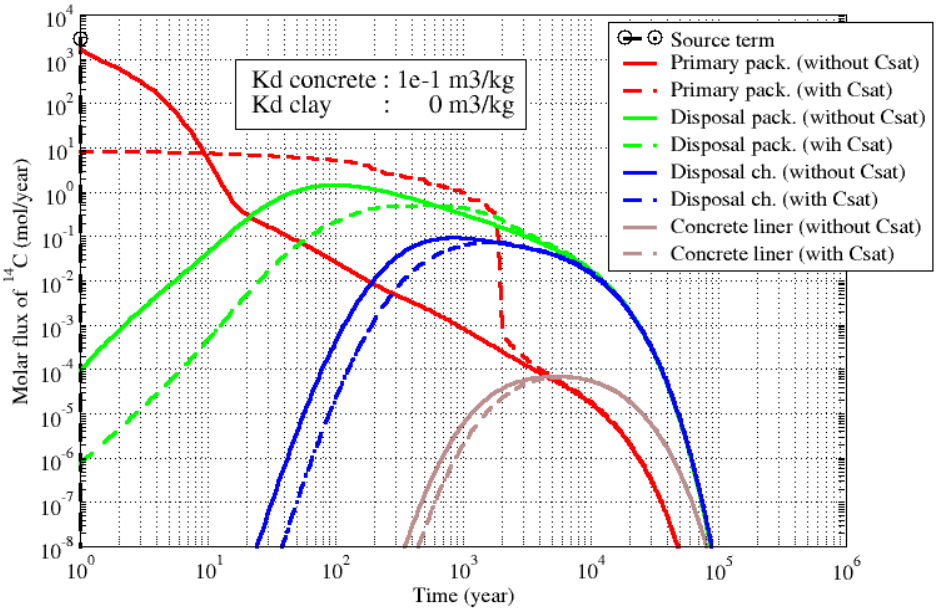

Figure 35: ^{14}C inorganic form (CO_3^{2-}) - "Envelope" case: molar fluxes evolution with time at different interfaces between materials for an instantaneous source term, $Kd=10^{-1}\ m^3/kg$ in cementitious components, no sorption in clay host rock and a solubility limit in primary packages ($Csat=9.5\times10^{-3}\ mol/m^3$) (dashed lines), compared to those of the initial "envelope" case considering no solubility limit ($Csat=0\ mol/m^3$), (solid lines)

It is to note that to fix a solubility limit has no effect in the case of kinetic ^{14}C source term, in same conditions ("Envelope" case, constant Kd value in cementitious components of 10^{-1} m^3/kg, no sorption in clay host rock), because ^{14}C concentration in primary packages remains about 30 times below the solubility limit value ($Csat=9.5\times10^{-3}$ mol/m^3) at any time.

3.3.2.2.4 Sensitivity to chemical reactivity (sorption) in clay host rock

Considering the effect of chemical reactivity (sorption), Figure 36 illustrates the effect of two constant Kd values of 10^{-3} m^3/kg and 10^{-2} m^3/kg for inorganic ^{14}C in clay host rock (Callovo-Oxfordian, damaged zones), in comparison with the initial "envelope" case considering no sorption in clay host rock (constant Kd value of 10^{-1} m^3/kg in cementitious components for the three cases).

Figure 36 shows that increasing sorption of inorganic ^{14}C in clay host rock drastically enhances the reduction effect brought by the damaged zones and the pristine clay host rock on the maximum molar flux (for instance, (i) reduction of almost 2 orders of magnitude (respectively almost 5 orders of magnitude) brought by the Kd value of 10^{-3} m^3/kg (respectively 10^{-2} m^3/kg) in damaged zones, (ii) reduction of almost 3 orders of magnitude (respectively almost 8 orders of magnitude) brought by the Kd value of 10^{-3} m^3/kg (respectively 10^{-2} m^3/kg) in the first 10 meters of clay, and (iii) reduction of more than 5 orders of magnitude brought by the Kd value of 10^{-3} m^3/kg in the first 15 meters of clay).

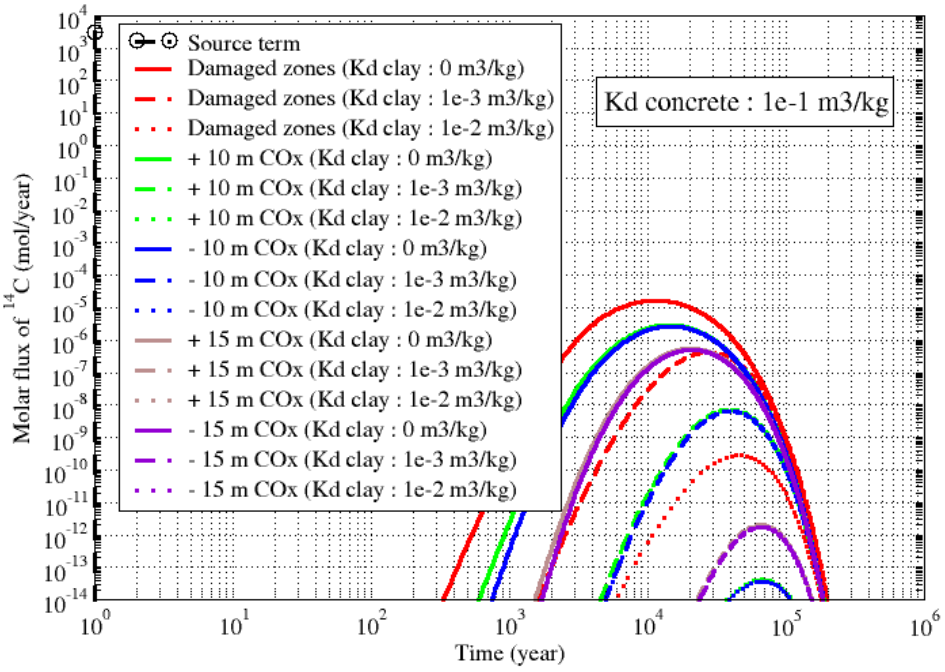

Figure 36: 14C inorganic form (CO_3^{2-}) – "Envelope" case: molar fluxes evolution with time at different interfaces between materials for an instantaneous source term, a constant Kd value in cementitious components of 10^{-1} m^3/kg, and two constant Kd value in clay host rock of 10^{-3} m^3/kg (dashed lines) and 10^{-2} m^3/kg (dotted lines), compared to those of the initial "envelope" case considering no sorption in clay host rock (solid lines)

3.3.2.3 Synthesis of maximum molar fluxes for ^{14}C inorganic form

Table 8 summarizes the ^{14}C inorganic maximum molar fluxes coming out of the disposal cell (surface "concrete liner") obtained for the different computed cases (cases considering an instantaneous source term and no precipitation in primary packages).

For the "phenomenological" case, the maximum molar fluxes coming out of the disposal cell are totally negligible (much lower than 10^{-14} mol/year), due to the expected performances for reactivity and transfer properties of cementitious components.

For the "envelope" case , the indicated results confirm that considering **sorption of ^{14}C inorganic in cementitious components** (constant Kd of 1m^3/kg, respectively 10m^3/kg,

compared to the initial Kd of 10^{-1} m^3/kg) brings a huge reduction of the maximum molar flux coming out of the disposal cell of (i) almost 3 orders of magnitude for Kd of 1 m^3/kg, and (ii) respectively at least 8 orders of magnitude for Kd of 10 m^3/kg.

Table 8: ^{14}C inorganic maximum molar fluxes coming out of the disposal cell

	Type of case	Sorption in cementitious components	Sorption in clay host rock	Type of ^{14}C source term (ST)	^{14}C maximum molar flux (level and date of occurrence)
^{14}C inorganic form (CO_3^{2-})	"Phenomenological" case	Kd=10^{-1} m^3/kg	Kd=0 m^3/kg	Instantaneous ST	<< 10^{-14} mol/year
		Kd=1 m^3/kg		Instantaneous ST	
		Kd=10 m^3/kg		Instantaneous ST	
	"Envelope" case	Kd=10^{-1} m^3/kg		Instantaneous ST	~ 7×10^{-5} mol/year (t ~ 5,400 years)
		Kd=1 m^3/kg		Instantaneous ST	~ 1.4×10^{-7} mol/year (t ~18,000 years)
		Kd=10 m^3/kg		Instantaneous ST	~ 2.5×10^{-13} mol/year (t ~ 57,000 years)

Table 8 summarizes the ^{14}C inorganic maximum molar fluxes coming out of the damaged zones and at a surface defined at 10 m within the clay host rock, obtained for the different computed cases (cases considering an instantaneous source term and no precipitation in primary packages).

For the "phenomenological" case, the maximum molar fluxes coming out of the damaged zones and out of a surface defined 10 m within the clay host rock are totally negligible (much lower than 10^{-14} mol/year), due to the expected performances for reactivity and transfer properties of cementitious components (same explanation as above).

For the "envelope" case , the indicated results confirm that considering **sorption of ^{14}C inorganic in clay host rock** (constant Kd of 10^{-3} m^3/kg, respectively 10^{-2} m^3/kg, compared to no sorption) brings a huge reduction of the maximum molar fluxes coming out of the damaged zones and out of a surface defined 10 m within the clay host rock: (i) almost 3 orders of magnitude for Kd of 10^{-3} m^3/kg, and (ii) respectively at least 8 orders of magnitude for Kd of 10^{-2} m^3/kg.

Table 9: ^{14}C inorganic maximum molar fluxes coming out of the damaged zones and out of a surface defined at 10m within the clay host rock

	Type of case	Sorption in cementitious components	Sorption in clay host rock	Type of ^{14}C source term (ST)	^{14}C maximum molar flux (level and date of occurrence)
^{14}C inorganic form (CO_3^{2-})	"Phenomeno-logical" case	Kd=10^{-1} m^3/kg	Kd= 0 m^3/kg	Instantaneous ST	Damaged zones and 10 m clay host rock: << 10^{-14} mol/year
			Kd= 10^{-3} m^3/kg	Instantaneous ST	
			Kd= 10^{-2} m^3/kg	Instantaneous ST	
	"Envelope" case		Kd= 0 m^3/kg	Instantaneous ST	Damaged zones: ~ 1.7×10^{-5} mol/year (t ~ 11,500 years) 10 m clay host rock: ~ 3×10^{-6} mol/year (t ~ 14,500 years)
			Kd = 10^{-3} m^3/kg	Instantaneous ST	Damaged zones: ~ 3×10^{-8} mol/year (t ~ 25,000 years) 10 m clay host rock: ~ 4×10^{-9} mol/year (t ~ 29,000 years)
			Kd= 10^{-2} m^3/kg	Instantaneous ST	Damaged zones: ~ 6×10^{-14} mol/year (t ~ 63,500 years) 10 m clay host rock: ~ 8×10^{-15} mol/year (t ~ 66,500 years)

4 ^{14}C transfer performance assessment in gaseous phase in the context of deep geological repository

This part addresses the performance assessment of ^{14}C transfer in gaseous phase, released from a deep geological repository. Since more than 10 years, extensive numerical phenomenological studies have been carried out taking advantage of a thorough experimental work in the Bure URL as well as on surface laboratories in order to implement models and parameters values for two-phase flow simulation. These simulations have shown that the system will evolve through several transient phases with respect to saturation, pressure, and thermal state and that these phases have significant impact on ^{14}C migration in gaseous form.

The work done specifically for the European Project CAST is based on the preliminary design phase of Cigéo. The aim of these evaluations is to assess operational range of several indicators linked to ^{14}C migration, especially at the interface between the bottom of the overlying aquifer and the top of the host rock.

4.1 *Conceptual modeling*

4.1.1 ^{14}C source term

As previously described (cf. 1.2), seven families of waste packages represent more than 98.5% of the total amount of carbon 14 inventory mole. In this assessment, the ^{14}C source term considers only these 7 families and the source terms from the other families is assumed to be null (so as not to impact the analysis). These waste packages are distributed in only 14 IL-LL waste disposal tunnels among the 50 available.

The following source terms were taken into account:

- A labile source term for one of the families of waste packages, which corresponds for less than 3% of the total ^{14}C inventory,
- Either a labile source term or a source term congruent with the corrosion of the metal for all other families of waste packages, corresponding to activated metallic waste. Both high and low corrosion rates were investigated.

The ^{14}C source terms are described in Figure 25 linked to the "sensitivity" section of the presented results (chapter 4.4.1).

4.1.2 Hydrogen source terms

In the deep geological repository, the underlying processes of gas generation and the amount of gas generated will depend on the zone considered (Figure 37). The main processes for gas production are the corrosion of the metallic materials mainly in anoxic conditions, and the radiolysis of water or organic materials. Hydrogen corresponds to about 95% of the total amount of generated gas.

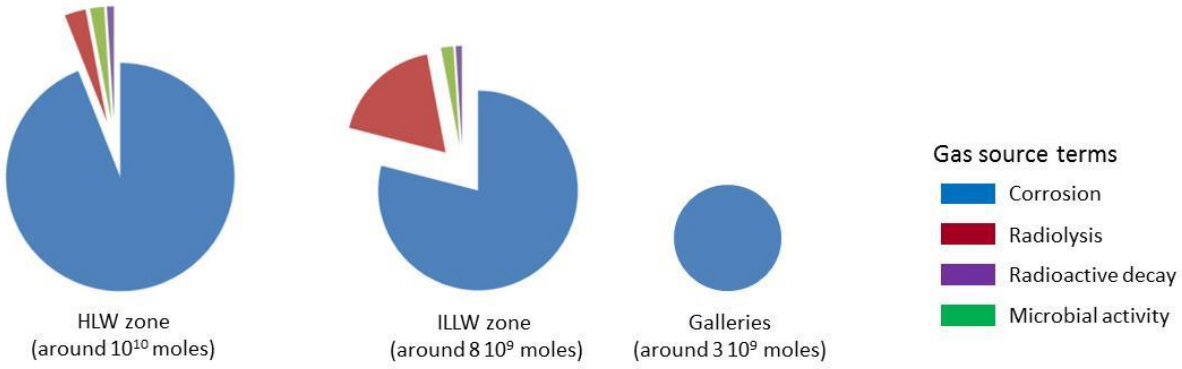

Figure 37: Principal type of gas generation processes in each zone

As all HL waste cells are conceptually the same concerning the amount of metallic materials, hydrogen source term is assumed to be the same for all of these several thousand cells (Figure 22). The evolution of hydrogen production results from the evolution of the temperature evolution (smooth evolution during the first part of the curve), the total consumption of a component (rapid decrease of the source term) and the failure of a component (rapid increase due to the corrosion on both sides of the component).

Taking these facts into account, this performance assessment considers only hydrogen resulting from corrosion and radiolysis as gas source terms. The total amount of hydrogen produced in Cigéo is of around 2×10^{10} moles (compared to 14,000 moles only for ^{14}C), half

of it produced in the HL waste disposal cells (carbon steel liner and carbon steel overpack), 40% in the IL-LL waste disposal cells (waste themselves, concrete container and concrete lining reinforcement) and 10% in the galleries (concrete lining reinforcement and host rock bolding).

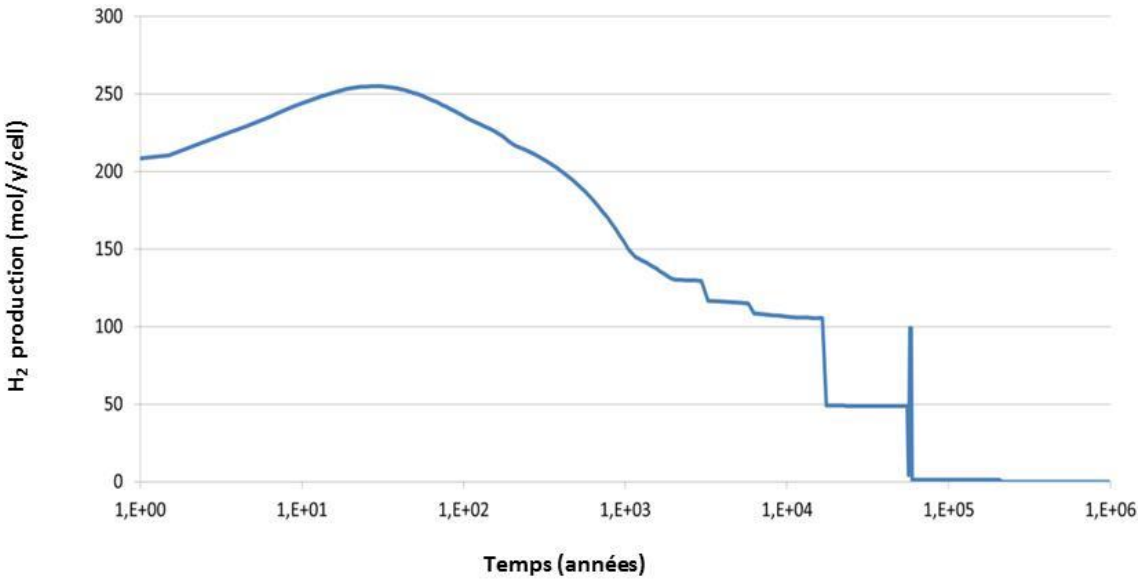

Figure 38: Hydrogen source term for a HL waste cell

In order to simplify the hydrogen source terms resulting from the different types of IL-LL waste, a clustering has been made which led to only eight different source terms to take into account in the evaluations (Figure 39). The total amount of hydrogen generated in a disposal cell may vary within a factor 100 from one disposal cell to another. An important uncertainty (over an order of magnitude) regarding hydrogen production is the corrosion rate of the metallic components. However, on the overall, hydrogen source term can last for several tens of thousands years in the repository.

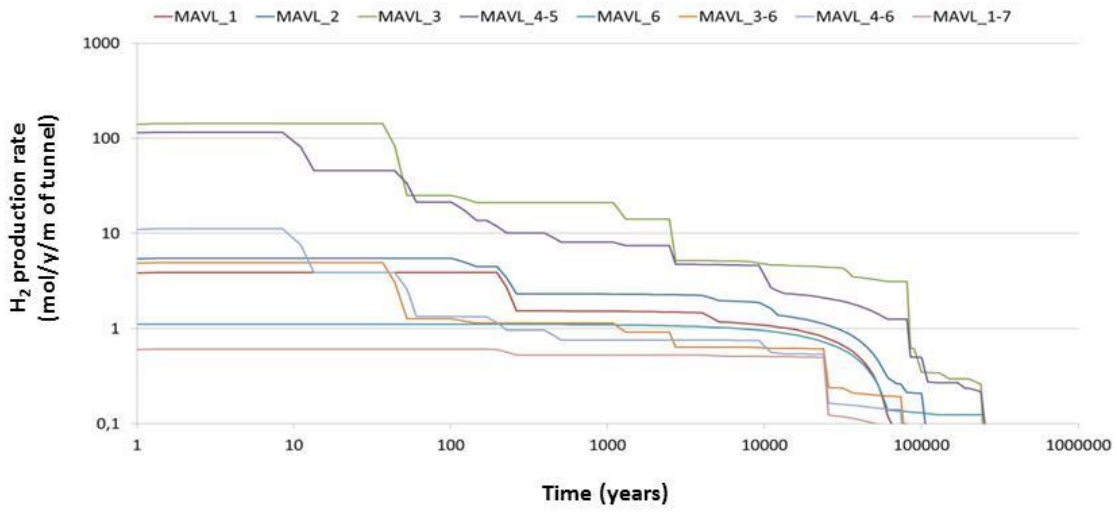

Figure 39: Gas source terms for IL-LL waste tunnels

4.1.3 Phenomenological two-phase flow representation

The two-phase flow modelling takes into account the following assumptions:

- The migration of gas and water results from convection (represented by extended Darcy flow equations) and by diffusion (represented by Fick law);
- Interactions between phases are simplified by using Henry's law for each gaseous component (mainly hydrogen and ^{14}C). The vapor pressure lowering is taken into account for water.
- Interaction between the non-vapor saturated ventilated air and the surrounding porous media (mainly cementitious materials and clay host rock) is taken into account via Kelvin's law.

Coupling between hydraulic and thermal process is complete and has a significant effect during the first hundred years after repository closure.

4.2 Numerical implementation

4.2.1 Simulation code and modeled processes

For this study, numerical simulations rely on the finite-volume code TOUGH2-MP. TOUGH2-MP is the parallel version of TOUGH2 and follows the concept of modules providing equations of state (EOS) for different components partitioned between phases. Further description and more details about Tough2/Tough2-MP codes are available from the Tough2 Homepage on the web, at http://esd.lbl.gov/TOUGH2, and from the Tough2-MP Homepage on the web at http://tough2.com.

For the present thermo-hydraulic two-phase flow and transport study the system can be well described by the TOUGH2-MP module EOS75Rx taking into account the following considerations and approaches:

- heat diffusion is supposed to be isotropic;
- the gas phase is considered as a mixture of hydrogen and water vapour;
- the ventilation during the operational phase is implemented using boundary conditions of fixed pressure, temperature, saturation and mass fractions in the ventilated drifts. The saturation is calculated from the given relative humidity and the corresponding capillary pressure according to Kelvin's equation;
- two chemical forms of ^{14}C are considered: methane and carbon dioxide;

4.2.2 Material properties

All the materials in the model are, according to the TOUGH2-MP philosophy, parameterized as porous materials, some of which with porosity one as e.g., for air in ventilated tunnels. The materials are defined through grain properties (e.g., dry grain density, dry grain specific heat) or bulk properties (e.g., porosity, tortuosity, heat conductivity at saturated conditions).

The two-phase flow properties and phase interaction are parameterized using

- the relative permeability saturation relationship following a modified version of the formulation by van Genuchten as a function of liquid saturation
- the capillary pressure saturation relationship following a modified version of the formulation by van Genuchten. It contains a linearization of the pressure for liquid

saturations between 0.999 and 1 as a common approach for improving numerical convergence.

In the modeling approach, some simplifications performed for mesh coarsening imply the definition of merged model materials that have average properties of several physical materials. In fact, several physical materials of rather small extent are modeled together as one equivalent material, which allows for coarser discretizations and can improve numerical performance and stability dramatically. The following merged materials were introduced for the present study:

- HL waste disposal cells: vitrified waste, stainless steel primary waste package, carbon steel overpack, buffer in-between waste packages, and the carbon steel liner;
- IL-LL waste disposal cells: IL-LL waste, primary waste package, concrete waste package, void spaces and concrete backfilling;
- EDZ materials: inner and outer EDZ and concrete lining along all the access and ventilation drifts.

The HL waste disposal cells are parameterized by a material with a porosity that represents the void space of the gaps between waste overpack and steel liner. Permeabilities, tortuosities, and most of the other hydraulic properties are assumed to be identical to the inner EDZ, while the density of the material is approximated by a volumetric average of the densities of the effectively present materials. The specific heat of the merged model material is then determined by averaging between the specific heat of the different materials weighted by volume and densities, i.e., by mass, and by considering the contribution of pore water. Since the prediction of the thermal evolution inside HL waste disposal cells is not of interest here, the heat conductivity of the merged material was assumed to be the one of steel.

For the IL-LL waste disposal cells and EDZ materials, the porosity and the grain density are defined as volumetric averages of the porosities and grain densities of the individual materials. The specific heat is a weighted average of the different specific heat values and the heat conductivity was set to the value of concrete for the MAVL-waste and to the value of both the inner and outer EDZ for the EDZ materials.

The different material properties used in the model are summarized in Appendix 1.

4.3 General TH-Gas evaluation

The results presented in this chapter are related to a simulation in which all the physical parameters have their reference value. In this sense, the following description represents the most representative evolution of available knowledge on the hydraulic-gas transient given the architecture chosen (concept by the end of 2014).

During the first thousand years, corresponding to a high gas production period, the gas phase is expanding at the repository scale and so does the gas pressure (Figure 24). This bulk gas phase is generated essentially by the production of hydrogen. In the HL waste zone, some transient phenomena, linked to an increase of temperature due to the heat generated by the wastes appear during the first centuries. The production of ^{14}C is too low to contribute to this expansion and to the increase of gas pressure into the repository, but gaseous ^{14}C is transported by the hydrogen generated gas phase. The gaseous phase (mainly hydrogen, but including also the gaseous ^{14}C) migrates preferentially by convection in the structures of the repository and very little hydrogen enters sound argillites due to their low desaturation and very high capillary potentials.

Due to the low gas entry pressure of seals and EDZ (some MPa at most), hydrogen can migrate at the repository scale and a significant flow can reach the access and pass into the Oxfordian (overlying aquifer). It's the same for gaseous ^{14}C in typically several thousand years (see more details on the next chapter).

Thereafter, typically beyond a few tens of thousands of years, due to the decline in hydrogen production, the expansion of the gas phase decreases (Figure 40) and the diffusion of dissolved hydrogen (and ^{14}C) in the Callovo-Oxfordian layer towards the overlying and underlying aquifers formations becomes the dominant transfer process.

At the repository scale, some hundreds of thousands of years after its closure, and after total resaturation (no more gas pressure, Figure 40), out of the total of around 2 10^{10} moles of hydrogen generated, approximately 85%-90% reached the over and under lying aquifers (Dogger and Oxfordian) under dissolved form via the Callovo-Oxfordian argillites and about 10% -15% of the volume of hydrogen produced has passed in gaseous form to the overlying Oxfordian aquifer via the access. Most of this flow goes through the shafts (90% of the total

hydrogen flux through the access) and only a very small part (about 10% of the total hydrogen flux through the access) migrates via the ramps.

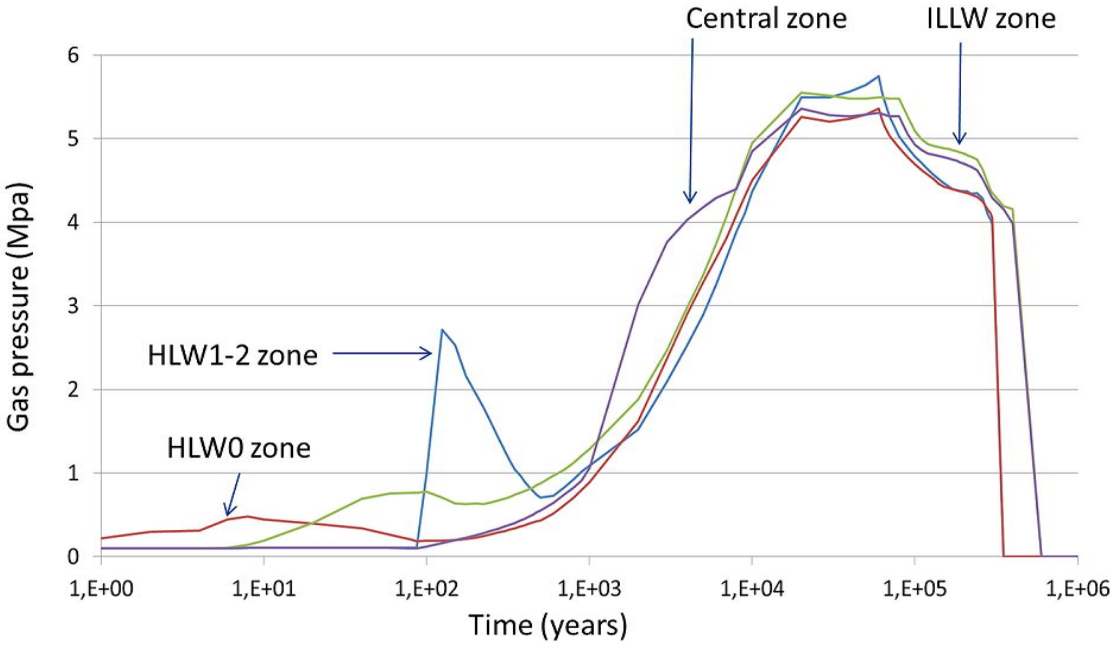

Figure 40: Evolution with time of the maximum gas pressure inside the Cigeo repository for the reference case

4.4 *Specific evaluations linked to ^{14}C migration*

4.4.1 Sensitivity analysis performed

As all IL-LL waste packages in the Cigeo project are emplaced in concrete "super-containers", themselves emplaced in concrete lined disposal cells, the chemical conditions around the waste are largely alkaline. Moreover, ^{14}C is mainly present in stainless steel, which implies a very low corrosion rate in alkaline conditions. As some uncertainties exist on the corrosion rate, a sensitivity analysis is proposed by considering a minimum (0,5 nm/y) and a maximum value (10 nm/y) (labelled respectively "Low_CorrR" and "High_CorrR").

Other sensitivities are carried out in order to take into the following uncertainties:

- thickness of the activated metallic pieces containing ^{14}C: minimum value 1 mm, maximum value 10 mm (this value has an impact on the duration of the ^{14}C source term), labelled respectively "Low_Th" and "High_Th";
- ^{14}C inventory: minimum value is the reference value (around 14,000 moles), maximum value is ten times the reference value (labelled respectively "Low_Inv" and "High_Inv");
- ^{14}C chemical form: each assessment assumes that the chemical for ^{14}C is either CH_4 or CO_2. For both chemical forms, the following parameters are assumed:

  ✓ Half life: 5,700 years

  ✓ Molecular diffusion in gas phase: $1{,}3\times10^{-4}$ m^2/s

  ✓ Molecular diffusion in liquid phase: $4{,}9\times10^{-11}$ m^2/s

  ✓ These forms differ from their molar mass (18 g/mol for CH_4 and 46 g/mol for CO_2) and their Henry's constant ($3{,}3\times10^{9}$ Pa for CH_4 / $2{,}0\times10^{8}$ Pa for CO_2)

  For CO_2 an evaluation considering a non-zero Kd (0.001 m^3/kg) in concrete elements was carried out (a zero Kd is assumed for CH_4).

For sake of simplicity, the corrosion rate of stainless steel is assumed to be independent from the hydrogen source term which results mainly from carbon steel corrosion. However, a sensitivity analysis on the hydrogen source term was performed taking into account a high corrosion rate and a low corrosion rate. The difference between these two corrosion rate regarding gaseous ^{14}C migration is that the former implies a more "rapid" development of the gas phase from the disposal tunnels toward the wells and ramps and a higher gas content in the seals (enhancing the migration of gaseous ^{14}C) at maximum gas pressure.

The following ranges of parameters drive the ^{14}C source terms:

- Low or high inventory of ^{14}C,
- 14C release labile or congruent to the corrosion rate (low or high corrosion rate),
- Low or high thickness of the activated metallic parts,

Based on these parameters, it is possible to define four cases (as shown on Figure 41) which give a good representation of ^{14}C source term.

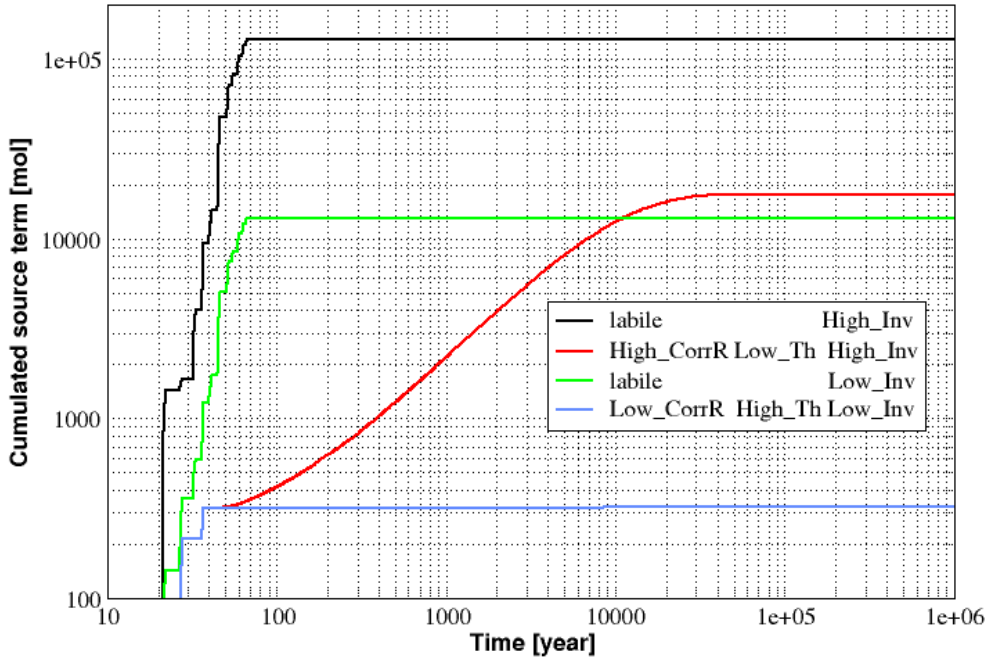

Figure 41: Cumulated molar source term of ^{14}C (form CH_4 or CO_2) used in the sensitivity analysis (includes radioactive decay)

A total of 17 sensitivity evaluations have been performed. The results are described below.

4.4.2 Results

Results focus on molar fluxes (instantaneous or cumulated over time) of gaseous ^{14}C reaching the upper aquifer via the access. The distance between the ramps intersection with the upper aquifer is significantly greater than the distance between the shafts intersection with the upper aquifer. As a consequence, the fluxes in the shafts are one order of magnitude higher than in the ramps (this is also true for hydrogen, see chapter 4.3). Furthermore, as the two represented shafts are close together, the results are similar for both of them and the same stands for the ramps, so only results for one of each are presented.

Instantaneous and cumulated fluxes of ^{14}C over time out of the host rock along the two shafts and along the two access ramps are presented from Figure 43 to Figure 46.

The main part of ^{14}C fluxes are advective fluxes in the bulk gas phase, which is generated by hydrogen. The times of occurrence of the maximum fluxes are thus strongly dependent on the corrosion rate related to the hydrogen generation (see also next chapter on "Discussions"):

- For higher hydrogen corrosion rates:
  - ✓ out of the shafts: between 4,000 and 6,000 years
  - ✓ out of the access ramps: between 4,000 and 7,000 years
- For lower hydrogen corrosion rates:
  - ✓ out of the shafts: between 13,000 and 21,000 years
  - ✓ out of the access ramps: between 16,000 and 27,000 years

Other parameters are of less importance with regards to the time occurrence of the maximum fluxes, showing that the bulk gas phase is not impacted by ^{14}C generation source term. But, on the contrary, maximum ^{14}C flux is significantly affected by the bulk gas phase (generated by H_2); in the cases tested, the difference is around one order of magnitude.

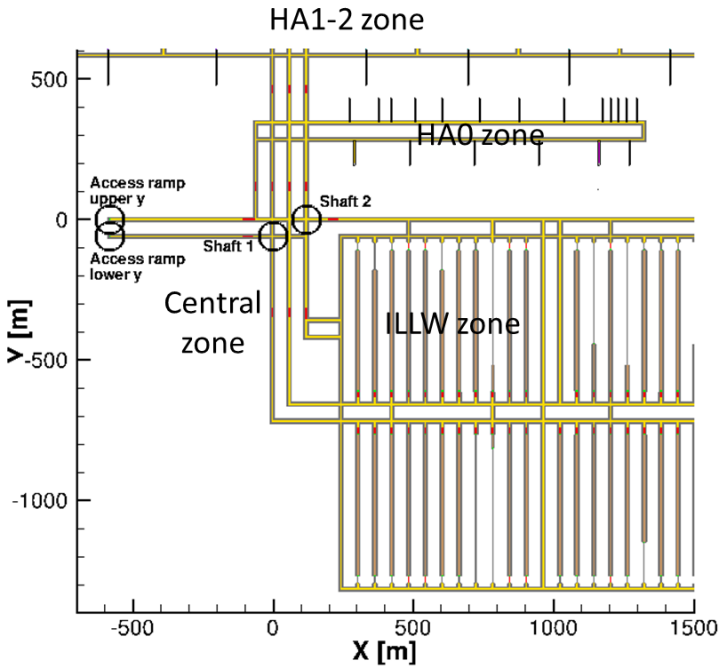

Figure 42: Positions of shafts and ramps in the modeled mesh

As expected, the higher instantaneous molar fluxes (for both ramps and shafts) correspond to a labile source term and a higher value of ^{14}C inventory ["labile High_Inv" curves on the figures]. On the contrary, the lower instantaneous molar fluxes correspond to the low corrosion rates for ^{14}C and the reference value of the ^{14}C inventory ["Low_Corr High_Th Low_Inv" curves on the figures].

The difference in behavior between $^{14}CO_2$ and $^{14}CH_4$ comes mainly from the Henry's coefficient (significantly higher dissolution possibility for CO_2 than for CH_4) and from the molar mass. This second term influences the mass fraction of the ^{14}C gas in the total gas phase and thus impacts also dissolution and diffusion processes. The difference in behavior is therefore complex to assess, but on the overall, everything else being the same, the behavior in terms of molar fluxes at the access is in the same order of magnitude for both chemical forms.

Based on the assumptions retained, everything else being the same, the total amount of ^{14}C reaching the upper aquifer is linear with the inventory. When ^{14}C is released congruently with the corrosion of the metallic pieces, the corrosion rate and the thickness of the metallic pieces drive the duration of the ^{14}C source term. In relation with the relatively short half-life of ^{14}C compared to the travel time, the total number of moles reaching the upper aquifer is all the more higher as the duration of the source term is low.

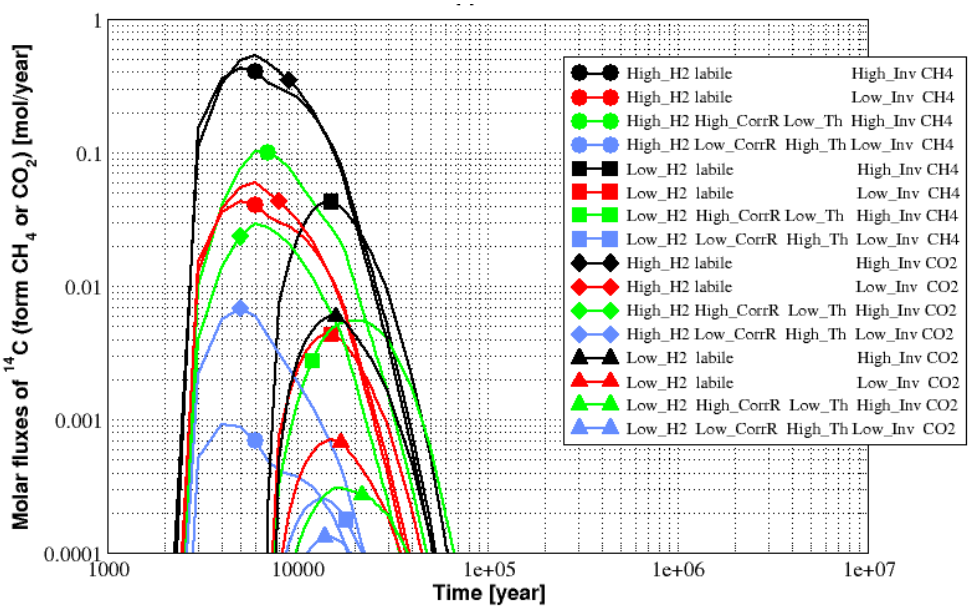

Figure 43: Instantaneous molar flux of ^{14}C at the upper limit of the Callovo-Oxfordian for shaft 1

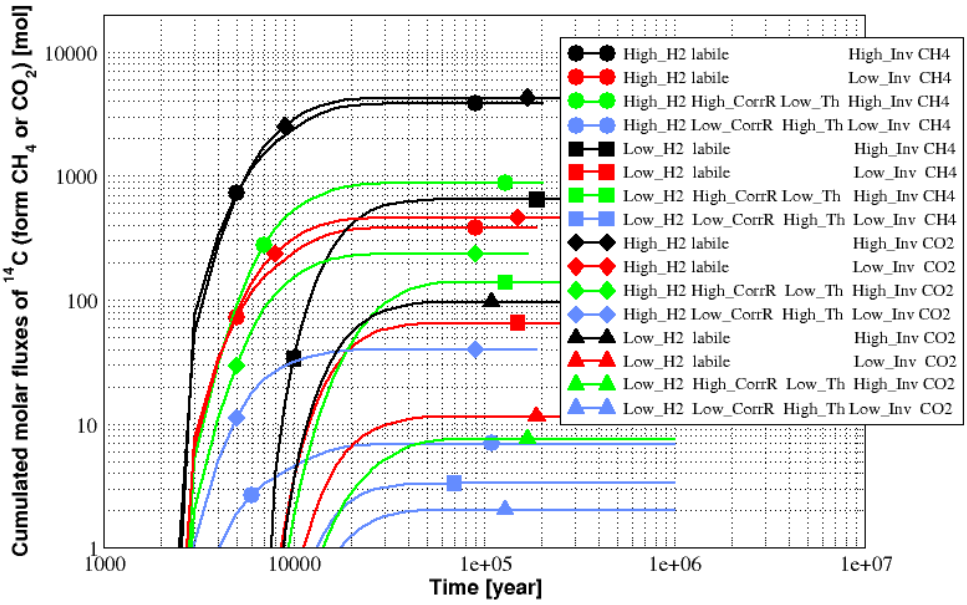

Figure 44: Cumulated molar flux of ^{14}C at the upper limit of the Callovo-Oxfordian for shaft 1

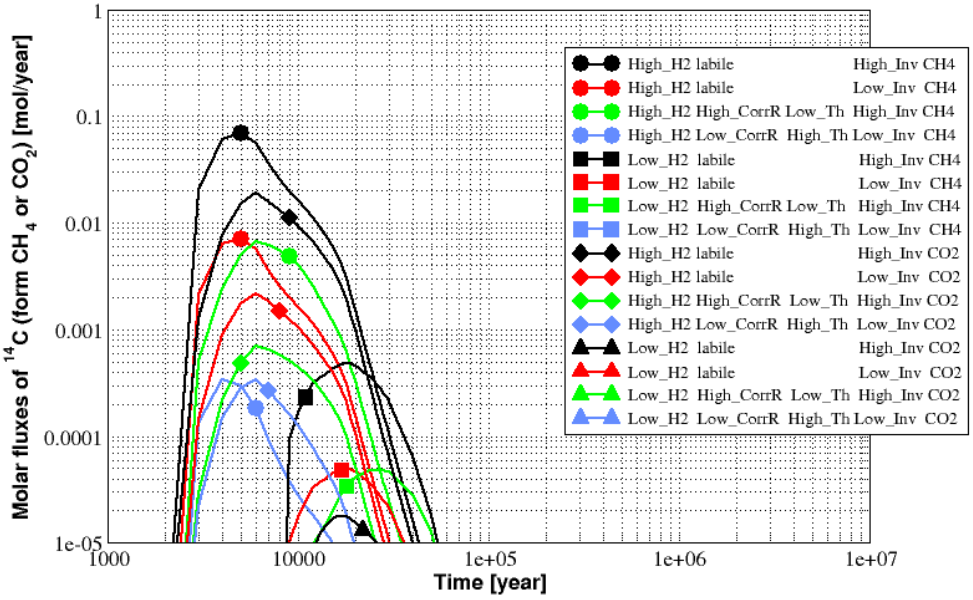

Figure 45: Instantaneous molar flux of ^{14}C at the upper limit of the Callovo-Oxfordian for Ramp "Lower y"

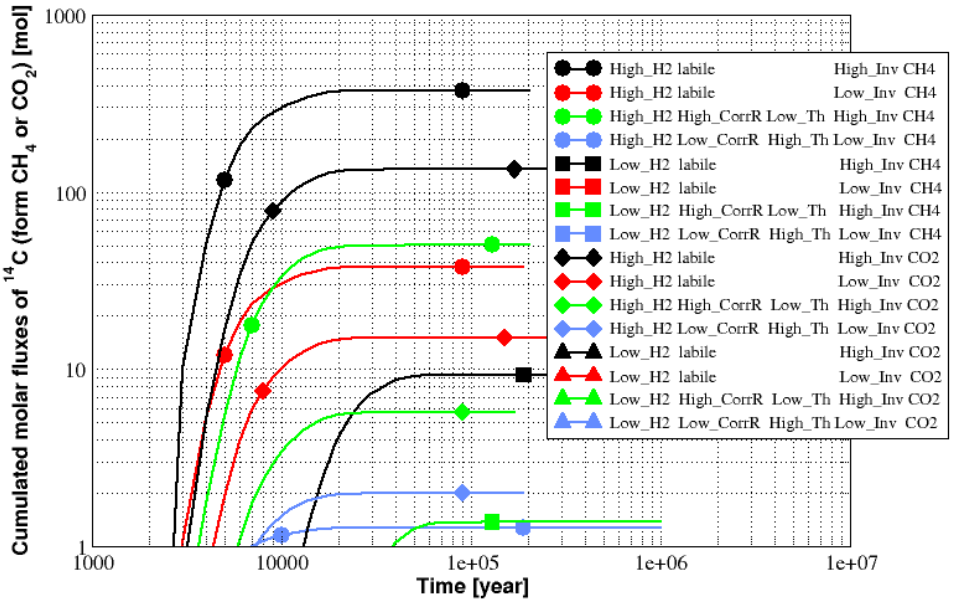

Figure 46: Cumulated molar flux of ^{14}C at the upper limit of the Callovo-Oxfordian for Ramp "Lower y"

An additional sensitivity case was performed to assess the influence of adsorption of CO_2 on concrete materials by using a reversible instantaneous linear sorption (Kd approach). This

case considers a high corrosion rate (with regard to H_2 generation), a labile source term for CO_2 and a high ^{14}C inventory together with a Kd in concrete materials equal to 0,001 m^3/Kg (Figure 47).

Sorption has a significant impact on fluxes of CO_2 over time out of the host rock along the two shafts and the two access ramps. Even with such a small value of Kd, implying a retardation factor around ten, cumulated fluxes out of the shafts are two orders of magnitude lower and fluxes out of the access ramps are five orders of magnitude lower. This effect is mainly due to a greater dissolution of CO_2 along the path toward the access as, due to the Kd in concrete, the concentration in concrete water is much lower than in the reference case (without any Kd).

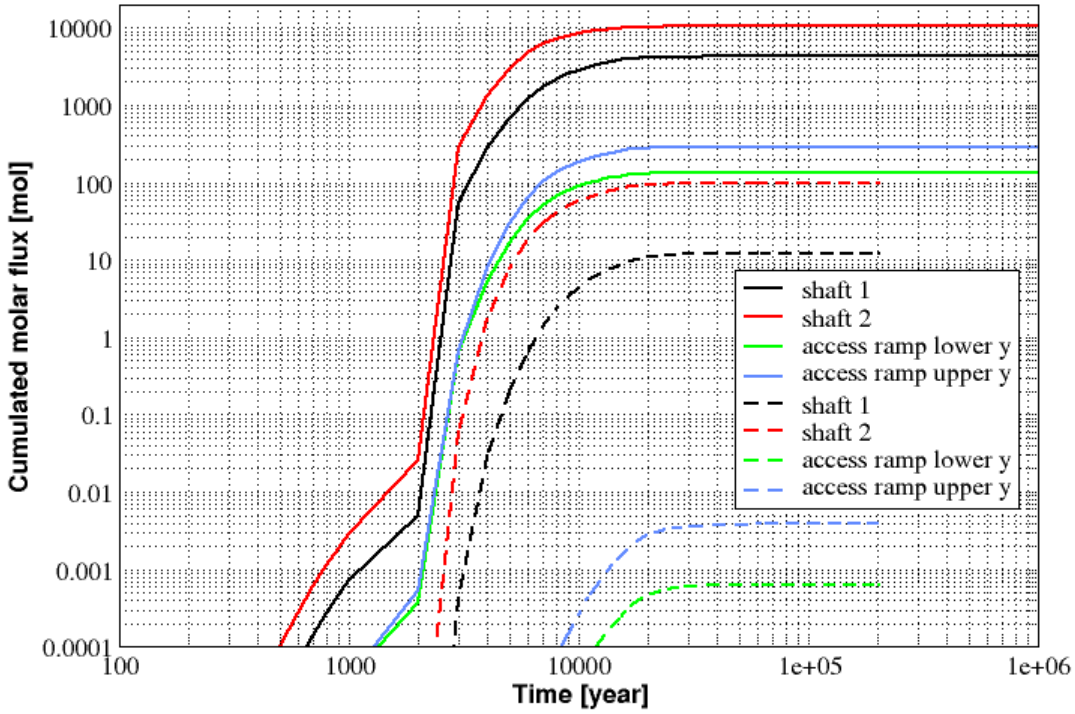

Figure 47: Impact on cumulated moral fluxes of CO_2 at the upper limit of the Callovo-Oxfordian layer of the use of a Kd in the concrete

4.5 *Discussion*

Several assumptions used for these evaluations could be seen as not phenomenologically representative. Some of them, linked to hydraulic processes, are discussed here after

4.5.1 Uncoupled gas source terms

For these simulations, part of hydrogen source terms and ^{14}C source terms are congruent to corrosion of metallic components present in the repository. Regarding hydrogen, more than half of the generated total volume/mass comes from anoxic corrosion and the generated flux is thus directly proportional to the corrosion rate. The same assumption has been used for ^{14}C: the source term is proportional to the corrosion rate of the metallic pieces which contain ^{14}C.

The corrosion rate of a metal depends on:

- The type of metal: in repository conditions, hydrogen flux comes mainly from carbon steel corrosion because its corrosion rate in such conditions is higher than the corrosion rate of stainless steel. On the contrary, most of the ^{14}C source term comes from the corrosion of stainless steel pieces.
- The chemical conditions (Eh, pH) and the surrounding materials: the corrosion rate may vary significantly depending on the type of material in contact with the metal. For instance, carbon steel corrosion rate is higher in contact with clay than in contact with cementitious material due (for example and among other reasons) to the pH value of the water in equilibrium with these porous matrixes.

Consequently, the corrosion rates which drive hydrogen production and ^{14}C production may be very significantly different: (an average corrosion rate for hydrogen production is around several µm/year whereas it is around several nm/years, i.e. thousand times smaller, for ^{14}C production. Moreover, uncertainty on both values is of an order of magnitude, without any correlation between these values, meaning that using different and uncoupled production rates for hydrogen and ^{14}C is phenomenologically representative of actual knowledge.

4.5.2 Water saturation of the repository seals

The bulk gas phase is generated by the production and migration of hydrogen over the whole repository. In the simulations, the main process for hydrogen migration under gaseous form is convection under two-phase flow assumptions. The main brakes on migration are the different seals places on different locations in the repository drifts. Under two phase flow assumption, this brake is related to water saturation: higher the water saturation, higher the drag.

Near the hydrogen generation source, HL waste or IL-LL waste disposal zones, the water saturation of the seals can be quite significant, depending on time and space, but the seals access, most of the gas has been dissolved during the migration from disposal zones and gas pressure is lower and water saturation is higher.

Gas saturation over time at the upper limit of the Callovo-Oxfordian along the two shafts and along the two access ramps is shown in Figure 48.

The distance between access ramps and IL-LL waste zone is greater than the distance between shafts and IL-LL waste zone. Gas saturation is therefore more important in shafts than in access ramps.

But for both types of access, gas saturation is very close to zero, i.e. water saturation is very close to one, and even if the validity of the two-phase flow assumption should still be valid some data show that in clayey rock some mechanical effects could appear at high water saturation.

Assuming mechanical coupling, from water saturation state, gas could drive its way inside the matrix by slightly moving the solid grains instead of moving water creating what is called “dilatant pathways”; This phenomenon is not taken into account in the two-phase flow formulation where gas drives its way into a porous media only by forcing water to move to take its place; there is no modification of the porosity structure of the medium.

The efficiency of “Dilatant pathway” for gas migration is supposed to be much higher than for simple two-phase flow, and taking this type of process in the assessment could increase significantly the ^{14}C flux and total volume passing to the upper aquifer.

However, this process is not well characterized in the Callovo-Oxfordian argillites, and no order of magnitude of its efficiency is available. In this context, using two-phase flow formulation is still the best way to estimate gas flow at the repository level and to fix the orders of magnitudes of the processes.

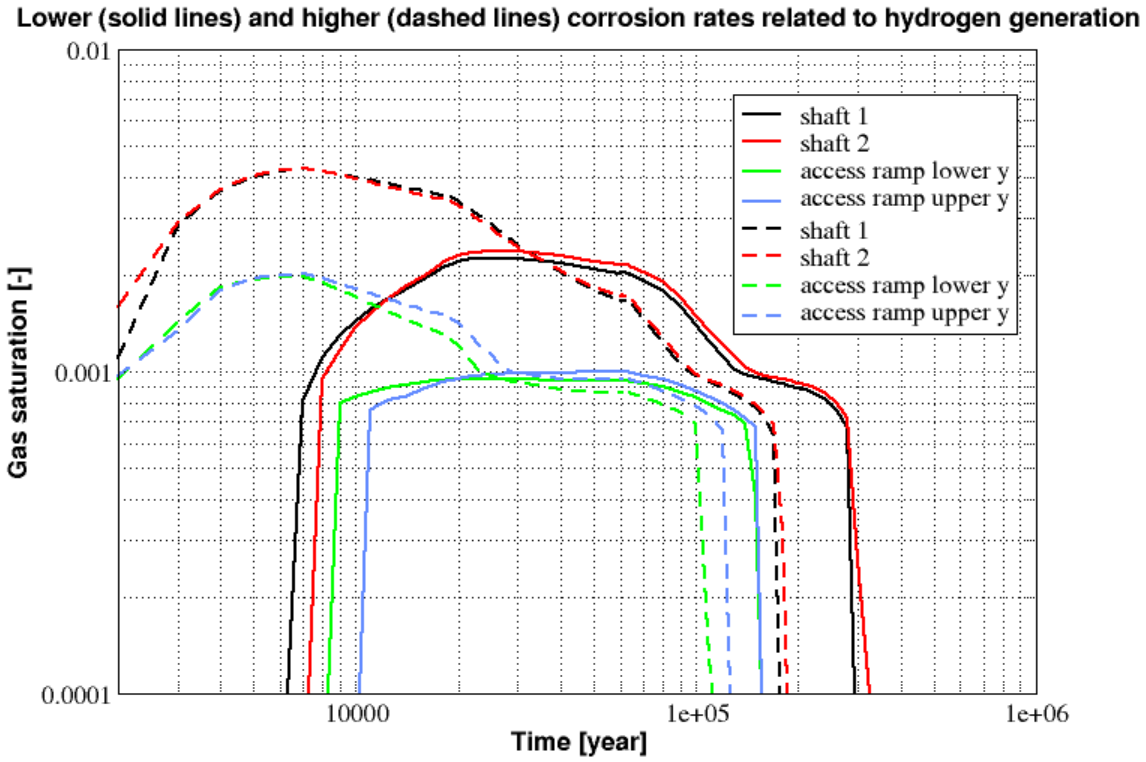

Figure 48: Gas saturation in the seals at the upper limit of the Callovo-Oxfordian

4.6 *Synthesis*

This work has shown that assessing ^{14}C migration at the repository level is feasible under generalized two-phase flow assumptions, taking into account this space scale (footprint of several tens of square kilometers, several tens of kilometers of drifts, several thousands of deposition tunnels) and this temporal scale (several hundreds of thousands of years).

Sensitivity analysis has been carried out on several key parameters like ^{14}C inventory, corrosion rate of the metallic waste containing ^{14}C, chemical form of ^{14}C (CO_2 and CH_4), hydrogen generated bulk gas phase and sorption for CO_2 in concrete.

Due to a quite small volume generated (14,000 moles for Cigeo), ^{14}C is not able by itself to generate a bulk gas phase at repository scale. This bulk gas phase has to be generated by another gas, which for Cigeo is the hydrogen produced mainly by corrosion of the metallic components and by water/organic radiolysis for certain types of waste.

The ^{14}C flux from the access toward the upper aquifer reaches a peak below 1 mol/year around 5,000 years after closure. The total mass reaching this aquifer is around 1,000 moles at the most, compared to the initial ^{14}C inventory close to 14,000 moles. It mainly goes through the nearest access compared to the position of the production zone (IL-LL waste zone for Cigeo). This illustrates the potential beneficial influence of the repository architecture with regard to ^{14}C migration under gaseous form. More precisely, and even if each repository is unique, one can expect that:

- The maximum flux of ^{14}C, somehow linked to the bulk gas phase generated inside the repository by anoxic corrosion and radiolysis, can be reduced by limiting as much as possible these processes for example by limiting the amount of steel left in the repository;
- A significant reduction of total mass of ^{14}C under gaseous form reaching the accesses compared to the initial inventory can be achieved by conceptual design allowing a minimum distance between production zones and the accesses to increase the efficiency of dissolution and diffusion under dissolved form processes.

References

ALLARD, B., TORSTENFELT, B., & ANDERSSON, K. 1981. SORPTION STUDIES OF $H^{14}CO_3^-$ ON SOME GEOLOGIC MEDIA AND CONCRETE. IN SCIENTIFIC BASIS FOR NUCLEAR WASTE MANAGEMENT. VOLUME 3.

ANDRA. 2005. DOSSIER 2005 ARGILE: SYNTHESIS - EVALUATION OF THE FEASIBILITY OF A GEOLOGICAL REPOSITORY IN AN ARGILLACEOUS FORMATION. http://www.andra.fr/download/andra-international-en/document/editions/288va.pdf

ANDRA. 2014. GL TRANSFERT – RAPPORT DE SYNTHESE 2007-2014. ANDRA REPORT NO. CGRPASTR140013.

BAYLISS, S., EWART, F. T., HOWSE, R. M., SMITH-BRIGGS, J. L., THOMASON, H. P., & WILLMOTT, H. A. 1987. THE SOLUBILITY AND SORPTION OF LEAD-210 AND CARBON-14 IN A NEAR-FIELD ENVIRONMENT. MRS ONLINE PROCEEDINGS LIBRARY ARCHIVE, 112.

FISLER, D. K., & CYGAN, R. T. 1999. DIFFUSION OF CA AND MG IN CALCITE. AMERICAN MINERALOGIST, 84(9), 1392-1399.

MATSUMOTO, J., BANBA, T., & MURAOKA, S. 1994. ADSORPTION OF CARBON-14 ON MORTAR. MRS ONLINE PROCEEDINGS LIBRARY ARCHIVE, 353.

POINTEAU, I., COREAU, N., & REILLER, P. E. 2003. ETUDE EXPERIMENTALE ET MODELISATION DE LA RETENTION DE $^{14}C0_3^{-2}$ PAR LES MATERIAUX CONSTITUANT LE BETON DANS LE CADRE DES ETUDES DE FAISABILITE D'UN STOCKAGE DE DECHETS GRAPHITES. ANDRA REPORT NO. FRPASDG03452A.

POINTEAU, I., COREAU, N., & REILLER, P. E. 2008. UPTAKE OF ANIONIC RADIONUCLIDES ONTO DEGRADED CEMENT PASTES AND COMPETING EFFECT OF ORGANIC LIGANDS. RADIOCHIMICA ACTA, 96(6), 367-374.

RASAMIMANANA, S., LEFEVRE, G., & DAGNELIE, R. V. H. 2017. ADSORPTION OF POLAR ORGANIC MOLECULES ON SEDIMENTS: CASE-STUDY ON CALLOVIAN-OXFORDIAN CLAYSTONE. CHEMOSPHERE, 181, 296-303.

TERTRE, E., BEAUCAIRE, C., JUERY, A., & LY, J. 2010. METHODOLOGY TO OBTAIN EXCHANGE PROPERTIES OF THE CALCITE SURFACE—APPLICATION TO MAJOR AND TRACE ELEMENTS: CA (II), AND ZN (II). JOURNAL OF COLLOID AND INTERFACE SCIENCE, 347(1), 120-126.

VINSOT, A., APPELO, C. A. J., LUNDY, M., WECHNER, S., CAILTEAU-FISCHBACH, C., DE DONATO, P., ... & DE CANNIERE, P. 2017. NATURAL GAS EXTRACTION AND ARTIFICIAL GAS INJECTION EXPERIMENTS IN OPALINUS CLAY, MONT TERRI ROCK LABORATORY (SWITZERLAND). SWISS JOURNAL OF GEOSCIENCES, 110(1), 375-390.

WIELAND, E., JAKOB, A., TITS, J., LOTHENBACH, B., & KUNZ, D. 2016. SORPTION AND DIFFUSION STUDIES WITH LOW MOLECULAR WEIGHT ORGANIC COMPOUNDS IN CEMENTITIOUS SYSTEMS. APPLIED GEOCHEMISTRY, 67, 101-117.

APPENDIX 1 – Material properties used for two-phase flow modelling

		External HLW cell void	Backfill of tunnels	Bentonite (seal)	Concrete (seal and concrete liner)	Inner EDZ (EDZ connect)	Outer EDZ (EDZ discrete)
		1	2	3	4	5	6
Parameter		JEU_E	BFILL	BENS_	CONC_	EDZ_I	EDZ_O
Density	kg/m³	2750,00	2710,00	2615,38	2750,00	2710,00	2710,00
Porosity		0,35	0,35	0,35	0,3	0,18	0,18
Permeability x/y/z	m²	9,59E-17	9,59E-17	9,59E-19	9,59E-18	9,59E-17	9,59E-19
Heat conductivity	W/m °C	2,3	1,3	1,5	2,3	1,7	1,7
specific heat	J/kg°C	341,08	739,35	694,59	469,43	720,64	720,64
pore compressibility	1/Pa	1,45E-10	1,02E-09	2,48E-09	2,43E-10	6,96E-10	6,96E-10
pore expansivity	1/°C	2,00E-05	2,00E-05	2,00E-05	2,00E-05	2,00E-05	2,00E-05
Relative permeability model	Mod vG	11	11	11	11	14	14
	Slr	0,01	0,01	0,4	0,01	0,01	0,01
Capillarity model	Mod vG	17	17	17	17	17	17
	n	1,3	1,6	1,6	1,5	1,5	1,5
	Pr	9,81E+05	5,89E+05	1,77E+07	1,96E+06	1,96E+06	7,85E+06
Mill-Quirk alpha in gas phase		0	0	0	0	0	0
Mill-Quirk alpha in liquid phase		2	1,6	1,6	2	1,6	1,6
Mill-Quirk beta in gas phase		5	1,8	1,8	5	1,8	1,8
Mill-Quirk beta in liquid phase		4,2	4,6	4,6	4,2	4,6	4,6

		Callovo Oxfordian	EDZSB (merged concrete liner and EDZ around drifts)	HLW0-waste	HLW1-waste	HLW2-waste	ILLW-waste
		7	8	9	10	11	12
Parameter		COX__	EDZSB	WAHA0	WAHA1	WAHA2	WAMA_
Density	kg/m³	2710,00	2712,21	3546,91	3652,73	3652,73	3020,81
Porosity		0,18	0,19	0,54	0,54	0,54	0,21
Permeability x	m²	3,84E-21	2,69E-17	9,59E-17	9,59E-17	9,59E-17	9,59E-17
Permeability y / z	m²	3,84E-21	1,73E-18	9,59E-17	9,59E-17	9,59E-17	9,59E-17
Heat conductivity	W/m °C	1,7	1,7	54	54	54	2,3
specific heat	J/kg°C	720,64	707,73	1595,78	2039,71	2039,71	628,58
pore compressibility	1/Pa	6,96E-10	6,55E-10	7,07E-11	7,53E-11	7,53E-11	4,79E-11
pore expansivity	1/°C	2,00E-05	2,00E-05	2,00E-05	2,00E-05	2,00E-05	2,00E-05
Relative permeability model	Mod vG	14	14	14	14	14	14
	Slr	0,01	0,01				0,01
Capillarity model	Mod vG	17	17	17	17	17	17
	n	1,6	1,5	1,5	1,5	1,5	1,5
	Pr	1,47E+07	1,96E+06				1,96E+06
Mill-Quirk alpha in gas phase		0	0	0	0	0	0
Mill-Quirk alpha in liquid phase		1,6	1,6	0	0	0	0
Mill-Quirk beta in gas phase		1,8	1,8	0	0	0	0
Mill-Quirk beta in liquid phase		4,6	4,6	1	1	1	1

CArbon-14 Source Term

CAST

Integration of CAST results to safety assessment: Contribution from Nagra to D6.3

Jens Mibus, Paul Smith, Thomas Kämpfer

Date of issue of this report: 05/06/2018

The project has received funding form the European Union's European Atomic Energy Community's (Euratom) Seventh Framework Programme FP7/2207-2013 under grant agreement no. 604779, the CAST project.		
Dissemination Level		
PU	Public	**PU**
RE	Restricted to the partners of the CAST project	
CO	Confidential, only for specific distribution list defined on this document	

Executive Summary

Nagra integrated the CAST results in a sensitivity study on dose computations that is based on the modelling approaches used in its former safety assessments for a HLW and L/ILW repository. On the one hand, the sensitivity analysis focus was on release processes and retardation by sorption. On the other hand, consequences regarding the way of analysing release paths along a groundwater and gas pathway have been analysed. The main conclusions are as follows:

Formerly made, partially conservative, assumptions regarding release fractions and rates as well as sorption coefficients could be confirmed and are likely to enter future safety assessments in the Swiss program, possibly in slightly refined or more precise ways.

The improved system understanding developed within CAST will help Nagra to improve its scenario development and the definition of assessment cases regarding ^{14}C release, in particular with respect to the groundwater and gas pathways.

List of Contents

1 Nagra Contribution to Modelling 14C in disposal systems

1.1 *Introduction*

In Switzerland, the Nuclear Energy Law requires that all types of radioactive waste be disposed of in deep geological repositories. The Swiss Radioactive Waste Management Programme (Nagra, 2008) foresees two types of deep geological repositories: A high-level waste repository (HLW repository) for spent fuel (SF), vitrified high-level waste (HLW) and long-lived intermediate-level waste (ILW), and a repository for low- and intermediate-level waste (L/ILW repository). In this concept, ILW are foreseen to be emplaced in separate tunnels within the HLW repository. In a later update [Nagra, 2016], the emplacement of the ILW in the L/ILW repository is considered as an option. This was, however, not considered specifically in this study.

The Swiss disposal system is based on a multi-barrier system. In the HLW repository it comprises the waste matrix (i.e. the glass matrix for vitrified waste or the spent fuel pellets), the cladding, the canister, the tunnel backfill, the seals and finally the host rock including confining units. In the L/ILW repository (including the ILW emplaced in the HLW repository) the barrier system consists of the waste embedded in the cement matrix in steel drums, the cement backfill, the gas permeable seals (implemented as Engineered Gas Transfer System, EGTS) and finally the host rock including confining units.

The last comprehensive safety analysis has been performed by [Nagra, 2014a,b] in the frame of the site selection procedure determined in the Sectoral Plan for Deep Geological Repositories Stage 2 (Sachplan Geologische Tiefenlager, Etappe 2), herein referred to as SGT-E2. The last safety case of Nagra for an HLW repository dates back to Project Opalinus Clay [Nagra, 2002a,b], where the feasibility of such a repository in Switzerland has been demonstrated.

In the present contribution, we perform a sensitivity analysis on dose calculations for ^{14}C that integrates the results and knowledge gain of the CAST project. The numerical

modelling is based upon the approach used in SGT-E2 for the transport path of soluble ^{14}C in the liquid phase and on the approach used in Project Opalinus Clay for the transport in the gas phase. The sensitivity analysis results are discussed and in the context of previous assessments and consequences for future safety cases in the Swiss disposal program deduced.

1.2 *Model description*

1.2.1 General modelling approach

Dose rates due to ^{14}C release from a L/ILW repository and from the SF emplacement rooms of an HLW repository have been evaluated by numerical modelling. Nagra's general modelling approach for the groundwater pathway is described in [Nagra, 2014b]. The approach to modelling the gas pathway is based on that developed in Project Opalinus Clay [Nagra, 2002b] and refined in [Nagra, 2004].

For both repository types, most of the nuclide inventory, including ^{14}C, is assumed to be embedded mainly in one or more homogeneous matrices. In the case of SF, two types of waste matrix are distinguished: (i) the spent fuel matrix, and (ii) the Zircaloy cladding and other structural elements. An instant release fraction (IRF) is, however, also considered.

Both repositories are considered to lie at the centre of a 100-metre thick Opalinus Clay host rock unit. The host rock has a low permeability, but, in modelling the groundwater pathway, advective as well as diffusive transport is considered, with retardation due to sorption.

Biosphere modelling is used to interpret radionuclide releases from the repository system in terms of effective dose rates.

1.2.2 L/ILW repository

1.2.2.1 ^{14}C inventory, speciation and release mechanisms

The total inventory of ^{14}C in the L/ILW repository is 1.38×10^{13} Bq. On the one hand, about 5 % of this inventory is estimated to be inorganic (carbonate). Consistent with the findings of CAST on retention processes, the inorganic ^{14}C inventory is assumed not to be safety relevant, since it is largely immobilised by precipitation in the cementitious near field. This immobilisation is conceptualised and parametrised in the present safety assessment but not discussed further. On the other hand, organic ^{14}C originates from activated metal parts and potentially from mixed wastes. ^{14}C from mixed wastes makes up about 26% of the total ^{14}C inventory and is conservatively assumed to be released instantaneously as organic ^{14}C of unknown speciation after an assumed containment time of 100 years. Organic carbon from activated metals makes up about 74% of the total organic ^{14}C inventory. The reference assumption (IRF = lower bound (LB)) is that it is released congruently with metal corrosion starting at 100 years. Corrosion rates for metals are given in Table 1.

Table 1: Corrosion rates of metal assumed in the L/ILW repository

Metal	**pH**	**Corrosion rate (µm/a)**		
		Lower bound (LB)	Reference (REF)	Upper bound (UB)
Stainless steel	≥ 10.5	0.0002	0.001	0.01
	<10.5	0.01	0.1	1 (10)*
Carbon steel	≥ 10.5	0.001	0.02	0.03
	<10.5	0.1	2	5 (10)*
Pb	-	0	0	1
Al	-	1	10	100
Zn	-	10	100	1000
Cu	-	0	0	0.08

* In the presence of graphite

The findings reported in CAST [Swanton et al., 2015] that the corrosion rates of stainless steel and carbon steel in alkaline, anoxic conditions have an upper limit of a nm/a and a few tens of nm/a, respectively, are broadly consistent with the ranges selected here. For comparisons, the results obtained using the same assumption as in SGT-E2, namely congruent release with a fraction release rate of 10^{-4} per year, are also shown in Section 1.3.

An alternative bounding assumption case (IRF = UB) is that a part of the ^{14}C in activated metals (5% of the inventory in steel and 20% of the inventory in other metals) is released instantaneously in organic form.

1.2.2.2 Migration pathways

The modelling study for the L/ILW repository considers release via both a groundwater pathway and a gas pathway.

To evaluate migration via the groundwater pathway, it is assumed that all organic ^{14}C released from the waste is dissolved in porewater and migrates through the engineered barriers and host rock by advection and diffusion. For the sensitivity study, linear equilibrium sorption on cementitious backfill and on the host rock is considered as a retardation mechanism. A range of sorption coefficients (K_d values) is considered for both media: 0, 10^{-5}, 10^{-4} and 10^{-3} m^3/kg (compiled from [Wieland et al., 2016 and Chen, 2017]). A zero K_d for the cementitious backfill has been used so far in the Nagra safety assessments and is considered here as a bounding assumption, given that a finding of CAST is that organic ^{14}C has low but non-zero K_d.

To evaluate migration via the gas pathway, it is assumed that all organic ^{14}C is released from the waste as volatile species that mix with repository-generated non-radioactive gases and then migrate through the engineered and natural repository barriers in gaseous form. Non-radioactive gases are generated primarily by the degradation of organic compounds and by the corrosion of metals at rates given in Table 1. The corresponding rates of gas production are given in [Poller et al., 2016]. Comprehensive, isothermal two-phase flow modelling studies reported in [Diomidis et al., 2016] show how gas accumulates in the waste

emplacement rooms and, as pressure increases, migrates (i) across the EDZ and into the host rock and (ii) along the repository underground structures and their EDZs and into the access ramp. The same modelling studies indicate that gas pressure and gas transport do not adversely perturb the safety-relevant properties of the repository media. The backfilling and sealing of the underground structures, collectively termed the Engineered Gas Transport System (EGTS), are designed such that they provide the dominant gas pathway, with migration to the ramp depending on the saturation state of the system but beginning the latest as the gas pressure exceeds hydrostatic. The flow of gas along this pathway is adopted from [Diomidis et al., 2016] and eventually considered when calculating the ^{14}C dose rate.

1.2.2.3 Biosphere and evaluation of dose

For the groundwater pathway, the biosphere model described in Chapter 4 of [Nagra, 2014b] is applied, and used to calculate steady-state biosphere dose conversion factors (BDCFs), which provide a convenient way to convert geosphere release rates into dose rates. Dose rates are calculated for a typical adult member of the population group that would receive the highest (additional) dose rates as a result of the presence of the repository. A simplified biosphere model is used for the gas pathway whereby, upon reaching the Malm aquifer, which is situated above the Opalinus Clay host rock, volatile ^{14}C is assumed to dissolve completely and to be transferred instantaneously to a near-surface aquifer used as a source of drinking water (see Section 4.4 of [Nagra, 2002b] for details).

1.2.3 HLW repository

1.2.3.1 ^{14}C inventory, speciation and release mechanisms

The total inventory of ^{14}C in the SF matrix and cladding in the HLW repository are 1.16×10^{14} Bq and 9.73×10^{13} Bq, respectively. The modelling study, however, focuses on releases from the cladding, since the SF matrix was not subject of CAST. The inventory in the cladding is conservatively assumed to be released in organic form, consistent with the recommendations of CAST. Release occurs congruently as the cladding corrodes at either an upper bound rate of 10 nm/a or a reference rate of 1 nm/a. Both rates are based on results presented in [Poller et al., 2016]. The range is the same as that proposed from CAST studies,

although these are for alkaline anoxic conditions, whereas the pH in the Nagra SF near field is expected to be near-neutral. The IRF is assumed to be either 1 % or 20 %, with the latter being the reference rate assumed in SGT-E2. This is the same as the range recommended by CAST.

1.2.3.2 Migration pathways

Only the groundwater pathway is considered for the evaluation of ^{14}C dose rates from an HLW repository. A range of sorption coefficients (K_d values) is considered for both the bentonite buffer and the host rock: 0, 10^{-5}, 10^{-4} and 10^{-3} m^3/kg. The gas path transport has not been considered, as both gas production and ^{14}C release are lower than in the L/ILW repository and no new insight is expected.

1.2.3.3 Biosphere and evaluation of dose

The same approach to biosphere modelling and the evaluation of dose is used as in the case of the groundwater pathway for the L/ILW repository.

1.3 *Results and discussions*

1.3.1 L/ILW Repository

1.3.1.1 Source terms

As noted in Section 1.2.2.1, ^{14}C from mixed wastes is assumed to be released in organic form of unknown speciation. A conservative assumption is made that organic ^{14}C from this source, in contrast to ^{14}C from activated metals, is assumed not to sorb on any of the components of a repository barrier system. The release of organic ^{14}C from mixed wastes to the biosphere is thus insensitive to variations in sorption coefficients. Given the focus of the present sensitivity analysis, the focus is thus on ^{14}C release from activated metals and contribution to the ^{14}C source term from mixed wastes is disregarded in the majority of the calculation cases reported below. One case is, however, calculated in which the impact of mixed wastes on overall ^{14}C release is evaluated.

Fig. 1 shows the ^{14}C source terms (release rates) from activated metals assuming no IRF (IRF = LB) for the L/ILW waste group containing most of the organic ^{14}C inventory. The figure shows the impact of corrosion rate, using data from Table 1. The maximum of the release rate is observed at the end of the assumed period of complete containment (100 years). Thereafter, the release rate decreases with time due to decay of ^{14}C and due to decrease of the corroding surface area with time.

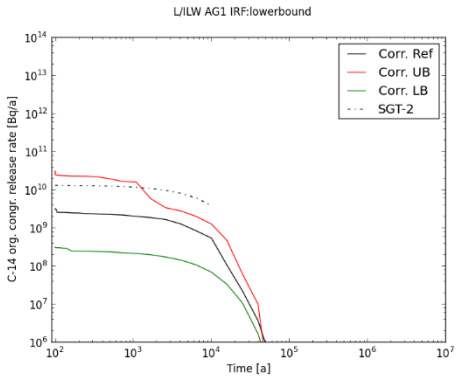

Fig. 1: L/ILW source terms of ^{14}C org. from activated metals for IRF = LB

1.3.1.2 Dose rates due to release via the groundwater pathway

Fig. 2 shows the dose rate histories due to release from activated metals assuming migration via the groundwater pathway (again with IRF = LB; i.e. no IRF).

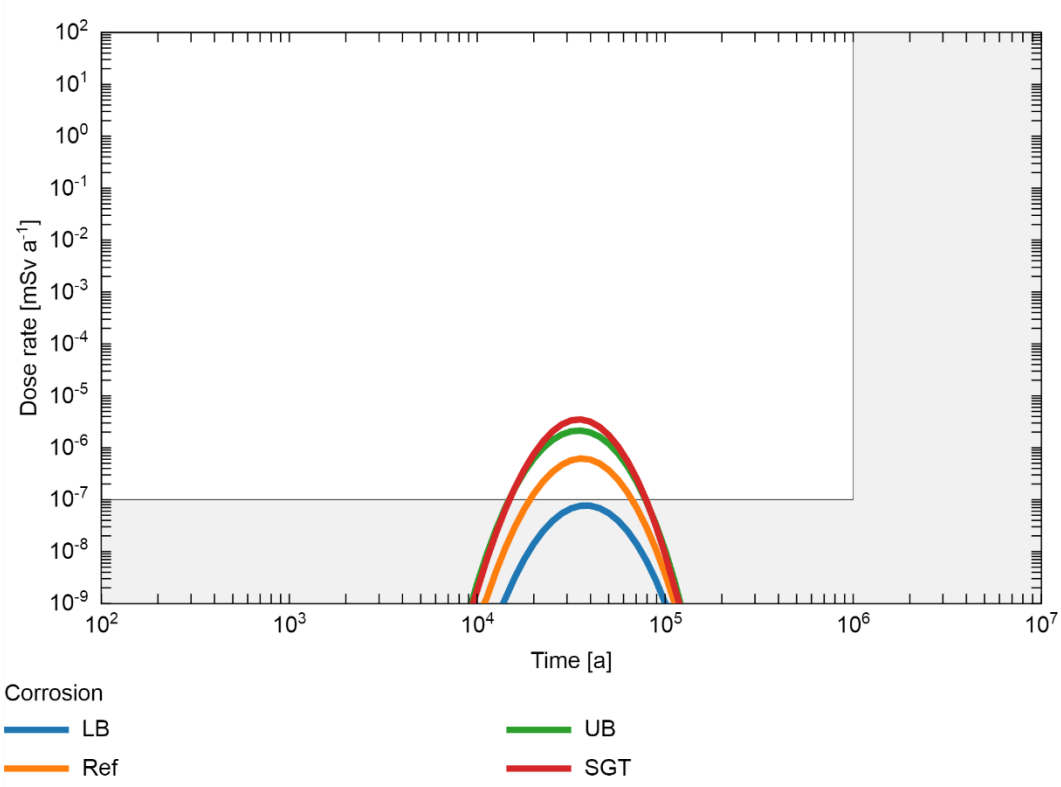

Fig. 2: ^{14}C dose rate as function of time due to entirely congruent release from activated metals for different release cases

In the reference case the maximum dose rate of 6.2×10^{-7} mSv/a is reached after 10,000 years. The maximum dose rate corresponding to the upper and lower bounding values of corrosion rates are 2.1×10^{-6} and 7.6×10^{-8} mSv/a, respectively, and are substantially below the Swiss regulatory guideline of 0.1 mSv/a.

The peak dose rates in these cases, and in additional cases in which a part of the ^{14}C in activated metals is released instantaneously in organic form (IRF = UB), are plotted in Fig. 3.

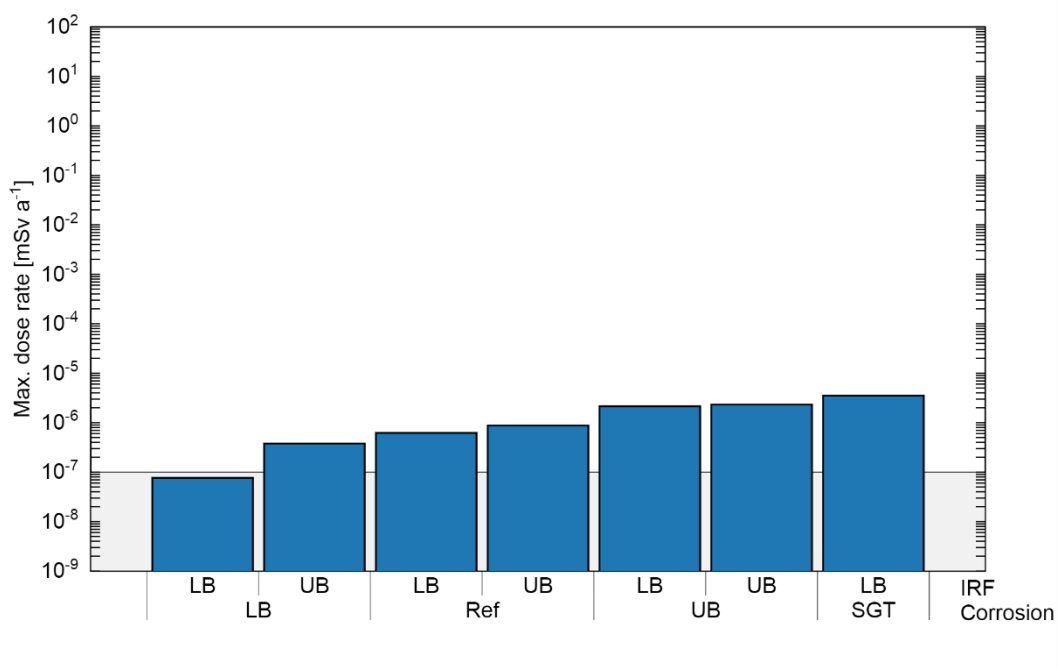

Fig. 3: Maximum dose rate of ^{14}C released from activated metals for different IRFs and different congruent release cases

The maximum dose rates increase when the IRF for activated metals is included. This effect is most pronounced in the case of low corrosion rates, where the difference is a factor of around five, but relatively small for the high corrosion rate cases. The highest peak dose rate remains more than 4 orders of magnitude below the Swiss regulatory guideline.

Fig. 4 shows the corresponding peak dose rates when the source term includes not only activated metals, but also ^{14}C from mixed wastes, which is assumed to be released instantaneously as organic ^{14}C and so increases the IRF. Due to the significant dose contribution from ^{14}C in the organic constituents of the mixed wastes, which is assumed to be released instantaneously and non-sorbing, the impact of the corrosion rate for activated metals on the total dose due to organic ^{14}C is less pronounced in Fig. 4 compared with Fig. 3. Nevertheless, the highest peak dose rate is again more than 4 orders of magnitude below the Swiss regulatory guideline.

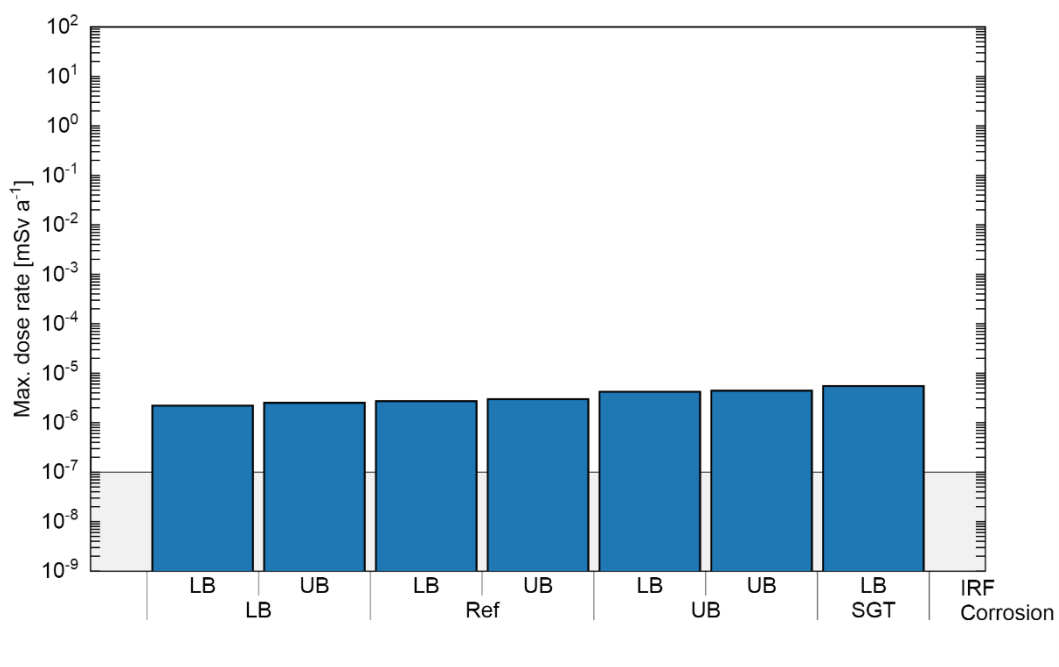

Fig. 4: Maximum total dose rate taking into account all organic ^{14}C for different IRFs and different congruent release cases

Fig. 5 shows the impact on peak dose rate of varying the sorption of organic ^{14}C in the near field and in the geosphere. In addition to the peak dose rates due to geosphere releases, peak dose rates are also shown for the hypothetical situation of direct release of ^{14}C from the near field to the biosphere. Comparing these two sets of peak dose rates, it can be seen that the peak rates are significantly attenuated by radioactive decay during geosphere transport, even if there is no sorption in the geosphere, such that the peak dose rate is at least 4 orders of magnitude below the Swiss regulatory guideline. This attenuation becomes larger still if geosphere sorption is taken into account. By contrast, near-field sorption has little impact on ^{14}C release across the range of sorption coefficients investigated.

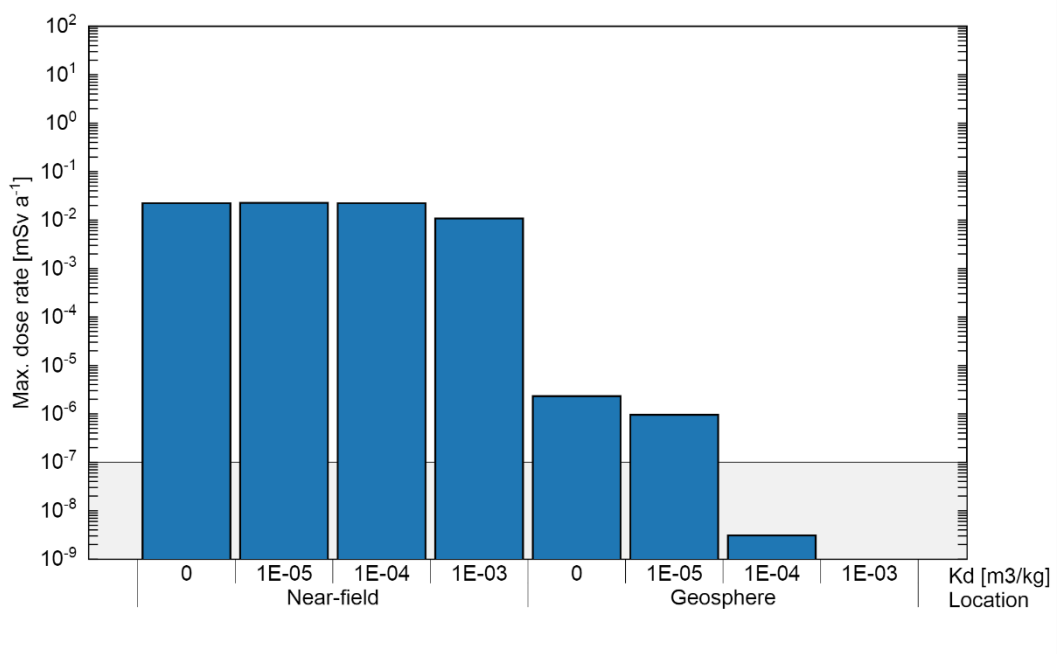

Fig. 5: Case IRF=UB, corrosion=UB: Maximum dose rate from the near-field and the geosphere for different sorption values

1.3.1.3 Dose rates due to release via the gas pathway

Fig. 6 shows drinking water dose rate histories due to assuming migration via the gas pathway. The figure shows the impact of corrosion rates, using data from Table 1. The impact of assumptions regarding the IRF is small, as also shown by the figure.

For the highest corrosion rates (and hence the highest production rates of bulk gas), the peak dose rate is a little over 10^{-3} mSv/y. It is reduced by around an order of magnitude if the reference corrosion rates are assumed, and by a further order of magnitude for the lower bound corrosion rates. The most pessimistic case (upper bound corrosion rate combined with upper bound IRF) is still more than an order of magnitude below the Swiss regulator guideline.

It should be noted that the gas transport model and drinking water dose model used in these gas pathway cases are highly simplified and would need to be reviewed and updated with site-specific information once a site is selected.

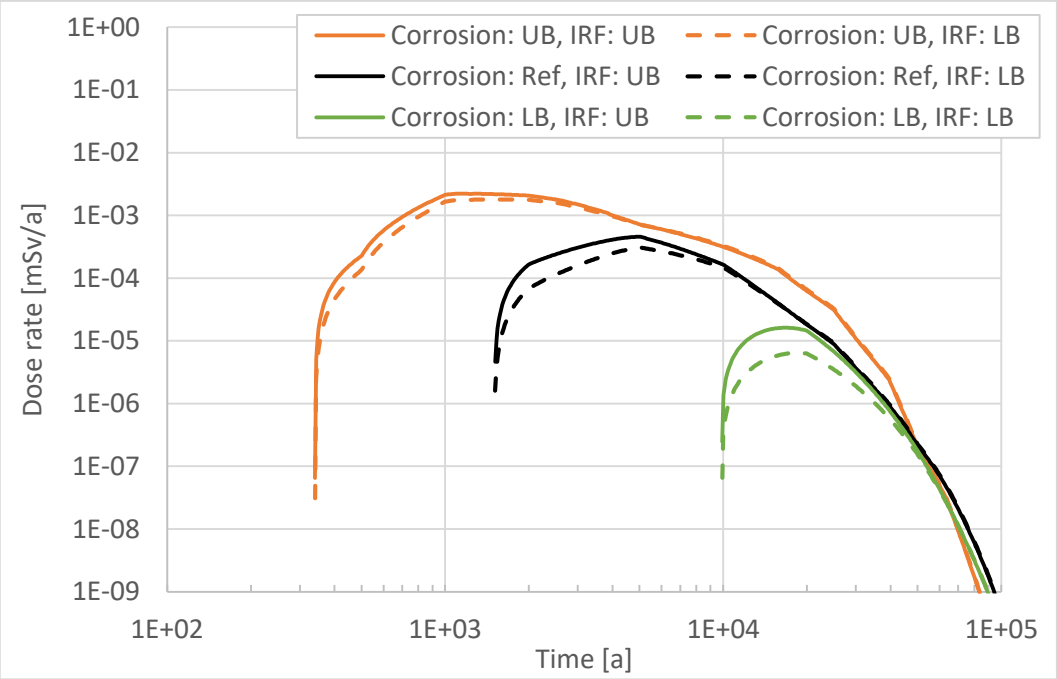

Fig 6: Drinking water dose rate due to release of volatile ^{14}C from activated metals for variants of the bulk gas production rate (and the associated corrosion rate) and the IRF.

1.3.2 HLW repository

Fig.7 shows the impact of the IRFs assumptions and of corrosion rates on the dose contribution of ^{14}C originating from spent fuel cladding in a HLW repository. As in the case of L/ILW, the effect of the IRF is most pronounced for low corrosion rates, but are somewhat masked by cladding release at higher corrosion rates.

The peak dose rate is very small in all cases, 10^{-8} to 10^{-7} mSv/a and hence 6 to 7 orders of magnitude below the Swiss regulatory guideline. It should also be noted that the contribution of ^{14}C from the cladding to the total dose rate due to spent fuel is small compared with that from ^{129}I.

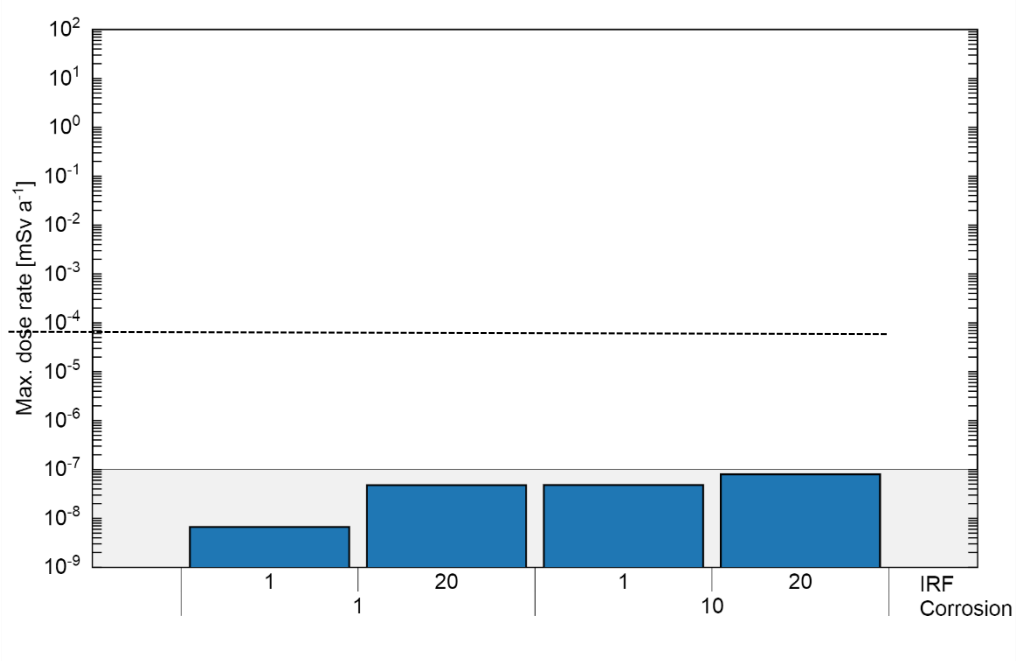

Fig. 7: Maximum dose rate of ^{14}C originating from the SF cladding for different IRFs and corrosion rates. The dashed line at 5.8E-5 mSv/a indicates the maximum total dose dominated by I-129.

Fig. 8 shows the impact on peak dose rate when varying the sorption of organic ^{14}C in the near field and in the geosphere. As in Fig. 5, in addition to the peak dose rates due to geosphere releases, peak dose rates are also shown for the hypothetical situation of direct release of ^{14}C from the near field to the biosphere. Similar to the case of L/ILW, it can be seen that the peak rates are significantly attenuated by radioactive decay during geosphere transport, even if there is no sorption in the geosphere, such that the peak dose rate is at least 6 orders of magnitude below the Swiss regulatory guideline. This attenuation becomes larger still if geosphere sorption is taken into account. Near-field sorption has relatively little impact on ^{14}C release, although some attenuation is observed, especially as the near-field sorption coefficient is increase above around 10^{-4} m^3/kg.

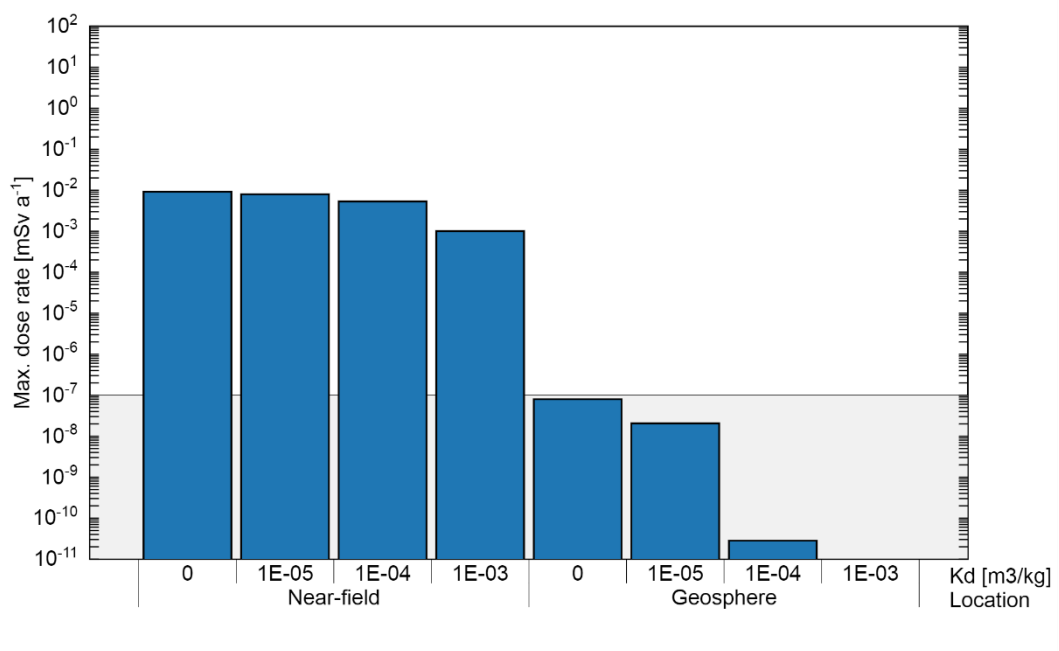

Fig. 8: Maximum dose rate from the near-field and the geosphere for different sorption values for IRF=20% and cladding corrosion rate = 10 nm/a.

1.4 *Integration of the CAST experimental outcomes at the level of the safety case.*

The results from CAST will mainly be used to better corroborate the conceptualisation of ^{14}C release and transport in future safety assessments. In particular, results of CAST and further studies inspired by it will form the basis to re-evaluate the definition of the scenarios to be considered and the parameter bandwidths used in assessment cases.

A particular CAST result is that the release and speciation of ^{14}C in the early stage of the leaching process could be derived from experimental results. Uncertainty still exists in i) the evolution of the speciation in the long term and ii) the further fate (stability and transport) of dissolved low-molecular organic compounds in the cementitious environment.

The main benefit from CAST is an improved system understanding. The uncertainty regarding the transport of ^{14}C either as dissolved or gaseous species could not be reduced as

the experimental findings do not sufficiently support that. However, there are valuable indications that, in contrast to former safety assessments at [Nagra, 2002a], the ^{14}C release to the gas phase deserves more attention. This will be considered when justifying the derivation of scenarios. In a former safety assessment [Nagra, 2002a], the reference scenario considered a dissolved transport of ^{14}C while the transport as gas phase was studied in an alternative scenario. As in CAST assumptions are made for a potential shift in the speciation from dissolved to gaseous organic ^{14}C compounds in the long term, it will be discussed how the transport will be conceptualised and how scenarios will be defined and weighted. E.g., two bounding cases (purely dissolved or gaseous transport) or a combination of both in one assessment case could be envisaged.

The experimental results on release of ^{14}C from activated steels indicate a fast release in the early phase of the experiment. This instantaneously released ^{14}C only amounts to a small fraction of the total ^{14}C inventory of the bulk material. Additionally, in the repository, the resaturation process is much slower and cannot be compared to the experiment. Furthermore, the sensitivity study reported here demonstrates that an IRF with an assumed value of 5% is not sensitive. Hence, an Instant Release Fraction (IRF) of ^{14}C released from steel will likely not be introduced in future safety analyses (i.e., no IRF assumed identical to former assessments).

Former safety assessments assumed an IRF of 20% for the release of ^{14}C from Zircaloy [Nagra, 2002b]. CAST results indicated that this might be a very conservative value and considered an IRF of <10% [Necib et al., 2018]. This lower value should be confirmed in an independent study before Nagra adapts it in future safety assessments.

Despite the new arguments that the importance of the gas pathway for ^{14}C transport increased, Nagra is convinced that the arguments from previous safety assessments that the repository is safe remain valid. However, the results of the quantitative analyses in the present sensitivity study will form the basis to additional, more specific analyses and possibly further optimisation measures. Accordingly, future work aiming at a less conservative treatment of ^{14}C in safety assessments at Nagra will have a particular focus on the ^{14}C transport via the gas pathway and its consequences for safety. This will involve a dedicated experimental study on

the long-term evolution of ^{14}C release as dissolved or gaseous species (continuation of a leaching experiment already running at PSI, see [Wieland et al. 2018]) that will help to better support the conceptual model of ^{14}C release and transport. Another important step will be the continued development of the gas transport model to enable the modelling of a combined consideration of ^{14}C transport together with the bulk gas following the lines of [Poller et al., 2016].

Finally, the activities with respect to interaction of dissolved ^{14}C species with clay rock will not be pursued since remaining uncertainties on the behaviour of these compounds in the near field dominate.

References

CHEN, Y. 2017. *Transport of low molecular weight organic compounds in compacted ilite, kaolinite and Opalinus Clay*. PhD Thesis, University of Bern, Bern, Switzerland.

DIOMIDIS, N., CLOET, V., LEUPIN, O., MARSCHALL, P., POLLER, A. AND STEIN, M. 2016. *Production, consumption and transport of gases in deep geological repositories according to the Swiss disposal concept*. Nagra Technical Report, NTB 16-03, Wettingen, Switzerland.

NAGRA 2002a. *Project Opalinus Clay – Safety Report «Demonstration of Disposal feasibility for spent fuel, vitrified high-level waste and long-lived intermediate level waste (Entsorgungsnachweis)»* Nagra Technical Report, NTB 02-05, Wettingen, Switzerland.

NAGRA 2002b. *Models, codes and data for safety assessment*. Nagra Technical Report, NTB 02-06, Wettingen, Switzerland.

NAGRA 2004. *Effects of post-disposal gas generation in a repository for spent fuel, high-level waste and long-lived intermediate-level waste sited in Opalinus Clay*. Nagra Technical Report, NTB 04-06, Wettingen, Switzerland.

NAGRA 2008. *«Entsorgungsprogramm 2008 der Entsorgungspflichtigen»*. Nagra Technical Report, NTB 08-01, Wettingen, Switzerland.

NAGRA 2014a. *SGT Etappe 2: Vorschlag weiter zu untersuchender geologischer Standortgebiete mit zugehörigen Standortarealen für die Oberflächenanlage «Charakteristische Dosisintervalle und Unterlagen zur Bewertung der Barrierensysteme»* Nagra Technical Report, NTB 14-03, Wettingen, Switzerland.

NAGRA 2014b. *Provisional safety analyses for SGT Stage 2. Models, codes and general modelling approach*. Nagra Technical Report, NTB 14-09, Wettingen, Switzerland.

NAGRA 2016. *«Entsorgungsprogramm 2016 der Entsorgungspflichtigen»*. Nagra Technical Report, NTB 16-01, Wettingen, Switzerland.

NECIB, S., AMBARD, A., BUCUR, C., CAES, S., COCHIN, F., FULGER, M., GRAS, J.M., HERM, M., KASPRZAK, L., LEGAND, S., METZ, V., PERRIN, S., SAKURAGI, T., SUZUKI – MURESAN, S. 2018. *Final report on ^{14}C behaviour in Zr fuel clad wastes under disposal conditions (D3.20).* CAST Project Report. Available from http://www.projectcast.eu.

POLLER, A., MAYER, G., DARCIS, M., AND SMITH, P. 2016. *Modelling of gas generation in deep geological repository after closure*. Nagra Technical Report, NTB 16-04, Wettingen, Switzerland.

SWANTON, S.W., BASTON, G.M.N. AND SMART, N.S., 2015, *Rates of steel corrosion and carbon-14 release from irradiated steels – state of the art review (D2.1).* CAST Project Report. Available from http://www.projectcast.eu.

WIELAND E., JAKOB A., TITS J., LOTHENBACH B., KUNZ D. 2016. *Sorption and diffusion studies with low molecular weight organic compounds in cementitious systems.* Appl. Geochem., Vol. 67, 101-117.

WIELAND, E., CVETKOVIC, B. 2018. *Corrosion of irradiated steel in alkaline conditions: First measurements of the carbon-14 speciation (D2.19).* CAST Project Report. Available from http://www.projectcast.eu.

CArbon-14 Source Term

CAST

Integration of CAST results to safety assessment: Contribution from NRG to D6.3

J. Hart, J.J. Dijkstra, J.C.L. Meeussen

Date of issue of this report: 21/09/2017

Executive Summary

Based on the Dutch OPERA reference concept for the final disposal of radioactive waste in Boom Clay, a conceptual model has been implemented in the computer code ORCHESTRA to assess the influence of system parameters on the C-14 flux, released from Zircaloy contained in a CSD-C canister, through the surrounding concrete and Boom Clay.

A full probabilistic uncertainty/sensitivity analysis (UA/SA) has been applied to assess how the C-14 flux through the disposal system depends on (1) the Instant Release Fraction (IRF) of C-14 from Zircaloy, (2) the long-term congruent release resulting from the corrosion of Zircaloy, (3) the K_d of C-14 in concrete surrounding the Source volume, and (4) the K_d of C-14 in Boom Clay as the host rock. The values of these system parameters have been varied according to the specifications laid down in [CAPOUET, 2016B].

The UA/SA has been performed for two different cases, (1) a "*Reference Case*", assuming a failure time of the CSD-C container 15'000 years after disposal and a deterministic value of the C-14 diffusion coefficient in Boom Clay, and (2) an "*Enhanced C-14 Migration Case*", assuming an immediate failure of the CSD-C container after disposal, and a significantly enhanced value of the C-14 diffusion coefficient in Boom Clay.

For analysing the sensitivities of the four system parameters on the calculated C-14 fluxes at different locations use has been made of scatter plots, the Pearson Correlation Coefficient (*PCC*) and the Rank Correlation Coefficient (*RCC*), and conditional Cobweb plots.

The results of the UA/SA show that in all cases and at all locations in the disposal system in Boom Clay the calculated C-14 fluxes hardly depend on the prescribed values of the IRF and the Zircaloy corrosion rate. On the other hand, the K_d values of concrete and Boom Clay do affect the C-14 fluxes throughout the disposal system. At 1 m into the Boom Clay, the C-14 flux is approximately equally influenced by the K_d values in concrete and Boom Clay. Further away from the repository, the influence of the K_d value in concrete decreases, whereas the K_d value in Boom Clay becomes more apparent. At the outer boundary of the Boom Clay, the K_d value in Boom Clay is the only remaining parameter influencing the C-14 flux.

Assuming expert values of the time of failure of the CSD-C container and the diffusion coefficient of C-14 in Boom Clay leads to calculated migration times of C-14 in the Boom Clay host rock which are sufficiently long for the disposed C-14 inventory to completely decay. In that case C-14 does not reach the outer boundary of the Boom Clay.

Assuming instant failure of the CSD-C containers upon disposal, and a significantly enhanced diffusion rate of C-14 in Boom Clay may lead to a fraction of C-14 reaching the outer boundary of the Boom Clay. For the present set of simulations, the C-14 fraction leaving the outer boundary of the Boom Clay ranges from 0.2% to 16% of the initial C-14 inventory, with an average value of 8%.

An important distinction between the *Reference Case* and the *Enhanced C-14 Migration Case* relates to the C-14 inventory that can be released from the CSD-C containers. A start of release immediately after disposal implies that the total initial C-14 inventory is available, whereas a start of release at 15'000 years (*Reference Case*) implies that more than 85% of the initially disposed inventory of C-14 has decayed.

The consequence of the difference in C-14 inventory that is available for release at t = 0 a and at t = 15'000 a in terms of C-14 flux through the system concrete/Boom Clay is minimal: in both cases, the K_d's in concrete and Boom Clay are the main parameters determining the C-14 flux through the system.

From the present UA/SA analysis it can be concluded that assessing the safety consequences of C-14 disposed in a deep geological repository in Boom Clay would benefit from enhancing the understanding of parameters and processes that determine the diffusion and sorption of C-14 both in concrete and Boom Clay.

For the OPERA disposal concept in Boom Clay the impact of C-14 on the ultimate dose rate in the biosphere, and also on other safety indicators (not reported here) is considered limited if not negligible. This is caused by the long transport time of C-14 from the waste containers through respectively the Boom Clay host rock and the overburden to the biosphere, compared to its half life. Only in case of an early release and a significantly enhanced migration rate,

e.g. in case of excessive gas generation and gas-mediated transport through the Boom Clay and the overburden, a noticeable amount of C-14 may ultimately appear in the biosphere. Even in that case it is anticipated that the contribution of C-14 to the dose rate in the biosphere will be limited compared to that of other radionuclides.

The current analyses have significantly deepened the understanding of processes considered relevant for assessing the impact of C-14 on the safety of a deep geological disposal facility in Boom Clay. The results of CAST are therefore significant for further demonstrating the long-term safety of the OPERA disposal concept.

List of Contents

1 NRG: Modelling C-14 in disposal systems

1.1 *Introduction*

In the Netherlands, extended (intermediate) surface storage of all radioactive waste in buildings has been chosen as the preferred policy. In due time, deep geological disposal in suitable host formations is envisaged for all categories of radioactive waste. During the interim storage period the geological disposal is prepared financially, technically and socially in such a way that it can be implemented when deemed necessary. At some point during the intermediate storage period (until around 2100), a decision is foreseen with the options being (1) to continue the surface storage, (2) to realize the GDF, or (3) to use new techniques or management options that may have become available during the period of interim storage. If it is decided to construct a geological disposal facility, it should become operational after 2130 [VERHOEF, 2014A].

In the Netherlands, safety assessments for the disposal have been performed in the past in the VEOS [Prij, 1989], PROSA [Prij, 1993], and METRO [Grupa, 2000] studies, but these referred to disposal in rock salt. For the disposal in a clay formation, scoping analyses have been performed as part of the Dutch CORA programme on the Dutch TRUCK-II design [Grupa, 2000], and within the EU-FP6 project PAMINA (SCHRÖDER, 2009). These simulations already showed that diffusion is the main driving process for the transport of any released radionuclides through the Boom Clay host rock, and that radionuclides are more or less adsorbed by the clay (retention), causing a significant slowdown of the transport rate of nuclides through the clay.

Safety assessment results from the present Dutch research programme for the disposal in Boom Clay are not yet available. The following section introduces the present Dutch concept for the disposal of radioactive waste in Boom Clay host rock in more detail.

1.1.1 Dutch OPERA disposal concept

COVRA, the Dutch waste management organisation, is considering the safety and feasibility of disposing of all radioactive wastes generated in the Netherlands in a geological repository. For a thorough substantiate of this topic the five-year research programme for the geological disposal of radioactive waste, OPERA[2], was established in 2011. The main objective of the OPERA research programme is to provide tools and data for the development of Safety Cases for Dutch repository concepts for radioactive waste disposals in two host rocks present in the Netherlands, Boom Clay, which is the primary focus of OPERA, and rock salt [VERHOEF, 2011].

The various types of radioactive waste, or "waste families", that have been investigated in the Dutch research programme OPERA are shown in Figure 1 [VERHOEF, 2015; Figure 2-1] . The number of waste packages intended for disposal (in green) and the expected activity for each waste package at disposal in 2130 (in black) are included.

For the OPERA Safety Case on Boom Clay, the 'OPERA reference concept' is the system concept under consideration [VERHOEF, 2014A]. The OPERA reference concept encompasses a disposal facility which is located at a depth of 500 m in the middle of a 100 m thick layer of Boom Clay. With respect to the disposal of heat producing waste, the OPERA reference concept is derived from the current Belgian 'Supercontainer' concept, but with different dimensions (smaller containers, shorter disposal galleries) that reflect the existing national differences in waste characteristics and amounts. Additionally, the OPERA concept addresses the requirement of retrievability of the waste, a major cornerstone of the Dutch policy on radioactive waste disposal.

[2] OPERA: *OnderzoeksProgramma Eindberging Radioactief Afval*; Dutch acronym translating as *Research Programme into the Geological Disposal of Radioactive Waste*

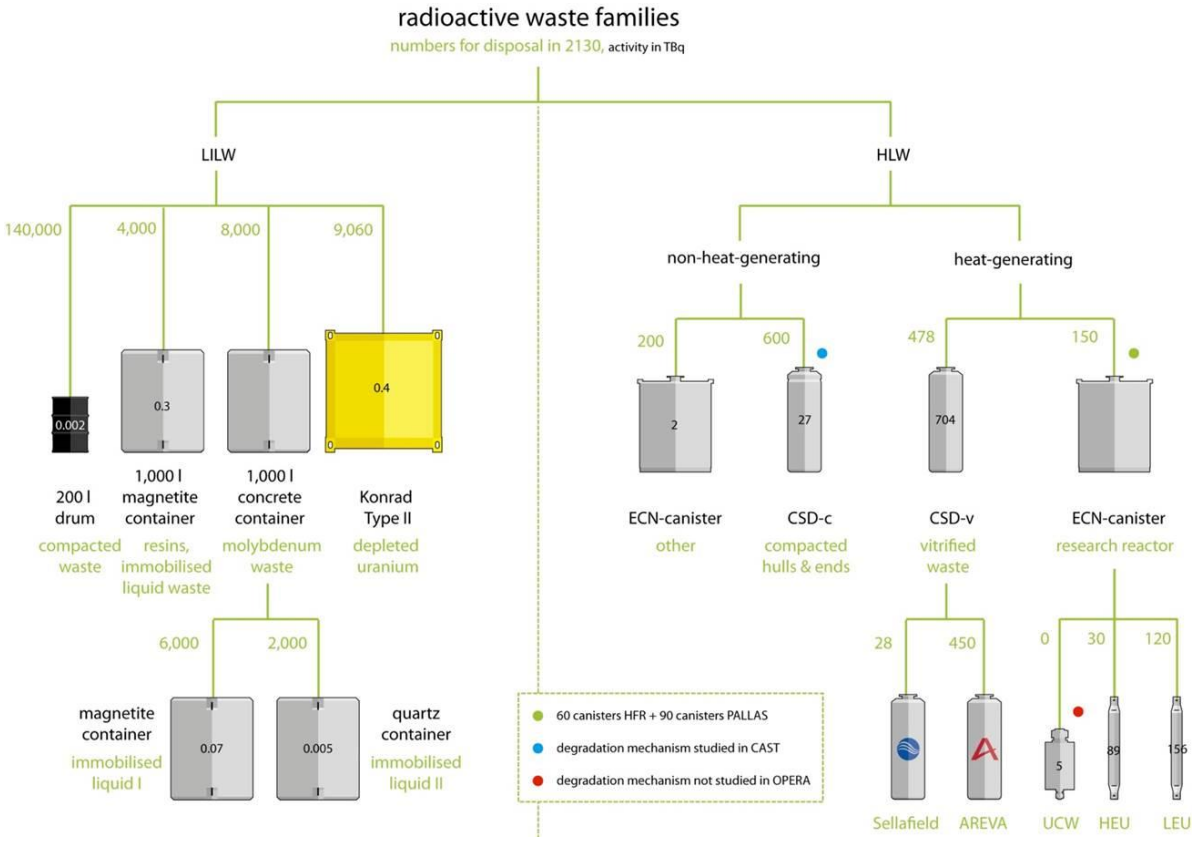

Figure 1: Distinction of waste families investigated in the Dutch research programme OPERA

Figure 2 depicts an outline of the surface and underground facilities of the OPERA disposal concept in Boom Clay [VERHOEF, 2014A; p.11/12]. The underground facilities contain separate disposal sections for the different types of wastes, a pilot facility and a workshop for maintenance work, all connected by the main gallery.

The facility contains four waste disposal sections for (1) vitrified HLW, (2) spent fuel from research reactors, (3) non-heat-generating HLW and (4) ILW/LLW and depleted uranium. Each disposal section is optimised with regard to dimensions and modes of transport of the waste containers through the galleries.

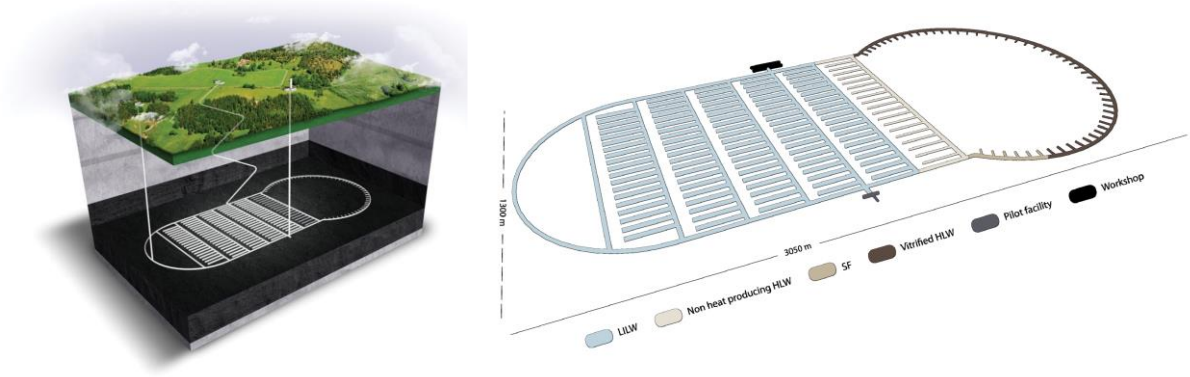

Figure 2: Artist impression of a geological repository for the disposal of radioactive waste in Boom Clay

The secondary galleries are branches of the main gallery and lead to the waste disposal drifts in the various waste sections (Figure 3).

Figure 3: Impression of the HLW waste sections and the OPERA supercontainer

To allow for a uniform storage and disposal, standardised waste packages are used. The LILW is already conditioned with concrete for the long-term interim storage which is assumed to be suitable for direct geological disposal, without further packaging or conditioning. The depleted uranium is disposed of in KONRAD type II containers. HLW containers will be overpacked in supercontainers ((Figure 3; VERHOEF, 2014A; p.15) before their emplacement

in the repository. In OPERA a supercontainer with uniform outer dimensions is used for the heat-generating HLW, spent fuel from research reactors as well as the non-heat-generating HLW (a.o. the CSD-C containers).

1.1.2 Present status of the Dutch safety assessment

The numerical OPERA performance assessment baseline model is implemented as a 1D-reactive transport model within the ORCHESTRA[3] framework. In the current PA model the following compartments are defined (SCHRÖDER, 2017; Ch. 2; see also Figure 4):

1) The *Waste-EBS* compartment, modelling the waste forms as well as the enclosing engineered barrier system;
2) The *Host Rock* (Boom Clay), through which any radionuclides released from the waste forms migrate from the waste sections to the surrounding aquifers by diffusion only. The transport rate of radionuclides in the Boom Clay depends on the distribution of radionuclides over the solid and solution phase (K_d) , and the diffusion coefficient of nuclides in solution (SCHRÖDER, 2017; Ch. 4).
3) The *Overburden* (surrounding rock formations) models the migration of the radionuclides from the Boom Clay to the biosphere both by advective transport and diffusion. The groundwater flow is conceptualized by an effective residence time (SCHRÖDER, 2017; Ch. 5) representing the hydraulic transport models developed in OPERA Task 6.2.1 (VALSTAR, 2016).
4) The *Biosphere*. In the BIOSPHERE compartment, dose rates are calculated on basis of the influx of water into a fixed compartment volume which is then mixed with the amount a radionuclides reaching the respective receptors Well, Rivers/Lakes, and/or Wetlands (SCHRÖDER, 2017; Ch. 6).

[3] see also Section 1.2.1

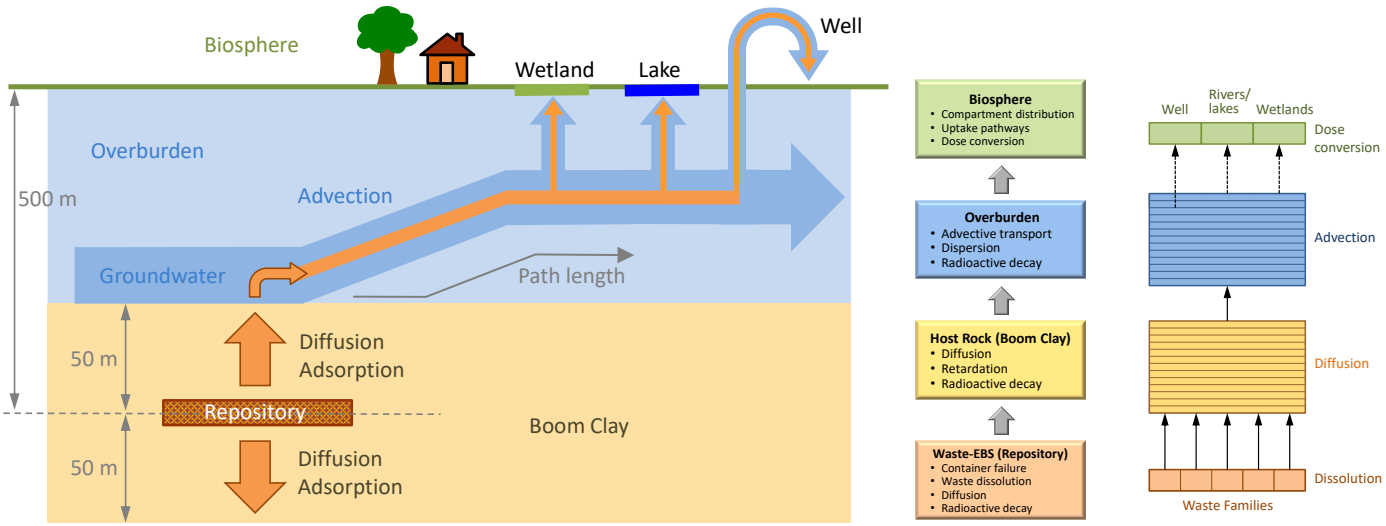

Figure 4: Overview of the conceptualization of the OPERA disposal concept

1.1.3 The Normal Evolution Scenario

The Normal Evolution Scenario (NES) is the most likely future evolution of the disposal system. The NES assumes normally progressing and undisturbed construction, operation, "passive" operation, and closure of the facility. However, natural processes affect the facility's engineered barriers in the long term.

Under in situ conditions in Boom Clay, carbon can exist in three stable forms: HCO_3^-, CH_4 and organic derivatives. The bicarbonates (HCO_3^-) are the dominant species [ONDRAF/NIRAS, 2001]. All C-14 species will dissolve in the ground water, mostly as HCO_3^-. The dissolved C-14 can migrate through the clay rock formation by diffusion only. The time to reach the overlying aquifer[4] by diffusion is on average several tens of thousands of years. Since the half-life of C-14 is 5700 years, this means that a significant fraction of C-14 released from the waste containers will decay in the clay host rock.

[4] Features of the geosphere, including any aquifer systems surrounding the Boom Clay host rock have been studied in Work Package 6 of the OPERA programme

1.1.4 C-14 Inventory

For the present analyses, only the release of C-14 from Zircaloy has been taken into account, as this is one of the main sources of C-14 in the OPERA disposal concept for deep geological disposal in the Netherlands. Zircaloy is utilized in hulls (cladding material) and end-pieces in LWR fuel rods. Hull dimensions are of the order 0.6-0.7 mm in diameter, and 0.65 mm in thickness [NEI, 2009; p.146]. During the reprocessing of LWR spent fuel, the Zircaloy hulls and end-pieces are separated from the fuel itself and compacted in a standard compacted waste container, i.e. a CSD-C Colis Standard de Déchets – Compactés (see also Figure 5). The C-14 waste inventory of the CSD-C containers has been determined as part of the OPERA research program [VERHOEF, 2015].

Figure 5: Zircaloy hulls and end-pieces separated from spent fuel (left) and a standard compacted waste container CSD-C

A comprehensive overview of the current status of knowledge on various aspects related to the C-14 content in Zircaloy and release of C-14 from zirconium alloys waste (hulls), which is of importance for long-term safety analyses of final repositories for long-lived Intermediate level waste, is provided in CAST Deliverable 3.1 [GRAS, 2014].

1.2 *Model description*

1.2.1 Conceptual model

The analyses on the release of C-14 from Zircaloy and the subsequent transport through concrete and Boom Clay have been modeled with the computer code ORCHESTRA, Objects Representing CHEmical Speciation and TRAnsport. ORCHESTRA [MEEUSSEN, 2003].

Figure 6 depicts the ORCHESTRA model for analyzing the release of C-14 from the Zircaloy in the CSD-C containers, and the subsequent transport through the concrete buffer of the OPERA supercontainer, the concrete backfill/lining of the disposal galleries, and the Boom Clay host rock. The aquifer overlying the Boom Clay has not been modeled; instead a zero C-14 concentration at the Boom Clay outer boundary has been imposed.

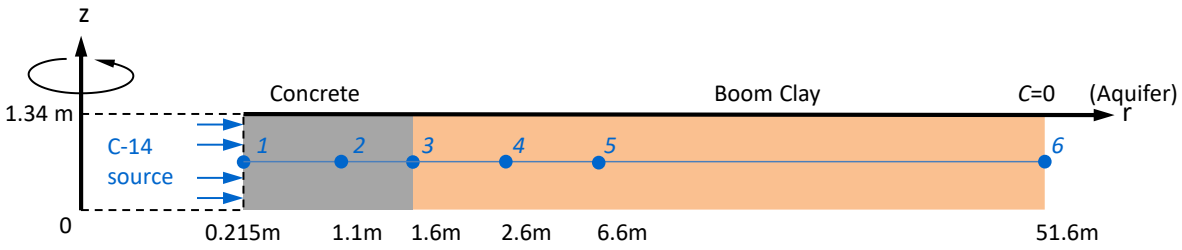

Figure 6: ORCHESTRA PA model for the C-14 release and transport

The model consists of a 360º circumferential radial slice of the repository with a length of 1.34 m, a width of 51.6 m and encompasses the following features:

- The C-14 source, i.e. the CSD-C container, with a length of 1.34 m, and a radius of 0.215 m (0.43 m diameter)
- The concrete supercontainer, ranging from radius r = 0.215 m to r = 1.1 m (0.885 m thickness)
- The concrete lining of the disposal gallery, ranging from radius r = 1.1 m to r = 1.6 m (0.5 m thickness)

- A 50 m thick layer of Boom Clay host rock, ranging from radius r = 1.6 m to r = 51.6 m

The total computational domain encompasses 100 cells in radial direction.

For the uncertainty/sensitivity analysis (UA/SA) 6 "observation points" are formulated in which C-14 fluxes and concentration profiles are calculated:

- r_1 = 0.215 m (radius of the CSD-C container)
- r_2 = 1.1 m (outer radius of the supercontainer)
- r_3 = 1.6 m (outer radius of the concrete liner)
- r_4 = 2.6 m (1 m into Boom Clay)
- r_5 = 6.6 m (5 m into Boom Clay)
- r_6 = 51.6 m (50 m into Boom Clay)

In the cell representing the CSD-C container (C-14 source), the initial C-14 inventory is 13.8 GBq, representing the total average C-14 inventory of a single CSD-C [VERHOEF, 2015; Table A-2]. At the outer boundary at 51.6 m, the C-14 concentration is set to the condition of zero C-14 concentration at all times, which maximizes the concentration gradient and therefore the diffusion rate of C-14 through the system.

The start of the release of C-14 from the CSD-C containers has been varied by assuming (1) an expert value determined based on considerations from the OPERA programme, i.e. at t = 15'000 a[5], and (2) an immediate failure of the CSD-C container after disposal, at t = 0 a.

In the absence of any driving force for water transport through the disposal system, only diffusive transport of C-14 through the modelled concrete and Boom Clay is taken into account. For assessing the influence of the diffusion coefficient of C-14 in Boom Clay two cases have been considered:

[5] At the time of performance of the simulations for CAST there were still discussions about times of failure of the OPERA supercontainer. Still unreported considerations indicate a range between 1'000 and 70'000 years for the NES.

- Case 1: "*Reference Case*", applying an expert value for the C-14 diffusion coefficient in Boom Clay, which is considered representative for the default transport rate by diffusion of bicarbonate, HCO_3^- in Boom Clay. In combination with the imposed expert failure time of the CSD-C container (at t = 15'000 a) this Case 1 represents conditions related to the OPERA normal evolution scenario in relation to the release of C-14 from the waste and its migration through the disposal system, i.e. concrete and Boom Clay.

- Case 2: "*Enhanced C-14 Migration*", a "What-If" case imposing a rapid C-14 diffusion rate in Boom Clay, which is considered representative for the relatively fast diffusion of a hypothetical C-14 containing chemical species through the Boom Clay. In combination with the imposed immediate failure of the CSD-C container (at *t* = 0 a) this Case 2 represents a very conservative approach in relation to the start of release of C-14 from the waste and the migration rate through the disposal system.

Table 1 summarizes key features of the ORCHESTRA model.

Table 1 Key parameters of the ORCHESTRA model for CAST analyses

Model parameter	Value	Reference
C-14 Inventory	$1.38 \cdot 10^{10}$ Bq/CSD-C	Verhoef, 2015; Table A-2
C-14 start of release	t = 15'000 a	"Case 1" - expert value (OPERA)
	t = 0 a	"Case 2" – early release
C-14 half life	5700 a	Kellett, 2009; p.53
Porosity	0.15 (concrete)	Schröder, 2017; Table 3-2
	0.23 (Boom Clay)	Schröder, 2017; Table 4-7
Density	2.6 kg/l (concrete+Boom Clay)	Expert value (OPERA)
C-14 Diffusion coefficient concrete	$2 \cdot 10^{-9}$ m²/s (0.063 m²/a)	Expert value (rapid diffusion)
C-14 Diffusion coefficient Boom Clay	$3.9 \cdot 10^{-11}$ m²/s (0.0012 m²/a)	Reference value; Schröder, 2017; Table 4-7
	$2 \cdot 10^{-9}$ m²/s (0.063 m²/a)	"Case 2" – rapid diffusion

1.2.2 Uncertainty/sensitivity parameters

The ORCHESTRA model described in the previous section was made fit for performing uncertainty/sensitivity analyses (UA/SA) in order to fulfil the following objectives of CAST WP6 [CAPOUET, 2016b; Chapter 1]:

- Implement experimental results of WP2-WP5 in safety assessment
- Transfer experimental specialist knowledge to safety assessment
- Determine most important properties and parameters
- Conduct uncertainty analysis to determine range of model outcomes and to guide future experimental efforts.

Based on the "Guidance for uncertainty analysis" [CAPOUET, 2016B] the following key factors have been assessed using the ORCHESTRA model:

- Corrosion rates
- IRF versus congruent release
- Sorption coefficients (K_d-values)

For each of these factors, ranges of parameters have been defined based on the minutes of the CAST technical meeting held at Wettingen, Switzerland, 8/9 March 2016 [CAPOUET, 2016A]. Table 2 summarizes the ranges of parameters which have been implemented in ORCHESTRA [CAPOUET, 2016B; Ch.2].

Table 2 Ranges of parameters for CAST uncertainty/sensitivity analyses

Model parameter	Value
Zircaloy corrosion rate	1 – 10 nm/a
C-14 Instant Release Fraction (IRF)	1 – 20% of the inventory
K_d values - cementitious materials	10^{-5} – 10^{-3} (10^{-4})* [m^3/kg]
K_d values – argillaceous rock	10^{-5} – 10^{-3} (10^{-4})* [m^3/kg]

* Minimum-maximum (average) values

Taking into account these ranges of the four parameters to be varied in the CAST UA/SA, a total number of 250 sets of randomly distributed values of these parameters mentioned were generated. Each combination of four parameters represents a different "state" of the disposal system. The total number of 250 combinations of the four input parameters provides a sufficiently large set of simulation results allowing for a robust sensitivity/uncertainty analysis.

In determining the 250 sets of parameter values, uniform distributions have been assumed for the Zircaloy corrosion rate and the C-14 instant release fraction, as well as for the ^{10}log values of the K_d's of C-14 in concrete and Boom Clay host rock. Figure 7 shows the distributions of values of the ranges of the four parameters for the CAST UA/SA. It can be seen that taking random samples from the imposed uniform distributions does not result in a completely "flat", uniform frequency distribution of the ranges of parameter values (i.e. the "Bins"). This non-uniformity does not significantly affect the outcomes of the UA/SA.

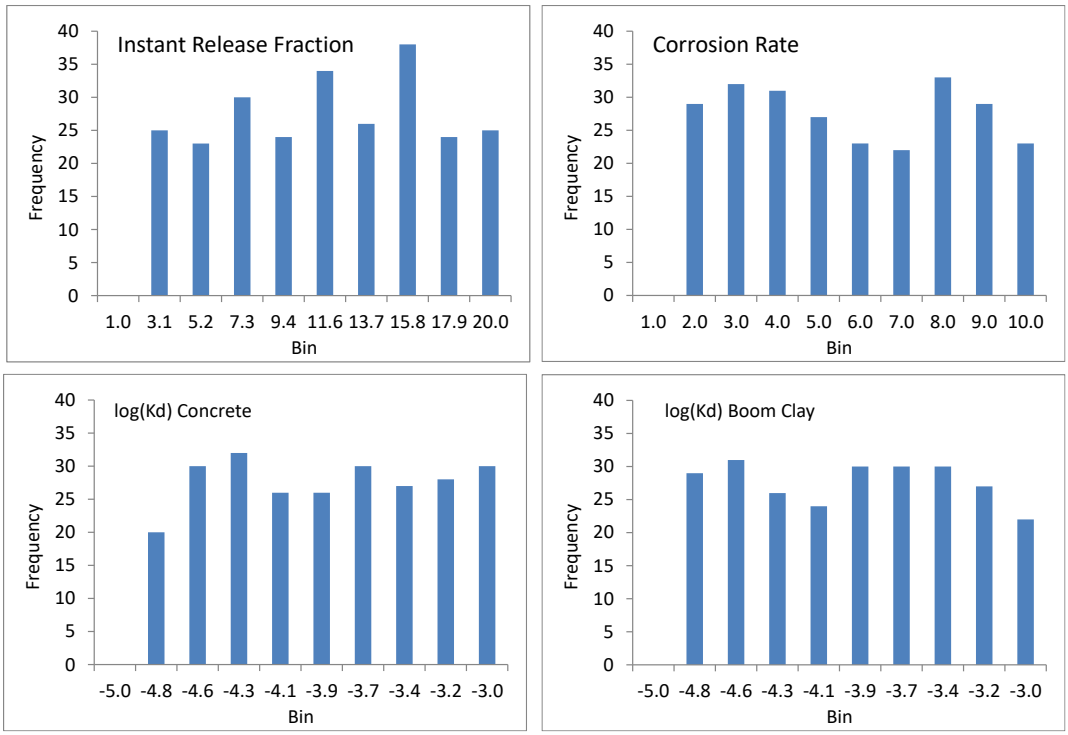

Figure 7: Distribution of sampled values of the ranges of parameters for the CAST UA/SA

1.2.3 Uncertainty/Sensitivity Analysis

For the uncertainty/sensitivity analysis the 250 calculations have been performed with ORCHESTRA with varying values of the four model parameters as indicated in the previous section, and for the two cases (see also Table 1):

- Case 1: "*Reference Case*"; expert values of the start of C-14 release and diffusion coefficient in Boom Clay;
- Case 2: "*Enhanced C-14 Migration Case*"; immediate start of C-14 release and enhanced rate of diffusion in Boom Clay.

The output variables of the simulations are the C-14 concentrations in and C-14 fluxes through the 6 observation points as indicated in Figure 6 as a function of time.

For the uncertainty analysis the results are presented as graphs indicating the calculated output parameter of each individual simulation as well as the average values and 5, 50, and 95 percentiles at each time step.

For the sensitivity analysis, the following methods have been applied for determining the influence of the four input parameters on the calculated output:

The *Pearson correlation coefficient*

The Pearson correlation coefficient (*PCC*) provides a measure of the strength of the linear relationship between any input factor (cf. Table 2) and the output, i.e. the C-14 flux or concentration at the observation points. The values of the *PCC* are between -1 and 1. A positive of *PCC* value means that both in input factor and the calculated output are increasing or decreasing together while a negative value means that when the input factor increases, the output decreases or vice versa. An absolute value of *PCC* close to 1.0 corresponds to a linear relationship between the input factor and the calculated output, while an absolute value close to 0.0 corresponds to the fact that there is no linear relationship.

The Pearson correlation coefficient can be estimated at each time step. This results in graphs showing the development in time of the influence of the input parameters on the respective output parameters.

The *Rank Correlation Coefficient*

Whenever a *nonlinear* but monotonic relationship between x_j (the value of the input parameter) and y (the value of the output parameter) exists, a rank transformation can be used to get a linear relationship. This transformation replaces the actual values of x_j and y by their corresponding ranks: the smallest value of a variable has the rank 1 and the largest one has the rank n. The *Rank Correlation Coefficient* , also referred to as the Spearman correlation coefficient, is computed in a similar way as the Pearson correlation coefficient except that the ranks of each variable are used instead of the actual values.

Cobweb plots

Cobweb plots have been designed to show the dependency of multidimensional samples in a two-dimensional graph [e.g. BOLADO, 2008]. The horizontal axis of a Cobweb plot lists the consecutive input variables x_i for which the dependency of the output variable y under consideration is investigated, and the output variable y itself. The vertical axis represents the values or, alternatively, the ranks of the sampled input variables x_i as well as the calculated output variable y. By connecting the values (ranks) of the sampled input variables x_i and the calculated output variable y with lines for each sampled run of the multiple simulation, the Cobweb plot may reveal the dependency of y on x_i. In the present study, *conditional Cobweb plots* based on the ranks have been used. In this type of plots, only a fraction of the total number of calculation runs are represented.

1.3 *Results and discussions*

This chapter presents a selection of the results calculated for the Case 1 ("Reference Case") and Case 2 ("Enhanced C-14 Migration") analyses. For limiting the amount of information provided, the results are restricted to analyzing the C-14 *fluxes* only.

1.3.1 Case 1 – Reference Case

1.3.1.1 C-14 Fluxes

The figures below show the calculated fluxes of C-14 through the subsequent observation points 1 (leaving the Source compartment, 4 (1 m into the Boom Clay; Figure 9), and 5 (5 m into the Boom Clay; Figure 10). The 250 individual runs are plotted in grey, whereas the thick colored curves represent the averages and indicated percentiles at all time steps.

The C-14 flux at the exit of the Boom Clay host rock (Point 6) is well below 10^{-3} Bq/a for all sampled runs, indicating that C-14 has almost completely decayed within the host rock.

The effect of the IRF versus the long-term congruent release of C-14 from Zircaloy is clearly visible in Figure 8. The steep flux following the C-14 IRF at 15'000 years is followed by a more gradual flux leaving the Source compartment, which is, due to the ongoing decay of C-14, continuously decreasing. About 40'000 years after disposal the C-14 flux leaving the Source compartment has fallen below 1 Bq/year.

From Figure 9 it can be seen that the effect of the IRF has already reduced significantly due to the dispersion of C-14 in the concrete and, subsequently, the Boom Clay. Beyond about 80'000 years (14 half lives) after disposal the C-14 has decayed almost entirely.

Figure 10 shows a significantly more pronounced effect of the dispersion of C-14 within the Boom Clay at 5 m (Point 5) than at 1 m (Point 4; Figure 9). The maximum values of the C-14 flux at this location vary by a factor of 100, mainly due to the variation of K_d-values in the concrete and the Boom Clay.

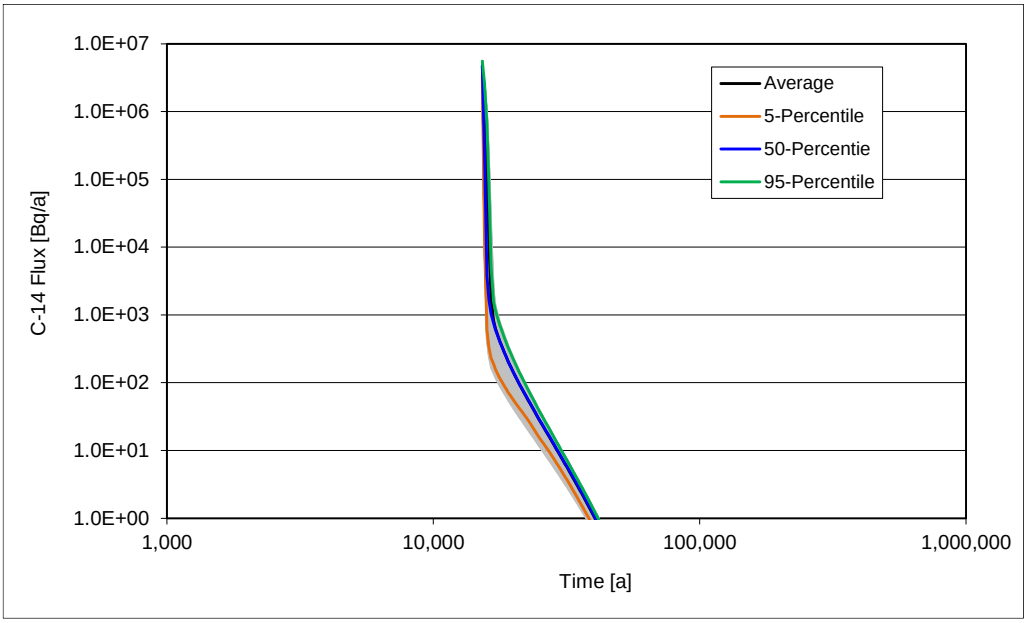

Figure 8: C-14 flux at the exit of the Source compartment – Point 1 (Case 1)

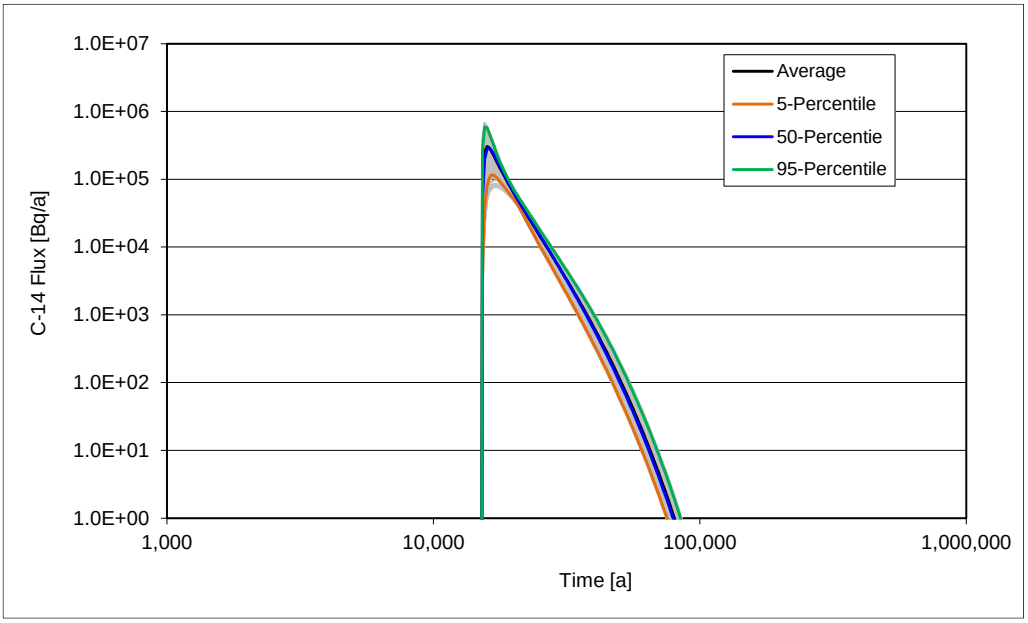

Figure 9: C-14 flux at 1 m into the Boom Clay – Point 4 (Case 1)

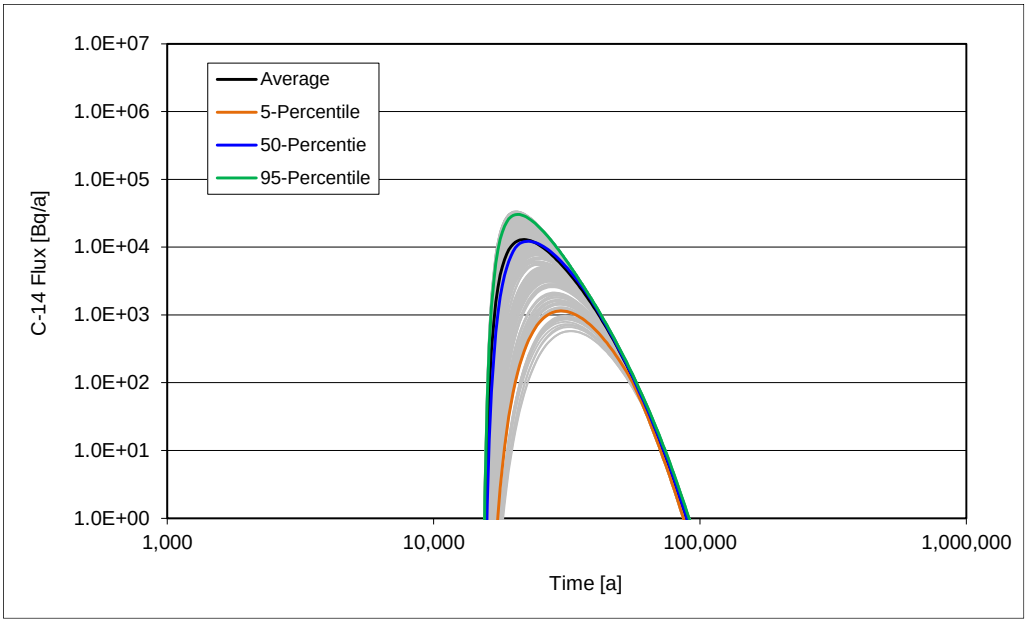

Figure 10: C-14 flux at 5 m into the Boom Clay – Point 5 (Case 1)

1.3.1.2 Scatter plots

Figure 11 shows scatter plots of the calculated C-14 fluxes (250 simulations) at the time of the maximum of the 50-Percentiles at 5 m into the Boom Clay – Point 5 (Case 1).

From these plots it is clearly seen that the C-14 fluxes at 5 m into the Boom Clay are not correlated to the IRF from Zircaloy nor the Zircaloy corrosion rate, as the points are scattered in a random-like pattern. The C-14 flux at this point is only slightly correlated with the K_d-values of concrete, as there is the tendency of lower values of the C-14 flux for higher values of the K_d of concrete. There is a definite correlation visible between the C-14 flux and the K_d of Boom Clay, although for larger K_d of Boom Clay ($K_d > 10^{-4}$ m^3/kg) this correlation is more pronounced than for lower K_d values.

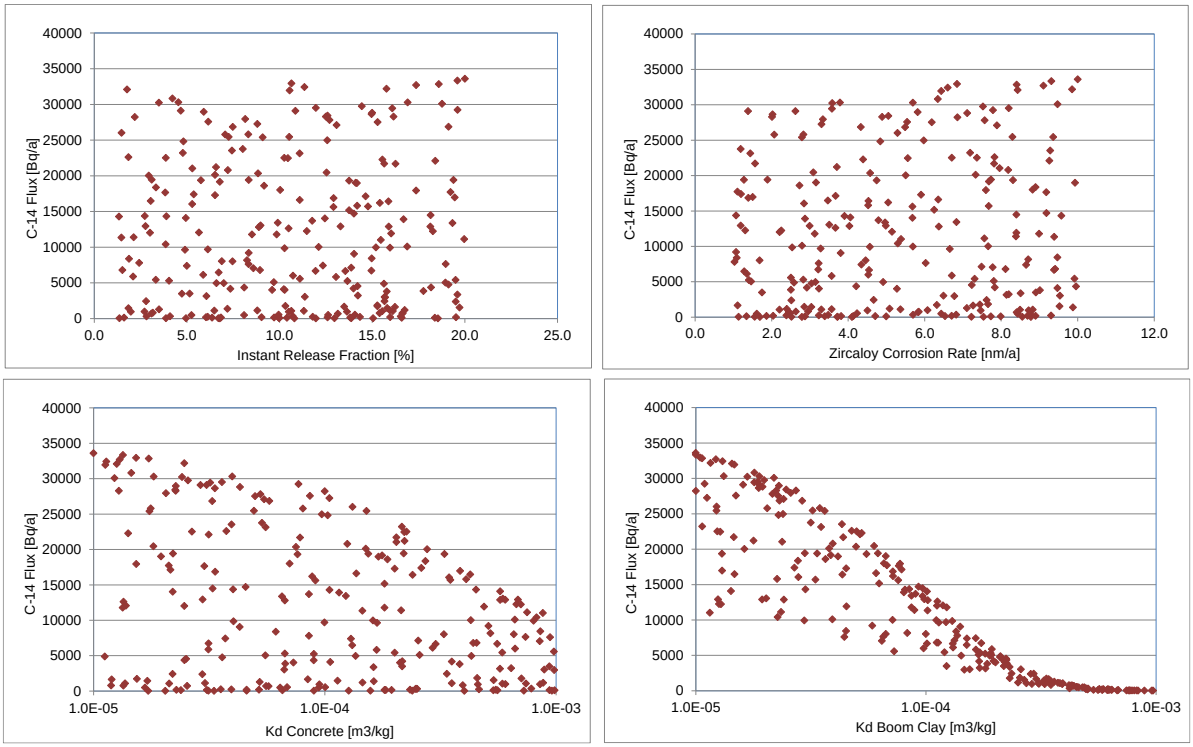

Figure 11: Scatter plots of C-14 flux at the time of the maximum of the 50-Percentiles at 5 m into the Boom Clay – Point 5 (Case 1)

1.3.1.3 Pearson and Rank Correlation Coefficients

The figures below show the Pearson Correlation Coefficients (*PCC*) and the Rank Correlation Coefficients (*RCC*) for respectively the C-14 flux at 1 m into the Boom Clay (Point 4; Figure 12 and Figure 13), and 5 m into the Boom Clay (Point 5; Figure 14 and Figure 15).

These figures clearly show that the IRF and the Zircaloy corrosion rate have a very limited influence on the C-14 fluxes through the disposal system, since the *PCC* and *RCC* values range most of the time from approx. -0.1 to +0.1, and for a limited time frame from approx. -0.3 to +0.3.

Compared to the IRF and the Zircaloy corrosion rate, the K_d values of concrete and Boom Clay show a more discernable correlation with the C-14 fluxes at 1 m and 5 m into the Boom Clay. The influence of the K_d values of concrete on the C-14 fluxes is more pronounced at

Point 4 (1 m into the Boom Clay), whereas the influence of the K_d values of Boom Clay is more notable at Point 5 (5 m into the Boom Clay). This is explained by the fact that the influence of concrete decreases as C-14 diffuses through the Boom Clay, further away from the source compartment.

The figures show that, after the release of C-14 from the CSD-C containers, the *PCC*'s and *RCC*'s related to the K_d's first indicate a negative correlation with the C-14 flux, followed by a positive correlation thereafter. The first period of negative correlation indicate that higher K_d- values, both for concrete and Boom Clay, lead to lower values of the C-14 fluxes at the successive locations in the Boom Clay. This is explained by the observation that higher K_d-values cause a delayed transport of C-14 through the concrete and Boom Clay, and therefore lower C-14 fluxes at this observation point.

At later stages in the transient the values of the *PCC*'s and *RCC*'s related to the K_d values change from negative to positive, indicating that higher K_d- values, both for concrete and Boom Clay, lead to higher values of the C-14 fluxes. This is caused by the fact that higher K_d- values lead to a more delayed C-14 transport in the first phase of the transient, and therefore an enhanced concentration ("inventory") of C-14 in the volumes enclosed by the subsequent observation points. This enhanced amount of C-14, hold back at the earlier stages, eventually leads to larger C-14 fluxes at later stages.

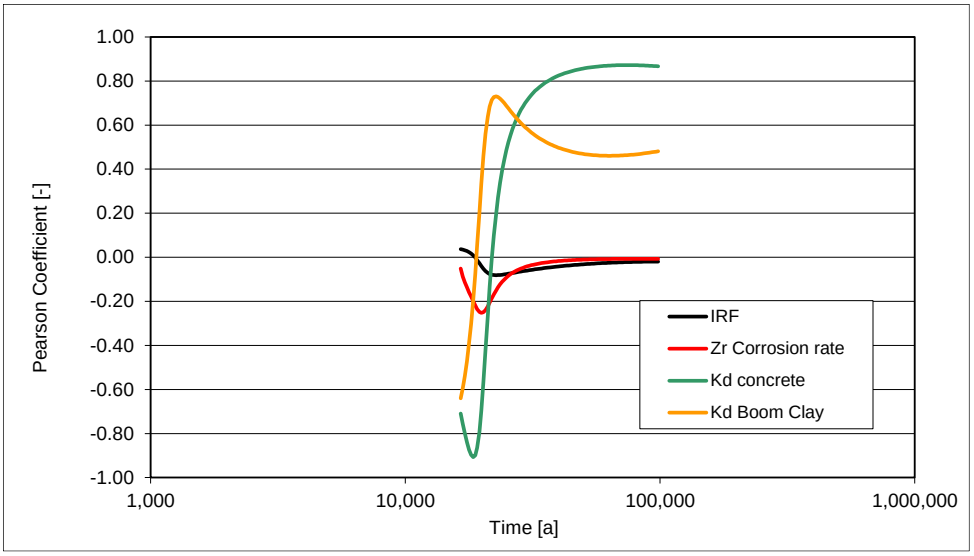

Figure 12: Pearson Correlation Coefficients for C-14 flux at 1 m into the Boom Clay – Point 4 (Case 1)

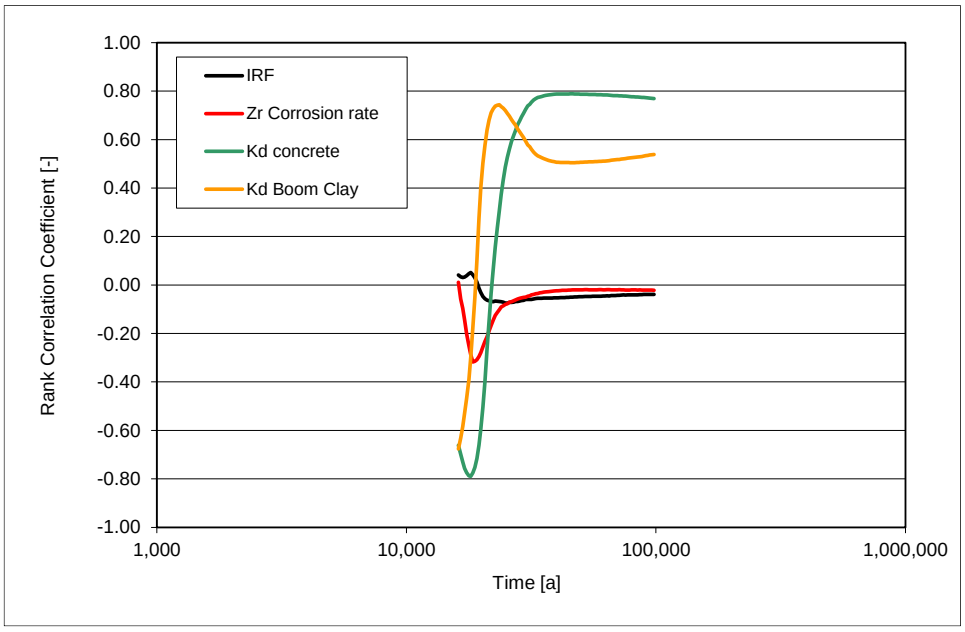

Figure 13: Rank Correlation Coefficients for C-14 flux at 1 m into the Boom Clay – Point 4 (Case 1)

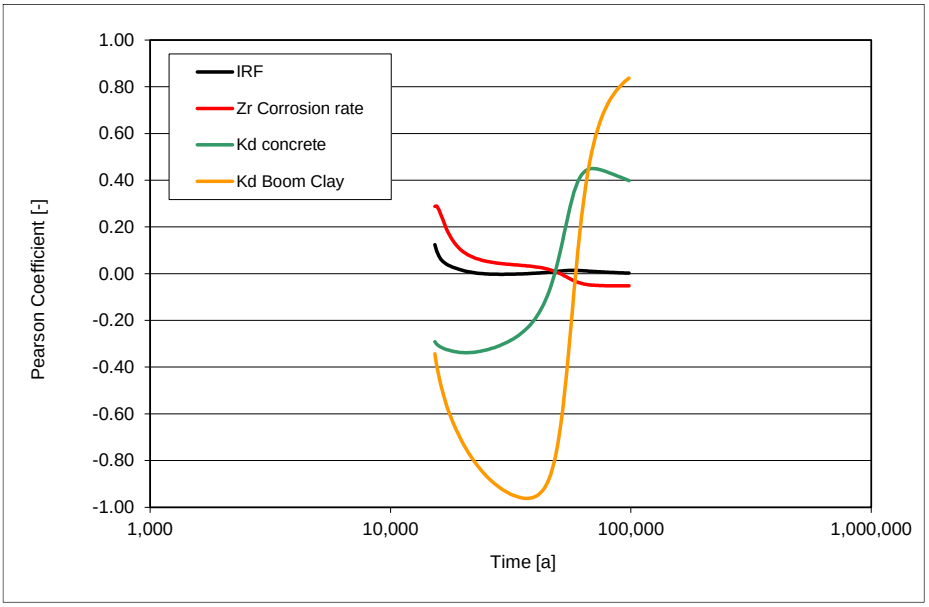

Figure 14: Pearson Correlation Coefficients for C-14 flux at 5 m into the Boom Clay – Point 5 (Case 1)

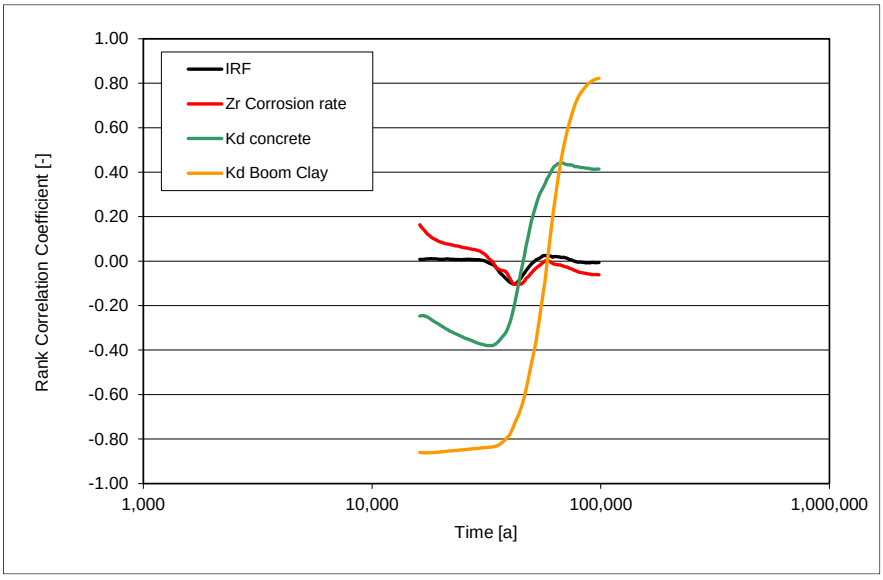

Figure 15: Rank Correlation Coefficients for C-14 flux at 5 m into the Boom Clay – Point 5 (Case 1)

From the *PCC*'s and *RCC*'s it can be concluded that the IRF and the Zircaloy corrosion rate have only a limited effect on the calculated C-14 fluxes at different locations in the disposal

system. On the other hand, the C-14 fluxes show a pronounced dependency on the K_d-values of concrete and Boom Clay. In the vicinity of the concrete, the influence of the K_d-values of concrete and Boom Clay on the C-14 flux is of concrete is of similar magnitude. Further away from the concrete, the K_d-values of Boom Clay become the dominant factor.

The Pearson correlation coefficient (*PCC*) provides a measure of the strength of the linear relationship between input factors and the calculated output, in this case the C-14 flux at different locations in the system. From the scatter plots (cf. Section 1.3.1.2), a linear relationship between the 4 input variables and the C-14 fluxes is however not apparent. In the case of a *nonlinear* but monotonic relationship between values of the input parameters and the output parameter, a rank transformation can be used to obtain a linear relationship. As a consequence, the resulting *Rank Correlation Coefficient*, *RCC*, is judged to provide more reliable results than the *PCC* to analyse sensitivities of input parameters on the output variables under consideration (e.g. SCHRÖDER, 2009; Ch. 7).

1.3.1.4 Cobweb plots

Figure 16 and Figure 17 show the conditional Cobweb plots for the maximum values of the C-14 flux for each simulation, respectively at 1 m (Point 4) and 5 m (Point 5) into the Boom Clay. In these plots the simulations producing the 40 highest *ranks* of the maximum values of the C-14 flux at these respective locations are connected with the corresponding *ranks* of the four input variables IRF, Zircaloy corrosion rate, and K_d values of concrete and Boom Clay.

By connecting the values of the ranks with lines for each sampled run of the multiple simulation, the plots clearly show that the highest calculated values of the C-14 flux correspond to low K_d values of concrete and Boom Clay.

Additionally, there is no clear correspondence between the highest values the of the C-14 flux and the input variables IRF and Zircaloy corrosion rate, since both high and low values of these variables can lead to high values of the C-14 flux.

Comparing Figure 16 and Figure 17 the correspondence between the highest values of the C-14 flux and the lower K_d values of concrete is more pronounced at 1 m into the Boom Clay

than at 5 m into the Boom Clay. This is explained by the longer pathway of the C-14 in Boom Clay in the latter case, resulting in a decrease of the influence of concrete on the C-14 flux.

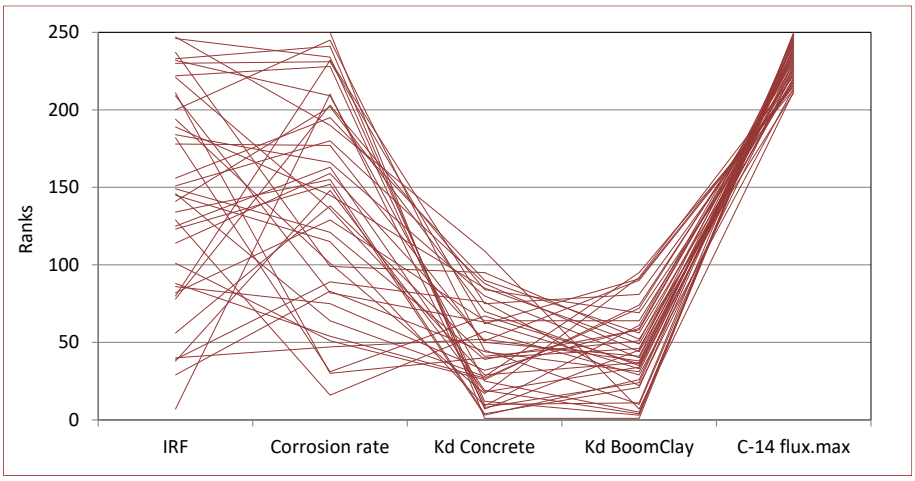

Figure 16: Conditional Cobweb plot for the maximum C-14 flux at 1 m into the Boom Clay – Point 4 (Case 1)

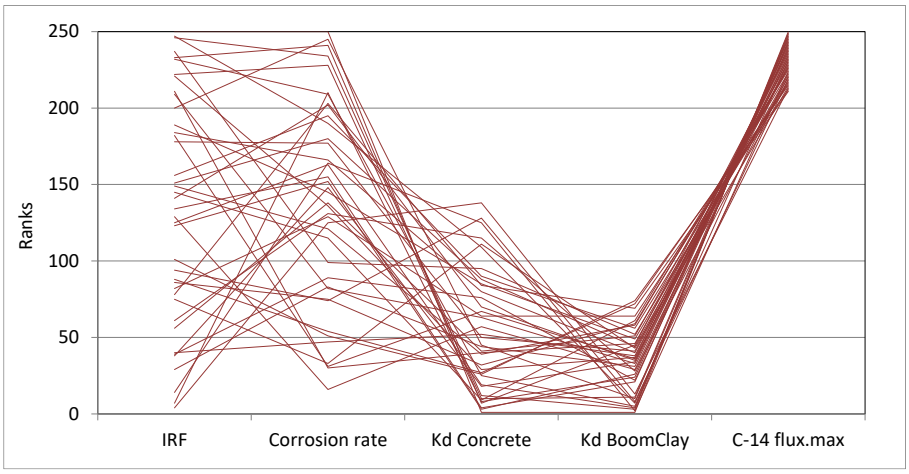

Figure 17: Conditional Cobweb plot for the maximum C-14 flux at 5 m into the Boom Clay – Point 5 (Case 1)

1.3.2 Case 2 – Enhanced C-14 Migration

Compared to Case 1, the Reference Case, Case 2 assumes the following modifications of model parameters:

- A start of C-14 release from the CSD-C containers immediately after disposal, i.e. at t = 0 a (instead of 15'000 a for the Reference Case);
- A diffusion coefficient of C-14 in Boom Clay D = 0.0012 m^2/a (instead of 0.063 m^2/a for the Reference Case").

1.3.2.1 C-14 Fluxes

Figure 18 shows the calculated C-14 fluxes at various locations of the disposal system.

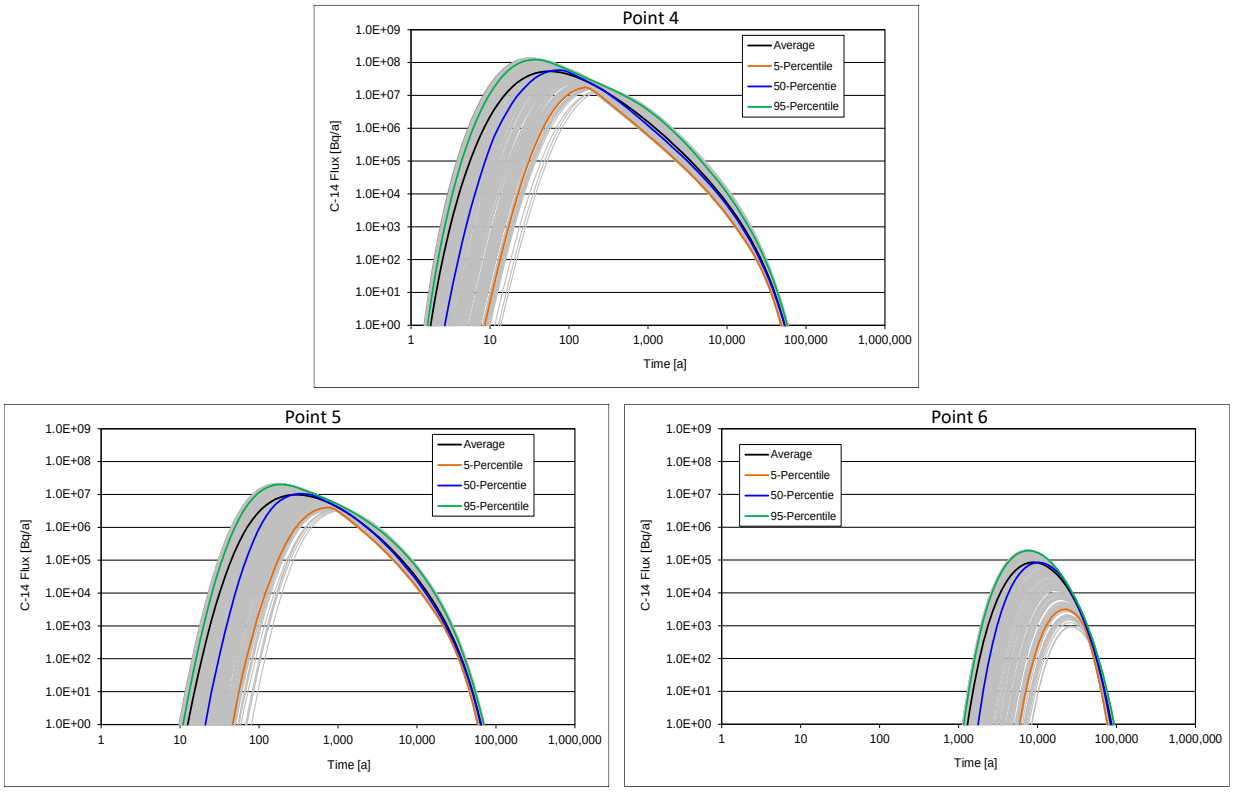

Figure 18: C-14 flux at various locations into the Boom Clay – 1 m (Point 4); 5 m (Point 5); exit (Point 6) - Case 2

It is seen that for this case of early C-14 release and enhanced migration rates in Boom Clay part of the C-14 may leave the outer boundary of the Boom Clay (Point 6). For the present set of simulations, the C-14 fraction leaving the outer boundary of the Boom Clay ranges from 0.2% to 16% (average 8%) of the initial C-14 inventory.

1.3.2.2 Scatter plots

Although not shown here, the scatter plots of the calculated C-14 fluxes (250 simulations) at the time of the maximum of the 50-Percentiles for Case 2 clearly reveal, similar to Case 1, that the C-14 fluxes are not correlated to the IRF from Zircaloy nor the Zircaloy corrosion rate at all locations, as the points are scattered in a random-like pattern. Additionally, the correlation of the C-14 flux with the K_d-values of concrete is apparent in the vicinity of the concrete compartment, but dies out further away from the concrete.

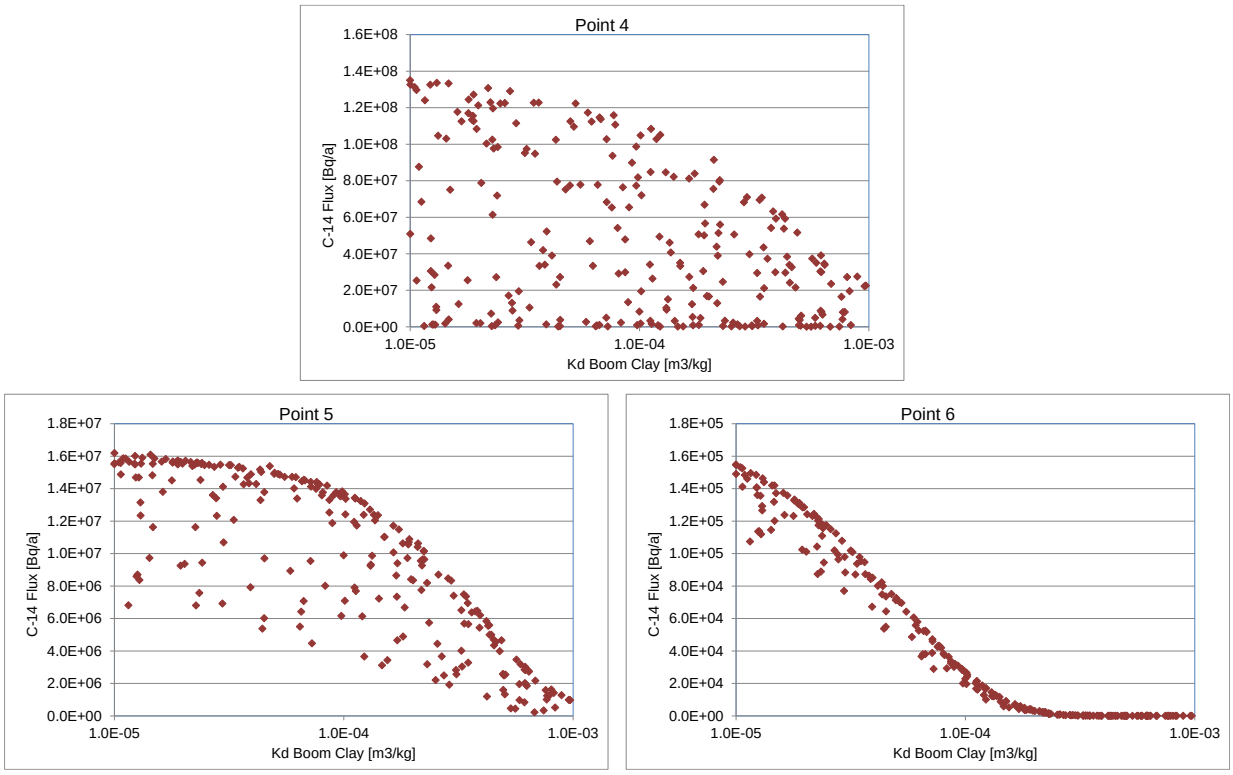

Figure 19: Scatter plots of C-14 flux at the time of the maximum of the 50-Percentiles at various locations into the Boom Clay – 1 m (Point 4); 5 m (Point 5); exit (Point 6) - Case 2

The correlation between the C-14 flux and the K_d–values of Boom Clay is apparent, and becomes more pronounced further away from the disposal area, as shown in Figure 19. At the outer boundary of the Boom Clay, i.e. Point 6, the K_d–value of Boom Clay is the only remaining parameter correlating with the C-14 flux.

1.3.2.3 Rank Correlation Coefficients

Figure 20 shows the *RCC*'s for the calculated C-14 fluxes, respectively at 1 m into the Boom Clay (Point 4), 5 m into the Boom Clay (Point 5), and at the outer boundary of the Boom Clay (Point 6).

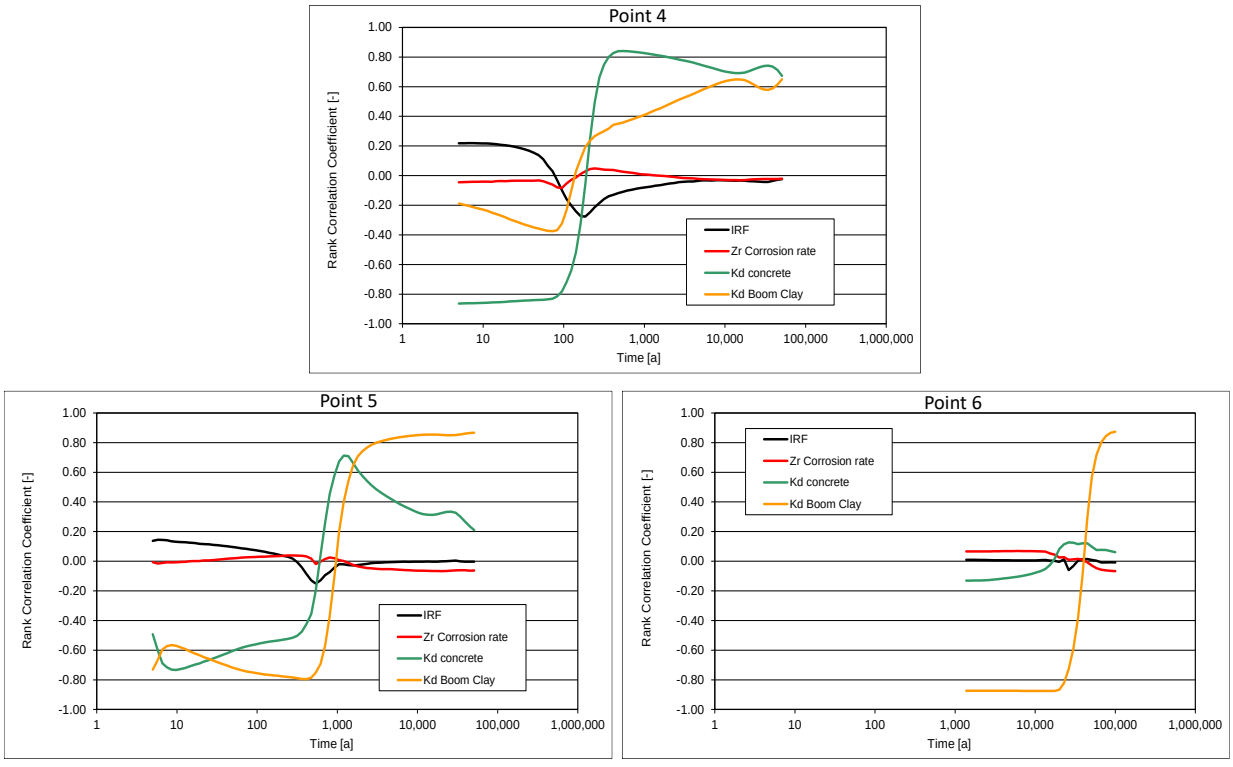

Figure 20: Rank Correlation Coefficients for C-14 flux at various locations into the Boom Clay – 1 m (Point 4); 5 m (Point 5); exit (Point 6) - Case 2

The observed trends of the dependency of the C-14 fluxes on the 4 input parameters at these locations is similar as can be established from the scatter plots. Both the IRF and the Zircaloy corrosion rate show hardly or no correlation with the C-14 fluxes since the *PCC*'s and *RCC*'s for these parameters range between only -0.2 and +0.2. On the other hand, the C-14 fluxes

show a pronounced dependency on the K_d-values of concrete and Boom Clay. Close to the disposal area, the K_d-value of concrete is the dominant factor influencing the C-14 flux, whereas further away into the Boom Clay K_d-value of Boom Clay becomes more relevant, if not dominant.

1.3.2.4 Cobweb plots

Figure 21 shows the conditional Cobweb plots for the calculated C-14 fluxes, respectively at 1 m into the Boom Clay (Point 4), 5 m into the Boom Clay (Point 5), and at the outer boundary of the Boom Clay (Point 6).

As already became apparent from the scatter plots and the *RCC*'s, the conditional Cobweb show that the maximum C-14 fluxes at all locations are uncorrelated with both the IRF and the Zircaloy corrosion rate. On the other hand and dependent on the location, the K_d-values of concrete and Boom Clay are the parameters which influence the C-14 fluxes throughout the disposal system.

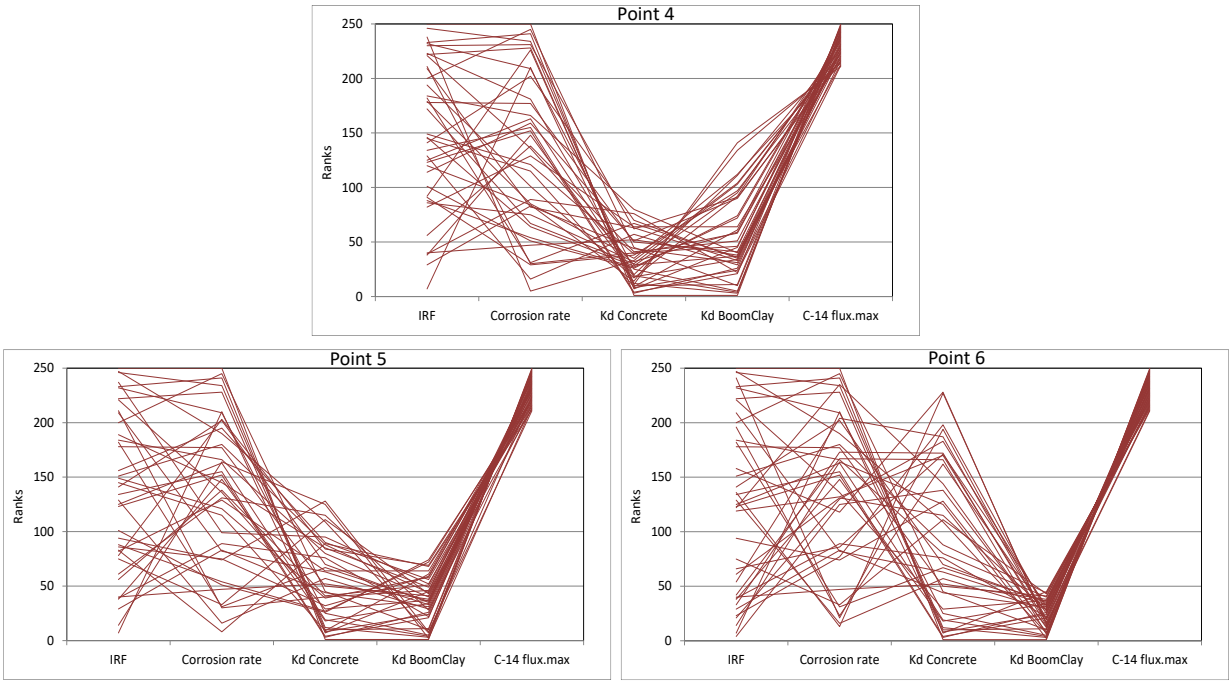

Figure 21: Conditional Cobweb plot for the maximum C-14 flux at various locations into the Boom Clay – 1 m (Point 4); 5 m (Point 5); exit (Point 6) - Case 2

1.4 Conclusions and Discussion

Based on the Dutch OPERA reference concept for the final disposal of radioactive waste in Boom Clay, a conceptual model has been implemented in the computer code ORCHESTRA to assess the influence of system parameters on the C-14 flux, released from Zircaloy contained in a CSD-C canister, through the surrounding concrete and Boom Clay.

A full probabilistic uncertainty/sensitivity analysis (UA/SA) has been applied to assess how the C-14 flux through the disposal system depends on (1) the Instant Release Fraction (IRF) of C-14 from Zircaloy, (2) the long-term congruent release resulting from the corrosion of Zircaloy, (3) the K_d of C-14 in concrete surrounding the Source volume, and (4) the K_d of C-14 in Boom Clay as the host rock. The values of these system parameters have been varied according to the specifications laid down in [CAPOUET, 2016B].

The UA/SA has been performed for two different cases, (1) a "*Reference Case*", assuming a failure time of the CSD-C container 15'000 years after disposal and a deterministic value of the C-14 diffusion coefficient in Boom Clay, and (2) an "*Enhanced C-14 Migration Case*", assuming an immediate failure of the CSD-C container after disposal, and a significantly enhanced value of the C-14 diffusion coefficient in Boom Clay.

For analysing the sensitivities of the four system parameters on the calculated C-14 fluxes at different locations use has been made of scatter plots, the Pearson Correlation Coefficient (*PCC*) and the Rank Correlation Coefficient (*RCC*), and conditional Cobweb plots.

The results of the UA/SA show that in all cases and at all locations in the disposal system in Boom Clay the calculated C-14 fluxes hardly depend on the prescribed values of the IRF and the Zircaloy corrosion rate. On the other hand , the K_d values of concrete and Boom Clay do affect the C-14 fluxes throughout the disposal system. At 1 m into the Boom Clay, the C-14 flux is approximately equally influenced by the K_d values of concrete and Boom Clay. Further away from the repository, the influence of the K_d value of concrete decreases, whereas the K_d value of Boom Clay becomes more apparent. At the outer boundary of the Boom Clay, the K_d value of Boom Clay is the only remaining parameter influencing the C-14 flux.

Assuming expert values of the time of failure of the CSD-C container and the diffusion coefficient of C-14 in Boom Clay leads to calculated migration times of C-14 in the Boom Clay host rock which are sufficiently long to for the disposed C-14 inventory to completely decay. In that case C-14 does not reach the outer boundary of the Boom Clay.

Assuming an instant failure of the CSD-C containers upon disposal, and a significantly enhanced diffusion rate of C-14 in Boom Clay may lead to a fraction of C-14 reaching the outer boundary of the Boom Clay. For the present set of simulations, the C-14 fraction leaving the outer boundary of the Boom Clay ranges from 0.2% to 16% of the initial C-14 inventory, with an average value of 8%.

An important distinction between the *Reference Case* and the *Enhanced C-14 Transfer Case* relates to the C-14 inventory that can be released from the CSD-C containers. A start of release immediately after disposal implies that the total initial C-14 inventory is available, whereas a start of release at 15'000 years (Reference Case) implies that more 85% of the initially disposed inventory of C-14 has decayed.

The consequence of the difference in C-14 inventory that is available for release at t = 0 a and at t = 15'000 a in terms of C-14 flux through the system concrete/Boom Clay is minimal: in both cases, the diffusion coefficient of C-14 in Boom Clay and the K_d's of concrete and Boom Clay are the main parameters determining the C-14 flux through the system.

From the present UA/SA analysis it can be concluded that assessing the safety consequences of C-14 disposed in a deep geological repository in Boom Clay would benefit from enhancing the understanding of parameters and processes that determine the diffusion and sorption of C-14 both in concrete and Boom Clay.

2 Integration of the CAST experimental outcomes at the level of the safety case.

The implications of the results obtained from the CAST project for the Dutch safety assessment presently performed in the OPERA programme as well as the safety case are discussed in the following sections.

2.1 *Implications of CAST results for the OPERA PA*

- The C-14 inventories in the various waste fractions are presently implemented in the OPERA PA model as homogeneously distributed. No distinction is yet made between variations in C-14 concentrations in e.g. claddings, structural parts, spent ion exchangers, etc. The present UA/SA analysis performed in CAST shows that the calculated C-14 fluxes in and from the Boom Clay hardly depend on the prescribed values of the IRF and the Zircaloy corrosion rates. Consequently, an implementation of more refined C-14 release forms into the OPERA PA model is, for the moment, judged unnecessary.
- The present OPERA PA model assumes a 100% IRF of the C-14 inventories following the assumed failure times of the respective waste containers, except for the vitrified HLW containers where a congruent release rate is assumed. In the present analysis performed in CAST these two system parameters were however shown to have a very limited effect on the C-14 migration in Boom Clay. Consequently, the current model assumptions for the OPERA PA will, for the time being, remain unchanged.
- The current OPERA PA model does not consider the retention of radionuclides in concrete, which is present in the supercontainer, the backfill of the disposal galleries, and the gallery lining. The current UA/SA analyses in CAST demonstrate that any retention in cement does affect the fluxes of C-14 through the disposal system, but only in the vicinity of the disposal cells. Further away into the Boom Clay, the effect of retention of C-14 in concrete dies out due to the slow, diffusive migration in Boom Clay and the simultaneous decay of C-14. Additionally, the thickness of the concrete of the EBS relative to the thickness of the surrounding Boom Clay is restricted, and therefore the potential influence of concrete on the C-14 migration is relatively limited.

Consequently, it is currently to considered to separately distinguish the concrete structures and retention of radionuclides therein in the OPERA PA model.

- Retention of radionuclides in Boom Clay is a most relevant process related to the long-term safety of the OPERA disposal concept. OPERA Work Package 6 thoroughly dealt with understanding and modelling of the retention (and also diffusion) of radionuclides in Boom Clay (MEEUSSEN, 2017; SCHRÖDER, 2017b). For C-14 however, the current OPERA PA model considers no retention of C-14 in Boom Clay (SCHRÖDER, 2017; Ch.4) . Even in that case, preliminary PA results show that the contribution of C-14 to the overall dose rate in the biosphere is negligible compared to other nuclides. This is caused by the relatively fast decay compared to the elongated residence time of C-14 in Boom Clay and the Overburden. Assuming, as in CAST, any retention of C-14 in Boom Clay will further delay the C-14 migration rate in Boom Clay, and therefore also the contribution of C-14 to the total dose rate in the biosphere.
- The current OPERA PA model models the transport rate of radionuclides in the rock formations surrounding the Boom Clay host rock, viz. the Overburden compartment, by means of a residence time, based on the hydraulic transport models developed in OPERA Task 6.2.1 (VALSTAR, 2016). These residence times range from 30’700 a to 853’000 a, i.e. approximately 5.4 to 150 half lives of C-14, implying a significant decay of C-14 during its transport from the Boom Clay to the biosphere.
- The current OPERA PA model does not consider retention of radionuclides in the rock formations surrounding the Boom Clay host rock, viz. the Overburden compartment. If any retention of C-14 in these formations can be demonstrated, the C-14 migration in the Overburden compartment will be significantly delayed, and therefore also the contribution of C-14 to the total dose rate in the biosphere.

2.2 Uncertainties

- The presence and formation of gaseous compounds after disposal were not yet implemented into the OPERA PA model, since it was substantiated that gas movement by solution/diffusion still carries a high level of uncertainty, especially at greater depths, i.e. at 500 m: the OPERA disposal concept. The aspect of "gas" including the associated processes (cf. Figure 22) have been investigated in the OPERA program (e.g. WISEALL, 2015), but no model has been developed yet for application in the OPERA PA.

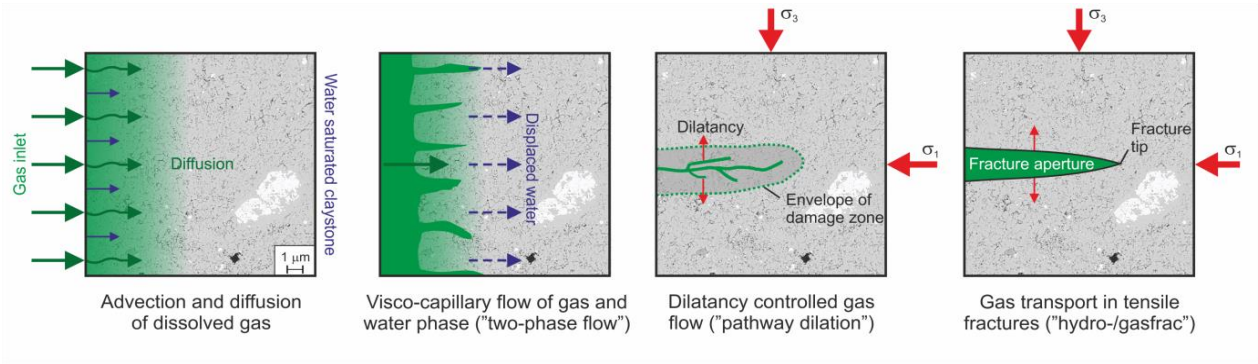

Figure 22: Overview of gas-related processes potentially affecting the radionuclide migration in Boom Clay

- Various CAST reports provide information about corrosion rates for materials which are also anticipated to be present in the OPERA disposal facility, e.g. stainless steel [SWANTON, 2015] and Zircaloy [GRAS, 2014]. Quantitative assessments were however not yet performed for the Dutch situation.

2.3 Implications of CAST results on OPERA scenarios

- The C-14 inventories in the various waste fractions are presently implemented in the current OPERA PA model as unspecified components; no distinction is yet made between organic/inorganic nor solid/gas fractions. For the normal evolution scenario this assumption seems plausible considering the elongated amount of time needed for C-14 to migrate from the waste compartments to the biosphere, which is sufficiently long for C-14 to decay more or less completely. For alternative evolution scenarios (e.g.

excessive gas generation) the speciation of C-14 may become relevant if it can be argued that the travel time of C-14 to the biosphere is relatively short compared to its half-life.

- In the normal evolution scenario of the OPERA PA, the C-14 transport in Boom Clay is assumed to occur by diffusion only as a soluble inorganic species. The release of gaseous material from the emplaced waste nor the transport of gases through the concrete engineered barriers and the Boom Clay are yet considered in the OPERA PA. As part of OPERA Task 6.1.6: *Gas migration in the EBS and in Boom Clay*, a critical evaluation was performed of fundamental processes for gas-related transport in Boom Clay, including pressure/temperature dependent gas penetration, two-phase flow, pathway dilation and the occurrence and relevance of preferential pathways in the EBS (WISEALL, 2015; cf. Figure 22).
- Concerning the consideration of scenarios as part of the OPERA safety assessment no additional AES's have been identified based on the results obtained in CAST. At present only the NES is being simulated in OPERA, but in due time also the simulation of AES's will be performed. CAST did stress the importance of gas-related scenarios (e.g. CAPOUET, 2016a); one of the OPERA AES refers to the excessive generation of gas, and it is apparent that the modelling of that scenario will benefit from the outcomes of CAST.

2.4 Implications for the OPERA Safety Case

- Preliminary simulations on the OPERA PA model show that the contribution of C-14 to the total dose rate in the biosphere is negligible for the normal evolution scenario. This is a confirmation of previously reported PA simulations, which also show that the time frame from the start of release from the waste containers to the arrival into biosphere is sufficiently long for C-14, mostly due to the slow migration through the Boom Clay host rock, to decay to such an extent that its contribution to the total dose rate is negligible (e.g. GRUPA, 2000; SCHRÖDER, 2009).

- The present simulations executed in CAST indicate that for the Reference Case the amount of C-14 reaching the outer boundary of the Boom Clay is negligible. On the other hand, for the case Enhanced C-14 Migration, a fraction of the initially disposed C-14 may reach the outer boundary of the Boom Clay. However, considering a dilution in the aquifer, the elongated travel times in the Overburden (at least 5 half-lives of C-14), and an additional dilution in the biosphere, the potential exposure in the biosphere resulting from C-14 will be insignificant.
- The CAST results confirm that, for a disposal facility in Boom Clay, the contribution of C-14 to the total dose rate in the biosphere is very small. However, the main remaining uncertainty relates to a situation where C-14 is released very early after disposal, in combination with a significantly enhanced transport through the Boom Clay, e.g. by the excessive formation of gaseous compounds.

2.5 *Future work*

- Considering the level of uncertainty about the production and transport of gas mentioned in Section 2.2 it is foreseen that in future safety assessment analyses, especially for gas-related alternative evolution scenarios, the topic of “gas” will be included into the PA model of the OPERA disposal concept.
- Special focus on gas-related issues will be placed on inventorying processes which potentially may lead to fast and vigorous production of gases, and the potential of gas to penetrate and damage the Boom Clay host rock in case of excessive gas generation processes.

2.6 *Summary*

Table 3 summarizes the implications of the present simulations performed by NRG within the CAST project for the modelling of C-14 in the Dutch safety assessment.

Table 3 Implications of CAST for C-14 modelling in the Dutch safety assessment

	Hypothesis used in safety assessment before CAST	Considerations for implementation in safety assessment based on CAST
Inventory	- Fixed inventories for considered waste fractions - No detailed distinction between C-14 in structural parts, claddings, SIER's, etc	Unchanged
Speciation	Reference case : Inorganic	Organic/gaseous species may accelerate the C-14 migration rate in Boom Clay
Leaching rate	Only considered for V-HLW; Congruent with various release rates: - Slow release case - Release base case - Fast release case	Unchanged; CAST revealed limited impact of this parameter
	Not considered for spent fuels, non-heat generating wastes, LILW	Unchanged; CAST revealed limited impact of this parameter
IRF	100% of the RN inventory for spent fuels, non-heat generating wastes, LILW	Unchanged; CAST revealed limited impact of this parameter
Gas; release and transport	Not considered	Consideration to implement gas models, esp. related to AES *Excessive gas generation*
Transport in Boom Clay	Diffusion as solute inorganic species	- Unchanged for NES - Possible enhanced diffusion for AES *Excessive gas generation*
Transport in overburden	Diffusion and advection (transport time) as solute inorganic species	- Unchanged for NES - Possible enhanced diffusion/advection for AES *Excessive gas generation*
Retention in concrete	Not considered; concrete presently not modelled	Not considered, even in case of modelling of concrete
Retention in Boom Clay	Not considered in NES	Unchanged, conservatively assumed
Retention in Overburden	Not considered in NES	Unchanged, conservatively assumed
Scenarios	-NES is presently being calculated -AES only inventoried and described, not yet simulated	-No additional AES's have been identified based on CAST -However, CAST stressed the consideration of gas-related scenarios

In conclusion it can be stated that for the OPERA disposal concept in Boom Clay the impact of C-14 on the ultimate dose rate in the biosphere is limited if not negligible in case of the presently adopted normal evolution scenario. This is caused by the long transport time of C-14 from the waste containers, through respectively the Boom Clay host rock and the overburden, to the biosphere, compared to its half life. Only in the case of an early release and a significantly enhanced migration rate, e.g. in the case of excessive gas generation and gas-mediated transport through the Boom Clay and the overburden, a noticeable amount of C-14 may ultimately appear in the biosphere. However, even in that case it is anticipated that the contribution of C-14 to the dose rate in the biosphere will be limited compared to that of other radionuclides.

In any case, the CAST project has significantly deepened the understanding of processes considered relevant for assessing the impact of C-14 on the safety of a deep geological disposal facility in Boom Clay. The results of CAST are therefore significant for further demonstrating the long-term safety of the OPERA disposal concept.

References

BOLADO, 2008: Bolado Lavín R, Röhlig K-J, Becker D-A, Sensitivity Analysis Techniques for the Performance Assessment of a Radioactive Waste Repository, Euradwaste '08, Seventh European Commission Conference on the Management and Disposal of Radioactive Waste, Luxembourg, 20-22 October 2008.

CAPOUET, 2016a: Capouet M., Wissmeier L., Minutes and Summary of CAST WP6 Technical Meeting from 8-9 March 2016, 27 September 2016.

CAPOUET, 2016b: Capouet M., CArbon-14 Source Term – CAST; Handling of C-14 in safety assessment - Guidance for uncertainty analysis, 2016.

CORA, 2001: Commissie Opberging Radioactief Afval, *Terugneembare berging, een begaanbaar pad? Onderzoek naar de mogelijkheden van terugneembare berging van radioactief afval in Nederland*, Ministry of Economic Affairs, The Hague, February 2001.

GRAS, 2014: Gras J.M, State of the art of 14C in Zircaloy and Zr alloys - 14C release from zirconium alloy hulls, Deliverable 3.1, Project CArbon-14 Source Term – CAST, Seventh Framework Programme FP7/2007-2013, Grant Agreement No. 604779, 04/08/2014.

GRUPA, 2000: Grupa J.B., Houkema M., Terughaalbare opberging van radioactief afval in diepe zouten kleiformaties Modellen voor een veiligheidsstudie, 21082/00.33017/P, Petten, March 2000.

KELLETT, 2009: Kellett M.A., Bersillon O., Mills R.W., The JEFF-3.1/-3.1.1 radioactive decay data and fission yields sub-libraries, JEFF Report 20, ISBN 978-92-64-99087-6, OECD/NEA No. 6287, Paris, 2009, 1-147.

MEEUSSEN, 2003: Meeussen JCL, ORCHESTRA: An Object-Oriented Framework for Implementing Chemical Equilibrium Models, Environmental Science & Technology 37 (6), 1175-1182, 2003. Website: orchestra.meeussen.nl.

MEEUSSEN, 2017: Meeussen J.C.L., Rosca-Bocancea E., Schröder T.J., Koenen M., Valega Mackenzie F., Maes N., Bruggeman C., Model representation of radionuclide diffusion in Boom Clay, OPERA-PU-NRG6131, 7 February 2017.

NEI, 2009: Nuclear Engineering International, 2009 World nuclear industry handbook, ISBN-978-1-903077-67-2, 2009.

ONDRAF/NIRAS, 2001: ONDRAF/NIRAS, Safety Assessment and Feasibility Interim Report 2, Section 11.3.8, NIROND 2001–06 E, December 2001.

PRIJ, 1989: Prij, J., Veiligheidsevaluatie van opbergconcepten in steenzout (VEOS), Eindrapportage Deelrapport 1, Samenvatting en evaluatie, ECN, Petten, January 1989.

PRIJ, 1993: Prij J., Blok J.B.M., Laheij G.H.M., van Rheenen W., Slagter W., Uffink G.J.M., Uijt de Haag P., Wildenborg A.F.B., Zanstra D.A., PRObabilistic Safety Assessment, Final report, of ECN, RIVM and RGD in Phase 1A of the OPLA Programme, 1993.

SCHRÖDER, 2009: Schröder T.J., Rosca-Bocancea E., Hart J., Costescu-Badea, A., Bolado Lavin R., PAMINA Task 2.1.D - Techniques for Sensitivity and Uncertainty Analysis; Analysis of a repository design in argillaceous rock, PAMINA Milestone Report M2.1D.12, NRG-21952/09.96187, 4 December 2009.

SCHRÖDER, 2017: Schröder T.J., Hart J., Meeussen J.C.L., Report on model parameterization - Normal evolution scenario OPERA-PU-NRG7251-NES, February 2017.

SCHRÖDER, 2017b: T.J. Schröder T.J., Meeussen J.C.L., Final report on radionuclide sorption in Boom Clay, OPERA-PU-NRG6123, 1 February 2017.

SWANTON, 2015, Swanton SW, Baston GMN, Smart NR, Rates of steel corrosion and carbon-14 release from irradiated steels – state of the art review, (D2.5) CAST project report (2015).

VALSTAR, 2016: Valstar J.R., Goorden N., *Hydrological transport in the rock formations surrounding the host rock*, OPERA report OPERA-PU-DLT621, 2016, 1-79.

VERHOEF, 2011: Verhoef. E., Schröder, T. Research Plan OPERA-PG-COV004 21 June 2011.

VERHOEF, 2014a: Verhoef, E., Neeft, E., Towards a safety strategy - Developing a long-term Dutch research programme into geological disposal of radioactive waste. OPERA-PG-COV014, 2014.

VERHOEF, 2014b: Verhoef E., Neeft E., Grupa, J., Poley A. Outline of a disposal concept in clay Revision 1, OPERA-PG-COV008, 13 November 2014.

VERHOEF, 2015: Verhoef E.V., Neeft E., Deissmann G., Filby A., Wiegers R.B., Kers D.A., *Waste families in OPERA*, OPERA report OPERA-PG-COV023, September 2015.

WISEALL, 2015: Wiseall A., Graham C., Zihms S., Harrington J., Cuss R., Gregory S., Shaw R., Properties and Behaviour of the Boom Clay formation within a Dutch Repository Concept, OPERA-PU-BGS615, December 2015.

CArbon-14 Source Term

CAST

Safety assessment of C-14 release from CSD-C waste in a geological disposal facility in poorly indurated clay

Contribution from ONDRAF/NIRAS to D6.3

Capouet M., Meert K., Vandoorne T., Gaggiano R. and Dorado E.
ONDRAF/NIRAS

Date of issue of this report: 09/03/2018

Executive Summary

The outcomes of the CAST project over C-14 release from Zy and steel waste provide ONDRAF/NIRAS the opportunity to revisit the assumptions used in the previous safety assessment study over the radiological impact of C-14 released from compacted waste (CSD-C) placed in a geological disposal in Boom Clay. On the basis of the experimental results of CAST revealing the presence of a non-negligible fraction of organic C-14 compounds in the four waste materials investigated, the C-14 speciation in the CSD-C waste was assumed to be in the form of dissolved methane in the ONDRAF/NIRAS normal evolution scenario (so-called "reference" scenario). This new hypothesis increases by more than two orders of magnitude the radiological impact of C-14 compared with the previous safety assessment study. However this result needs to be put in perspective: Indeed, the knowledge over the C-14 release mechanism from Zircaloy claddings have greatly improved. Qualitative arguments suggest an extremely slow degradation of Zy hulls in disposal conditions resulting in the decay of a major part of C-14 in the metal mass. The C-14 radiological impact would then be negligible. These arguments are indicative of the safety margin taken in this scenario. With CAST, the quantitative impact of C-14 on long-term safety has increased, but also the confidence that this impact is extremely conservative. Safety assessment modelling accounting for both the Zircaloy corrosion and the zircone solubility should give a more realistic picture of C-14 release from CSD-C waste.

List of Contents

1 ONDRAF/NIRAS: Safety assessment studies of ^{14}C from CSD-C in a geological disposal in clay

1.1 *Geological disposal design and C-14 inventory*

ONDRAF/NIRAS, the Belgian Agency for Radioactive Waste and Enriched Fissile Materials, is considering the safety and feasibility of disposing of low level and intermediate-level long-lived radioactive waste (category B waste), and vitrified high level radioactive waste and spent fuel (category C waste) in a geological repository excavated in poorly indurated clays. Boom Clay and Ypresian clays are currently investigated as potential host formations. In this study, we assume that the disposal system is located in the mid-plane of a Boom Clay host formation of 80 meters.

Primary waste packages will be emplaced into pre cast concrete disposal waste packages: the "supercontainer" for category C waste and the "monolith" for category B, examples of which are illustrated in Figure 1. In the supercontainer, containment is achieved by placing the primary waste container in a carbon steel overpack surrounded by a Portland Cement concrete buffer. An outer stainless steel envelope is currently foreseen around the buffer. The supercontainer is designed to provide complete containment of radioactivity at least during the thermal phase. Category B waste does not generate significant amounts of heat, but does not meet the radiological criteria to be compatible with surface disposal. Generally, these wastes have been encapsulated in cement, or immobilized in a bitumen matrix. The primary waste containers are emplaced in large pre-cast concrete containers (the monolith) and the void space is filled with mortar. A concrete lid closes the monolith. The monolith is designed to facilitate contact handling during emplacement, but has no specific post-closure safety function assigned to it.

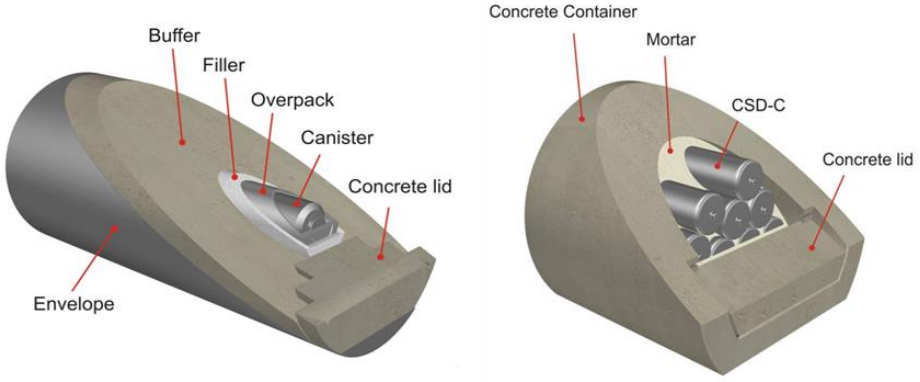

Figure 1: Example of a supercontainer and a monolith design for vitrified HLW canisters and compacted waste ('CSD-C'), respectively.

The 2016 estimation of the C-14 inventory of the main waste families of the Belgian programme relevant for long term safety is given in Table 1. A fraction of the spent nuclear fuel inventory is reprocessed at La Hague. The waste resulting from this reprocessing is returned to Belgium in the form of compacted (CSD-C) and vitrified (CSD-V) waste. The CSD-C are filled with sliced hulls (cladding tubes), grids and springs of typically 3-4 cm long, sections of nozzles of typically 10-15 cm long and a fraction of chips and fines. The CSD-C family shows the most important inventory of C-14 with a total activity of 6.1 x 10^{13} Bq. The C-14 activity in a CSD-C includes the inventories of the claddings and of the structural parts. The specific activity ranges between 3.9 x 10^{10} and 6.5 x 10^{10} Bq/canister depending on the incorporation rate and burn-up. The average burn-up is about 48 GWd/tHM (PWR). The C-14 inventory is estimated by ONDRAF/NIRAS on basis of the nitrogen content. The maximum of the tolerance in zircaloy material permitted by the waste producer is taken for the content of nitrogen (80 ppm). With regards to stainless steel, the precursor content is set to the conservative value of 1000 ppm. This inventory is conservative with respect to the initial enrichments. An additional contribution of 0.2% of the fuel inventory is also included to consider the short-depth penetration of nuclides into the cladding as a result of both atomic diffusion and fission recoil, and not leached out during the fuel nitric dissolution (Vandoorne, 2016).

C-14 inventory of the core internals resulting from the dismantling of the Belgian PWR's amounts a total around 1 x 10^{14} Bq, resulting in a best estimate of 3 x 10^{8} Bq/kg of stainless

steel. On the other hand, a C-14 activity of 1 x 10^7 Bq /kg for the resin waste originating from the primary circuits of PWRs is reported. The chemical speciation of carbon sorbed on these resins is an unknown as well as the impact of the conditioning processes (drying) thereon (ONDRAF/NIRAS, 2017).

The inventory of the high level waste is as follows: The C-14 inventory amounts around 1.3 x 10^{10} Bq/canister of CSD-V. It corresponds to an average burn-up of about 48 GWd/tHM. The C-14 activity of a 12 feet UOX assembly is around 5.6 x 10^{10} Bq/assembly. The claddings are mainly made of M-5/ZIRLO (1/2) and standard zirconium alloy (1/2). C-14 is also present in Be-waste and bitumen waste and other NPP operational waste but in a less important amount (ONDRAF/NIRAS, 2017).

Table 1: C-14 Belgian inventory as of 2016

Waste type	**C-14 activity (Bq/unit)**	**Uncertainty**
CSD-C	3.9-6.5 x 10^{10} /canister	Reasonably conservative
Core internals	3 x 10^8 Bq/kg metal	Best estimate for the most activated parts, uncertainty within one order of magnitude
Resins (PWR primary circuit)	1 x 10^7 Bq/kg resins	Best estimate, uncertainty more than one order of magnitude not excluded.
CSD-V	1.3 x 10^{10} Bq/canister	Reasonably conservative
Spent fuel total	5.6 x 10^{10} Bq/assembly 12 ft	Reasonably conservative
Fuel	4.1 x 10^{10} Bq/assembly 12 ft	
Struct. parts	0.4 x 10^{10} Bq/assembly 12 ft	
Claddings	1.1 x 10^{10} Bq/assembly 12 ft	

1.2 *Modelling of a diffusive scenario in saturated conditions*

The sensitivity analysis discussed here considers the disposal of CSD-C waste. The different cases treated are synthesised in Table 2. The *base case* describes the assumptions of the previous safety assessment (Weetjens et al., 2012), with the exception of the inventory that have been revised by (Vandoorne, 2016). The *base case* is a conservative realisation of the normal evolution scenario (reference scenario in ONDRAF/NIRAS terminology). *Case Org*

is an update of the *base case*. It integrates the experimental results from CAST. Additional cases are also treated to consider the impact of alternative hypothesis or uncertainties identified in the project.

The hypotheses considered in the *base case* are as follows: Containment of the primary package and chemical interactions such as calcite precipitation in the cemented EBS are not accounted for. C-14 is assumed to diffuse without retention through the near field. The only barrier to C-14 migration are the limited degradation of the waste form and the diffusive transport in the geological formation. It is assumed that the inventory is distributed homogeneously in the CSD-C waste and is released congruently. The lifetime is based on the corrosion rate of 10 nm/y of a Zy-4 hull of 550 µm thick. An instant release fraction (IRF) from C-14 originating from the oxidised zone of the hull is not considered in the *base case*. In previous studies of the Belgian program, C-14 released from the waste is assumed to be in inorganic form. Diffusion measurement of carbonates in Boom Clay show a weak retention (Aertsens *et al.*, 2010), which is neglected for C-14 in safety assessment.

The experimental results in CAST on the speciation of C-14 released from Zircaloy and steel suggest that a dominant fraction of organic compounds is released from the corrosion of the CSD-C waste form (Necib *et al.*, 2017). This main result from the CAST program is captured in *Case Org.* We consider conservatively that the entire content of C-14 migrates under the form of dissolved methane in Boom Clay. The experimental studies of diffusion of methane in Boom Clay samples indicate an effective diffusion rate of 2.4×10^{-10} m^2/s and a porosity of 0.37 (Jacops *et al.*, 2015) which are incorporated in *Case Org.*

The C-14 release rate is governed by the corrosion rate in the safety assessment model. (Gras, 2014) reports in its state-of-the-art review over Zircaloy that the uniform corrosion rate of the metal in anoxic, alkaline conditions is a few nm/yr at the most. This rate would correspond to a cladding lifetime approaching 10^5 years. More recently, (Sakuragi *et al.*, 2016) have carried out measurements of the gaseous hydrogen produced by the corrosion of Zy-4 during more than 6 years under representative cementitious conditions in disposal systems. Their data are indicative of a cladding lifetime longer than 10^5 years. However, these measurement data must be confirmed by additional experimental studies in order to be abstracted in safety

assessment modelling. On this knowledge basis, ONDRAF/NIRAS sets the lifetime of the CSD-C waste to 50 000 years for the *case Org*, which is about twice the value used in past safety assessment. This lifetime is based on the corrosion rate of a few nm/y a Zy-4 hull of 550 µm thick, from which an inner and an outer part are already both oxidized. The characteristic thickness of the outer oxide layer is 100 µm maximum for the Zy-4 alloys whereas the inner oxide is only 10 µm thick. Taking the density difference between the oxide and the metal into account, it results that only 13% of the Zircaloy metal have been oxidized. In order to take account of the potential increase of the reactive surface due to compaction and shearing processes the calculated lifetime is arbitrary reduced of a third. This lifetime is conservative for the C-14 released from the structural parts because these steel pieces show a larger thickness and their full corrosion will thus take more times than for Zy-4 hulls.

(Gras, 2014) indicates that the long duration corrosion tests performed on Zy-4, M-5 and Zirlo in alkaline conditions did not allow to differentiate the behaviour of the three alloys. M-5 and Zirlo are known to be more corrosion resistant than Zy-4 in operational conditions, resulting in a thinner outer oxide layer.

The CSD-C lifetime value proposed in *case Org* is considered as a defensible conservative value covering pH variability over the alkaline range, reasonable temperature variation, irradiations influence, salt ground water conditions, other cladding types of the Belgian inventory, as well as the smaller amount of stainless steel included in the CSD-C showing a C-14 release rate lower than for Zy-4.

Applying an IRF to the CSD-C is a matter of debate. In theory, the IRF assumed for the claddings of disposed spent fuel assemblies should also be applicable to CSD-C. However, the acid treatment of the material during reprocessing might remove accessible C-14 from the surfaces (Capouet, Boulanger, Vandoorne, Gaggiano, Norris, Williams, Schumacher, Rübel, Nummi, Poskas, Narkuniene, Grigaliuniene, Vokál *et al.*, 2017). In the following, we will conservatively consider that the reprocessing has no influence on the C-14 inventory of the claddings.

The CAST results confirm the hypotheses formulated fifteen years ago by the Japanese program of a mechanism in which C-14 is not released immediately by Zircaloy corrosion but is incorporated into the oxide film and then released at later stages (references in Gras, 2014). Indeed, the total leached fraction of C-14 from a long-term experiment on PWR cladding samples performed by (Sakuragi *et al.*, 2016) is less than 0.1% after two years of measurements. Longer experimental studies (up to 6 years) performed on BWR samples do not show an increase of C-14 after that period. Assuming that PWR and BWR have similar behaviours, the early and uncongruent release from PWR hulls would be less than 1%. Based on kinetic relationships derived at high temperature in operational conditions, (Sakuragi *et al.*, 2016b) calculate that the C-14 released in this experiment originates almost entirely from the oxide layer. These experimental results tend to confirm the strong conservatism of 20% used traditionally in safety assessment. Unfortunately, there are not enough data and currently no consensus over the release mechanism of C-14 from the oxide layer to abstract this hypothesis in quantitative safety assessment. Consequently, an IRF of 20% is considered in *Case Org* to represent the early fast release of C-14 supposed to be in the oxide layer. Note that the IRF is conservatively applied to the whole C-14 inventory of the CSD-C waste, thus also to the C-14 fraction in the stainless steel of the structural pieces sliced and included in the waste form, although results from CAST have confirmed that a negligible IRF can be considered for steel (on the contrary to Zy-4, the oxide layer of steel is thin and dense).

Congruent release with corrosion could not be demonstrated in CAST due to the very low rates measured. Congruency is actually uncertain since measurements on LWR hulls suggest that the C-14 concentration in the oxide layer is roughly two to four times its concentration in the bulk metal (Gras, 2014). However, we consider that the IRF of 20% covers this uncertainty as well as the possible fast release from shearing fines of small dimensions (< 200 µm) assumed to represent less than 1% of the ONDRAF/NIRAS CSD-C inventory.

The next cases illustrate the impact of three factors: The inventory uncertainty, the release rate and the potential retention effect in the host formation if C-14 is in the form of carboxylic acids.

Experimental data on C-14 inventory in Zy-4 cladding materials show that, on average, actual C-14 content in high burn-up claddings is rather representative of nitrogen content of 20-40 ppm, that is, at least twice lower than the specifications (Capouet, Boulanger, Vandoorne, Gaggiano, Norris, Williams, Schumacher, Rübel, Nummi, Poskas, Narkuniene, Grigaliuniene, Vokál *et al.*, 2017). This effect is represented in the calculation *case N/2*.

Corrosion rates on irradiated Zy-4 samples in CAST show contrasted results that are not in line with the literature: Rates up to 100 nm/y were measured. These high measured values could be assigned to the use of electrochemical methods, which are known to overestimate the actual corrosion rate. Additional measurement studies in irradiation conditions are required to clarify the discrepancy between these data and the literature. *Case CR* investigates the effect of a shorter cladding lifetime resulting from such a high corrosion rate. No IRF is considered in this case.

Different chemical specifications are then tested. A literature study as well as experimental works performed by PSI and Nagra suggest that small oxygenated, i.e. carboxylic acids could exhibit a weak retention in clay and in the cementitious environment (Capouet, Boulanger, Vandoorne, Gaggiano, Norris, Williams, Schumacher, Rübel, Nummi, Poskas, Narkuniene, Grigaliuniene, Vokal *et al.*, 2017). In this sensitivity analysis, *Case Kd_4* is performed to investigate the impact of possible release of carboxylic acids by assuming a Kd of 1×10^{-4} m^3/kg. An alternative case *Case IRF_100* is also considered where the C-14 inventory is assumed to be released instantaneously. This case addresses the release of C-14 due to the formation of zirconium hydrides in disposal conditions resulting potentially in different corrosion or release behaviours. This perturbation cannot be totally excluded currently.

Table 2: Cases considered in the sensitivity analysis. "Inv", "LT", "IRF" and "D" stands for inventory, CSD-C waste matrix lifetime, instant release fraction and diffusion coefficient, respectively.

Base case	**Inv.: 6.1 x 10^{13} Bq, LT=27500 years, IRF: 0%, D(carbonate)**
Case Org	Hypothesis *base case* with D(methane), LT=50000 years, IRF:20%
Case CR	Hypothesis *Case Org* with LT=1500 years, IRF:0%
Case N/2	Hypothesis *Case Org* with Inv/2
Case Kd_4	Hypothesis *Case N/2* with Kd: 1 x 10^{-4} m^3/ kg
Case IRF_100	Hypothesis *Case Org* with IRF: 100%

1.3 *Results and discussions*

The activity flux of C-14 released at the top boundary of the host formation (travelled distance is 40 meters) is represented in Figure 2. The large sensitivity of the results is due to the fast decay of the radionuclide.

The organic speciation of C-14 shows the most important impact. The flux increases by more than two orders of magnitude with respect to the previous safety assessment case where C-14 was considered in its inorganic form. The lifetime of the waste form influences the activity flux for values higher than a few tens of thousands of years, which means for Zy-4 corrosion rates below 10 nm/y. As illustrated by the case (*CR*), a short lifetime of 1500 years (corresponding to about 100 nm/y) has almost no impact on the C-14 flux.

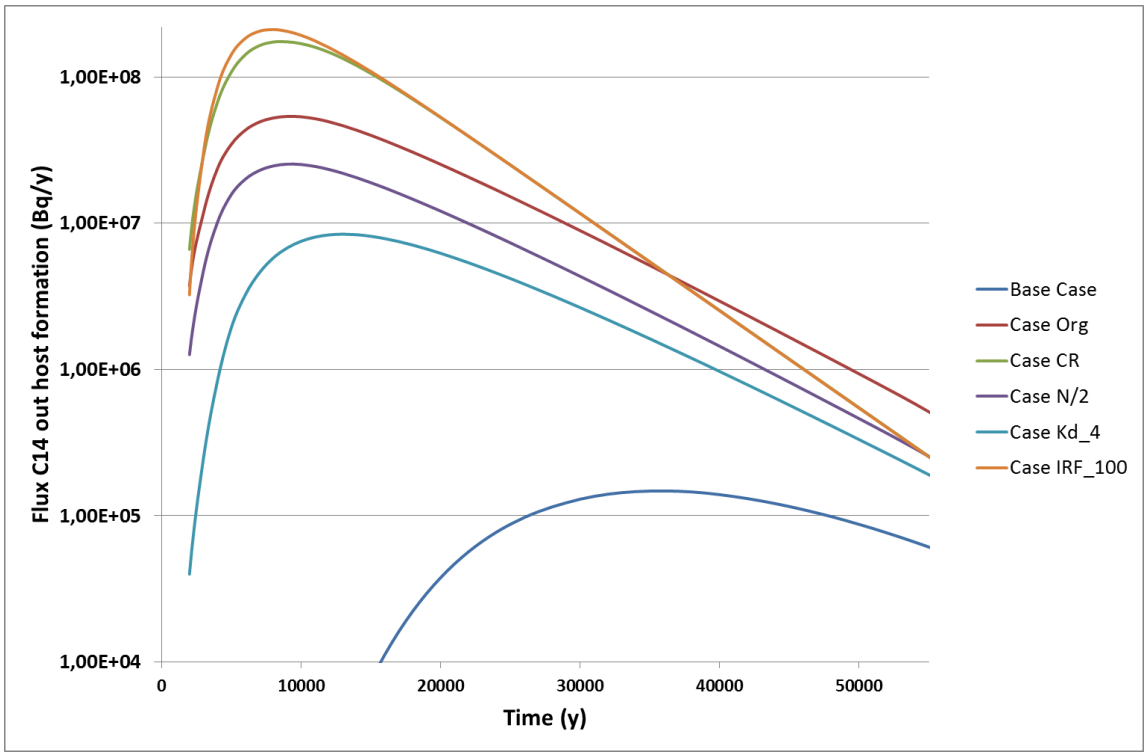

Figure 2: Sensitivity analysis of C-14 flux at the top of the host formation

The CAST results suggest that the release rate of C-14 from the oxide layer of the hull could be controlled by diffusion processes or by the solubility of zirconia (Gras, 2014; Sakuragi *et al.*, 2016). From a safety assessment point of view, a C-14 diffusion through the oxide layer should have an unrealistic high characteristic time to affect the hypothesis of congruent release with the corrosion. The solubility of the zircaloy oxide seems to be around 10^{-6} mol/l at pH=12. It increases with higher alkalinity (Gras, 2014). The mass of Zr is about 500 kg per CSD-C primary waste (4500 moles). It results that even a very limited solubility of Zr oxide, orders of magnitude higher than current estimations, would be sufficient to hinder the zircone dissolution and ensure a complete decay of C-14 in the metal mass. Modelling the release of C-14 controlled by Zy-4 corrosion and Zy oxide dissolution would be a more consistent representation than the current modelling, based solely on the corrosion rate.

The alternative *case N/2,* based on a more realistic inventory is indicative of a minimum safety margin with a more realistic, averaged, estimation of the inventory.

Although there are evidences of retention of small oxygenated organics in clay and cement, in particular the carboxylic acids, there are currently no firm results in CAST to support a release of these species in the long-term in disposal conditions. A Kd of at least 10^{-4} mol/l in Boom Clay would be necessary to obtain a sizeable effect of the retention in clay on the radioactive flux at the clay boundary.

2 Integration of the CAST experimental outcomes at the level of the safety case.

The experimental results of CAST have improved the knowledge regarding different factors influencing the C-14 source term. First, the experimental results of CAST reveal the presence of a non-negligible fraction of organic C-14 compounds in the four waste materials investigated. This conclusion has important consequences in the ONDRAF/NIRAS safety case, since, on this basis, C-14 will be considered to be released as an unretarded organic species (methane) from Zircaloy and steel waste in safety assessment of a geological disposal. The impact of C-14 as gaseous species needs to be investigated by ONDRAF/NIRAS in specific advective scenarios where hydrogen gas produced from the metal corrosion might act as a radionuclide carrier.

Next to the C-14 speciation, the investigation of the release rate of C-14 in CAST has allowed an important reduction of the uncertainty on the corrosion rates of both Zircaloy and, carbon and stainless steels. Very low rates are confirmed in reducing conditions. In particular, the understanding of the claddings degradation in disposal conditions has increased. There are indications of the capacity of the oxide layer to retain C-14. CAST results suggest that C-14 release is controlled by the corrosion of the Zy metal and a slow subsequent processes taking place in the oxide layer (diffusion or dissolution). If this conceptualisation is validated, C-14 would decay in the metal mass before being released.

The integration of the CAST outcomes at the level of the ONDRAF/NIRAS safety case shows a contrasted picture: Accounting for the organic speciation of C-14 from steel and Zircaloy in safety assessment scenarios results in a higher impact on long-term safety compared to

previous studies. However, this quantitative evaluation has to be put in perspective with the phenomenological understanding of C-14 release mechanisms. This knowledge has greatly improved in CAST. There are qualitative arguments suggesting an extremely slow and low C-14 release from steel and Zircaloy in disposal conditions. These arguments are indicative of the safety margin taken in safety assessment scenarios. With CAST, the quantitative impact of C-14 on long-term safety has increased, but also the confidence that this impact is extremely conservative.

References

Aertsens M., Dierckx A., Moors H., De Cannière P. and Maes N. (2010). Vertical distribution of H14CO3- transport parameters in Boom Clay in the Mol-1 borehole and comparison with data from independent measurements. SCK•CEN. External Report ER-66.

Capouet M., Boulanger D., Vandoorne T., Gaggiano R., Norris S., Williams S., Schumacher S., Rübel A., Nummi O., Poskas P., Narkuniene A., Grigaliuniene D., Vokal A., Mibus J., Rosca-Bocancea E., Hart J., Ferrucci B., Levizzari R., Luce A., Diaconu D., Cunado Peralta M., Owada H., Kienzler B., Wieland E., Van Loon L. and Walke, R. (2017). Knowledge supporting Safety Assessments of 14C. CAST D6.2.

Gras J.-M. (2014). State of the art of 14C in Zircaloy and Zr alloys - 14C release from zirconium alloy hulls. CAST report D3.1.

Jacops E., Wouters K., Volckaert G., Moors H., Maes N., Bruggeman C., Swennen R. and Littke R. (2015). Measuring the effective diffusion coefficient of dissolved hydrogen in saturated Boom Clay. Applied Geochemistry **61**, 175–184.

Kato O., Tanabe H., Tomofumi S., Tsutomu N. and Tsuyoshi T. (2014). Corrosion Tests of Zircaloy Hull Waste to Confirm Applicability of Corrosion Model and to Evaluate Influence Factors on Corrosion Rate under Geological Disposal Conditions. Mater. Res. Soc. Symp. Proc **1665**.

Kienzler B., Metz V., Duro L. and Valls A. (2013). 2nd Annual Workshop Proceedings of the Collaborative Project "Fast / Instant Release of Safety Relevant Radionuclides from Spent Nuclear Fuel." KIT SCIENTIFIC REPORTS 7676.

Maeda T., Chiba N., Yamaguchi T. and Tateishi T. (2014). Consideration on application of empirical corrosion rate model of Zircaloy at 280-400 °C to deep underground temperature. Corrosion Engineering, Science and Technology **49** (6).

Necib S., Mibus J., Diomidis N. and Capouet M. (2017). Work packages 2&3 meeting Minutes. European Commission, CAST project. Minutes of Meeting CAST-2017-29032017.

ONDRAF/NIRAS. (2016). Présentation de l'inventaire technique des déchets radioactifs 2016, note 2017-0752, 27/03/2017.

Sakuragi T., Ueda, H., Kato O., Yoshida, S., Tsuyoshi T. and Yamashita Y. (2016). Corrosion behavior of irradiated and non-irradiated zirconium alloys: investigations on corrosion rate, released ^{14}C specie, and IRF, poster presentation, Final symposium in Lyon.

Sakuragi T., Yamashita Y., Akagi M. and Takahashi R. (2016b). Carbon 14 Distribution in Irradiated BWR Fuel Cladding and Released Carbon 14 after Aqueous Immersion of 6.5 Years. Procedia Chemistry **21**.

Tanabe H., Sakuragi T., Miyakawa H. and Takahashi R. (2014). Long-Term Corrosion of Zircaloy Hull Waste under Geological Disposal Conditions: Corrosion Correlations, Factors Influencing Corrosion, Corrosion Test Data, and Preliminary Evaluation. Mater. Res. Soc. Symp. Proc **1665**.

Vandoorne T. (2016). Calculation of spent fuel and reprocessing waste inventory for SFC-1. ONDRAF/NIRAS. NIROND Note 2017–1497.

PART 2 – Crystalline host rock

CArbon-14 Source Term

CAST

Integration of CAST results to safety assessment: Contribution from FORTUM to D6.3

Nummi, O.

Date of issue of this report: 08/1/2018

Executive Summary

The safety assessment calculations rely on the scientific understanding of barrier performance and radionuclide migration as well as on the conservative assumptions to account for the uncertainties. The increased understanding of the C-14 release and transport gathered during the CAST project will be transferred to the safety case for the Loviisa LILW repository. The impacts of the CAST results are qualitatively discussed here along with a more quantitative sensitivity analysis describing the impacts of C-14 speciation and sorption.

The sensitivity analysis focuses is on the spent ion-exchange resins which are solidified with concrete and surrounded by concrete barriers. The results clearly demonstrate that the organic C-14 is released more rapidly than the inorganic C-14 due to its weaker - but non-negligible - sorption onto cement and backfill. Since the organic fraction forms a considerable proportion of the C-14 released, it governs the whole C-14 release. Similar behaviour is expected in case of activated steel parts, although the steel corrosion rate has a major impact on the overall release rate and majority of C-14 are released as organic species. The increased understanding of C-14 sorption on cement and host rock as well as transport in biosphere also reduces the C-14 related uncertainties.

List of Contents

1 FORTUM: Modelling ^{14}C in disposal systems

1.1 *Introduction*

The Loviisa low and intermediate level waste (LILW) repository is located at the Loviisa NPP site, approximately 80 km East of Helsinki. The on-site repository for the operational waste from the Loviisa NPP has been excavated in crystalline bedrock at the approximate depth of 110 m and has been in operation since 1998. The caverns for the decommissioning waste from Loviisa NPP will later be licensed and excavated as an extension of the repository as shown Figure 1. The repository hosts different types of waste caverns: maintenance waste halls, solidified waste hall, decommissioning waste halls, primary circuit component hall and two pressure vessel silos. At the closure, the crushed rock backfilling and concrete plugs at the entrance of the waste caverns and along the access tunnel and shafts will be set in place.

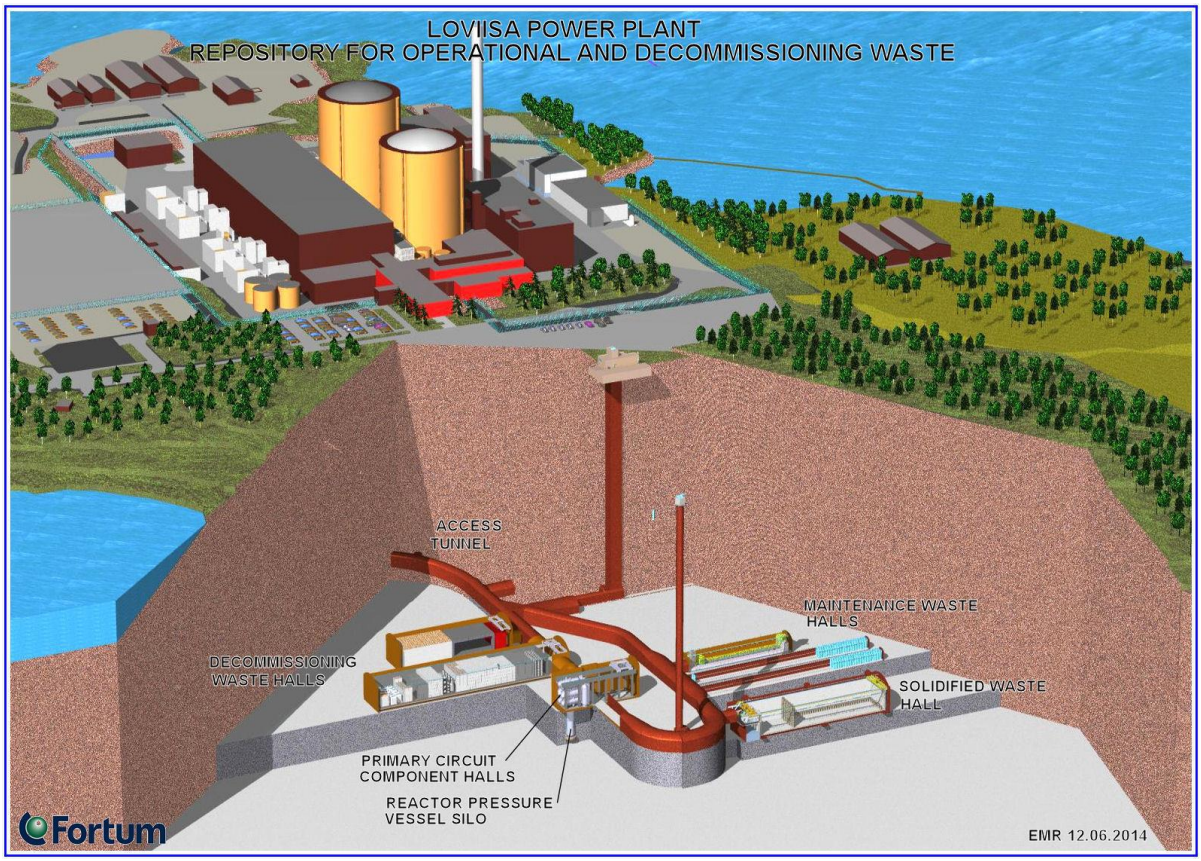

Figure 1: The LILW repository located at Loviisa NPP site. The existing waste caverns of the operational waste are located on the right side of the connection tunnel, whereas the future decommissioning waste caverns are located on the left.

1.2 *Model description*

The majority of the C-14 in the repository resides in the activated metal parts and, to a lesser extent, in the spent ion-exchange resins. The modelling described here focuses on the C-14 released from the spent ion-exchange resins. To highlight the impact of the C-14 release and speciation, the modelling is simplified to make the model more transparent and easier to communicate. All carbon C-14 is assumed be released and migrated in dissolved form. A proportion of C-14 can be released gaseous form, but its migration is assumed to be rather similar to that of organic C-14 in dissolved form due to low sorption. For simplicity, the modelling endpoint is chosen to be the release rates into bedrock.

The modelling focuses on features governing the release and transport of C-14: activity content, release rate, speciation and sorption. Their impact is studied in deterministic calculation cases to provide a relatively simple and transparent view of the modelling and the factors affecting the results. Probabilistic modelling would explore the combined impacts of various uncertainties in more detail, but would lead to a more complex description of the modelling outcomes. The calculations are carried out specifically for this report and differ from those in the previous or upcoming safety assessments.

1.3 *Solidified ion-exchange resins*

The spent ion-exchange resins are solidified in concrete containers by mixing the resins with cement. The containers will be emplaced inside a concrete basin and the empty space between the cylindrical containers will be backfilled with concrete. The waste form, containers, concrete filling and the basin are assumed to constitute a massive concrete block that limits the groundwater flow through it. Thus, the radionuclide release is mainly diffusive and limited by the properties of the concrete. Eventually, concrete degradation will accelerate both the diffusive and advective release.

Here the modelling is based on two compartment description of the solidified waste hall (see Figure 2). The first compartment is inside the basin and assumes waste matrix, containers and concrete filling to form a rather homogenous and sorbing medium. The second compartment outside the basin is backfilled with crushed rock and also provides sorption. The transport between these two compartments is governed by diffusion and advection. The groundwater flow to the bedrock governs the release from the backfill into the bedrock.

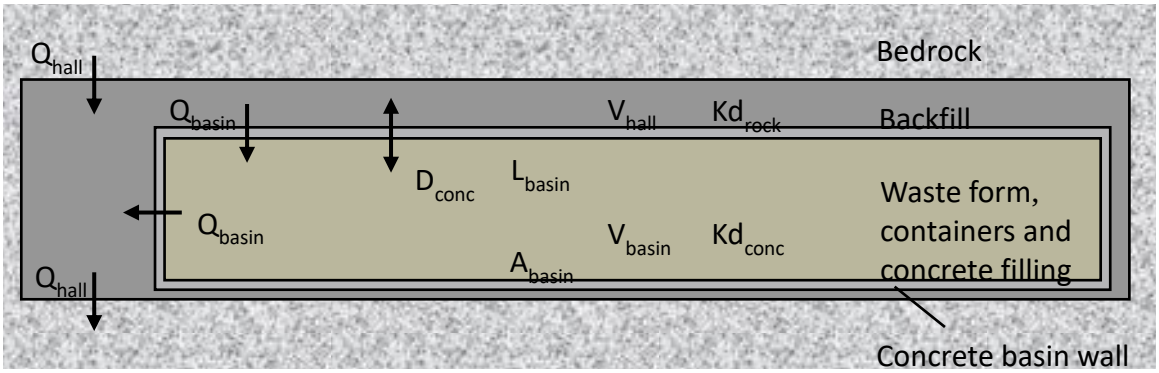

Figure 2: Conceptual model of C-14 release from inside the concrete basin into backfill and furthermore into bedrock. The figure indicates the main processes (Q stands for groundwater flow and D for diffusion) governing the release and parameters affecting the release (L=thickness, A=area, V=volume and Kd=distribution coefficient). The parameters and their values are further explained in Table 1.

The groundwater flow through solidified waste hall and the concrete basin results from a separate groundwater flow modelling. The groundwater flow through the hall is here assumed to remain constant, although in reality it will be increased by degradation of the closure materials and altered by the land uplift and the global sea level change. Despite the constant groundwater flow through the hall, the proportion of groundwater flowing through the basin increases due to the chemical degradation of concrete and especially the concrete fracturing. The time dependent effective diffusion coefficients and hydraulic conductivities (based on which the groundwater flows have been calculated) in concrete are adapted from [SKB 2014].

The C-14 released from the solidification product is divided into organic and inorganic parts, based on the earlier measurements from the ion-exchange resins. The distribution coefficients for organic C-14 originate from sensitivity analysis guidance, whereas the distribution coefficients for inorganic C-14 are taken from [SKB 2014].

Table 1: Parameters used in modelling the release from the solidified ion-exchange resins in the solidified waste hall. The ranges of parameters that a varied are given in parenthesis.

C-14 parameters	**C-14 organic**	**C-14 inorganic**
Initial activity (GBq)	75 (0…500)	425 (0…500)
Distribution coefficient in concrete, Kd_{conc} (m^3/kg)	$1 \cdot 10^{-4}$ ($1 \cdot 10^{-5}$…$1 \cdot 10^{-3}$)	0.2 (0.5…5)
Distribution coefficient in crushed rock, Kd_{rock} (m^3/kg)	$1 \cdot 10^{-4}$ ($1 \cdot 10^{-5}$…$1 \cdot 10^{-3}$)	$1 \cdot 10^{-3}$ ($1 \cdot 10^{-4}$…$1 \cdot 10^{-2}$)
Diffusion coefficient in concrete (m^2/s)		
- 0…100 a	$3.5 \cdot 10^{-12}$	
- 100…10 000 a	$1 \cdot 10^{-11}$	
- 10 000…20 000 a	$5 \cdot 10^{-11}$	
- 20 000…100 000 a	$1 \cdot 10^{-10}$	
Groundwater flow through	**the hall, Q_{hall} (m^3/a)**	**the basin, Q_{basin} (m^3/a)**
- 0…10 000 a	2.50	0.01
- 10 000…20 000 a	2.50	0.11
- 20 000…100 000 a	2.50	1.10
Parameters related to geometry		
Water filled volume in the hall, V_{hall} (m^3)	1108	
Water filled volume inside the basin, V_{basin} (m^3)	2000	
Concrete basin wall thickness, L_{basin} (m)	0.6	
Concrete basin wall area, A_{basin} (m^2)	3770	

1.4 *Results and discussions*

The resulting release rates from solidified ion-exchange resins, in Figure 3, indicate that overall C-14 release rate is controlled by the organic species. The release of inorganic species is effectively retarded by the sorption in concrete and furthermore into backfilling material (crushed rock). Also, the advective release appears to be insignificant compared to the diffusive release indicating that the concrete basin fulfils its safety function to limit the groundwater flow through it.

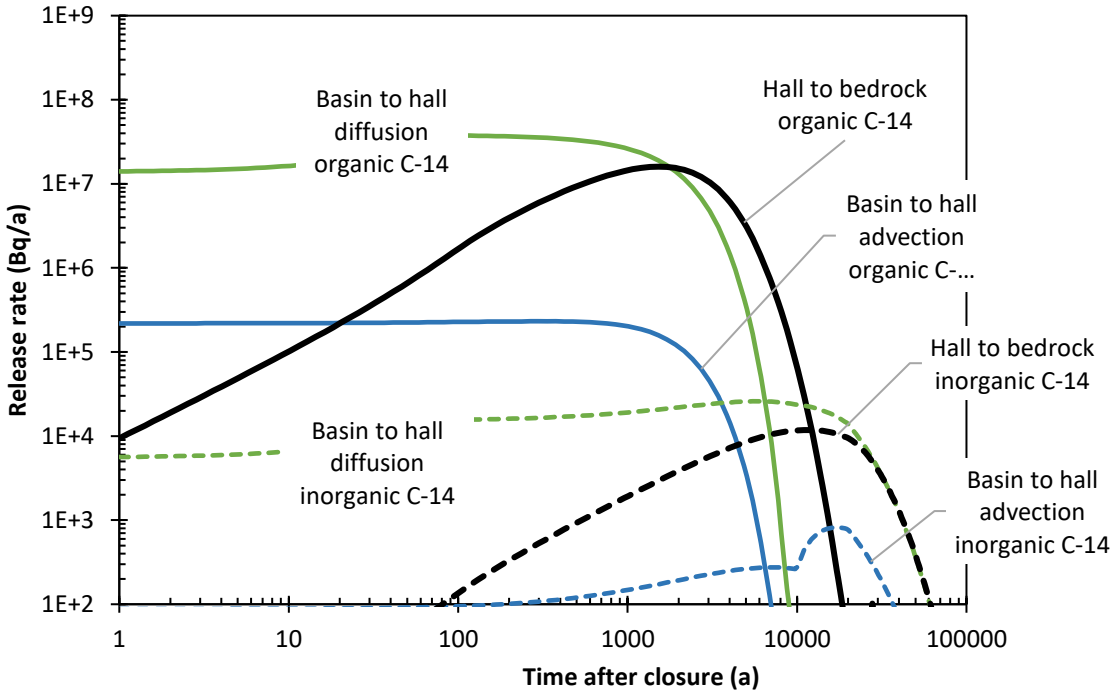

Figure 3: Resulting release rates from basin to hall and from hall to bedrock in the reference case. The organic C-14 (solid lines) is released considerably faster compared to the inorganic C-14 (dashed lines) due to the higher sorption of inorganic C-14. Also the advective release is small compared to the diffusive release.

The importance of the C-14 speciation and sorption into concrete and crushed rock are analysed in various sensitivity cases described in Table 2. The sensitivity cases have been selected to highlight the importance of the C-14 related parameters and their combined effects.

Table 2: Description of the different calculation cases for the release from the ion-exchange resins.

Calculation case	Difference from the reference case
All organic	All C-14 is assumed to be in organic form
All inorganic	All C-14 is assumed to be in inorganic form
Low Kd	Distribution coefficients to rock and concrete are selected from the lower end of their ranges
High Kd	Distribution coefficients to rock and concrete are selected from the higher end of their ranges
No Kd rock	No sorption to crushed rock is assumed
No Kd concrete	No sorption to concrete is assumed
No Kd	No sorption to crushed rock or concrete is assumed

The temporal behaviour of the sensitivity cases is rather similar to the reference case; hence only the maximum release rates are shown in Figure 4. The difference between the organic and inorganic species is several orders of magnitude, highlighting the importance of the C-14 speciation. The uncertainty in the distribution coefficient values appears also to be important factor, but the range is smaller than between the different C-14 species.

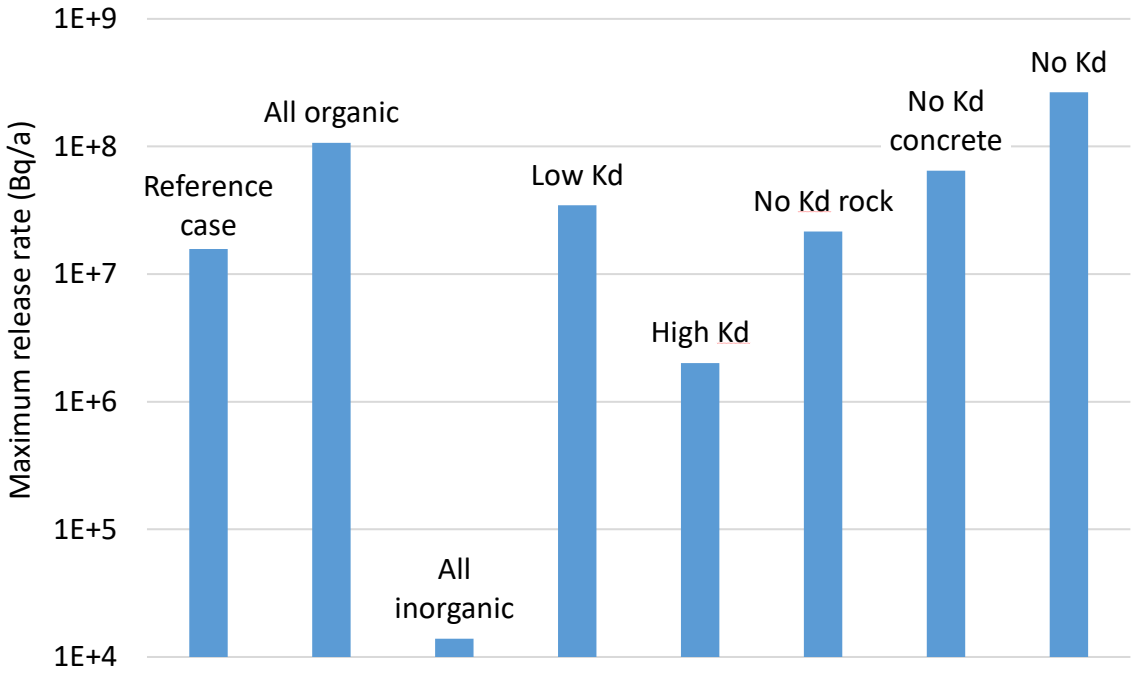

Figure 4: Maximum releases rates into bedrock in all calculation cases. The calculation cases are explained in Table 2.

The model assumes an instant release from the waste matrix. The slower release rate would (i) reduce the overall release rates and (ii) possibly enhance the difference between organic and inorganic release rates. Furthermore, the simplified compartment model is considered to be mostly conservative and more detailed modelling is expected to result in lower release rates.

2 Integration of the CAST experimental outcomes at the level of the safety case

The aim of research and development in the context of the radioactive waste disposal is to demonstrate - with increasing confidence - that the disposal is safe. To achieve this, uncertainties and their impacts need to the reduced which has also been the aim of the CAST project. In this chapter, the outcomes of the project and their impacts to the Loviisa safety case are discussed.

Despite the related uncertainties, the C-14 activity content or its speciation does not as such give rise to a formulation of different scenarios, because the scenarios - in the Finnish regulatory context [STUK 2014] - describe the performance of the disposal system, not the radionuclide release. The factors affecting the C-14 release and migration are being varied inside various scenarios both in the deterministic and probabilistic modelling.

While the exact chemical form of the C-14 has been determined in many experiments, the safety case for Loviisa LILW repository does not address them directly, but groups them into 'organic' and 'inorganic' species to increase the robustness of the analysis.

2.1 *Spent ion-exchange resins*

At Loviisa NPP, the C-14 inventory of solidified ion-exchange resins has been determined based on direct measurements. The C-14 activity in carbonate form was first determined using acid treatment after which the residual C-14 activity was measured by incineration. The exact composition of the residual C-14 is not known, but it is most likely organic. The main uncertainties in the inventory are due to uncertainties in the measurements of C-14 in the ion-exchange resins and variability between the samples. As a result, 15 % of C-14 was assumed organic and the remaining 85 % inorganic.

The CAST results indicate a large variability in organic C-14 proportion between resins used the PWR and BWR reactor types: in PWR resins the organic C-14 proportion can be tens of

percents, whereas in the BWR resins the corresponding proportion is typically only few percent [Rizzato et al. 2014, Aronsson et al. 2016]. There is also variability between different power plant units and resulting from the different treatment of the spent ion-exchange resins.

Overall the CAST results from the spent ion-exchange resins support the earlier measurements of Loviisa NPP ion-exchange resins, thus providing more confidence in the results. However, the variability both in the Loviisa measurements and in the results provided by CAST indicate that the organic proportion is not necessarily conservative and may need to be increased. To capture the uncertainty in the proportion of organic species, a range or probability distribution will be established for the probabilistic modelling.

Another uncertainty results from the C-14 release during the storage and solidification: to which extent are the different C-14 species released during these phases prior to disposal and does it affect the amount of C-14 in any way.

The C-14 release rate from the solidification product is rather specific to the solidification method used. Currently the available data regarding this is sparse and definite conclusions cannot be drawn. Thus, as discussed above, the both C-14 species are conservatively expected to be released from solidification product rather easily, i.e. they are not bound to the waste matrix. However, the waste matrix retards the C-14 release, especially the inorganic species.

2.2 *Activated steels*

The activation calculations at Loviisa NPP have been carried out using MCNP calculation and nitrogen impurity content of 0.04 - 0.14 % in steels were used [Eurajoki & Ek 2008]. The main uncertainties in the C-14 activation calculations are due to material properties, especially the nitrogen content in the steel components. The most activated components are reactor internals and, to a lesser extent, the reactor pressure vessel. The speciation was highly uncertain; thus all C-14 was assumed to be released in organic or gaseous forms. The corrosion rates of stainless steel were assumed to lie between 0.01 - 1 μm/a depending on the pH conditions and the degree of conservatism.

A literature review carried out within CAST [Swanton et al. 2015] indicates a fairly low corrosion rate under alkaline and anoxic conditions. Based on recent experiments:

- uniform corrosion rate of carbon steel is clearly below 100 nm/y and
- uniform corrosion rate of stainless steel is clearly below 10 nm/y.

This supports earlier assumptions and allows for even lower corrosion to be used in the safety assessment.

The speciation of released C-14 was found to the mainly organic, thus supporting the earlier conservative assumption. While this new information does not give rise to a reduction in the C-14 release rates, the uncertainty in the C-14 speciation is considerably reduced. The CAST results are limited to an early corrosion period (six months), whereas the steady state low corrosion rate can be assumed only after a few years. Whether this affects the speciation of C-14 released remains uncertain. No indication of instant release was found in the experiments which supports the earlier assumptions.

2.3 *Migration of C-14*

CAST is a source term project and does not directly address the C-14 migration. However, to provide a more comprehensive picture of the C-14 also these aspects were touched within the CAST [Capouet et al. 2017].

In the previous safety assessments, no sorption of organic C-14 was assumed, but according to new measurements, a low sorption in to concrete has been measured. While there are uncertainties in the distribution coefficient of organic C-14 (partly because distribution coefficient is a lumped parameter), the measured values provide a considerable advance compared to the previously applied conservative assumption. According to the results discussed in section 1.4, the introduction of distribution coefficient for organic C-14 reduces the maximum release rates by a factor of three. The sorption of organic C-14 is also excepted to retard its migration through the bedrock, but to a lesser extent due to the relatively fast groundwater flow in the bedrock.

Also the C-14 treatment in the surface environment (biosphere) will be improved compared to the previous modelling. According to [Capouet *et al.* 2017] almost all C-14 that has migrated to the soil layers will be transformed to CO_2. The plants can uptake this CO_2 via photosynthesis or directly through the plant roots.

References

ARONSSON, P.-E., LILLFORS-PINTÉR, C. AND HENNING, Å. 2016. C-14 Accumulated in Ion Exchange Resins in Swedish Nuclear Power Plants. Part 1: Results from Analyses and Calculation of Accumulation Factors based on Samplings 2008-2015. Version 8.

CAPOUET, BOULANGER, GAGGIANO, NORRIS, WILLIAMS, SCHUMACHER, NUMMI, POSKAS, NARKUNIENE, GRIGALIUNIENE, VOKÁL, MIBUS, ROSCA-BOCANCEA, HART, FERRUCCI, LEVIZZARI, LUCE, DIACONU. CUÑADO PERALTA, KIENZLER, WIELAND, VAN LOON AND WALKE 2017. Knowledge supporting Safety Assessments of ^{14}C, CAST report D6.2.

EURAJOKI, T. 2006. Loviisa Low and Intermediate Level Waste Repository, Safety Case. *Fortum Nuclear Services Oy, Espoo, Finland*, Report LOKIT-5243.

EURAJOKI, T. 2008. Loviisa NPP Safety Case for the Final Disposal of the Decommissioning Waste. *Fortum Nuclear Services Oy, Espoo, Finland*, Report TJATE-G12-114.

EURAJOKI, T. & EK, M. 2008. Loviisa NPP, Decommissioning Plan 2008, Activity Inventory. Report TJATE-G12-104. *Fortum Nuclear Services Oy, Espoo, Finland.*

SWANTON, S.W., BASTON, G.M.N. AND SMART, N.R., 2015. Rates of steel corrosion and carbon-14 release from irradiated steels - state of the art review. *AMEC*, CAST report D2.1.

RIZZATO, C., RIZZO, A., HEISBOURG, G., VEČERÍK, P., BUCUR, C., COMTE, J., LEBEAU, D., AND REILLER, P. E. 2014. State of the art review on sample choice, analytical techniques and current knowledge of release from spent ion-exchange resins (D4.1). CAST report D4.1.

SKB 2014. Data report for the safety assessment SR-PSU. Technical report TR-14-10. Svensk Kärnbränslehantering AB (SKB), Stockholm, Sweden.

STUK 2014. YVL Guide D.5. Disposal of nuclear waste. Radiation and Nuclear Safety Authority, Helsinki, Finland. Available at http://www.finlex.fi/data/normit/41785-YVL_D.5e.pdf

CArbon-14 Source Term

CAST

Integration of CAST results to safety assessment: Contribution from INR to D6.3

Daniela Diaconu, Alina Constantin, Crina Bucur

Date of issue of this report: 20/11/2017

Executive Summary

Romania operates in open fuel cycle two CANDU 600 units. The spent fuel (SF) and the long-lived intermediate level waste (ILW-LL) are foreseen to be disposed of in a geological repository starting with 2055. Since no host rock was yet selected, the in-house safety assessments are aimed to the comparison of different types of rocks from the point of view of their performances as repository host rock. The modelling is based on a generic concept similar to the Canadian one. The previous simulations used as input data assumptions and values from the Canadian studies.

As C-14 plays an important role in the total annual dose, any improvement in C-14 source term can decrease the associated uncertainty. Therefore, as part of the CAST project, INR continued to elaborate on the performance assessment of SF disposal in granite, refining and updating the input data related to C-14 inventory and release. Based on the updated model, the sensitivity analysis followed the influence on the total dose summing the biosphere pathway of:

- the C-14 instantaneous release fraction from UO_2;
- the C-14 release rate from Zy-4;
- the organic/inorganic ratio in the C-14 release from Zy-4 claddings;
- the diffusivity coefficient in bentonite and granite;
- the Kd in bentonite and granite.

The sensitivity analysis (addressing only C-14 from spent fuel) pointed out that the most sensitive parameters are the IRF from the UO_2 pellets and the Kd in bentonite.

Apart of the model update, the results of the experimental work on the C-14 content and release from Zy-4 claddings and SIERs from Cernavoda NPP done by INR in CAST will be used to improve the C-14 inventory for geological development.

The values obtained on Zy-4 samples irradiated in the Romanian NPP showed a very good correlation with the ORIGEN calculations, increasing the confidence in the total inventory of

C-14 in the Zy claddings. Using these data, the new safety assessments, presented in this study, included therefore more realistic values for the C-14 inventory in Zy-4 claddings.

Experimental data on C-14 release from Zy-4, SIER and graphite contributed to a better understanding of the governing processes and provided the first data on the organic/inorganic ratio of C-14 released in liquid phase, in alkaline conditions. Based on data obtained on irradiated Zy-4, the new calculations made in CAST included C-14 speciation, considering the experimental values as a reference case, and differentiated for the first time the radiologic impact of CO_2 and CH_4.

List of Contents

1 INR: Modelling C^{14} in disposal systems

1.1 *Introduction*

Currently, Romania operates in an open fuel cycle two CANDU 600 units. According the Energy Strategy, other 2 CANDU Units are planned to be completed on the Cernavoda NPP site in the coming years. Recently it was decided the refurbishment of Unit 1 for an extended life time up to 40 years. According to the Romanian strategy for radioactive waste management, the spent fuel shall be disposed of in a geological repository [ANDRAD, 2004] started with 2055.

As result of a desk research screening, six different types of host rock have been identified as suitable for a deep geological repository but no decision has been taken on site selection approach yet. Nevertheless, one aspect will be the safety performance of the host rock for a generic concept of the repository.

The first safety assessments were made for spent fuel disposal in salt [Pavelescu et al., 2003] and granite [Buhmann et al., 2003]. Both considered a generic concept of the repository similar to the Canadian one [Capouet, 2015], using as input data the results of the ORIGEN simulations [NWMO, 2012], but only the later one considered C-14 in the inventory (Figures 1 and 2).

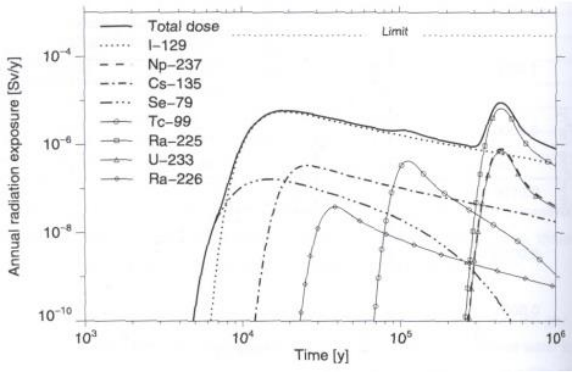

Figure 1: Total dose evolution for geological disposal of CANDU SF in salt (generic concept) [Pavelescu et al., 2003]

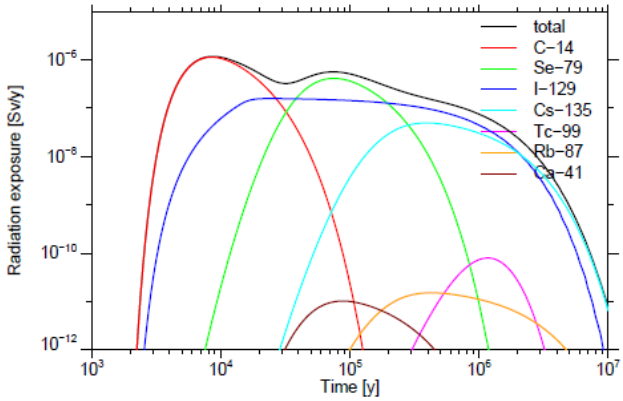

Figure 2: Total dose evolution for geological disposal of CANDU SF in granite (generic concept) [Buhmann et al., 2003]

As part of the CAST, INR continued to elaborate on the performance assessment of SF disposal in granite, refining and updating the input data related to C-14 inventory.

The disposal system considered in the calculations consists in a deep geological repository in granite, in which double-walls canisters in steel and cupper containing the spent fuel boundless are emplaced in vertical boreholes buffered by compacted bentonite (similar to the Canadian concept). Bentonite-based materials are used to backfill and seal the repository. Excavation disturbed zones with different lengths/depths surround the main galleries and the boreholes.

The wastes considered in these calculations were the CANDU spent fuel generated by 2 Units during 40 years of operation. The total C-14 inventory was based on ORIGEN calculations, including the decay corresponding to 50 years of wet and dry storage [NWMO, 2012].

The scenarios considered in this study included for the first time the C-14 speciation, in particular the organic/inorganic ratio for the Zy-4 claddings, using experimental data obtained on irradiated Zy-4 regarding corrosion, C-14 release and speciation.

The sensitivity analysis considered the influence on the total dose accumulated by ingestion by a member of the critical group of:

- the C-14 instantaneous release fraction from UO_2
- the C-14 release rate from Zy-4;
- the organic/inorganic ratio in the C-14 release from Zy-4 claddings
- the diffusivity coefficient in bentonite and granite;
- the Kd in bentonite and granite

The modelling is done in the framework of a first development and implementation of an in-house safety assessment model, as preliminary work for the host rock selection.

1.2 *Model description*

1.2.1 Conceptual description of the model

CANDU spent fuel generated by 2 Units operating 40 years and stored for minimum 50 years are disposed of in a deep geological repository in granitic rock, at 500m depth. The closest fractures to the repository are located at 50m from the lateral disposal cells. The fractures lead directly to the aquifer, placed 400 m above the repository, which supplies the well used for water consumption by the critical group.

A number of 1350 steel/cupper canisters are emplaced in vertical bore holes. The compacted bentonite saturates and prevents the cupper degradation for 1500 years.

After 1500 years, the barrier effect of the canister and cladding fails, and the C-14 immediately releases into the volume of dissolution both from the Zy-4 and UO_2.

A small fraction of C-14 is released instantaneously from the fuel pellets, the rest of it being released at a constant rate equal to the UO_2 degradation rate; all C-14 is considered to release in an inorganic form, dissolved in the pore water. In the same time, a small amount of the C-14 from the oxide layer of the fuel cladding releases rapidly; the rapid release is followed by a constantC-14 release equal to the Zy-4 corrosion rate. Both organic and inorganic C-14 compounds are released during the two stages (instantaneous release phase and congruent release phase), in the same proportion. Compared to the previous model, the scenario on the C-14 from Zy-4 introduces the IRF as proved by the leaching experiments on cladding samples performed under CAST project.

The two C-14 species considered ($^{14}CO_2$ and $^{14}CH_4$) are transported in liquid phase by diffusion through the bentonite buffer and granite matrix and by advection through the EDZ and the granite fractures. The diffusion coefficients in bentonite and respectively in granite are different for the two C-14 species. No sorption was considered for methane (neither in bentonite, nor in granite) and distinct Kd was assigned for CO_2 in bentonite and granite.

The ratio organic/inorganic leaving the repository is not affected by biological processes.

Once arrived in the shallow aquifer, the C-14 dilutes. A well drilled in this aquifer supplies with water a critical group established above the repository. The members of the group drink water and use it to irrigate crops and cereals and to grow cows, and to prepare meals. The plants will uptake the $^{14}CO_2$ through their roots and canopy, entering into the entire food chain, contributing therefore to the ingestion pathway, while the $^{14}CH_4$ will be released into the atmosphere, contributing to the ingestion pathway only with the CH_4 still dissolved in water, and to the inhalation pathway.

Since ingestion pathway is the most important contributor to the total annual dose, only this pathway was considered in the sensitivity analysis performed under this study.

The GOLDSIM simulations modelled one canister with the surrounding bentonite, EDZ, fracture, granite matrix and aquifer. The C-14 concentration into the aquifer was then calculated for the total number of canisters. The dose calculation accounted for the two different species applying a conversion factor of $5.80 \cdot 10^{-10}$Sv/Bq [Buhmann et al., 2003] for C-14 ingested from drinking water (both as methane and CO_2) and a factor of 1.00 10^{-7} (Sv:y)/(Bq:m^3) for the biosphere dose conversion of CO_2 [Buhmann et al., 2003].

1.2.2 Scenarios/sensitivity analysis envisaged

Starting from the conceptual model described in the previous section, the reference scenario considered:

- an instantaneous release fraction of 3% from UO_2 followed by a constant release rate congruent with the UO_2 corrosion of 9.10^{-5} y^{-1} [Buhmann et al., 2003], 100% as $^{14}CO_2$;
- 20% of total C-14 in the Zy-4 is rapidly released from the ZrO_2 layer, with inorganic species representing 40% of the total release, as resulted from RATEN experimental measurements in CAST [Bucur et al., 2017]. The remaining C-14 is released at a constant rate of 10nm/year equal to the Zy-4 corrosion rate [Buhmann et al., 2003];
- No sorption for CH_4 in bentonite and granite;
- Low sorption of CO_2 in bentonite and granite (Kd in bentonite= $10^{-5}m^3$/kg; Kd in granite ($10^{-4}m^3$/kg);
- Distinct diffusion coefficient for CO_2 and CH_4 in bentonite ($1.92x10^{-9}$ m^2/s and respectively $1.42x10^{-9}$ m^2/s) and in granite ($5.18x\ 10^{-13}$ m^2/s and respectively $4.023x\ 10^{-13}m^2$/s).

The parameters relevant for the reference case are summarized in Table 1.

Table 1. Reference case data for SF disposal in granite

IRF[C-14_UO2]	3%
C-14 inorg fraction [UO_2]	100%
Fractional release rate of C-14	9.00E-05 1/yr
IRF[C-14_Zy]	20%
C-14 inorg fraction [Zy]	40%
Corrosion rate of Zy cladding	10 nm/yr
(C-14 inorg, C-14org) Diffusion coefficient in bentonite	(1.92E-9; 1.49E-9) m^2/s
(C-14 inorg, C-14org) Diffusion coefficient in granite	(5.18E-13; 4.023E-13) m^2/s
Kd_C-14inorg in bentonite	1E-5 m^3/kg
Kd_C-14 inorg in granite	1E-4 m^3/kg

The sensitivity analysis was intended to evaluate the relevance of C-14 speciation in the safety assessment, as well as the weight of the transport parameters in the main components of the disposal system (buffer and rock matrix). In this regard, the following cases have been investigated:

a. different IRF of C-14 from the UO_2 than the reference value (1%; 5%)
b. different release rates from UO_2 than the reference value (1.10^{-5}; $1.10^{-4}y^{-1}$)
c. smaller IRF from Zy-4 than reference value (1%; 10%)
d. different congruent C-14 release rates from Zy-4 (5 nm/year; 50 nm/year)
e. larger inorganic fractions in the C-14 release from Zy-4 (50%; 60%)
f. lower diffusion of C-14 in bentonite (10^{-10} m^2/s)
g. lower diffusion of C-14 in granite (10^{-14} m^2/s)
h. stronger sorption of CO_2 in bentonite (Kd=10^{-4} m^3/kg; Kd=10^{-3} m^3/kg)
i. stronger sorption of CO_2 in granite (Kd=10^{-3} m^3/kg)

1.2.3 Key parameters used in safety assessment.

The input data used in the simulations are grouped in the Table 2.

Table 2 Input data used in the GOLSIM simulations of SF disposal in granite

Species:	(C14inorg, C14org)
Inventory Data	
Inventory of C-14 in SF [Bq/canister]: - In UO_2 - in Zy-4	 8.94e+10 1.69e+10
Time at which release starts [yr]	1500
Instantaneous release fraction from UO_2	3% of inventory
Fractional release rate inorganic C14 from UO_2	9e-05 1/yr
Instantaneous release fraction from Zy-4	20% of inventory
Zy-4Corrosion rate	10 nm/yr
Number of canisters	7200
Solubility limit C14inorg	0.83 mol/m3
Solubility limit C14org	0.83 mol/m3
Canister Data	
Canister Height, m	3.842m
Canister Outer Diameter, m	1.247m
Bentonite Data	
Bentonite Density, m	1610 kg/m3
Bentonite Saturation	0.65
Bentonite Porosity	0.413
Bentonite Thickness	0.26 m
C14inorganic Kd in bentonite, m3/kg	1e-5 m3/kg
C14organicKd in bentonite, m3/kg	0.0 m3/kg
Diffusion coefficient in water C14anorg (CO_2)	1.92e-10 m2/s
Diffusion coefficient in water C14org (CH_4)	1.49e-10 m2/s
Granite Data	
Distance to fracture, m	50 m
Granite thickness, m	400m
Granite density, kg/m3	2000 kg/m3
Granite porosity	0.003
Granite tortuosity	0.09
C14 inorg Kd in granite, m3/kg	1e-4 m3/kg
C14org Kd in bentonite, m3/kg	1e-3 m3/kg
Granite saturation	1.0
EDZ	
EDZ Thickness, m	0.2m
EDZ Porosity	0.003
EDZ Tortuosity	0.09
EDZ Groundwater Flow	1.5 m/yr
EDZ Density, kg/m3	2000 kg/m3
C14 inorg Kd in EDZ, m3/kg	0.0 m3/kg

C14org Kd in EDZ, m3/kg	0.0 m3/kg
EDZ Saturation	0.65
Hydraulic conductivity in fracture, m/s	1e-6 m/s
Fracture length, m	462 m
Dispersivity in granite	20 m
Fracture aperture, m	1e-3 m
Fracture Groundwater Flow	2.4 m/yr

The conceptual modell transposed in GOLSIM is illustrated in Figure 3.

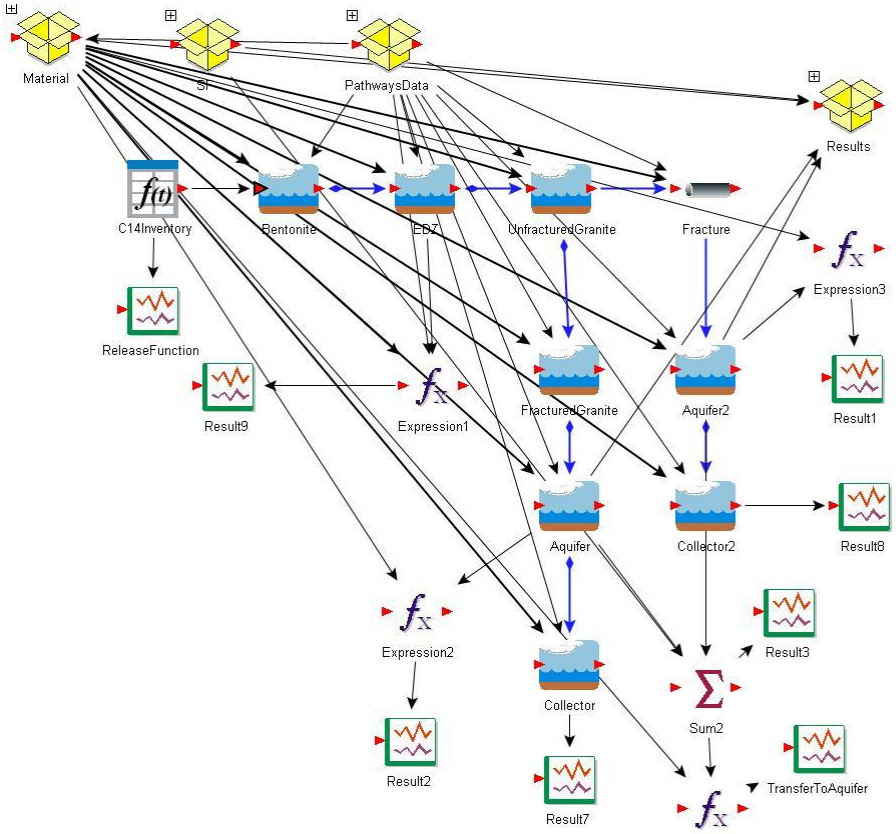

Figure 3: Schematic view of the model used in GOLDSIM simulation of the spent fuel disposal in granite

1.3 Results and discussions

For the reference case considered for sensitivity analysis, the C-14 release in the aquifer shows that, due to the advective flow through the fractures, the maximum concentration is reached at 2600 years, only 1100 years after canisters failure (Figure 4), while the component corresponding to the diffusive transport through granite which represents the larger part of the C-14 inventory, reaches the maximum release at 9800 years (Figure 5).

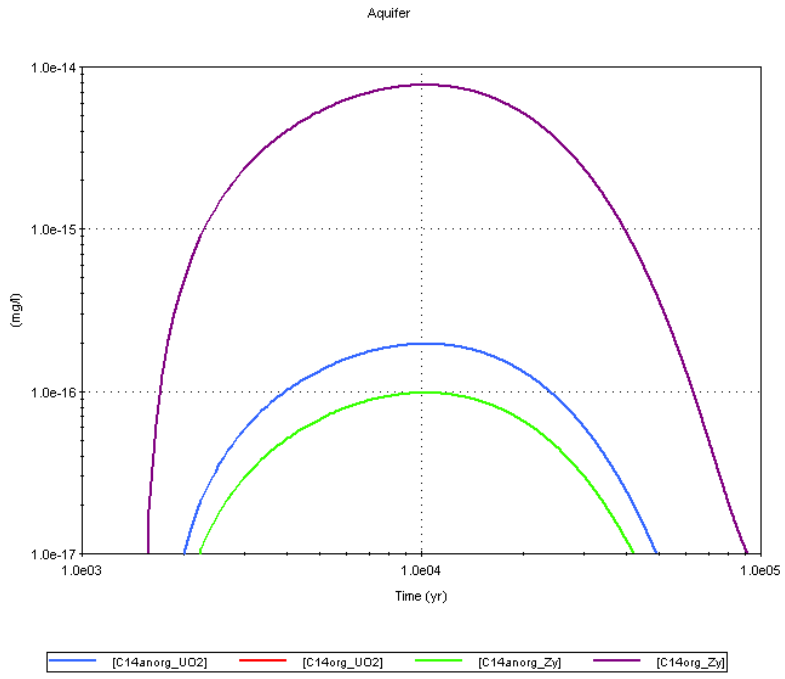

Figure 4: Concentration in aquifer after passing through the granite matrix and through the fracture for the reference case

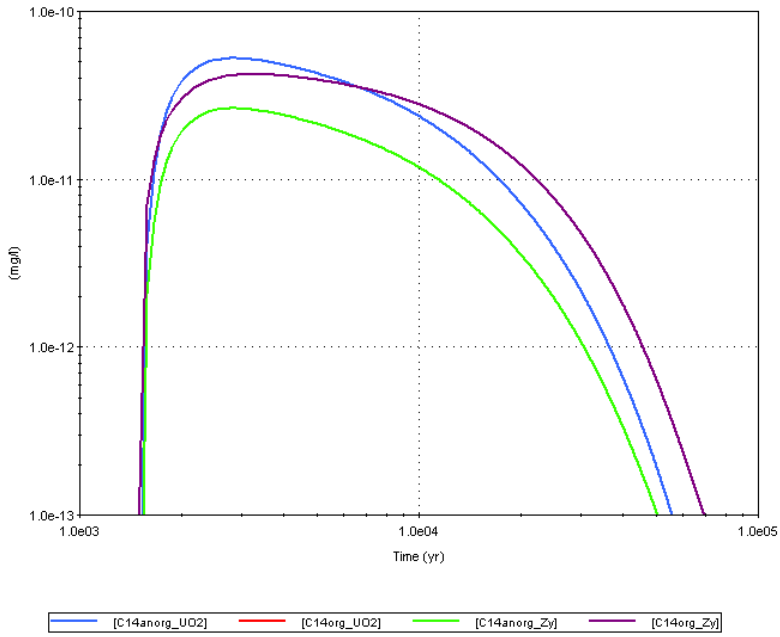

Figure 5: Concentration in aquifer after passing through the granite matrix for the reference case

As indicated by Figures 6 and 7, the contribution of C14 in the annual dose from drinking water received by a member of the critical group has much lower impact than the impact of C14 in the annual dose for biosphere. Consequently, only the annual dose for biosphere was considered for the sensitivity analysis. The contributions given by C14 released from UO_2 pellets and Zy claddings have the same order of magnitude.

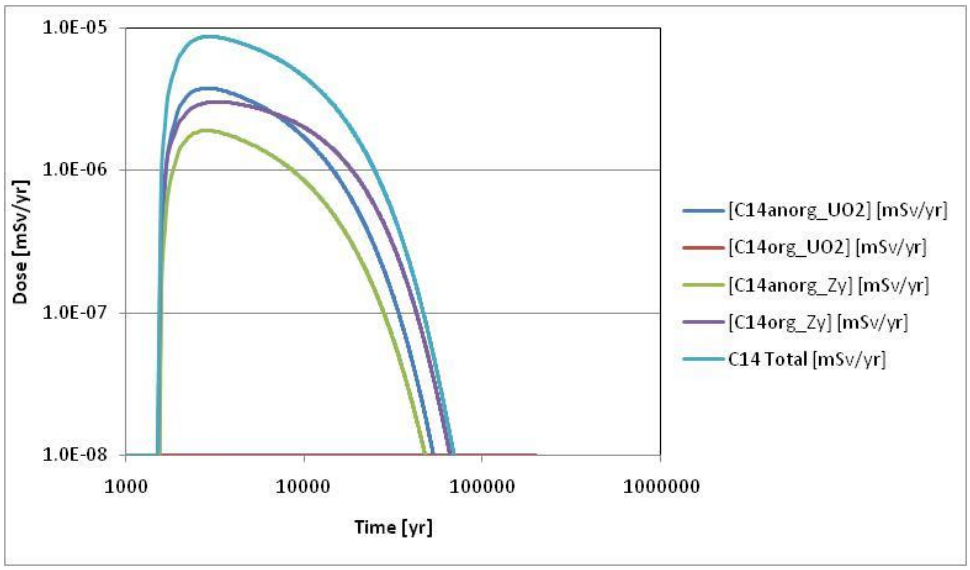

Figure 6: Contribution of C-14 speciation to the water intake dose for the reference case

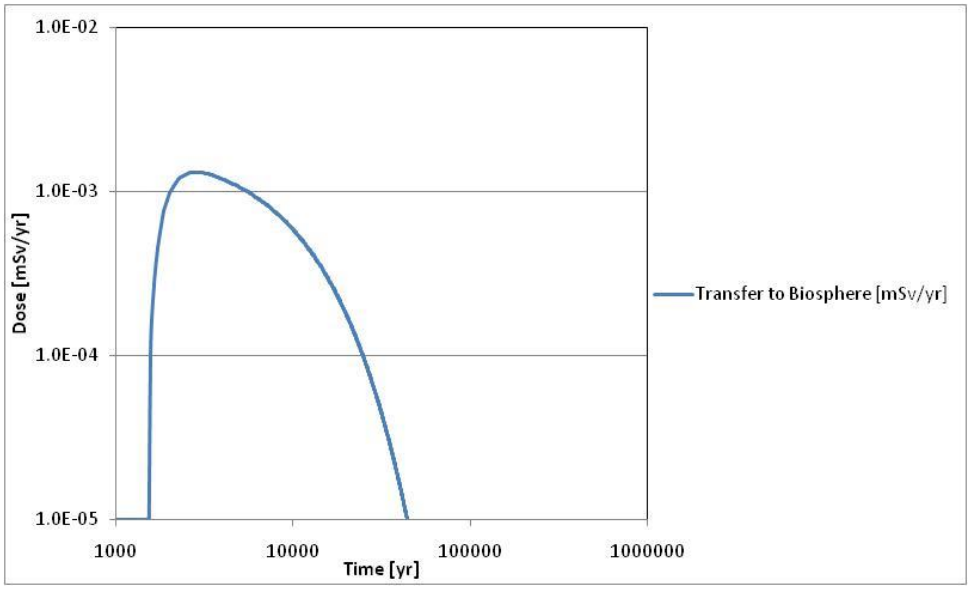

Figure 7: Contribution of C-14 to the biosphere dose for the reference case

Instantaneous release fraction

The Canadian studies [NWMO, 2012] on the C-14 release from UO_2 indicate IRF values of 2.7%. For sensitivity analysis lower and higher fractions compared to the reference value of 3% have been considered.

INR leaching tests on Zy cladding samples indicated an IRF lower than 1% but this value could be affected by preliminary washing of the samples and therefore, higher instant release could occur. To investigate the impact of the uncertainty related to the instant release from Zy oxide layer, different IRF values have been considered (1% and 20%, the latter value being recommended by the results obtained in the framework of the CAST project). For an IRF of C-14 from Zy claddings varying in this range the maximum annual dose to biosphere has a magnitude order of 10^{-3} mSv/yr.

The model also shows that the influence of IRF variation brings changes in the dose in both cases (Figure 8) and pointed out a higher sensitivity for IRF from UO_2 compared to Zy-4, for which larger levels of variation the IFR produce much lower changes in the dose. This is consistent with the assumption that C-14 releases from UO_2 entirely CO_2, while the 60% from the C-14 released from Zy-4 is organic and do not contribute to the dose.

a)

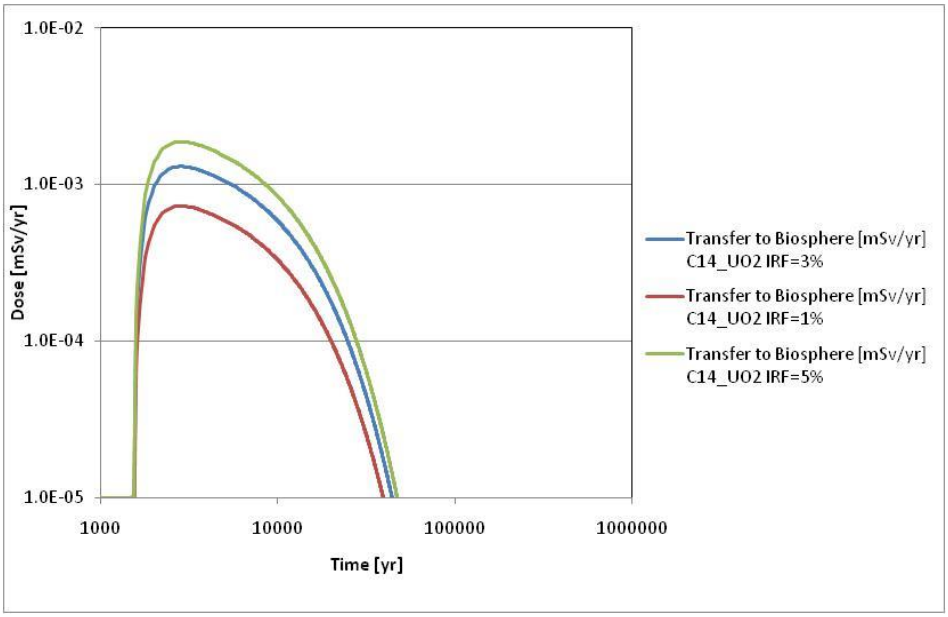

b)

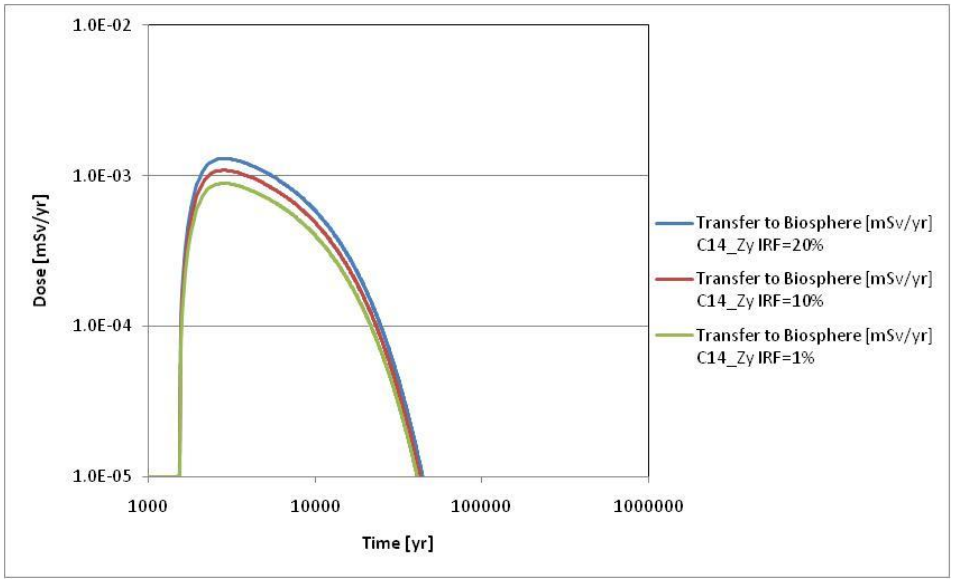

Figure 8: The influence of IRF from UO2 pellets (a) and Zy-4 claddings (b) on the biosphere dose

Congruent release rate

The values used in the sensitivity analysis for the congruent release of C-14 from Zy ranged between the upper limit of 50nm/yr (representing the experimental corrosion rate resulted from the electrochemical tests performed in CAST on irradiated Zy-4 samples from a CANDU SF transferred from Cernavoda NPP [Bucur et al., 2017]) and a less conservative value of 5nm/yr. Variations of the congruent release of C-14 from Zy claddings do not show impact on the maximum dose, which is practically given by the IRF. The impact of different corrosion rates considered for the sensitivity analysis can be observed only at times higher than 100000 yr and when the dose drops below 10^{-6}mSv/yr (Figure 9).

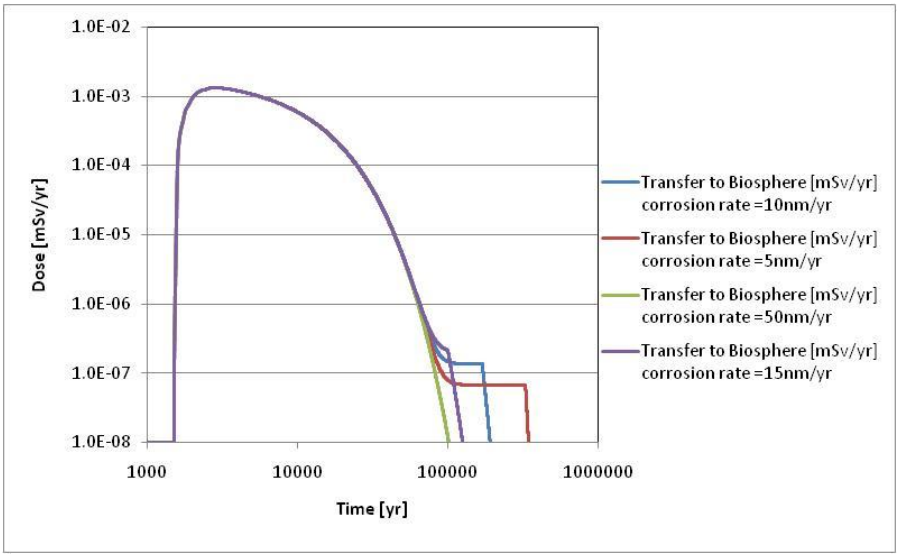

Figure 9: The influence of the C-14 congruent release rate from Zy-4 claddings

C-14 speciation

The increase of inorganic C-14 has, as expected, an impact on the dose due to the CO_2transfer into the biosphere, but the model does not show significant deviations from the reference case for larger amounts of inorganic C-14 released from the Zy claddings, as shown in Figure 10.

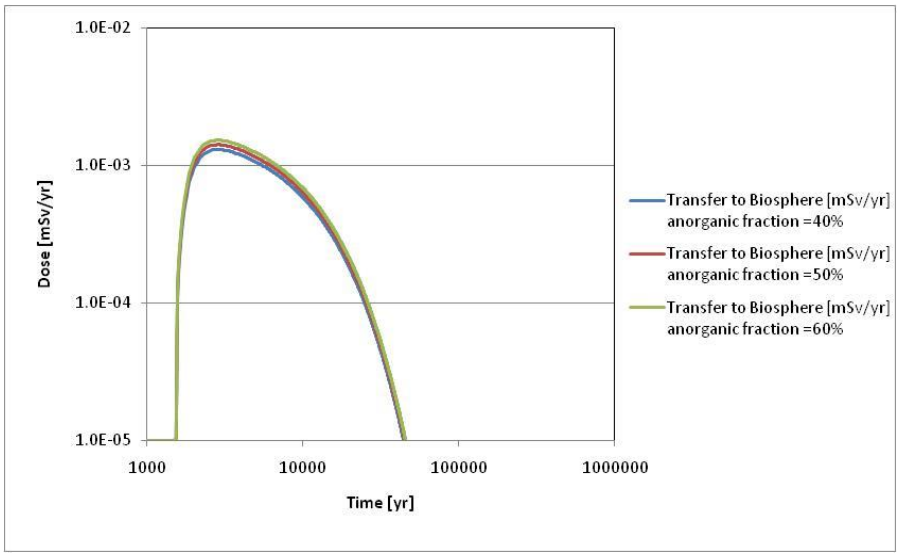

Figure 10: The influence of the C-14 speciation release from Zy-4 claddings

$^{14}CO_2$ sorption on bentonite and host rock

$^{14}CO_2$ sorption on bentonite and host rock could diminish the total inorganic C-14 released into the biosphere, contributing therefore to a lower dose. Stronger sorption of CO_2 both in bentonite and granite decreases indeed the maximum value of the dose, and shifts it at longer times (Figure 11).

a)

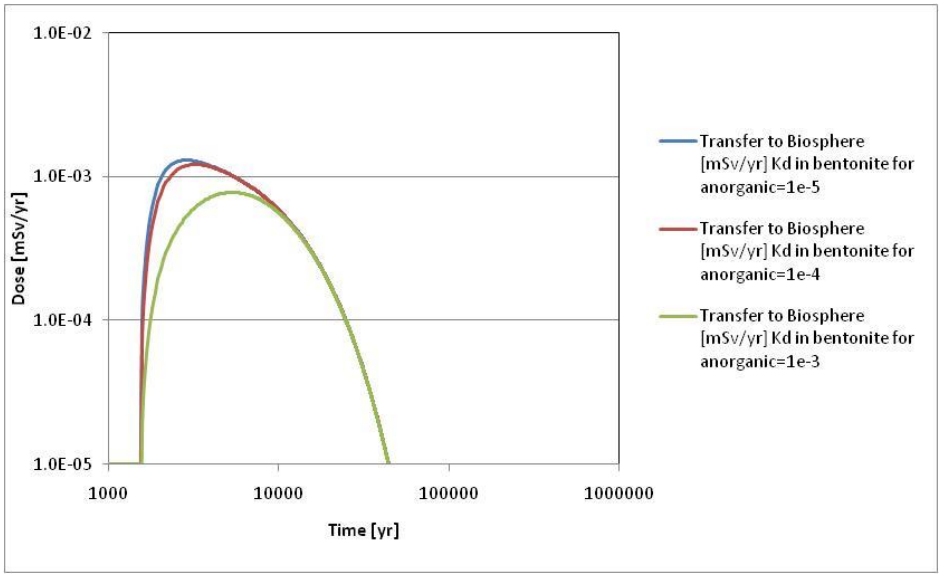

b)

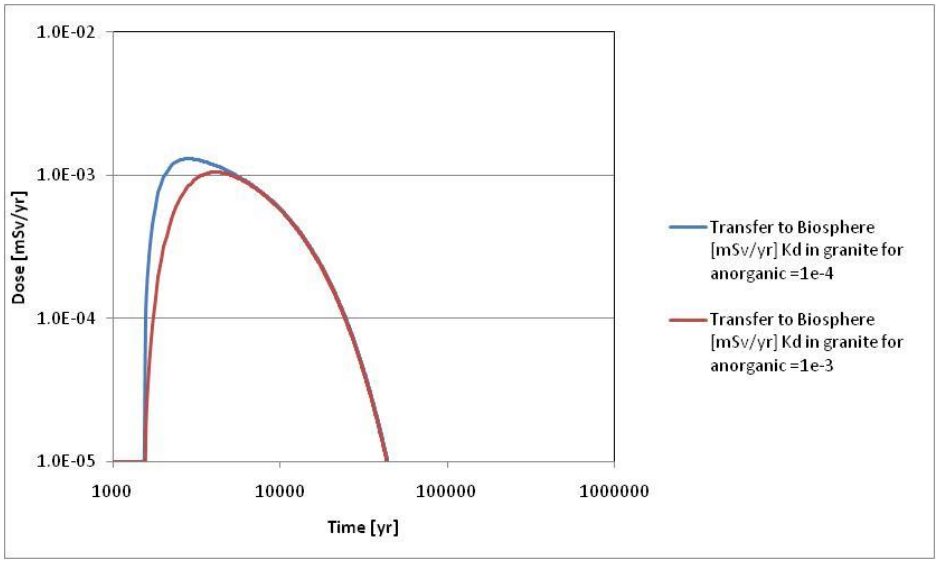

Figure 11: The influence of the inorganic C-14 sorption on bentonite (a) and respectively in granite (b)

The most significant deviation was observed for a variation with two orders of magnitude of the Kd in bentonite (at Kd=10^{-3} m^3/kg). For the same variation in Kd (one order of magnitude), sorption in bentonite have a stronger impact on the maximum dose than sorption in granite due to the fact that the major element contributing to the C-14 release in the aquifer is the fracture where no C-14 sorption is assumed.

Diffusion in bentonite and rock matrix

No significant influence has been found for the increase with one order of magnitude of the diffusion coefficients in bentonite and granite compared to the reference case (Figure 12), as long as the fractures remain the most effective transport pathway for radionuclides.

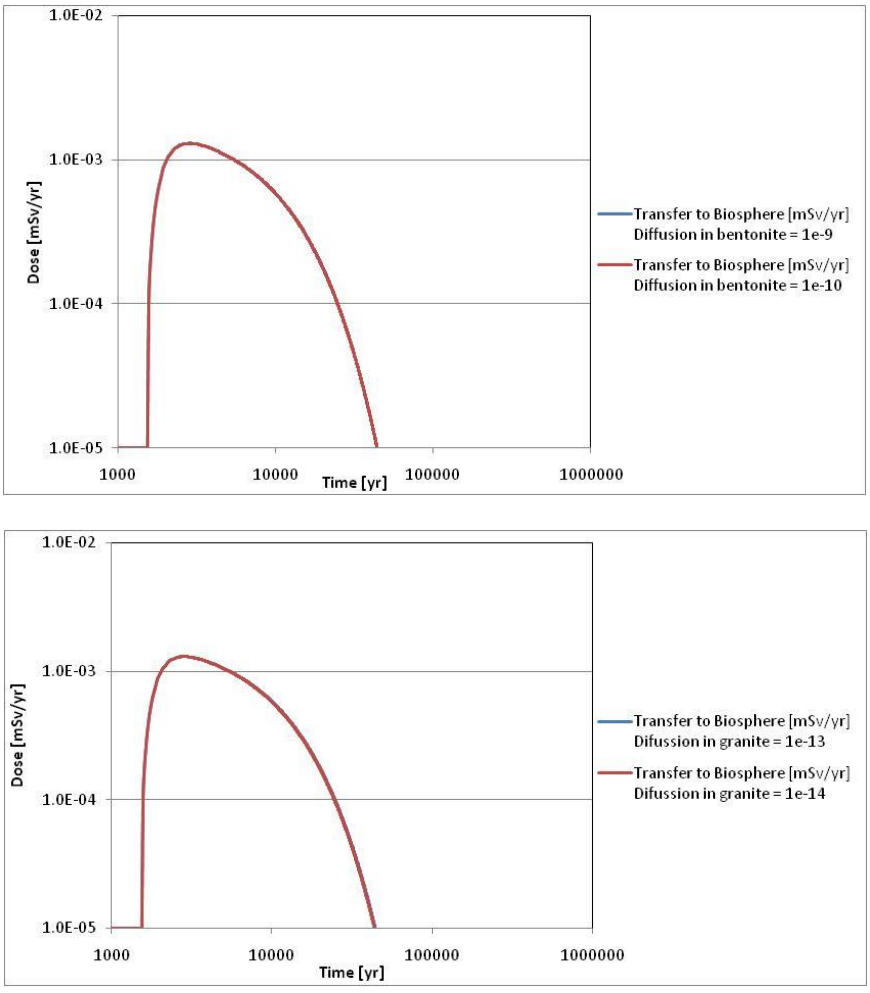

Figure 12: The influence of CO_2 diffusion coefficients in bentonite (up) and granite (down)

Integrating new achieved experimental data on C-14 release and speciation from Zy-4 claddings, as well as the better understanding of the processes governing the C-14 releases, the calculations performed under CAST project improved the previous safety assessment of a generic geological repository in granite for the spent fuel disposal. Table 3 summarises this

progress, illustrating changes made in the assumptions regarding C-14 release, C-14 speciation.

Table 3: Safety Assessment of the Spent Fuel

	Hypothesis used in safety assessment before CAST	**Hypothesis used in safety assessment based on CAST**
Inventory	C-14 in spent fuel: - C-14 from UO2 as resulted from Canadian ORIGEN calculations; - C-14 from Zy-4 as measured on irradiated samples which confirmed calculations for a 30ppm N in Zy cladding	Unchanged for the C-14 in UO2; Inventory based on CAST measurements for C-14 in Zy
	Not considered.	No sensitivity analysis on the inventory
Speciation	Reference case: Inorganic	Dissolved CO_2 and dissolved methane.CO_2 contribution to the dose given by specific biosphere conversion factor and ingestion dose coefficient In Zy: 40% inorganic C-14 as measured in CAST for the reference case;
		Sensitivity analysis with different ratio CH_4/CO_2both in UO2 and Zy-4.
^{14}C distribution	Homogeneous distribution.	Unchanged.
Leaching rate	Congruent with the UO_2 dissolution rate $9.10^{-5}y^{-1}$ Congruent with corrosion rate of Zy:10 nm/y.	Congruent with the UO_2 dissolution rate $9.10^{-5}y^{-}1$ for the reference case; lower and higher rates considered for sensitivity analysis Congruent with corrosion rate of Zy: 10 nm/y as reference;
	Not considered.	Sensitivity analysis for corrosion rate (considering 50nm/y as higher value, corresponding to INR data achieved in CAST) and a lower rate (less conservative) considered for sensitivity analysis
IRF	For fuel pellets: 3% from inventory without considering the speciation For Zy-4 not considered	Unchanged IFR for the reference case; Lower and higher IRF considered for sensitivity analysis. 20% of the C14 inventory of the cladding is instantaneously released from the oxide layer (reference case); No contribution from shearing fines. Lower IRF considered for sensitivity analysis.
Transport in granite	In matrix: Diffusion as soluble inorganic species Fracture: Advective as soluble inorganic species.	- Diffusion as dissolved CO_2 and methane. -Advective transport of dissolved CO_2 and methane through fracture Lower diffusion coefficient in granite of CO2 considered for sensitivity analysis

	Hypothesis used in safety assessment before CAST	Hypothesis used in safety assessment based on CAST
Retention in bentonite and granite	Considered for CO_2	Retention in bentonite and granite considered in the reference case only for CO_2
		Sensitivity analysis with a weak and strong retention of the CO_2.

2 Integration of the CAST experimental outcomes at the level of the safety case

Deep geological disposal of the spent fuel and long-lived intermediate level waste generated from Cernavoda NPP is expected to become operational not early than 2055. Since a host rock was not yet selected, at this moment only a generic repository concept is considered. In this context, the main focus is a better definition of inventory and of the source term for the evaluation of different options regarding the host rock.

Results achieved by INR ICN in CAST project brought the first experimental data on the C-14 content in Zy-4 claddings and SIERs from Cernavoda NPP. The values obtained on Zy-4 samples showed a very good correlation with the ORIGEN calculations. These findings increased the confidence in the total inventory of C-14 in the Zy claddings. Using these data, the new safety assessments presented in this study included therefore more realistic values for the C-14 inventory in Zy-4 claddings.

Experimental data on C-14 release from Zy-4, SIER and graphite contributed to a better understanding of the governing processes and provided the first data on the organic/inorganic ratio of C-14 released in liquid phase, in alkaline conditions. Based on data obtained on irradiated Zy-4, the new calculations made in CAST included C-14 speciation, considering the experimental values as a reference case.

Data on SIER, an important component of the deep geological repository, will be further included in the safety assessment, completing the source term of the generic safety case.

The sensitivity analysis (addressing only C-14 from spent fuel) pointed out that the most sensitive parameters are the IRF from the UO_2 pellets, and the Kd in bentonite.

References

[ANDRAD, 2004] National medium and long-term strategy for the safe management of radioactive waste and spent nuclear fuel, ANDRAD, 2004

[Bucur et al., 2017] C. Bucur et all., Final report on experimental results on long term corrosion tests and C-14 release assessment, CAST Project, D3.16, 2017

[Buhmann et al., 2003] D. Buhmann, M. Pavelescu, A. Ionescu, A. Rizoiu, R.Storck - Comparison of Long-Term Safety of repositories for Spent CANDU or LWR Fuels in Hard Rock, GRS – 196SCN-NT 261/2003

[Capouet, 2015] M. Capouet - Handling of C-14 in current safety assessments: State of the art - CAST project, D6.1, 2015

[NWMO, 2012] Adaptive Phased Management. Used Fuel Repository Conceptual Design and Post-closure Safety Assessment in Crystalline Rock - NWMO TR-2012-16, December 2012

[Pavelescu et al., 2003] M. Pavelescu, A. Ionescu, A. Rizoiu, D. Buhmann, R.Storck - Deep Geological Disposal Research in Romania, 2003

CArbon-14 Source Term

CAST

Integration of CAST results to safety assessment: Contribution from LEI to D6.3

D. Grigaliuniene, P. Poskas, A. Narkuniene

Date of issue of this report: 09/06/2017

Executive Summary

There are two RBMK-1500 type reactors at the Ignalina NPP in Lithuania where graphite was used as a neutron moderator and reflector. These reactors are under decommissioning now and Lithuania has to find a solution for safe disposal of the irradiated graphite. The graphite cannot be disposed of in a near surface repository due to great amounts of ^{14}C; thus a deep geological repository (DGR) is analysed as an option. This study had the following aims: to perform evaluation of ^{14}C migration from the RBMK-1500 irradiated graphite disposed of in a potential DGR in crystalline rocks; to evaluate the impact on humans based on the research performed under the CAST Project; and to identify the potential for conservatism reduction. The gathered information was used to model ^{14}C transport in the near-field and far-field environment by the water pathway, to perform uncertainty and sensitivity analysis and to illustrate the impact on humans by evaluating the radiological impact occurred due to consumption of well water contaminated with ^{14}C. It was demonstrated that substantiated more realistic assumptions could reduce ^{14}C flux to the far-field environment by approximately one order of magnitude in comparison with the previous estimation based on very conservative assumptions. The evaluated dose to humans would make a few percent from the dose constraint of 0.2 mSv.

List of Contents

1 LEI: Modelling C^{14} in disposal systems

1.1 *Introduction*

The Ignalina nuclear power plant (Ignalina NPP) in Lithuania has two RBMK-1500 type reactors under decommissioning now. The RBMK-1500 type reactors contain graphite as a neutron moderator and reflector. After dismantling of both reactor cores, about 3800 t of irradiated graphite (i-graphite) will be accumulated. Due to large amounts of ^{14}C, it cannot be disposed of in a near surface repository. As a solution for i-graphite disposal, an option of i-graphite disposal in a deep geological repository (DGR) for the spent nuclear fuel (SNF), at a certain distance from SNF emplacement tunnels, is analysed. As a basis for ^{14}C release and transport analysis a generic repository concept of RBMK-1500 SNF disposal in crystalline rock in Lithuania described in [POSKAS, 2006] is considered. According to this concept, graphite blocks are placed into metal containers which are stacked in a tunnel and backfilled with cement backfill. Two options regarding packaging are considered: graphite waste in metal containers without encapsulant (Alternative 1) and encapsulated waste (Alternative 2).

Initial evaluation of ^{14}C migration from the RBMK-1500 graphite in case of disposal in crystalline rock was performed by Narkuniene et al. [NARKUNIENE, 2014] where ^{14}C migration with the groundwater flow was analysed. The focus was mainly on the evaluation of the importance of waste leaching rate to the ^{14}C transfer into geosphere and potential radiological impact. In the absence of data on the source term the evaluation was performed with very conservative assumptions.

Research performed under the CAST project provided more information on the ^{14}C release from i-graphite, its speciation and behaviour in the near field. In addition, ^{14}C inventory in the Ignalina NPP graphite was updated. Based on this information an updated safety assessment of the i-graphite disposed of in a DGR in crystalline rocks is performed. The aim of this assessment is to evaluate ^{14}C flux to geosphere using more realistic assumptions and data gathered from CAST project, estimate potential radiological impact and to identify the importance of the different components of the disposal system on ^{14}C transfer. For this purpose transport of ^{14}C in the near-field environment by the groundwater pathway was

evaluated and uncertainty and sensitivity analysis were performed. Then a more realistic site model (so called Site A) was developed where available data on crystalline basement and sedimentary cover were incorporated and ^{14}C transfer in the far-field environment was evaluated. In addition, possibility of the ^{14}C transfer to the biosphere through the gas pathway was analysed. The results of this assessment provide the understanding of the potential impact of the disposed i-graphite and prioritization of the future research areas.

1.2 *Model description*

For the updated safety assessment as a basis the model of the previous assessment presented in [NARKUNIENE, 2014] and summarized in the CAST project deliverable D6.1 [KENDALL, 2015] is used. Scheme of the disposal tunnel and intersecting fractures is presented in Figure 1.

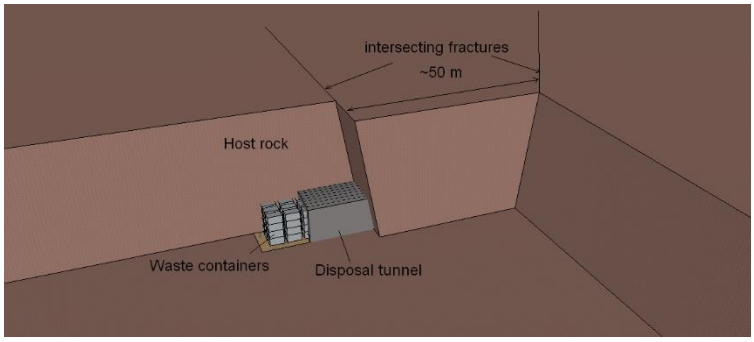

Figure 1: Scheme of the disposal tunnel and intersecting fractures.

^{14}C from i-graphite could be released in aqueous or gaseous form [AMEC, 2016]. In the previous assessment ^{14}C transport only by groundwater pathway was considered. During the CAST project it was intended to analyse the possibility of the ^{14}C transfer in a gas phase as well. In order to reach the biosphere by the gas pathway, a free gas phase should form and there should be a pathway for gas to migrate through geosphere. A free gas phase can form only if sufficient gas is generated.

In general, the ^{14}C release rate from i-graphite is very slow and for bulk gas formation other sources (e.g. metal corrosion) play more significant role. In addition, gas that is formed may dissolve in water. The review of available experimental results indicated that majority of ^{14}C

release from i-graphite occurs to the solution and only small amounts of gaseous releases (about 1% of the released ^{14}C) have been measured [TOULHOUT, 2015]. This suggests that even if the gaseous ^{14}C could reach the surface environment, the impact to biosphere would be insignificant. The peculiarity of the Site A, which is considered for this assessment, is more than 500 meters thick sedimentary cover overlaying the crystalline basement and consisting of several layers of aquifers and aquitards. This feature is supposed to prevent the gas to reach the biosphere as the gas may be trapped beneath the low permeability rock or dissolve in water. Therefore, further investigation on ^{14}C transport in a free gas phase to biosphere at this stage is not considered. However, when more information about the DGR concept, inventory and site specific data are available, the potential ^{14}C migration by the gas pathway should be examined.

For the updated safety assessment, a normal evolution scenario with ^{14}C leaching from i-graphite and transfer through the engineered barriers and geosphere up to the biosphere by the groundwater pathway is analysed. The disposal system was divided into compartments and the mass balance equation was solved numerically using computer tools AMBER (near field modelling) and GOLDSIM (far field modelling). Conceptual model of the disposal system is presented in Figure 2 and conceptual model of the geosphere – in Figure 3.

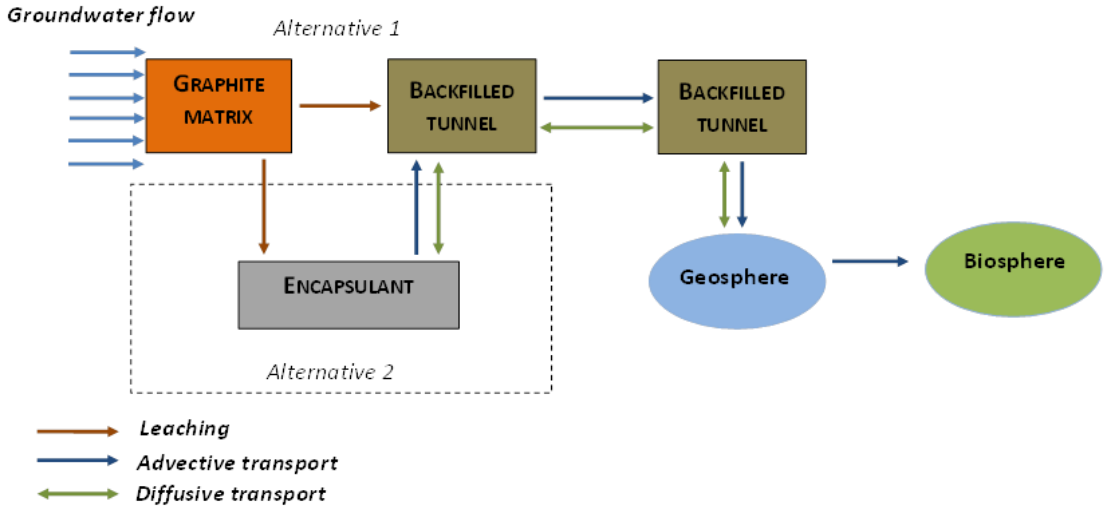

Figure 2: Conceptual model of the disposal system used in the updated safety assessment

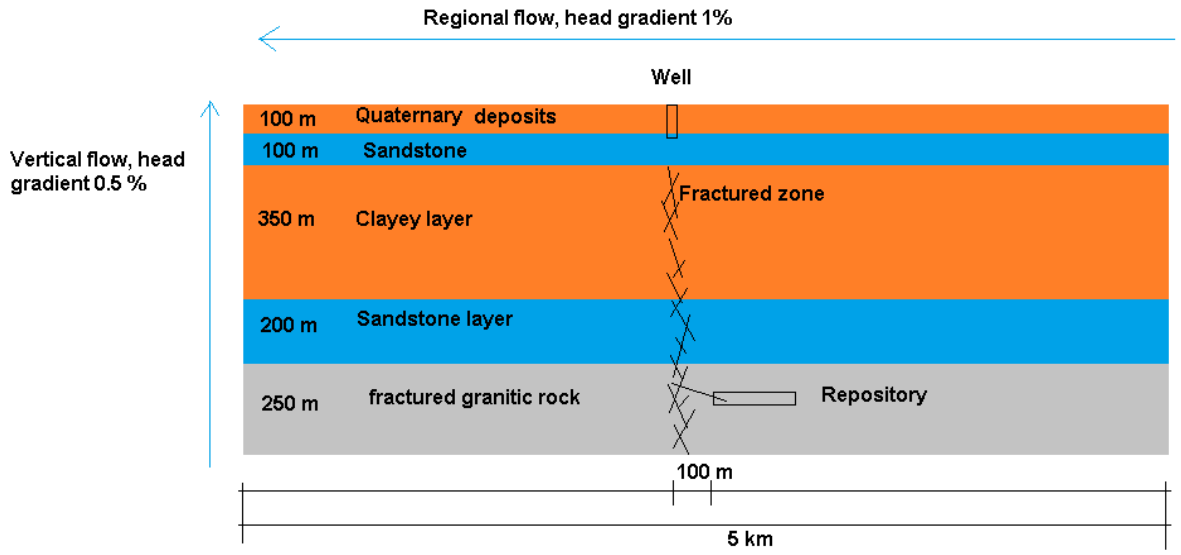

Figure 3: Conceptual model of the Site A used in the updated safety assessment

The main focus in the updated safety assessment is given to the ^{14}C inventory in the i-graphite, ^{14}C release rate, speciation and sorption, which were investigated in the CAST project. Selection of these parameter values are discussed below. More detailed description of the engineered barrier system could be found in the CAST project deliverable D6.1 [KENDALL, 2015].

Inventory. ^{14}C inventory in i-graphite depends on the location in the reactor core, operating power history, initial concentration of impurities, amount of cooling gases, etc. In the previous assessment the inventory was selected based on the activation modelling with very conservative assumption on N impurity. The estimated ^{14}C specific activity in i-graphite was about 9.9E+05 Bq/g. During the CAST project some new experimental data on ^{14}C activity in RBMK-1500 graphite were published [MAZEIKA, 2015]. These data were used for calibration of numerical modelling data in the CAST project deliverable D5.17 [NARKUNAS, 2017] and based on this averaged specific activity value of 1.9E+05 Bq/g with standard deviation of +/- 36.7% was defined. These values were used in the updated safety assessment.

Release rate. Experimental results indicate that initially ^{14}C from i-graphite is released at a higher release rate followed by a decreased release rate in the long-term. However, for the treated graphite the initial rapid release was not identified. Release rate also depends on the geometry of the sample: higher release rate for crushed graphite is observed. Based on such information, in the previous assessment several deterministic calculations were performed varying long-term fractional release rate from 1.83E-05 1/y to 0.1 1/y. To represent rapid release, for the first 10 years after repository closure fractional release rate of 0.1 1/y was assumed.

In the course of the CAST project some more information regarding the release rate from i-graphite was obtained, mainly as part of the UK programme. Leaching experiments with UK graphite provided evidence that a significant proportion of the ^{14}C content is unleachable (is incorporated in the graphite matrix). According to [AMEC, 2016; NDA, 2016] not more than 30% of the ^{14}C could be released. The fraction of the inventory associated with rapid release can vary in the interval from 0 to 0.2 % with the best estimate value as 0.02%. Therefore, in the updated safety assessment the releasable fraction of 30 % from the total ^{14}C inventory was assumed with the rapid release fraction as indicated above. The rest from the releasable inventory is associated with the slower long-term release.

A number of leaching experiments indicated that the (quasi)steady state conditions are reached in a period less than one year [TOULHOUT, 2015]. Also in [AMEC, 2016] it is reported that the rapid release occurs over such a short time for long-term modelling, that it may be better considered as an initial instant release. Rate constant for the slower release of ^{14}C provided in [AMEC, 2016; NDA, 2016] vary from 0.001 1/y to 0.1 1/y with the best estimate value of 0.01 1/y. These values are assumed for the modelling ^{14}C release from RBMK-1500 i-graphite in the updated safety assessment. However, it should be noted that these values are only indicative and have to be updated when new data for RBMK-1500 i-graphite are obtained.

Speciation and sorption. ^{14}C released from irradiated graphite can form either organic or inorganic compounds with different retention and solubility in the environment. Due to lack of data on partitioning of the released ^{14}C between organic and inorganic compounds, in the

previous assessment two cases were analysed: in one case it was assumed that the released ^{14}C is non-sorbed and in another case strong sorption in cementitious material was assumed. The partition of the released ^{14}C between organic and inorganic compounds is still not well defined and sometimes contradictory. Some sources reported in [TOULHOUT, 2015] indicate the amount of inorganic compounds to be 65–75% while from the recent leaching studies of moderator and reflector graphite from the Tokai (Magnox) reactors in Japan it was found that about 80% of the released ^{14}C was in organic form [AMEC, 2016]. Taking this into account for the uncertainty analysis in the updated safety assessment, the fraction of organic compounds in solution is assumed to vary between 20 and 80% with the best estimated value of 50 %. The appropriate remaining fraction is assigned to inorganic compounds.

It was assumed in the previous assessment that non-sorbed ^{14}C released from i-graphite has no interaction with the cementitious backfill and encapsulant and migrates without retardation. No sorption of organic compounds is also assumed in a number of works collected in the CAST deliverable D6.1 [KENDALL, 2015]. During the CAST project it was obtained information that sorption of the small organic molecules in cement may be non-negligible: there are some experiments indicating k_d values in the interval from 10^{-3} m^3/kg to 10^{-5} m^3/kg with a best-estimate value of 10^{-4} m^3/kg [CAPOUET, 2017]. However, the dataset on k_d values for organic ^{14}C is rather limited and no compound-specific k_d values can be recommended. Therefore in the updated safety assessment it is assumed that organic compounds released from i-graphite (mainly as $^{14}CH_4$) migrate without retention. However, for the uncertainty analysis the range of the k_d values from 0 to 1E-04 m^3/kg is assumed. Inorganic compounds (expected to be $^{14}CO_2$) is prone to precipitate and is trapped in the cementitious engineered barriers. This phenomena is not modelled explicitly, but is reflected to some extent in the sorption coefficient assuming k_d value of 0.2 m^3/kg [TOWLER, 2010] with +/- one order of magnitude variation for the uncertainty analysis.

Comparison of the assumptions in the previous safety assessment and in the updated safety assessment with integrated CAST project results is presented in Table 1.

Table 1: Comparison of the assumptions in the previous and in the updated safety assessment

Parameter	Hypothesis used in previous safety assessment (before CAST)	Hypothesis used in updated safety assessment (based on CAST)
Inventory	Based on conservative modelling.	Based on updated modelling and experimental results.
	No sensitivity and uncertainty analysis.	
Release rate		
Releasable inventory	Total	Fraction from total inventory based on experimental results.
Rapid release fraction	For 10 years with release rate of 0.1 1/y.	Based on experimental results.
Rapid release rate		Instant.
Long-term (slower) release fraction	Variant calculations with different release rate based on measurements and modelling.	Based on experimental results, depends on releasable inventory and rapid release fraction.
Long-term (slower) release rate		Based on experimental results.
Speciation	Not considered.	Organic compounds –methane; inorganic compounds – $^{14}CO_2$/carbonate.
		Ratio between organic and inorganic compounds based on measurements.
Sorption in cement	Two calculation cases analysed: in one case all released ^{14}C is non-sorbed and in another case – all released ^{14}C is well-sorbed.	Inorganic compounds: well sorbed.
		Organic compounds: no sorption for the best estimate calculations; weak retention for uncertainty analysis.
Transport in near field	Advection, diffusion-dispersion of dissolved ^{14}C compounds	Advection, diffusion-dispersion of dissolved ^{14}C compounds.
Transport in far field	Advection, diffusion-dispersion of dissolved ^{14}C compounds, no retention.	Advection, diffusion-dispersion of dissolved ^{14}C compounds, no retention. Site A model developed.
Transport by gas pathway	Not analysed.	Substantiation of exclusion from analysis at this stage of assessment.

1.3 Results and discussions

In order to evaluate potential impact of ^{14}C released from RBMK-1500 i-graphite, to illustrate the impact of uncertainties and investigate the importance of different components of the near field, a set of calculations were performed. At first as the base case ^{14}C flux into geosphere was evaluated with the best estimate parameter values. To identify the role of different processes and associated parameters to the maximal ^{14}C flux into geosphere, a local sensitivity analysis was performed and presented as tornado diagrams. In order to illustrate the influence of the parameter uncertainties to the ^{14}C flux into geosphere a stochastic modelling was performed applying the Monte-Carlo technique.

Base case (best estimate calculations)

The base case modelling results for Alternative 1 and Alternative 2 are presented in Figure 4. The total ^{14}C flux into geosphere is expressed as total fractional flux, i.e. in terms of estimated flux Bq/y per Bq of ^{14}C disposed of in the repository. In addition, the results of the previous assessment (variant with the maximal flux) are presented in the figure. It can be seen from Figure 4 that there are some peaks in the updated safety assessment graphs. The first peak corresponds to the organic ^{14}C flux to geosphere and the second one – to the inorganic ^{14}C flux to geosphere. Similarly the first peak in the previous assessment line indicates release of the non-sorbed ^{14}C while the second one corresponds to the case when ^{14}C sorption in cementitious material was assumed. The maximal fractional flux of organic ^{14}C into geosphere in the updated safety assessment in Alternative 1 as well as in Alternative 2 is approximately 1E-04 1/y and appears about 500 years after the repository closure. The difference of the organic ^{14}C maximal fractional flux into the geological environment between the two Alternatives (non-encapsulated/encapsulated waste) is insignificant. This indicates that the encapsulant does not act as an additional barrier to reduce the flux of organic ^{14}C from the repository.

Inorganic ^{14}C is well sorbed in the cementitious materials and its maximal fractional flux into geosphere is significantly lower. In Alternative 1 the maximal fractional flux of inorganic ^{14}C is approximately 5E-12 1/y and in Alternative 2 it is about one order of magnitude lower. The

lower fractional flux in Alternative 2 results mainly from the cementitious encapsulant where sorption plays its important role. The maximal inorganic ^{14}C flux into geosphere is observed at approximately 50,000 years after the repository closure.

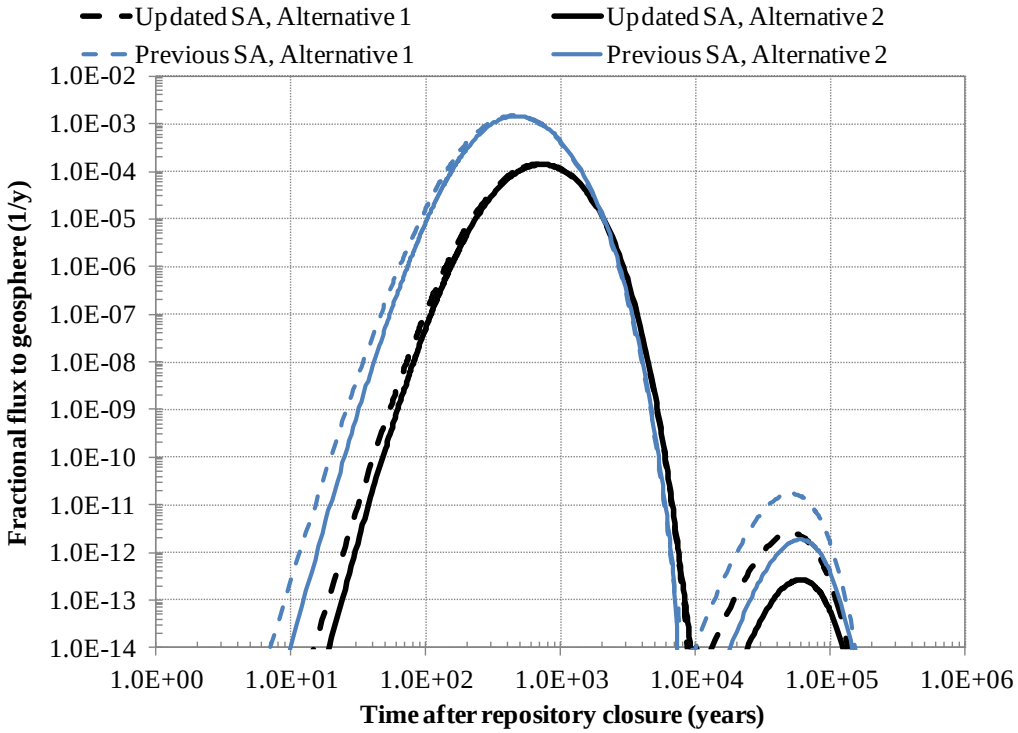

Figure 4: ^{14}C fractional flux into geosphere in case of updated safety assessment and previous safety assessment

Comparison of the updated safety assessment base case results with the results from the previous assessment indicates that the maximal fractional flux to geosphere in the updated safety assessment is reduced by about one order of magnitude. Therefore substantiated more realistic assumptions could significantly reduce the conservatism.

Local sensitivity analysis

As an example of the results of the local sensitivity analysis, a tornado diagram for maximal organic ^{14}C flux to geosphere in case of Alternative 2 (encapsulated waste) is presented in Figure 5. It can be seen from the Figure 5 that the parameter with the highest importance in this case is backfill hydraulic conductivity. Since the retention of organic ^{14}C is insignificant, the hydraulic properties of the engineered barriers become the key factor for organic ^{14}C

transfer. However, uncertainties in inventory and rapid release fraction have also significant impact. This indicates the importance of the issues related to graphite treatment and characterization. The treatment of graphite by removing the rapid release fraction could result in perceptible decrease of the organic ^{14}C peak flux. In case of ^{14}C release in inorganic form, the distribution coefficient in cementitious material and the backfill hydraulic conductivity are the parameters with the highest importance for the peak flux to geosphere.

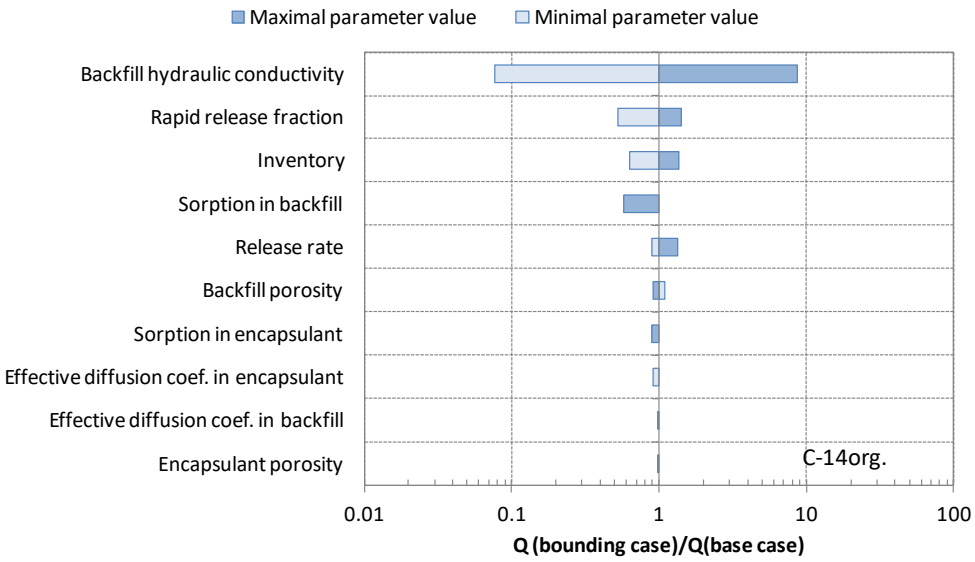

Figure 5: Results of local sensitivity analysis for organic ^{14}C, Alternative 2 (encapsulated waste)

Uncertainty analysis

The results of the uncertainty analysis for the Alternative 1 (non-encapsulated waste) are presented in Figure 6. It provides plots showing the fractional ^{14}C flux to geosphere for the best estimate case, the mean fractional flux and the 95th percentile. It should be noted, that the flux estimated using stochastic approach vary in a large interval and median value of the flux might be seen as a better indication of the central tendency (less sensitive to the large values in data) than the arithmetic mean value. Therefore, for comparison purposes the median flux value is added in the figure.

It can be seen from Figure 6 that the maximal fractional flux values corresponding to the organic ^{14}C release differs between the median value and the 95th percentile by about factor of 5. The maximal fractional flux to geosphere for the best estimate calculations is about 1.4E-04 1/y, the maximum of the 95th percentile is about 3.7E-04 1/y and the maximum of the median flux is about 7.2E-05 1/y.

The maximal fractional flux corresponding to the inorganic ^{14}C release varies in much wider interval than in case of organic ^{14}C: from 2.5E-12 1/y (best estimate case) to 3.2E-07 1/y (the 95th percentile). It is supposed that this is related to the changes in sorption coefficient values. It was mentioned above that for inorganic ^{14}C sorption in the cementitious barriers has the highest impact on the ^{14}C flux.

It should be noted that the results for Alternative 2 are very similar to Alternative 1 in the shape, with about one order of magnitude lower peak corresponding to inorganic ^{14}C.

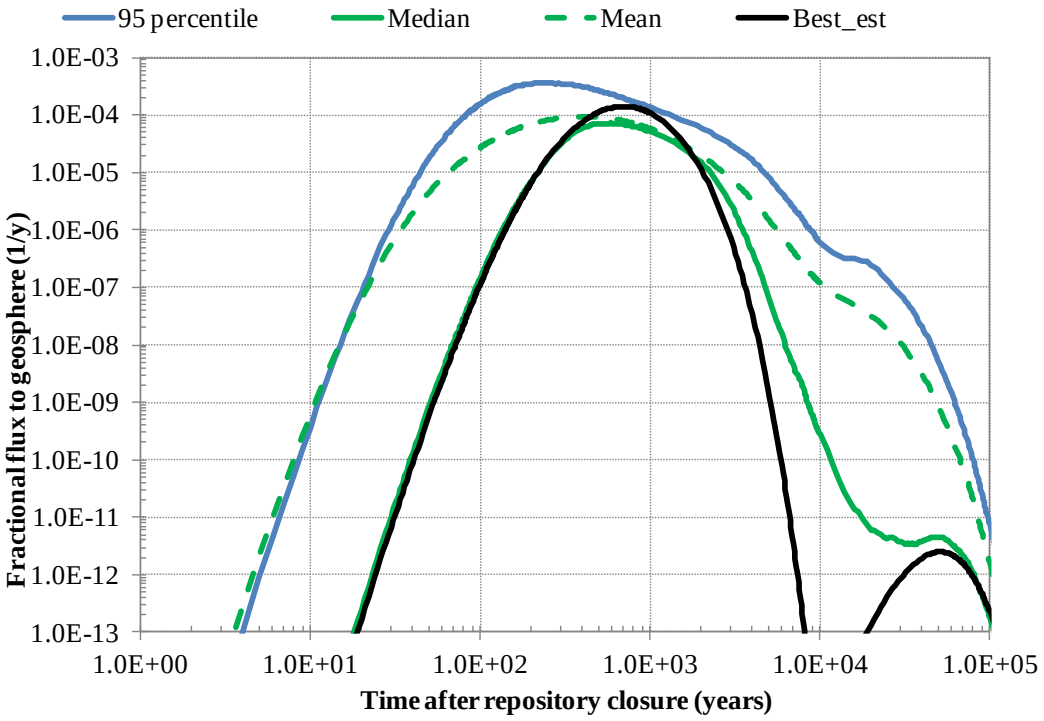

Figure 6: Results of uncertainty analysis, Alternative 1 (non-encapsulated waste)

From the uncertainty and sensitivity analysis it can be concluded that further investigations in partitioning of the released ^{14}C between organic and inorganic compounds and sorption of the released compounds in the cementitious environment could reduce the range of uncertainties and provide more realistic picture of the system capability to provide adequate level of safety. It also should be pointed out that the information on ^{14}C release from i-graphite obtained during the CAST project should be used with care since the results for RBMK-1500 i-graphite might be somewhat different. Therefore, there is a need for research on RBMK-1500 i-graphite.

Impact to human

In order to illustrate the impact of the released ^{14}C from i-graphite disposed of in the DGR to a human, the flux to geosphere in case of the best estimate calculations was imported to the GOLDSIM Site A model (far field model) and radiological impact due to consumption of water from a well was evaluated. The estimated maximal dose in case of Alternative 1 makes

about 5.5 % from the dose constraint (0.2 mSv/y). The results for Alternative 2 are very similar since the main contributor to the maximal dose is organic ^{14}C and encapsulant considered in the Alternative 2 has a minor role in this case.

2 Integration of the CAST experimental outcomes at the level of the safety case

One of the strategic goals indicated in the national Program of Radioactive Waste Management Development is safe management of all radioactive waste and spent nuclear fuel available in Lithuania. As an option for irradiated RBMK-1500 graphite from Ignalina NPP disposal could be a separate tunnel in a DGR for spent nuclear fuel. Initial evaluation of possibilities on i-graphite disposal in DGR was performed in the frame of CARBOWASTE project. The results of these investigations are summarized in the CAST deliverable D6.1 [KENDALL, 2015]. The assessment was performed for a generic site, limited to the migration by groundwater pathway and with some very conservative assumptions on the source term. One of the work packages in the CAST project was dedicated to investigations of the i-graphite characteristics. Based on the outcomes of these investigations, an updated safety assessment was performed in the frame of the CAST project. Information on inventory, rapid and slow release fractions and release rate as well as on speciation and sorption were applied in the updated assessment, however, in some cases with cautious assumptions, taking parameter values from the uncertainty interval with the worst effect on ^{14}C release. Despite this, the use of the provided information in general reduced conservatism in the updated assessment by about one order of magnitude. The differences between assumptions in the previous assessment and in the updated assessment are discussed in Section 1.2 and summarized in Table 1.

One more point is that information on ^{14}C release and speciation obtained during the CAST project was for other types of i-graphite than RBMK-1500 reactor. Taking this into account the results of the updated safety assessment should be regarded with care. In any case the

obtained information increased knowledge on the ^{14}C behaviour and provided understanding of its potential impact. However, further investigations are needed, especially with RBMK-1500 i-graphite, in order to increase confidence in selection of parameter values and to get more realistic representation of the system.

References

AMEC, 2016. Carbon-14 Project Phase 2. Irradiated Graphite Wastes. *AMEC for Radioactive Waste Management Limited*, Report RP50, AMEC/200047/004 Issue 2.

CAPOUET M., ET AL., 2017. Knowledge supporting Safety Assessments of ^{14}C (D6.2). *RWM, ONDRAF/NIRAS, ANDRA, RATEN ICN, GRS, ENEA, RWMC, FORTUM, LEI, NRG, SURAO, SKB, ENRESA, NAGRA,* CAST report D6.2.

KENDALL H., ET AL, 2015. Handling of C-14 in current safety assessments: State of the art. *RWM, ONDRAF/NIRAS, ANDRA, RATEN ICN, GRS, ENEA, RWMC, FORTUM, LEI, NRG, SURAO, SKB, ENRESA, NAGRA,* CAST report D6.1.

MAZEIKA, J., LUJANIENE, G., PETROSIUS, R., ORYSAKA, N., OVCINIKOV, S., 2015. Preliminary evaluation of ^{14}C and ^{36}Cl in nuclear waste from Ignalina Nuclear Power Plant decommissioning. *Open Chemistry,* Vol. 13 (1), 177–186.

NARKUNAS E., POSKAS P., 2017. Report on modelling of C-14 inventory in RBMK reactor core. *LEI*, CAST report D.5.17.

NARKUNIENE, A., ET AL., 2014. The study of the relationship between treatment and disposal on the performance of RBMK-1500 graphite disposal in crystalline rock. In: Proceedings of the 8th EC Conference on the Management of Radioactive Waste Community Policy and Research on Disposal EURADWASTE'13; 2013 Oct 14–17; Vilnius, Lithuania. EUR 26846 EN. Luxembourg: Publications Office of the European Union; 2014. p. 447–450. (Available from: http://cordis.europa.eu/fp7/euratom-fission/docs/euradwaste-low.pdf).

NDA, 2016. Geological Disposal. Carbon-14 Project Phase 2: Overview Report. *Nuclear Decommissioning Authority (NDA)*, NDA Report NDA/RWM/137.

POSKAS, P. ET AL., 2006. Generic repository concept for RBMK-1500 spent nuclear fuel disposal in crystalline rocks in Lithuania. *International topical meeting TOPSEAL 2006*, Olkiluoto, Finland, September 17-20.

TOULHOUT N., ET AL., 2015. Review of Current Understanding of Inventory and Release of C14 from Irradiated Graphite. CAST report D.5.5.

TOWLER, G., PENFOLD, J., LIMER, L., METCALFE, R., KING, F., 2010. PCPA: Consideration of Nonencapsulated ILW in the Phased Geological Repository Concept. Quintessa Limited (Report No.: QRS-1378ZD-R1).

Publication of CAST results

The preliminary results of investigations performed in the frame of the CAST project were published in the paper *Poskas, P. et al., 2016. Modeling of irradiated graphite ^{14}C transfer through engineered barriers of a generic geological repository in crystalline rocks. Science of the Total Environment, Vol. 569-570, 1126-1135*.

CArbon-14 Source Term

CAST

Integration of the CAST results into the safety assessment: SURAO contribution to D6.3

Antonín Vokál, Aleš Vetešník

Date of issue of this report: 23/03/2018

Executive Summary

The main objective of this study was to evaluate the latest scientific knowledge and understanding of the behaviour of carbon-14 provided by the CAST project in the context of the Czech deep geological repository development programme. The report addresses the performance of the sensitivity analysis of the release of carbon-14 in both its organic and inorganic forms from a deep geological repository for intermediate-level waste located in a crystalline host rock environment. The sensitivity analysis methodology employed in the study was based on the pseudo-random selection of values from a range of selected parameter values. The first order and total sensitivity indices, which express the contribution of individual parameters to the calculated output parameters over time, were calculated. This report briefly summarises the most important results obtained. The analysis revealed that carbon-14 in the organic form only is capable of exerting a non-negligible impact on repository safety; that the release of carbon-14 in the free gas phase may exert an important impact; and that the leaching rates of carbon-14 from the waste forms and the equivalent flow rates, which express the transport rates of carbon-14 from the backfill to the surrounding host rock fractures, make up the most important parameters with respect to influencing the release of carbon-14 into the crystalline host rock environment. It was also demonstrated that if the sorption of organic forms of carbon-14 on the host rock is substantiated, then it may exert a significant impact on the release rates of carbon-14 into the biosphere.

List of Contents

1 SURAO: The modelling of ^{14}C in disposal systems

1.1 *Introduction*

The Czech DGR concept assumes the disposal of spent fuel assemblies from Czech nuclear power plants in a deep geological repository at a depth of ~ 500m below the surface in a crystalline host rock environment. Intermediate-level waste (ILW) that cannot be disposed of in the near-surface repositories available in the Czech Republic will also be disposed of in the deep geological repository. Due to the planned use of robust two-layer canisters for the spent fuel assemblies with an estimated lifetime of more than 100 000 years, the majority of the carbon-14 contained in the spent fuel assemblies will decay to a negligible level within the canisters. However, with respect to the waste created from the decommissioning of nuclear power plants (NPPs), the use of short-lifetime canisters is envisaged, the lifetime of which will be insufficient for the decay of carbon-14 to an insignificant level. It has been estimated that the total activity of carbon-14 in the radioactive waste created from the decommissioning of NPPs will amount to around 5 x 10^{14} Bq, which is only slightly less than the activity of all the carbon-14 expected to be contained in the NPP spent fuel assemblies.

The main objective of this study was to evaluate the new scientific knowledge and understanding of the behaviour of carbon-14 provided by the CAST project in the context of a Czech deep geological repository for intermediate level waste located in a hypothetical crystalline host rock environment. The aim of the sensitivity analysis was to highlight which of the parameters analysed in the CAST project were expected to have the most significant influence on the release of carbon-14 into the environment. The sensitivity analysis methodology employed in the study was based on the pseudo-random selection of values from a range of selected parameter values. The first order and total sensitivity indices, which express the contribution of individual parameters to the calculated output parameters over time, were calculated. This report briefly summarises the most important results obtained. The results of the sensitivity analysis calculations, which were conducted by the Czech Technical University, are described in more detail in the SURAO report [VETEŠNÍK *et al.*, 2017].

1.2 Model description

The conceptual model (Figure 1) of a vault containing intermediate level waste from the decommissioning of Czech nuclear power plants assumes that the canisters containing the waste will be surrounded by a cement backfill material (backfill 1) inserted into the spaces between the canisters and a second cement backfill material (backfill 2) along the interface between the vault containing the canisters and the crystalline host rock. It is assumed that the maximum concentration of carbon-14 will be contained only in a limited number of canisters (the red canisters in Fig. 1); this is a conservative assumption aimed at avoiding the so-called dilution effect. It is possible that carbon-14 will be released directly from backfill 2 into the fracture network, or into the rock matrix and then into the fracture network. Further, it is assumed that carbon-14 may be released into the surrounding components in both the aqueous and free gas phases and as either organic or inorganic species. The expected range of transport parameter values used in the sensitivity analysis, taken partly from the results of the CAST project, is provided in Table 1.

Table 1: Selected range of parameter values used in the sensitivity analysis of the release of carbon-14 from a deep geological repository

Parameter	Unit	Min	Max	Mean
μ (lifetime of the canisters)	a	10	100	31
τ (leaching rate)	a^{-1}	$1 \cdot 10^{-5}$	0.1	0.001
Porosity (backfill)		0.2	0.5	0.35
Reference diffusivity	$m^2\ s^{-1}$	$2 \cdot 10^{-9}$	$2 \cdot 10^{-9}$	$2 \cdot 10^{-9}$
Relative diffusivity (backfill)		1	10^*	
Tortuosity		0.5	1	0.75
Porosity (granite)		0.005	0.02	0.01
Solubility (Inorganic)	$mol\ l^{-1}$	$1 \cdot 10^{-6}$	$1 \cdot 10^{-5}$	$5 \cdot 10^{-6}$
Solubility (organic)	$mol\ l^{-1}$	unlimited	unlimited	unlimited
K_d (backfill1, 2) (Inorganic/organic) [OCHS ET AL., 2016]	$m^3\ kg^{-1}$	2/1e-7/0*	20/1e-2	5/1e-4

Parameter	Unit	Min	Max	Mean
K_d (geosphere) (Inorganic/organic)	$m^3\,kg^{-1}$	2/1e-7/0*	20/1e-2	5/1e-4
Geo^{IN} (flow rate)	$m^3\,a^{-1}$	0.01	100	1
Geo^{T} (transport time)	A	10	$1\cdot10^{4}$	316
Q_{eq}	$l\,a^{-1}$	0.01	1	0.1
Inventory in one WP	Bq	$5\cdot10^{12}$	$5\cdot10^{13}$	$1.6\cdot10^{13}$
Volume of the repository (waste only)	m^3	160	800	480
Total number of WPs		40	200	120
Maximum activity of all the WPs	Bq	$1\cdot10^{14}$	$1\cdot10^{15}$	$3.2\cdot10^{14}$

*In some of the calculations, the sorption of the organic forms of carbon-14 with respect both to the granite and the backfill was assumed to be zero.

The calculations were performed in the GoldSim Transport Code [GOLDSIM, 2014].

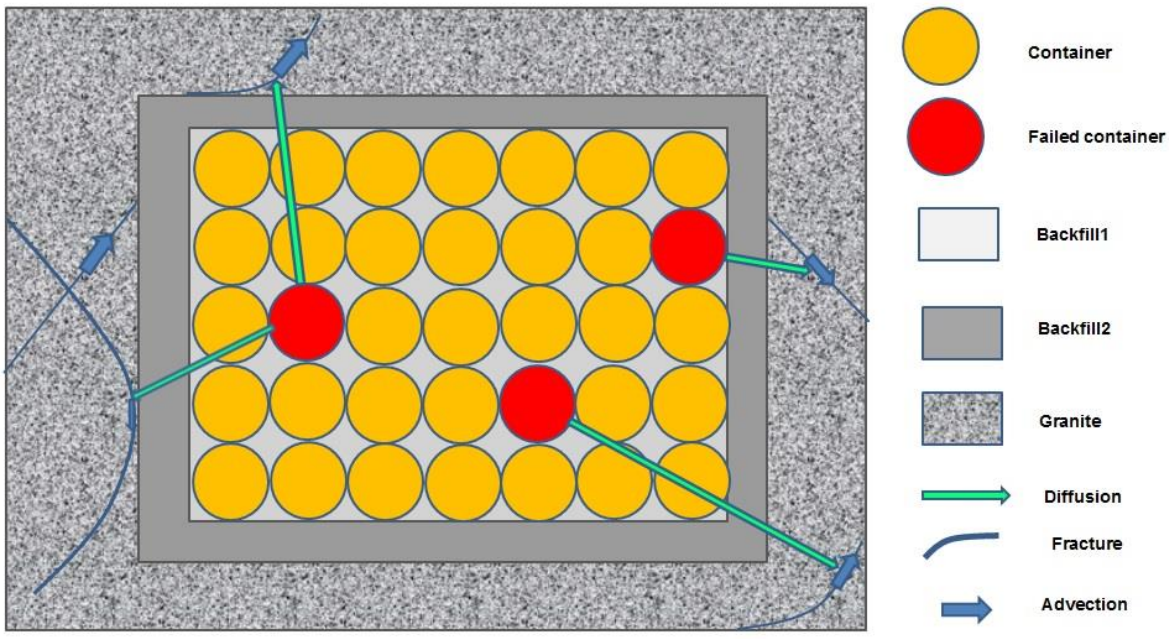

Figure 1: Conceptual model of a disposal cell for calculation purposes

1.3 *Results and discussion*

1.3.1 Comparison of the release of carbon-14 in its organic and inorganic forms

The first study focused on a comparison of the release of carbon-14 in both its organic and inorganic forms. The results of the calculations of the release of carbon-14 through different compartments according to the mean data provided in Table 1 are shown in Table 2. They clearly show that the release of carbon-14 species into the environment in its inorganic forms leads to effective doses several orders of magnitude lower than the release of carbon-14 in its organic forms. Thus, most of the calculations provided in this summary are related primarily to the release of carbon-14 in its various organic forms.

Table 2: Comparison of the maximum flow rate values of carbon-14 through the model compartments in its inorganic and organic forms for the mean values provided in Table 1 ($F_{C\text{-}B1}$ flow from the waste package to backfill 1, $F_{B1\text{-}B2}$ flow of carbon-14 from backfill 1 to backfill 2, and $F_{B2\text{-}G}$ flow of carbon-14 from backfill 2 to the host rock matrix)

Carbon-14 form	$F_{C\text{-}B1}$ [Bq/yr]	$F_{B1\text{-}B2}$ [Bq/yr]	$F_{B2\text{-}G}$ [Bq/yr]	Well dose [mSv/yr]
Inorganic	1.56×10^{10}	4.33×10^{8}	7697	3.25×10^{-10}
Organic	1.12×10^{10}	1.05×10^{10}	4.42×10^{9}	1.87×10^{-4}

1.3.2 Sensitivity analysis of the release of carbon-14 with respect to changing leaching rate, inventory and equivalent flow rate

The second study focused on the sensitivity analysis of the impact of the leaching rate, the inventory of carbon-14 in one waste package and the so-called equivalent flow rate, which express the transport rates of carbon-14 from the backfill to fractures in the surrounding host rock [NERETNIEKS ET AL., 2010], the change in the mass of carbon-14 in the waste packages (Fig. 2 A), the change in the concentration of carbon-14 in the waste packages (Figure 2 B), the flow of carbon-14 from a waste package to the backfill (Figure 2 C) and the flow of carbon-14 from the backfill to the fracture network (Figure 2 D). Other parameter values were

kept constant as given in Table 1. It was conservatively assumed in the analysis that the sorption of carbon-14 in its organic forms on both the backfill materials and the host rock was zero and the solubility of organic forms of carbon-14 in the groundwater was unlimited. The results of the calculations over time are provided in Figure 2.

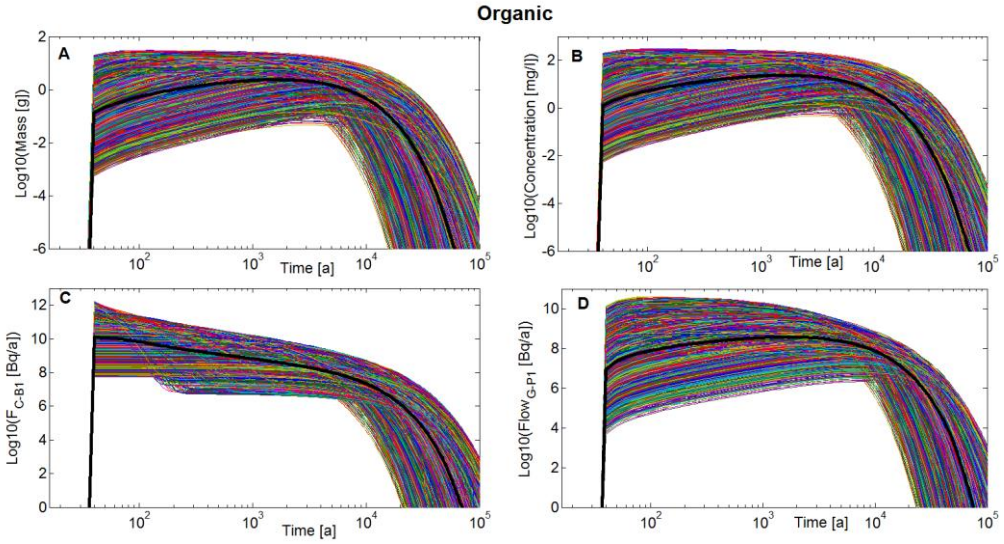

Figure 2: Evolution of the output parameters over time for organic forms of carbon-14. Change in the mass of carbon-14 in the waste packages (A), concentration of carbon-14 in the waste packages (B), flow of carbon-14 from a waste package to the backfill (C) and the flow from the backfill to the fracture network (D)

From the results provided in Figure 2, it is difficult to estimate the impact of the uncertainty of the input parameter values on the calculated output parameters and, therefore, the so-called sensitivity indices, which allow the estimation of those parameters which exert the most significant influence on the output parameters, were calculated according to the method proposed by Saltelli [SALTELLI *ET AL.*, 2010] described in more detail in the SURAO report [VETEŠNÍK *ET AL.*, 2017]. The results of the calculations of the sensitivity indices are shown in Fig. 3. It is clear that, initially, the most significant effect on the all output parameters is exerted by the leaching rate of carbon-14 from the waste forms (black lines); subsequently, however, the equivalent flow rate (green lines) can be seen to have the greatest influence on the output parameters. The maximum effect of the carbon-14 inventory in the waste packages

(blue lines) is exerted at a time approaching 10 000 years following the release of carbon-14 from the waste forms.

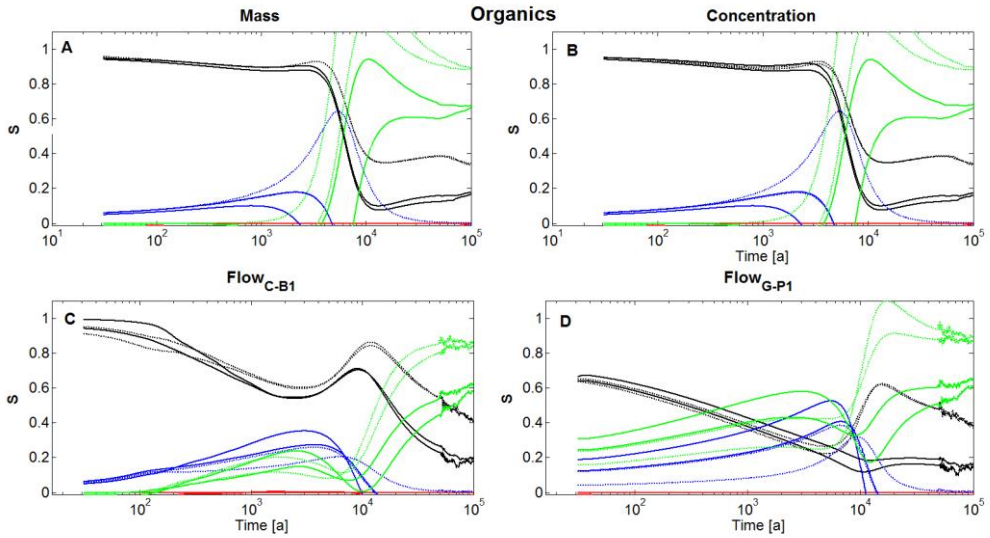

Figure 3: Dependence of the sensitivity indices over time for variations in the leaching rate, solubility, inventory and equivalent flow rate (Table 2) for organic carbon-14 species (mass of organic carbon-14) (A), concentration in the waste package (B), the flow of carbon-14 from a waste package to the backfill (C) and the flow from the backfill to the fracture network (D). Sensitivity index for organic species (leaching rate - black lines, solubility - red lines, inventory - blue lines, Q_{eq} - green lines).

1.3.3 Sensitivity analysis of the release of carbon-14 with respect to changing sorption coefficients, porosity and equivalent flow rate

Subsequent sensitivity analysis focused on highlighting the influence of the sorption coefficients of carbon-14 on both the backfill and the host rock with simultaneous changes in porosity and equivalent flow rates. The range of selected parameters applied is provided in Table 1. Figure 4 shows the results of the evolution of the concentration of carbon-14 in the free water in the waste packages (A), the flow of carbon-14 from the host rock matrix to the host rock fracture network (B) and the respective sensitivity indices over time. All the other parameters exhibited the mean constant values as shown in Table 1. The solubility of the organic species of carbon-14 was assumed to be unlimited.

It is clear that upon the commencement of the release of carbon-14 from the waste packages, a change in the sorption coefficients of carbon-14 on the host rock exerted the most significant impact on the variance of the release of carbon-14 into the host rock. Subsequently, however, once again the equivalent flow rate was seen to exert the greatest influence on the release of carbon-14 into the host rock.

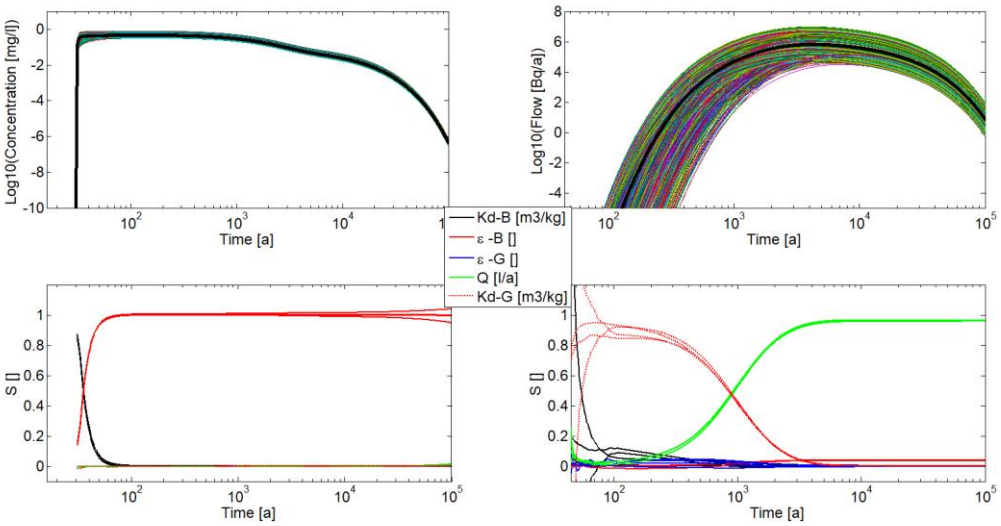

Figure 4: Dependence of the sensitivity indices over time with respect to varying sorption, porosity and the equivalent flow rate (Table 4) for the transport of organic carbon-14 species (mass of inorganic carbon-14) (A), concentration in the canister (B), the flow of carbon-14 from a waste package to the backfill (C) and the flow from the host rock matrix to the fracture network (D). Sensitivity index for organic species (K_d backfill - black lines, K_d granite – dotted red lines, porosity backfill - red lines, porosity granite - blue lines, Q_{eq} - green lines).

1.3.4 Release of carbon-14 in the free gas phase

The thermodynamic equilibrium calculations performed as part of the CAST project [WIELAND AND HUMMEL, 2015] revealed that hydrocarbons, primarily methane, made up the predominant species released from activated carbon steels, both in the aqueous and gaseous phases depending on the level of saturation of the host rock environment. The partitioning of methane between the aqueous and gas phases was calculated with the assistance of the Henry relationship, which expresses the relationship between the

concentration of species in the water and the partial pressure of the gas above the water. The results of the calculations of the release of carbon-14 through the DGR compartments for a saturation level of 0.5 are provided in Table 3. In view of the high reference gas diffusivity value obtained for the gaseous phase and the Henry constant value, it is evident that flow in the gaseous phase is capable of exceeding that in the liquid phase by many orders of magnitude. Details of the calculation of the release of carbon-14 in a partly-saturated environment depending on the level of saturation of the host rock are provided in the SURAO report [VETEŠNÍK ET AL., 2017].

Table 3: Comparison of the maximum flow rate values of carbon-14 through model compartments in the gaseous and aqueous forms ($F_{C\text{-}B1}$ flow of carbon-14 from the waste package to backfill 1, $F_{B1\text{-}B2}$ flow of carbon-14 from backfill 1 to backfill 2, $F_{B2\text{-}G}$ flow of carbon-14 from backfill 2 to the granite)

Medium/saturation	$F_{C\text{-}B1}$ [Bq/yr]	$F_{B1\text{-}B2}$ [Bq/yr]	$F_{B2\text{-}G}$ [Bq/yr]	Well dose [mSv/yr]
Gas/0.5	1.57×10^{10}	1.34×10^{10}	5.99×10^{9}	2.53×10^{-4}
Water/0.5	1.57×10^{5}	6.18×10^{5}	9.68×10^{4}	4.10×10^{-12}

2 Integration of the CAST experimental outcomes at the safety case level

The sensitivity analysis revealed that carbon-14 in the organic form only is capable of exerting a non-negligible impact on repository safety; that the release of carbon-14 in the free gas phase may exert a significant impact; and that the leaching rates of carbon-14 from the waste forms and the equivalent flow rates between the backfill and the host rock fracture network make up the most important parameters with respect to influencing the release of carbon-14 into the environment. It was also shown that if the sorption of organic forms of carbon-14 on the host rock is substantiated, then it may exert a significant impact on the release rates of carbon-14 into the biosphere.

The latest results of the CAST project make a significant contribution to the understanding of the behaviour of carbon-14 in deep geological repositories and will, in the future, assist in the compilation of advanced safety assessments for the future Czech deep geological repository. However, the results of the CAST project relating to the determination of the ratio of inorganic and organic forms of carbon-14 expected to be released during the degradation of the radioactive waste remain ambiguous. It seems, as suggested by Wieland and Hummel [WIELAND AND HUMMEL, 2015], that neither the experimental evidence obtained to date, nor the thermodynamic modelling allow for the drawing of well-supported conclusions in this respect from the current results.

References

GOLDSIM, GoldSim Contaminant Transport Module User's Guide. − GoldSim Technology Group, version 6.4., 2014

NERETNIEKS I., LIU L., MORENO L. Mass transfer between waste canister and water seeping in rock fractures. Revisiting the Q-equivalent model, SKB Technical Report TR-10-42, March 2010

OCHS M., MALLANTS D., WANG L. ,2016,: Radionuclide and Metal Sorption on Cement and Concrete. Topics in Safety, Risk, Reliability and Quality, 29, 300 s.

SALTELLI A., ANNONI P., AZZINI I., CAMPOLONGO F., RATTO M., TARANTOLA S. (2010): Variance based sensitivity analysis of model output. Design and estimator for the total sensitivity index. COMPUTER PHYSICS COMMUNICATIONS 181, 259-270.

VETEŠNÍK A., REIMITZ D., BABOROVA L., VOPÁLKA D., 2017 Development of model for CARBON-14 transport in a DGR environment, uncertainty and sensitive analyses, SURAO report 171/2017, April 2017

WIELAND E., HUMMEL W., Formation and stability of 14C-containing organic compounds in alkaline iron-water system, MINERALOGICAL MAGAZINE, NOVEMBER 2015, VOL 79, PP. 1275 – 1286

PART 3 – Salt host rock

CArbon-14 Source Term

CAST

Integration of CAST results to safety assessment: Contribution from ENEA to D6.3

B. Ferrucci, R. Levizzari, A. Luce

Date of issue of this report: 09/02/2018

Executive Summary

The present work, performed within the European CAST project, has the purpose to evaluate the radiological impact of gaseous 14C in a hypothetical geological repository hosted in salt rock, within the context of HLW-LL and ILW final disposal.

In Italy the agreement for final disposal of HLW-LL and ILW has not yet been taken, while an interim storage in a near surface repository has been selected as provisional solution. Past Italian studies about geological disposal do not comprehend safety analysis or, in modern approach of the term, safety assessment. Therefore, this work is a preliminary safety analysis for the disposal of radioactive waste intended for geological repository.

The conceptual model of the system "waste-repository-salt rock" has been developed using data of Italian past studies about salt formation, information from literature and analogies with other GDF projects (e.g., WIPP). The hypothetical repository should be realized in a deep salt formation, about 800 m depth, with geometry features similar to the US WIPP repository. The data of radioactive waste inventory have been elaborated from previous Italian studies and thanks to information gathered from Italian waste management organisation (Sogin S.p.a.). These data have been the fundamental input to size the underground structure and to define the key parameters used in simulation code.

Simulations about the emission and migration of gaseous 14C from radioactive waste in GDF have been carried out by means of TOUGH2 software. Three simulations have been performed: the first one, related to the whole inventory (multi-room model), to test the reliability of the conceptual model; the second one (single-room model with a conservative approach), related only to the emissions of gaseous 14C from the graphite waste, representing the most important radiological source for the Italian inventory; the third model, similar to the previous one (single-room model), but with a more realistic approach (less conservative). A preliminary sensitivity analysis, with different scenarios, has been performed to evaluate the effect of key parameters variation on final results.

Results of different simulations have highlighted the low radiological impact of 14C gaseous emissions in underground facility and in the shaft toward the surface, using appropriate sealing materials. The results of the detailed simulations, to evaluate the emission and migration of gaseous 14C from the graphite, have highlighted the low radiological impact of this waste disposed in deep salt formation and have highlighted the possibility to correlate the features and location of sealing materials to the amount of 14C emitted toward the surface facility.

List of Contents

1 ENEA: Modelling 14C in disposal systems

In Italy, the solution for radioactive HLW-ILW final disposal is under discussion. At the moment, a solution for the final disposal of LLW and for interim storage of ILW and HLW-LL has been identified in a near surface disposal, but the area has not been yet selected.

Current work supports future Safety Assessment studies (post-closure safety) for a hypothetical GDF in a favourable geological Italian site in salt rock, analysing the dynamic and the radiological impact of gaseous 14C in underground facility. The numerical modelling has been performed using the TOUGH2/EOS7R multi-phase code, by means of PetraSim software as graphical interface [Oldenburg and Pruess, 1995]. To understand the dynamic and the radiological impact of gaseous 14C, three models have been developed: one referred to a 3D "multi-room" model and two referred to a 3D "single-room" model. The main purpose of the first one has been to test the reliability of the conceptual model and of the code capabilities; in this case a whole simplified geologic repository in salt rock has been modelled. In the second one (single-room model with conservative approach) only one storage room has been modelled, containing the 14C activity of the graphite waste, that represents the major radiological contribution to the whole 14C in Italian radioactive waste inventory. The third model (single-room model with "realistic" approach) is similar to the second one, but with a more realistic approach (less conservative) for what concern the sealing materials and gaseous 14C release rate.

1.1 *Introduction*

The work has been performed taking into account data by previous Italian studies and by literature (when site data were not available) and taking into account the Italian radioactive waste inventory; for what concern the underground disposal facility, analogies with other existing geological repository projects have been considered (e.g., WIPP).

The current inventory of Italian radioactive HLW-LL and ILW containing 14C, to be placed in a geological disposal, is reported in Table 1; it does not contain the residues coming from

the reprocessing of irradiated fuel sent abroad (UK and France) to be returned to Italy as vitrified waste.

Table 1: Inventory of Italian ILW and HLW-LL containing 14C

Origin	**Materials**	**Volume (m^3)**	**Inventory of 14C (GBq)**	**Quality of information Uncertainty**
GCR-Magnox Reactor (Latina NPP)	Graphite	3.30+E3	2.83E+04	Estimated Moderate
Nuclear Power Plants	Resins, metals	n.a.	3.30E+03	Estimated High
Medical, industrial, research	Conditioned sources	172.60 (863 drums 200 dm^3)	0.42	Estimated Moderate
	Not treated sources	6.78 (113 metallic drums 60 dm^3)	92.80	Estimated Moderate
	Cemented sources	113.60 (284 metallic drums 400 dm^3)	106.28	Estimated Moderate
	Solid treated sources	42.00 (105 drums)	11.00	Estimated Moderate
	Not treated liquid waste	4.19 (192 plastic 20 dm3; 2 metallic drums 120 dm3; 1 metallic 110 dm^3)	4.05	Estimated Moderate
	Not treated solid waste	15.06 (251 metallic drums 60 dm^3)	2.36	Estimated Moderate

Volume of graphite is referred to not-conditioned waste. The high uncertainty of data about resins and metals is due to the worst characterization of waste.

As previously underlined, the performed simulations represent the first implementation of a preparatory safety analysis, useful for future safety assessment of a hypothetical Italian geological repository, with particular reference to the dynamic of 14C gaseous release and transport. The three simulations have been focused on the performances of the engineered barrier system, referred to different filling and sealing materials, with particular reference to

the variation of their distribution coefficient (K_d). The multi-room model provides three main study cases, in which the 14C amount (Bq) has been calculated under different configuration of sealing material within the repository. The two single-room models take into account only one storage room of the repository, increasing the calculation domain above the storage room, to reduce the discretization grid and to better detail the migration of gaseous 14C. The objective of these models is to evaluate the capability of containment of the salt body and the capability of the engineered barrier system to delay the 14C migration toward the top of the shaft, using different values of K_d, for the filling and sealing materials within the repository.

1.2 *Model description*

In all models, an underground facility located to a depth of ~800 meters has been considered; the repository should be hosted in a salt body, 200 m thick, below clay rock about 700 m tick (Figure 1).

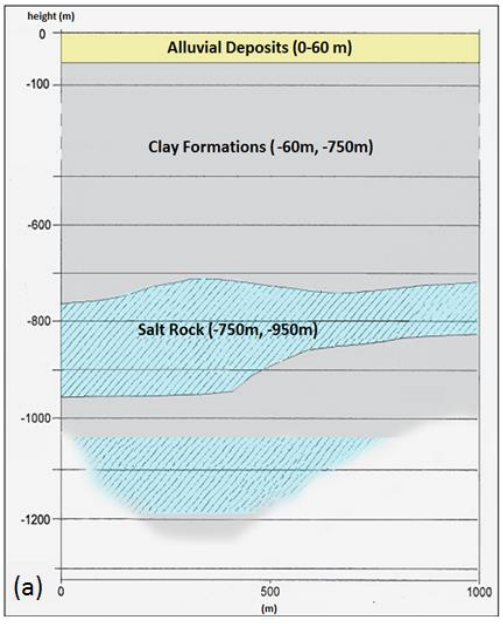

Figure 1: Geological stratigraphy of host rock

Geological barrier is guaranteed by the salt rock, isolated from the surface by two different clay formations; the salt formation is considered quite homogeneous, although some discontinuities, as clay inclusions, cannot be excluded. The host formation is supposed strictly

dry and no water circulation is considered. Sealing material (clay, concrete, asphalt and salt) are used as engineered barriers to slow radionuclides migration**.**

The gas generation for all the three models has been modeled on the basis of three main hypotheses: the corrosion of steel containers (assumed corrosion rate of 1 nm/y) cause a release of hydrogen (H_2) in the gaseous phase, generated in accordance with the steel corrosion reaction and a consequent release of carbon; in the first two models, the rate of gaseous 14C release is constant for all waste and equal to the 10% per year of the activity content during the calculation time. This Instant Release Fraction (IRF) is considered to adopt a conservative approach in the first two simulations. In the third simulation, a less conservative approach has been adopted, reducing the emission rate to a congruent release of 1% per year [Poskas *et al.*, 2016]. The steady-state initial conditions provide a pressure profile that generates a gas flow in the system. Taking into account the US WIPP experience, a lithostatic pressure of ~15 MPa is considered at ~800 m depth. This pressure is never exceeded by the previous gas flow during the simulation time in the repository.

An important fraction of the 14C in graphite is not releasable, because strongly bounded to the graphite matrix. Moreover, the total fraction and the fraction of each gaseous species (mainly CO_2 and CH_4) depend on the "history" of graphite (i.e. irradiation history, operational conditions, etc.) etc. [Toulhoat *et al.*, 2018]. Unfortunately, it was not possible to take into account these evidences in current simulations, because cited data are not available at the moment for the graphite inventory.

In all models, only the normal evolution scenario has been modelled. Two main time steps have been considered: the first from 0 to 300 years after repository closure, when no release of radionuclides occurs and waste package integrity is maintained; the second from 300 y to 300.000 y after the repository closure, when steady-state conditions are established, waste packages corrosion and 14C release take place.

1.2.1 Description of the 3D multi-room model

The multi-room model comprehends 16 rooms, arranged in two *panels* separated by a central *pillar* of intact salt, as showed in Figure 2.

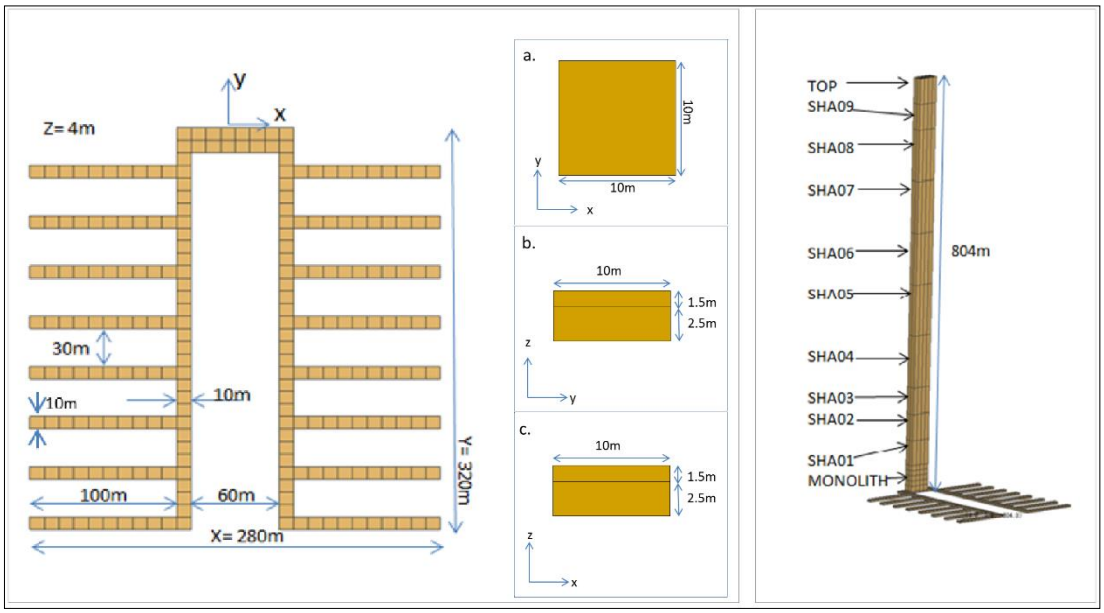

Figure 2: 3D multi-room conceptual model

The sealing system comprises four materials that completely fill the shaft, rooms and drifts, as showed in Figure 3 in which the white areas will be filled with different materials depending on the considered scenario, which will be discussed later. The engineered barrier system consists of waste containers, backfill and shaft seal. No damaged zone has been included in this conceptual model and only one shaft to surface is considered.

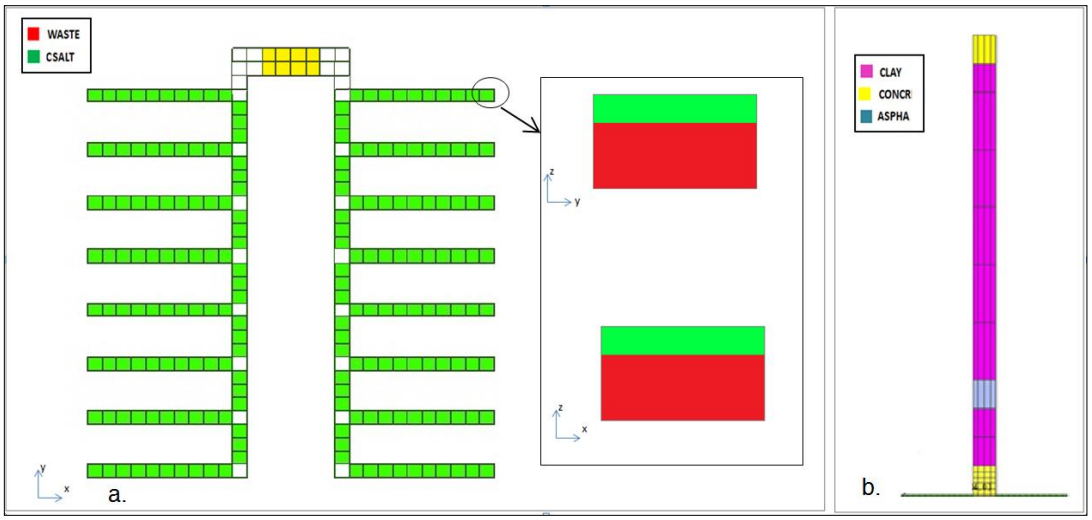

Figure 3: Configuration of sealing materials in the repository domain

Due to lack of detailed data regarding waste inventory and due to lack of detailed information about specific site for GDF, preliminary hypotheses were adopted. For each kind of waste, the total amount of the estimated 14C activity is equally distributed and the features of waste material do not affect the 14C release processes. The 14C is released only in the gaseous phase and the gas generation will persist during all the calculation time; migration takes place only by diffusion. The arrangement of waste into the rooms has been carried out dividing the waste on the basis of their origin. The total number and type of drums have been used to calculate the number of storage rooms and to estimate the total amount of active metal surface in each room (where applicable). No overpack is provided to contain drums (conservative approach); in each room, waste is assumed as disposed in a compacted volume of 2500 m^3 (x=100 m; y=10 m, z=2,5 m dimensions) divided into 10 cells of 250 m^3.

To deepen the dynamic of gaseous 14C migration, a preliminary sensitivity analysis has been carried out in the first simulation; the K_d value of sealing materials is selected as sensitive parameter in the simulation cases. Three main study cases have been analyzed by changing the materials combination at the repository level, as shown in Figure 4. In all cases, K_d = 1 m^3/kg for the clay, K_d=1E-5 m^3/kg for asphalt, concrete and waste, K_d = 1 m^3/kg for

crushed salt have been assumed. These approximated values have been selected to verify the capabilities of the code and the validity of the performed conceptual model.

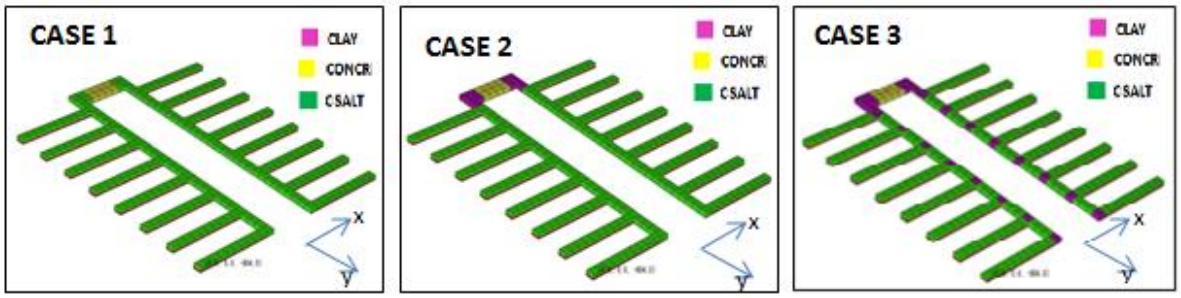

Figure 4: Materials configuration in the study cases

1.2.2 Description of the 3D single-room model (conservative approach)

In the 3D single-room model (conservative approach), only one storage room has been simulated. A new barrier system configuration has been taken into account, based on [Freeze *et al.*, 2013]. Where not explicated in following description, input data assumed for simulation are the same assumed as input for the multi room model.

The engineered barrier system consists of the waste form, waste container, backfill, and shaft seal. A disturbed rock zone (DRZ), surrounding the excavated zone, has been considered (Figure 5). In the storage room there are 196 cubic waste containers, representing the graphite waste of Italian inventory, with a volume of 1 m^3 each one; they are divided into four rows of 49 elements, placed at the same distance of 1 m from each other. The void between and above the containers is filled with salt. The base of the shaft consists of a monolith of concrete 4 m high, 9 m long and 9 m thick.

The source term is modelled as a gaseous emission of 14C with a release rate of 10% per year of total 14C activity of the graphite (IRF is considered to adopt a conservative approach); it's assumed equally distributed throughout the 196 fictitious containers. Four main cases have been simulated (Table 2).

Table 2: K_d values (m^3/kg) used for the 3D single-room model (conservative approach) study cases

	DRZ	Clay	Waste Containers	Backfill (salt)	Shaft Sealing	Concrete (Monolith)
Case 1	0	0	0	0	0	0
Case 2	0	0	0	0	0	4
Case 3	0	0	1	0	0	0
Case 4	0	0	0	0	1	0

Assuming different values for the K_d featuring the sealing materials, it is possible to create different scenario and to analyze their contribution to delay the migration of 14C through the system. Furthermore, it allows to know if the location of the material with the highest K_d value affects the performance of the whole barrier system. The highest value of K_d is referred to concrete, to enhance its real capability to retain radionuclides [Yim and Caron, 2006].

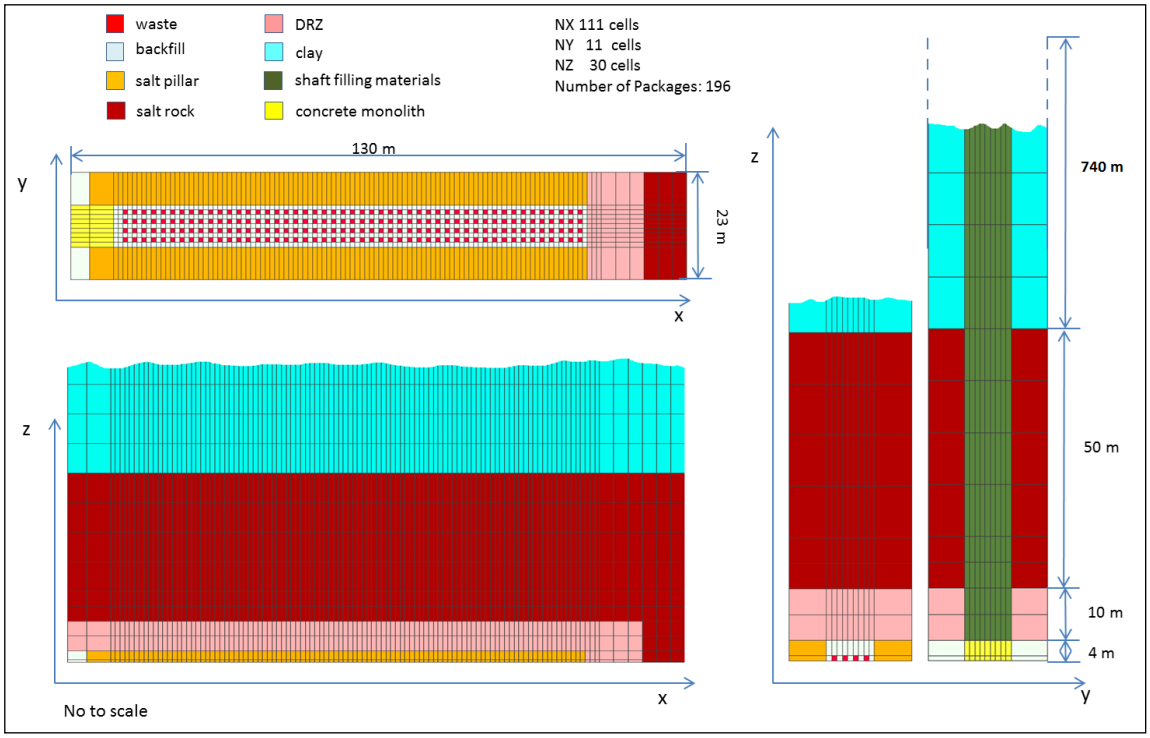

Figure 5: Salt repository TOUGH2/PetraSim in 3D single-room model (conservative approach)

The 14C speciation occurring during the repository evolution cannot be simulated using TOUGH2/EOS7R; then, at the moment no assumption has been made on the 14C speciation.

1.2.3 Description of the 3D single-room model ("realistic" approach)

The third model has been developed to reduce conservativeness of previous models and to evaluate in a more realistic way the radiological impact of 14C. The main features of the previous conceptual model have been preserved, but a different and more detailed configuration of sealing materials has been performed. Figure 6 illustrates a possible configuration of materials featuring the shaft sealing system for simulations, as defined for a generic vertical shaft in US WIPP. Materials comprehend concrete, asphalt, salt and clay, whose physical and mechanical properties are referred to [Sandia National Laboratories, 1996].

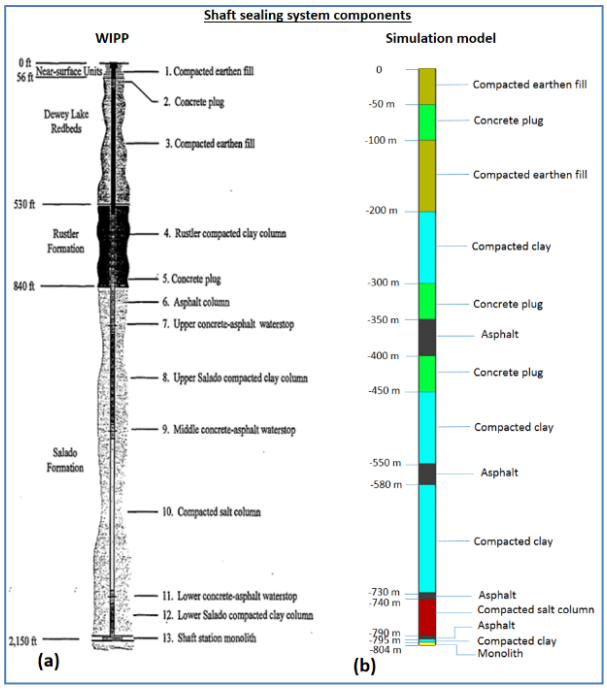

Figure 6: Sealing system of the shaft developed for simulations (b) in analogy with US WIPP (a) [Sandia National Laboratories, 1996]

At the moment, considered the necessity to evaluate the impact of sealing materials on migration of 14C, the predominant form of gaseous 14C considered for the this simulation is methane (CO_2 is not considered, unlike the previous models), with no adsorption capacity into the salt rock formation (K_{d_salt} = 0 m^3/kg) and a capacity of adsorption into the concrete sealing material (K_{d_concr}= 0,5 m^3/kg) [Enssle et al., 2014]. Chemical reactions, i.e. oxidation of CH_4 or carbonation as an attenuating process of 14C migration, are neglected. A congruent release of gaseous 14C starts at the moment of the repository closure, with a release rate of 1% per year (t=0 at the repository closure) [Poskas *et al.*, 2016]. No IRF is considered and migration takes place only by diffusion. All other simulation characteristics are the same already implemented in the previous 3D single-room model.

1.3 *Results and discussions*

In the following tables are reported the simulation results. The values of 14C amount have been calculated on two specific blocks common to the three models: the top of the shaft and the monolith. However, the results of the first two simulations (multi-room and single-room conservative approach) are not comparable, because of the different discretization and conceptualization of the two models; therefore, the data are reported in different tables.

Table 3: Simulation results for multi-room model

	14C amount (Bq) after 300.000 years			
	Case 1	Case 2	Case 3	Case 4
Top of the shaft	5,0E-04	1,0E-15	1,0E-15	-
Monolith	3,4E03	3,2E04	5,1E02	-

Table 4: Simulation results for single-room model (conservative approach)

	14C amount (Bq) after 300.000 years			
	Case 1	Case 2	Case 3	Case 4
Top of the shaft	1,3E-03	8,5E-06	9,7E-05	5,36E-06
Monolith	1,9E-03	3,62E-05	1,3E-03	2,1E-05

Table 5: Maximum amount of 14C at the top of the shaft over the time for multi-room model

		Case 1	Case 2	Case 3	Case 4
Multi-Room	*(y)*	*50.000*	*100.000*	*100.000*	
	Bq	2,2E-01	1,3E-02	1,1E-03	

The multi-room model simulation results (Table 5) show that in Case 1 the amount of 14C at the top of the shaft reaches the maximum value in half the time than the Case 2 and 3, with a value of two and three order of magnitude higher. After 300.000 years the release in the Case 1 become negligible, while in the Case 2 and 3 falls to zero.

The single-room model simulation results (Table 6) show that the peak of 14C amount at the top of the shaft occurs between 20.000 y and 30.000 years in the first three cases, with a maximum value of 2,7E07 Bq at 22.000 years in the Case 1. In the Case 4 the peak is reached earlier than the other cases, having a value four order of magnitude lesser than the Case 1. After 300.000 years the 14C amount at the top of the shaft become negligible in all cases, with a minimum value of 8,5E-06 Bq in the Case 2.

Table 6: Maximum amount of 14C at the top of the shaft over the time for single-room model (conservative approach).

		Case 1	Case 2	Case 3	Case 4
Single-Room	*(y)*	*22.000*	*25.400*	*28.500*	*19.000*
	Bq	2,7E07	3,8E06	4,2E05	4,1E03

In the single room model ("realistic" approach) the peak of the 14C gaseous emission in the monolith occurs at 1270 years after the repository closure (Table 7), while at the top of the shaft at 4750 years (about 2.800 Bq).

Table 7: Maximum amount of 14C at the top and at the bottom of the shaft for the single-room model ("realistic" approach)

	Time (years)	14C (Bq)
Monolith	1270	1,6E+07
Top of the shaft	4750	2,8E+03

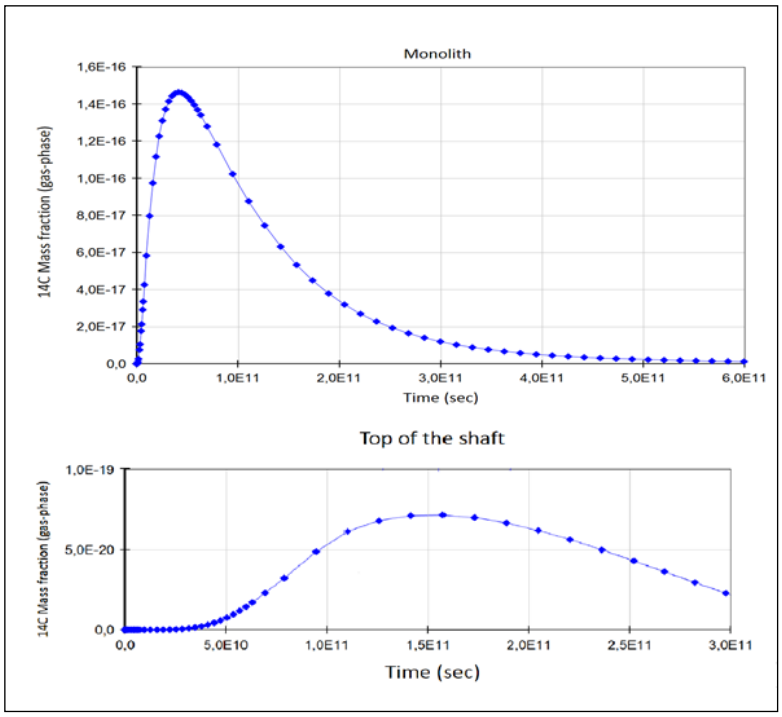

Figure 7: Peak of 14C mass fraction at the top and at the bottom of the shaft for the single-room model ("realistic" approach)

2 Integration of the CAST experimental outcomes at the level of the safety case

This work performed within the CAST project is a preliminary analysis of the radiological impact of gaseous 14C from HLW-LL and ILW disposed in a hypothetical Italian GDF in salt rock. Before this work, no safety assessment or generic safety studies had been developed in the Italian context for geological disposal. So, radioactive inventory data and literature data have been used as primary data for simulations. The outcomes of the CAST project have been used to better detail the phenomena occurring in the repository. Unfortunately, no comparison is actually possible with past studies, especially for what concern the reduction of uncertainties and scenario hypothesis.

The conceptualization of a hypothetical geological repository and the following simulations have improved the knowledge about the future safety issues that will have to be discussed for final disposal of Italian HLW-LL and ILW. In particular, data and information gathered form others WPs of the CAST project, have permitted to reduce the conservative approach normally used in simulations, especially for what concern the improvement of model development from the second to the third simulation.

The main contribution to the delay of the gaseous 14C migration through the repository is given by using appropriate filling and sealing materials, as quantified in simulations. From the simulation results of the multi-room model, taking into account the Cases 2 and 3, it's evident that, for equal values of K_d, the performance of the filling material is proportional to its volume/density: increasing of three times the total volume of the clay, moving from the Case 2 to the Case 3, the amount of 14C in the monolith is reduced of two orders of magnitude. The same conclusion can be drawn from the single-room model simulations results. But in this case the difference in the 14C amount, occurring by increasing three times the volume of the highest K_d material, is about four orders of magnitude. This result depends on the grid spacing discretization of the calculation domain. In fact, the grid spacing of the second model domain has been drastically reduced. In order to have more realistic results, the discretization grid should be the smallest possible, but this lead to longer calculation time and it could be developed in future studies.

The third simulation performs a more realistic evaluation (less conservative) about the low radiological impact of gaseous 14C emission from graphite, hosted in a deep geologic repository. The mitigation of 14C migration towards the surface and the following low radiologic impact, are due to the combined actions of low conductivity of salt host rock, adsorbing capacity of sealing/filling materials and radioactive decay.

References

Enssle, C. P., Brommundt, J., Kaempfer, Th. U., Mayer, G., Wendling, J., 2014. Full-scale 3D modelling of a nuclear waste repository in the Callovo-Oxfordian clay. Part 1: thermo-hydraulic two-phase transport of water and hydrogen. In: Norris, S., Bruno, J. et al. (eds) Clays in Natural and Engineered Barriers for Radioactive Waste Confinement. Geological Society, London, Special Publications, 400

Freeze, G. P., Gardner, P., Vaughn, P., Sevougian, S.D., Mariner, P., Mousseau, V., Hammond, G., 2013. Enhancements to generic disposal system modeling capabilities. FCRD-UFD-2014-000062. SAND2013-10532P. Sandia National Laboratories, Albuquerque, NM

Oldenburg, C., Pruess, K. 1995. EOS7R: Radionuclide transport for TOUGH2. Berkeley, California. Report LBL-34868

Poskas, P., Grigaliuniene, D., Narkuniene, A., Kilda, R., Justinavicius, D., 2016. Modeling of irradiated graphite 14C transfer through engineered barriers of a generic geological repository in crystalline rocks. Science of the Total Environment 569–570, 1126–1135, 2016

Sandia National Laboratories, 1996. Waste Isolation Pilot Plant Shaft Sealing System. Compliance Submittal. Design Report. Volume 1 of 2: Main Report. Appendices A, B, C, and D. SANDIA REPORT. SAND96-1326/1, UC-721

Toulhoat, N., Moncoffre, N., Narkunas, E., Poskas, P., Bucur, C., Ichim, C., Petit, L., Schumacher, S., Catherin, S., Capone, M., Shcherbina, N., Bukaemskiy, A., Rodríguez Alcalá, M., Magro, E., María Márquez, E., Piña ,G., Fachinger, J., Fugaru, V., Norris, S., Borys, Z., 2018, Final report on results from Work Package 5: Carbon-14 in irradiated graphite (D5.19). CAST project Report; 2018. Available from: http://www.projectcast.eu/publications

Yim M., Caron, F., 2006, Life cycle and management of carbon-14 from nuclear power generation. Progress in Nuclear Energy, 48, 2–36

CArbon-14 Source Term

CAST

Integration of CAST results to safety assessment: Contribution from GRS to D6.3

André Rübel

Date of issue of this report: 22/06/2017

List of Contents

1 GRS: Modelling C^{14} in disposal systems

1.1 Introduction

1.1.1 Repository concept

The strategy of the site selection and licensing procedure for a nuclear waste repository for high-level waste in Germany is under discussion at the moment of writing. While salt has been regarded as main option for the host rock for deep geological disposal, the three host rock types salt, clay and crystalline rock are to be considered equally in the future. Although there has been research on repository concepts in clay and crystalline rock, the repository concept for geological disposal in salt host rock clearly is the most advanced at this time. Therefore, this document describes the repository concept developed for the Gorleben site.

The Gorleben salt dome has been investigated as potential site for a repository for high-level waste since the end of the 1970s. Until now, it has been made neither a decision in favour of Gorleben as repository site nor a final statement on the actual suitability of the site. A site-specific research project, the Preliminary Safety Analysis for Gorleben (VSG), has been conducted from July 2010 to March 2013 to sum up the results of the Gorleben investigation achieved so far, to update the concepts like for emplacement, repository layout, sealing and performance assessment and to compile remaining open questions. The repository layout and the sealing concept for the Gorleben site developed during the VSG project were adapted to the site-specific geological boundary conditions.

The following description of the disposal concept refers to the drift disposal concept developed within the scope of the VSG [Bollingerfehr et al. 2011] and [Bollingerfehr et al. 2012]. The emplacement fields for spent fuel and HLW are located in the north-eastern part of the repository (see figure 1.1). The emplacement fields are tailored in such a way that they are completely embedded in the main salt (z2HS) of the salt dome. The repository layout took into account the known and expected geologic situation at the emplacement level (870 m below surface) of the salt dome. Two main transport drifts are the northern and southern boundaries of the twelve emplacement fields (East 1 to East 12). Each emplacement field

consists of a crosscut and several parallel emplacement drifts in which the waste containers are emplaced on the floor. After the containers have been emplaced, the void spaces of the emplacement drifts are backfilled with dry crushed rock salt. There is no requirement to seal each single emplacement drift. Optionally, the emplacement field is sealed with a 10-m-long sorel concrete (MgO) plug at both ends of the crosscuts for operational reasons. Sorel concrete consists of magnesium oxide as adhesive cement and crushed salt as aggregate. These plugs have no specified requirement for the post-operational phase. The main transport drifts are backfilled with crushed salt as well, but with a water content of 0.6%wt, to accelerate the compaction process.

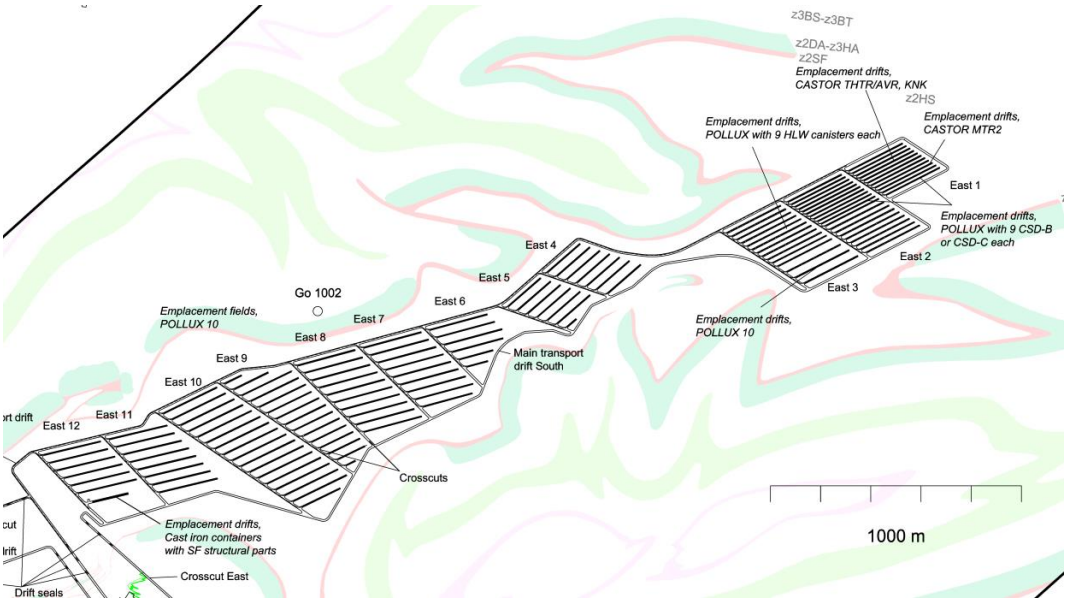

Fig 1.1: Layout of the north-eastern part of the repository [Bollingerfehr et al. 2012]

1.1.2 C-14 inventory

The inventory of the repository consists of heat generating waste. Waste types with negligible heat generation which are foreseen to be disposed of in the already licensed repository Konrad are not considered here. The data given was collected in the German research project Preliminary Safety Analysis for Gorleben (VSG). It considers the disposal of the following heat generating waste types:

1. Spent fuel elements (SF) for direct disposal from pressure water (DWR), boiling water (SWR), water-water (WWER) and research reactors as uranium oxide (UO2) or mixed oxide (MOX) fuel,
2. Vitrified reprocessed spent fuel (CSD-V) mainly from reprocessing in France and Great Britain,
3. Vitrified effluents and sludges from reprocessing (CSD-B) and
4. Compacted Zircaloy hull material and metal parts from disassembled SF-elements (CSD-C).

The absolute amount of the wastes to be disposed of in the future that fall into these four categories are fairly well known due to the phase out from nuclear energy in Germany. The expected inventories are given in [Pfeiffer et al. 2012]. The radionuclide inventory of the spent fuel given in table 1 was calculated using the OREST-code assuming a burn-up of 50 GWd/t_{hm} for SWR fuel elements, and 55 GWd/t_{hm} for DWR fuel elements with a potential Nitrogen impurity of 30 ppm. Information on other impurities, the uranium enrichment of the fuel, the chemical composition of the hull material and information on the burn-up calculations, like neutron fluxes are also given in [Pfeiffer et al 2012]. The inventory of the CSD-C waste was obtained from the same OREST simulations with assumed Nitrogen impurities in the Zircaloy hull material of 45 ppm [Hummelsheim & Hesse 2001]. Nitrogen impurities in the metal parts are not given in the documentation of the calculations. The inventory of the CSD-V type of waste was also received from OREST calculations regarding DWR fuel elements with a burn-up of 33 GWd/t_{hm} and the same values for nitrogen impurities as for the spent-fuel given above. This inventory used in VSG for CSD-V does not correctly take into account the actual distribution of C-14 in the different waste streams during the

reprocessing at La Hague. This is why the inventory is expected to be by far too high. A more realistic estimation comes to the conclusion that the 14C inventory per CSD-V canister delivered to Germany from La Hague can be estimated to range between the minimum value of 84.6 MBq and the maximum value of 517 MBq with an expected, average value of 238 MBq [Meleshyn & Noseck 2012].

The type of packaging is not yet decided and depends on the repository concept and host rock type. The drift disposal concept (concept B) of the VSG assumes the use of POLLUX containers which can hold up to 30 SWR fuel elements with 0.177 tons heavy metal (t_{hm}) each or 10 DWR fuel elements with 0.52 t_{hm} each.

As an option, the additional storage of waste types with negligible heat generation in a separate second repository wing with a distance between both wings of about 400 m was examined within the scope of the VSG (concept A). The waste types considered in this option are:

5a. wastes containing graphite which mainly stem from neutron reflector shields from the high temperature rector (AVR),
5b. depleted Uranium tails which stem from the production of fuel elements and
5c. other, non-specified wastes which are not applicable to be disposed of in the future Konrad repository.

The waste categories listed under items 5 are on the one hand still ill-defined in terms of waste amount, packaging and chemical form and on the other hand, it is not yet decided whether those types of waste will be deposited in a future repository primarily constructed for heat generating waste at all. Therefore, these waste types are not considered in the following and the data given in table 1.1 only refers to the given list items one to four. The full nuclide vectors of the given waste types and additionally for the spent fuel from six research reactors are also listed in [Pfeiffer et al. 2012].

The uncertainty of the C-14 inventory of spent fuel and hull material directly results from the uncertainty in the assumptions of the burn-up calculations for spent fuel and additionally from the assumptions concerning the reprocessing process for reprocessed CSD waste types. The

assumed Nitrogen impurity of 30 ppm in the spent fuel used for the calculations of the numbers given in table 1 is an upper bound of the expected range. The lower range can be assumed to be 4 ppm resulting in an uncertainty of the resulting C-14 inventory of a factor 3.6 [Hummelsheim & Hesse 2001]. Impurities of Nitrogen in Zircaloy-4 were assumed to be in the range of 45 to 75 ppm. The numbers in table 1.1 refer to the latter value. No information is given on the bandwidth of the other assumptions used in the burn-up calculations or of the resulting uncertainty of the calculated activities. No information is available on the uncertainties regarding the assumptions for the reprocessing process of the CSD waste types. However, since some uncertainties were already identified in [Meleshyn & Noseck 2012] regarding the CSD-V waste types the inventories of the other two CSD wastes might also be subject to higher uncertainties. No information is available on the chemical form of the C-14.

Table 1.1: Inventory of C-14 for the main heat generating waste families stemming from the use of power reactors

Waste type	**Number of fuel elements**	**C-14 activity [GBq/t_{hm}]**
SF (SWR) UO2	14,350	37.7
SF (SWR) MOX	1,250	21.9
SF (DWR) UO2	12,450	37.3
SF (DWR) MOX	1,530	23.1
SF (WWER) UO2	5,050	10.2
	canisters	[GBq/canister]
CSD-V	3,735	17.9
CSD-B	308	not listed
CSD-C	4,104	13.8

1.2 Model description

The German safety requirements [BMU 2010] allow the possibility to perform a simplified long-term radiological statement that is achieved without modelling the dispersion of substances in the adjoining rock and the overburden. In this case, the radionuclide fluxes are calculated at the boundary of the so called isolating rock zone[6] (IRZ). The IRZ is part of the repository system and could be regarded as an envelope boundary around the whole repository mine. A maximum allowed release of radioactive substances from the IRZ of 0.1 person-millisieverts per year for a reference group of ten persons is defined for probable developments to comply with the safety requirements. For less probable developments a criteria of 1 person-millisieverts per year is defined. To neglect dispersion, dissolution and retention in the overburden for the simplified long-term radiological statement could be called a conservative approach. Especially since the IRZ can be quite close to the emplacement areas of the waste with additional low permeable rock formations around the IRZ.

The results from the safety assessment performed are presented as a safety indicator called RGI (Radiologischer Geringfügigkeitsindex) representing the relative radionuclide outflux compared to the regulatory criterion given above. An RGI of 1 denotes for a radionuclide release equal to the maximum value allowed in the safety requirements. If the RGI is lower than 1, the regulatory criterion is achieved.

Since the salt host rock itself is impermeable for radionuclide flow, the RGI indicator is calculated from radionuclide fluxes in the mine drifts, at the position where the envelope of the defined isolating rock zone intersects the mine drifts. For the case of VSG, this is at the outer face of the drift seals in the access drifts, which is still inside the repository mine and on the repository depth.

6 In German called einschlusswirksamer Gebirgsbereich (ewG). The VSG project used the term containment providing rock zone (CPRZ) in English.

1.2.1 Reference scenario

The reference scenario is chosen according to the work performed for the preliminary safety assessment for Gorleben (VSG) [Larue et al. 2013]. In the reference case, the sealings behave for at least 50 000 years as designed and the porosity of the salt grit backfill in the drifts reduces down to 1% within a few hundreds to a few thousands of years. The according permeability of the salt grit is estimated to be $k = 3 \cdot 10^{-20}$ m², which is sufficiently low to reduce the inflow along the drifts into the mine to a value that the repository mine is still not fully saturated at the end of the reference period of one million years. No advection, but only diffusive transport is effective for the radionuclides dissolved in the liquid phase for such conditions. No dissolved radionuclides are released from the isolating rock zone during the whole reference period. Consequently, the contribution of dissolved radionuclides to the RGI is zero for the reference scenario.

For the simulations of the gas transport pathway, a lifetime of 500 years is assumed for the waste containers, with the exception of four containers which are assumed to have initial defects already at the time of emplacement. As a conservative assumption, it is assumed that the volatile radionuclides can be instantaneously released from these containers.

For the release of C-14 from the spent-fuel containers, the instant release fraction (IRF) of C-14 is assumed to be 10% for the UO_2 fuel matrix, 10% for the Zircaloy and 20% for the metal structural parts. For the CSD-C containers from reprocessing, no IRF of C-14 was assumed due to the acid treatment of the material which removes the oxide layers. No bandwidths have been assumed for those values. No information is available if those are realistic or rather conservative values.

C-14 from the IRF in the matrix and in the metal parts is assumed to be released not before a contact of external water with the waste. However, the 10% of the C-14 in the IRF of the Zircaloy disposed with the spent fuel is assumed to be in oxide layers and is assumed to be released instantaneously as CO_2-gas after container failure, even without a contact of the waste matrix with external waters. This assumption is based on [Smith et al. 1993] and subsequent publications and is clearly a conservative assumption.

A flow of non-radioactive gases in the mine is caused from the beginning of the post-closure phase by the displacement of air from the mine. This is due to the convergence of the salt host rock and the decreasing porosity in the salt grit. Additionally, a gas flow also results from hydrogen production caused by iron corrosion by the small amount of water initially emplaced with the containers and the salt grit backfill. External waters that might reach the emplacement fields closest to the shaft can potentially lead to a more significant corrosion and gas production, however to late times which are not relevant for the C-14 release.

The C-14 instantaneously mobilised from the IRF of the Zircaloy is released from the four initially defect spent fuel containers directly at the beginning of the post-closure phase and further on is transported along with the non-radioactive gases through the unsaturated drifts to be released through the drift seal from the IRZ.

1.2.2 Simulation model

TOUGH2 was used to model the gas and radionuclide transport in the mine to perform the simulations as part of the CAST project. The modelling with TOUGH2 needs a representation of the repository as a segment structure. The segment structure used for the simulations presented in the following is based on the one used for the simulation of the dissolved radionuclides using the near-field module LOPOS for repositories in salt from the RepoTREND code family [Buhmann et al. 2016]. The structure consists of 46 segments (see figure 1.2) representing the full repository layout. The LOPOS segment structure is directly converted into a TOUGH2 segment model. For the TOUGH2 simulations in the project CAST only the spent fuel in Pollux-containers and the compacted hull material in CSD-C containers are regarded. These waste forms are stored in the emplacement areas in the east wing. Therefore, all segments representing the west wing were removed from the segment model (shaded in grey in figure 1.2).

The standard version of TOUGH2 regards temporal constant porosity and permeability material parameters. This is not representative for the situation in salt, where the convergence of the backfill leads to a decrease in permeability and porosity and consequently in a gas flow of the air being expelled from the pore space during compaction acting as carrier gas for

volatile radionuclides. The latter effect is of most importance for the release of radioactive gases. In the VSG a modified version of the TOUGH2 code has been used that was extended to be capable of considering the convergence process. Since this modified version of the TOUGH2 code is not public available, a different approach has been used in the following to regard the effect of the flow of expelled air acting as carrier gas for the radioactive gases: The convergence of the salt and the resulting reduction of the porosity of the salt grit is simulated by assuming a source of air at a constant low porosity. However, the effect of changing porosity and permeability cannot be regarded by this approach.

The change of porosity of the segments as modelled in the LOPOS model is shown in figure 1.3 for three segments. This temporal behaviour is calculated during the simulation and is segment specific due to the different temperature at different locations. For the TOUGH2 simulation, the convergence has been assumed similar for all segments and the pore volume of each segment is reduced by 1/8 of its volume each year, what fits quite well to the behaviour calculated in the LOPOS model. Due to the different initial size of the segments, the resulting gas flow is however different for each segment (see figure 1.4). Segment 16 for example has an initial volume of about 23,000 m^3. With an initial porosity of the backfill of 0.35 the initial pore volume is about 8,050 m^3. The porosity is reduced with time by convergence resulting in either an outflow of nearly 8,000 m^3 of air from this segment or in an increase of air pressure. A combination of both happens in reality. After 200 to 300 years, most of the air is generated by the assumed sources and has either been expelled from the mine or lead to an increase of gas pressure using this approach. The convergence finally comes to an end at 500 years. After that point in time further gas flows only occur by either equalling out existing gas pressure differences or by diffusion to equal out concentration gradients.

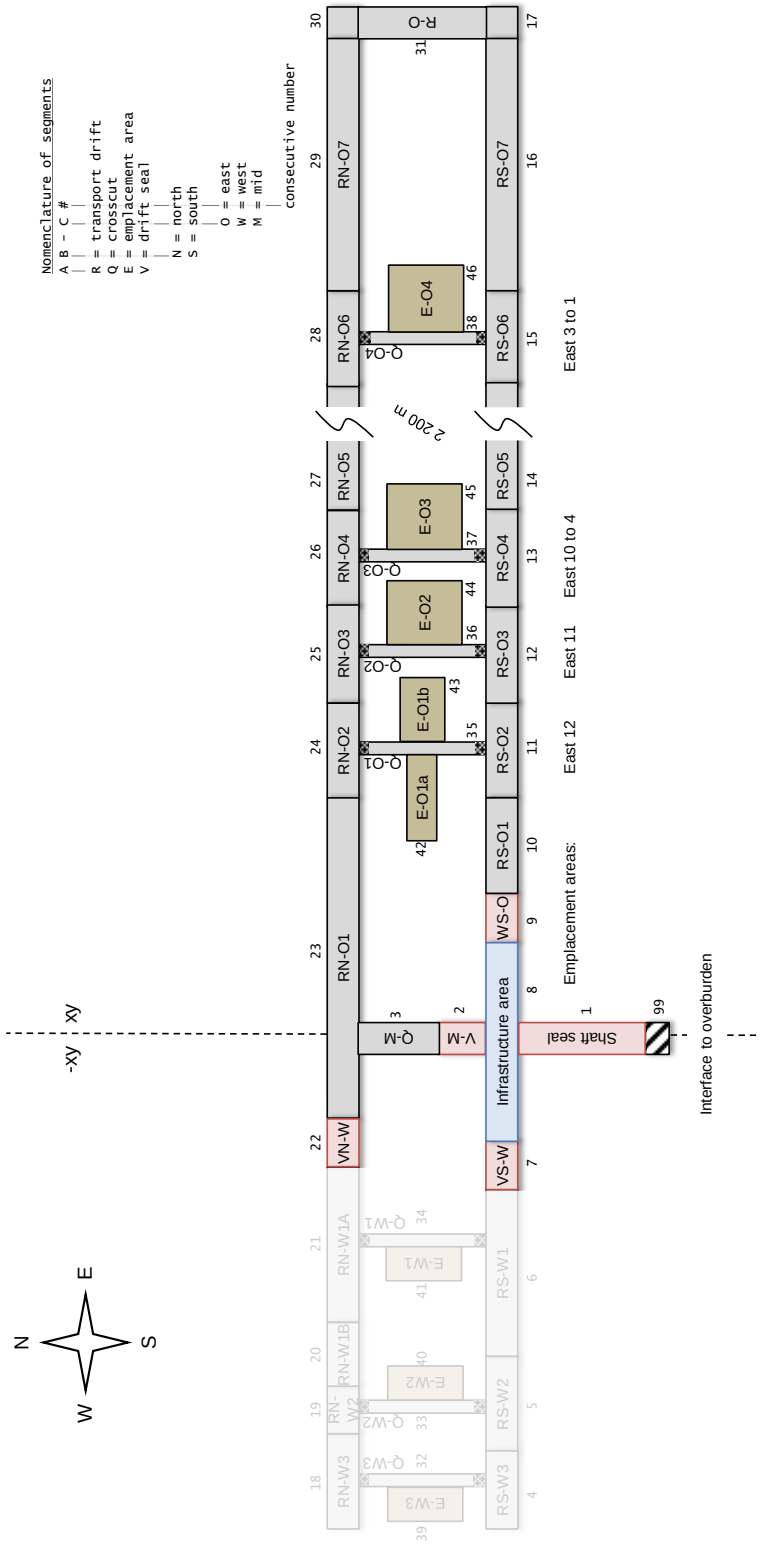

Figure 1.2: Segment structure of the repository model (not to scale)

Since permeability and porosity are constant in TOUGH2, effective mean values have to be assumed for both parameters. Effective (mean) porosity and permeability have not necessarily fit together according to the porosity-permeability-relationship of crushed salt, since both work on different scales and the effective mean value results from different weighing. Constant values have been chosen of 5 % for the porosity and 10^{-15} m^2 for the permeability of the salt grit.

Two initially defect containers are assumed, one in each of the emplacement areas E-O1a and E-O1b. Each of the two containers releases the IRF of C-14 of $5.6 \cdot 10^{-9}$ Bq into the air of the emplacement area during one year after time t = 0 resulting in a release rate of $1.08 \cdot 10^{-12}$ kg/s of C-14. Additionally, all other containers in those two emplacement areas, i.e. 10 containers in emplacement area E-O1a and 100 containers in E-O1b have been assumed to fail after 500 years and releasing their IRF of C-14 into the gas phase.

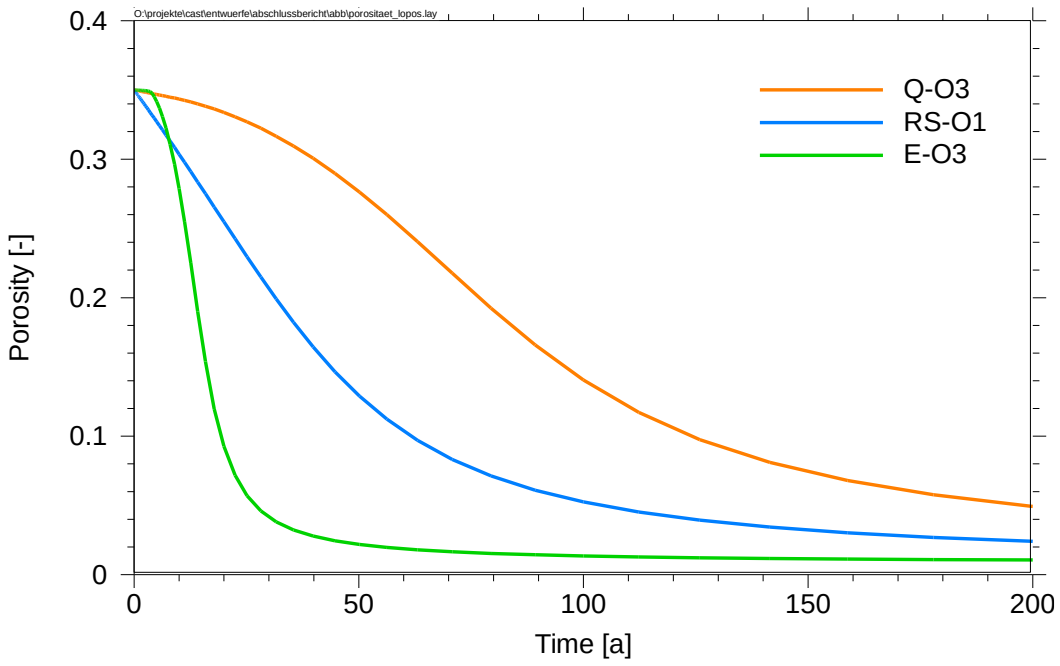

Figure 1.3: Temporal evolution of three segments in the LOPOS model

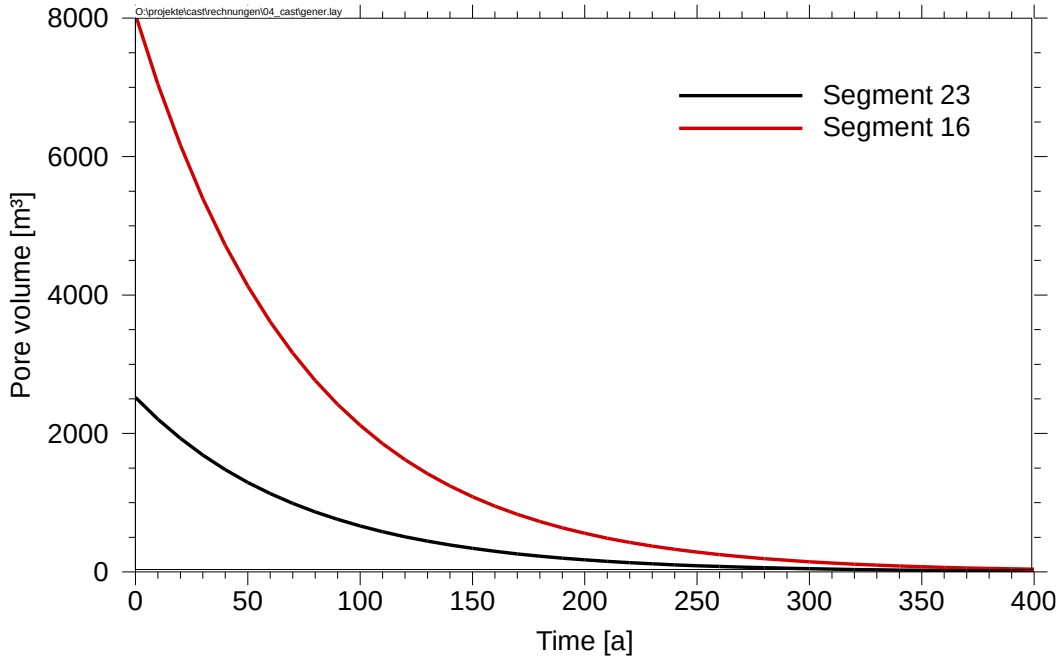

Figure 1.4: Temporal evolution of pore volume for selected segments

1.3 Results and discussions

1.3.1 Reference case

The results of the simulations are presented as RGI values and are therefore directly comparable to the results presented in the VSG [Larue et al. 2013]. For the model presented, the RGI values are calculated as sum of the C-14 fluxes at the drift seals V-M (segment 2) and WS-O (segment 9). Since the standard TOUGH2 code used in the simulations presented here is not able to allow for temporal variable porosity and permeability values, parameter variations have been performed to estimate their influence on the maximum RGI value. Table 1.2 shows the maximum RGI value depending on the porosity and permeability values given. In principle it can be said that in this model, higher porosity values lead to lower RGI-values and for higher permeability values there is a tendency to obtain a curve with for two peaks. Lower permeability values result in two effects which are that the first peak is moving towards later times and has a lower RGI value. Lower permeability and porosity values also tend to result in higher gas pressures in the mine. The first peak in the RGI-plot may even fall together

with second peak, resulting in one single peak. The result of the simulations shows a variation of the RGI of about one to two orders of magnitude for reasonable parameter variations. A permeability of 10^{-15} m^2 and a porosity of 0.05 have been chosen for the further simulations.

The major contribution of the overall RGI is from the flux out of segment WS-O (segment 9) and results from the two initially defect containers. Other containers failing after 500 years only result in a minor relative maximum in the curve after about 83 000 years with an RGI lower than 10^{-7}. The peak of the RGI-plot is much wider than presented in the VSG-simulations [Larue et al. 2013]. The reason is most probably that the convergence in the emplacement areas is much faster in the VSG-simulations: the convergence is already finished after some tens of years for the emplacement areas, resulting in a much faster movement of the gases and a much sharper peak of the RGI.

Table 1.2: Maximum calculated RGI-value when varying the parameters of the backfill for porosity *n* and permeability *k*

k **[m^2]** / ***n*** **[-]**	10^{-14}	10^{-15}	10^{-16}
0.02	3.5	2.1	0.9
0.03	0.7	0.4	0.3
0.05	0.1	**0.1**	0.1
0.10	0.02	0.02	0.02

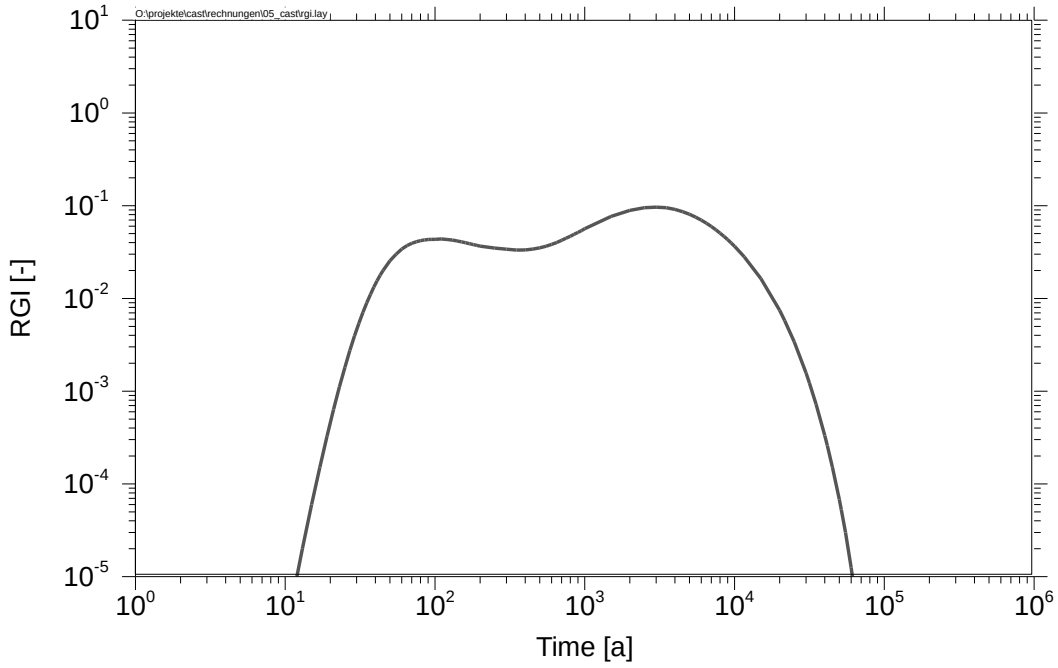

Figure 1.5: Temporal evolution of the RGI-value for a reference parameter combination for porosity and permeability of n = 0.05 and k = 10^{-15} m^2

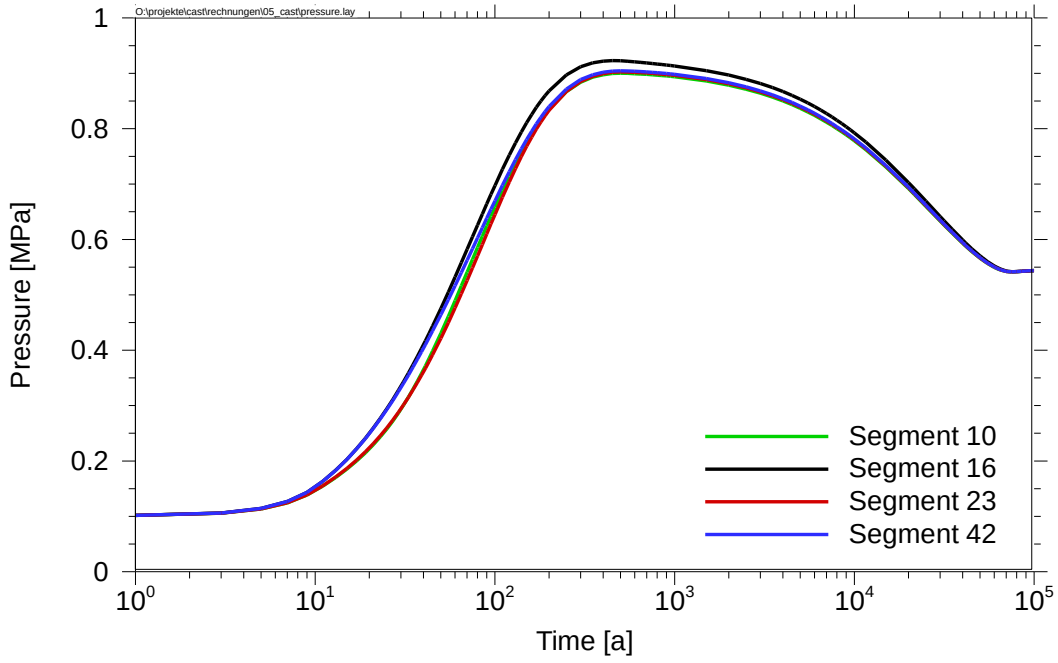

Figure 1.6: Temporal evolution of pressure for selected segments for a reference parameter combination for porosity and permeability of n = 0.05 and k = 10^{-15} m^2

1.3.2 Parameter variations of the C-14 source term

The boundary conditions of the experiments performed in the CAST project do not match the ones expected in the reference evolution of a repository in salt. This is on the one hand because of unsaturated conditions prevailing over the time of interest for the release of C-14 and on the other hand because of the fact that those small amounts of fluids existing in the repository show salt concentrations at saturation. Therefore, the results from the CAST project cannot be directly transferred to the safety case. Since the experimental result obtained in CAST are not directly applicable to the situation in salt, parameter variations are performed to vary the following influencing factors of the source term:

Instant release fraction (IRF): The IRF was varied to be 10, 1 and 0.1 percent of the C-14 inventory equally for all compartments of the spent fuel waste package.

Release rate: The release rate was varied in a way that the release started at the beginning of the simulation and lasted for 1, 10, 100 and 1000 years respectively.

Release start time: The time of the IRF release start was varied to be 1, 10, 100 and 500 years with a release of the full IRF within 1 year after the release time.

The reference values considered are always the ones given at first in the list above. All other parameters have been used as described before for the reference case. The simulations presented in the following aim to investigate how the variation of the source-term of C-14 does affect the outflow of C-14 from the repository i.e. the radiotoxicity indicator RGI.

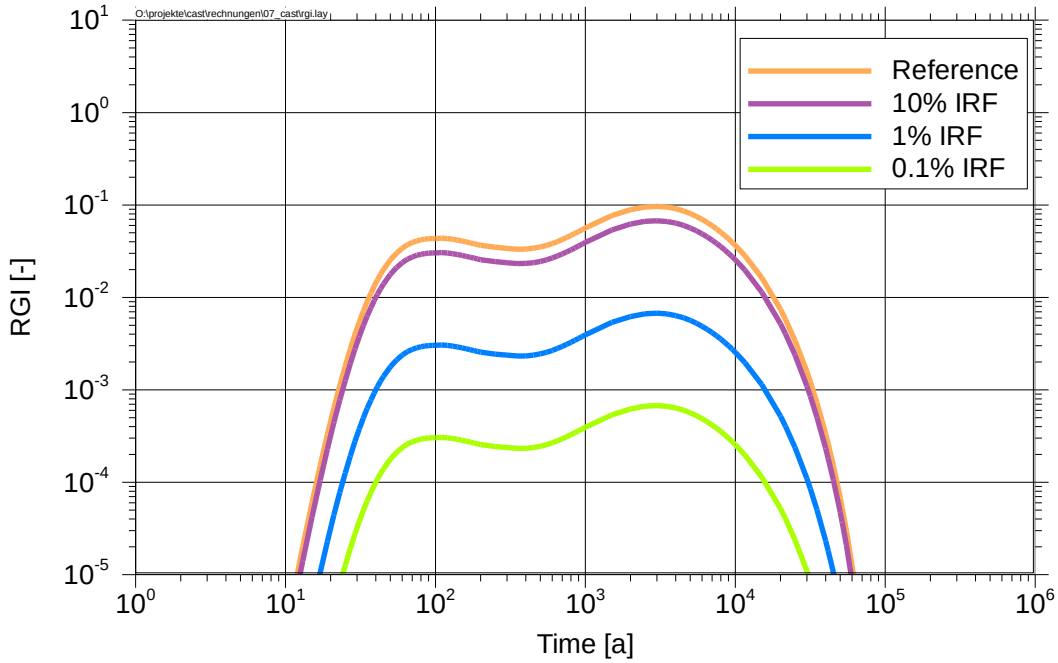

Figure 1.7: Dependence of the radiotoxicity indicator RGI from the C-14 IRF

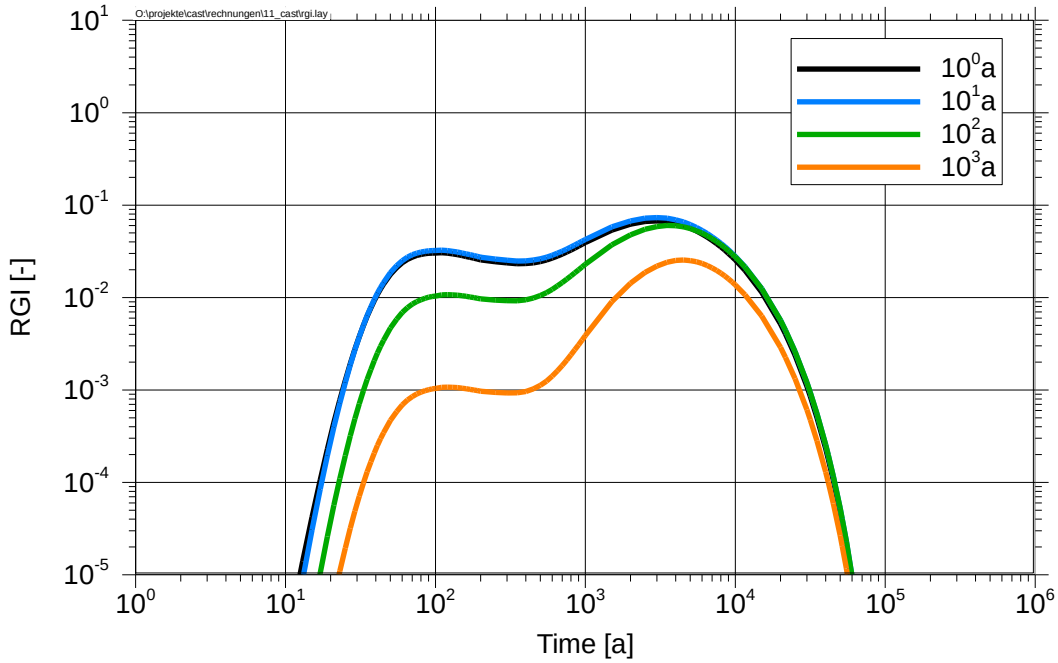

Figure 1.8: Dependence of the radiotoxicity indicator RGI from the release rate of C-14 for an IRF of 10 %

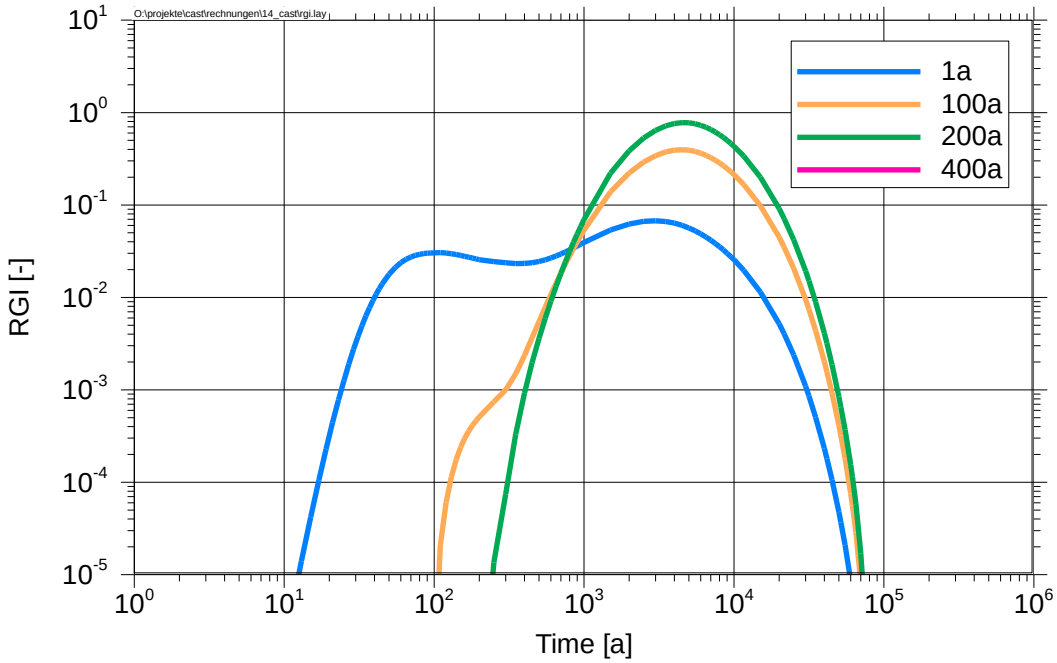

Figure 1.9: Dependence of the radiotoxicity indicator RGI from the release start time

Figure 1.7 shows the result of simulations varying the instant release fraction (IRF) of the C-14. In the reference case of the VSG, a value of 20 % was used for metal parts and 10 % for Zircaloy and the fuel matrix. For the parameter variations performed in this project, values for the IRF of 10, 1 and 0.1 % were used equally for all types of wastes. The simulation results plotted in figure 1.7 show that a reduction of the IRF causes a reduction of the RGI by the same factor, suggesting a linear relationship of the IRF and RGI.

The first experimental results from CAST suggest values for the IRF in the range of 1 %, i.e. at the lower boundary of the range used in the parameter variations and therefore also much lower than assumed in the VSG reference case. However, the samples used and the type of experiments performed in CAST were not suitable to rule out the existence of a fraction of C-14 being initially in the gas phase of the spent fuel waste as a result of diffusion at high temperature from the waste as suggested by experiments reported in [Smith et al. 1993]. On the other hand, such type of gas phase was not found in experiments performed as part of the EC First Nuclides project which are reported by Kienzler et al. [2014]. A maximum amount of only 0.2 % of the assumed C-14 inventory was found to be present initially in the gas phase

of a fuel element tested in the First Nuclides project. As a result of both projects, First Nuclides and CAST it can be expected that the release of C-14 into the gas phase during the first 500 years under the assumed boundary conditions is lower than 10 % of the value assumed in the preliminary safety case for Gorleben or even less than 1 %. The reduction of conservatism in the assumption of the release behaviour of the IRF of C-14 in the waste is therefore a promising way to reduce the calculated RGI values in long-term safety assessment.

Figure 1.8 shows the result of simulations varying the release rate of C-14 from the waste using values of 1, 10, 100 and 1,000 years for the time span of release. The release rate was considered to be constant in time throughout the respective periods. The curves plotted in figure 1.8 show that the RGI value is reduced somewhat at early times due to a slower release, however for late times the RGI value remains unchanged or is only slightly lowered. This is especially true for expected release times of some tens to a few hundred years at maximum.

Figure 1.9 shows the result of simulations varying the start time of the C-14 release from the waste container using values of 1, 100, 200 and 400 years. As expected, a later start of the C-14 release also results in a later rise of the RGI value. For a start time of 400 years and later, no release of C-14 from the repository is occurring and the RGI value is consequently zero. The reason for this effect is that the convergence is already very low at that point in time and finally stops after 500 years. A subsequent gas transport therefore only occurs from pressure gradients already existing before that time. These pressure gradients are obviously too low to lead to a relevant gas transport after the convergence has stopped. More generally it can be pointed out that a C-14 release at a point in time where the porosity of the salt is close or even at its final value does not lead to a notable release from the repository. This clearly shows that the assumption of initially defect containers is critical for the C-14 release. A guaranteed container life-time of more than 500 years might prevent the release of gaseous C-14 from the repository.

As a summarizing conclusion it can be stated that the consequences of the C-14 release from the waste in the early phase of the repository, determined by the RGI indicator, are to a large part controlled by the quantity of the C-14 released. The temporal behaviour of the C-14 release only shows a minor impact on the RGI indicator. The potential to reduce the

conservatism in the assumption of the amount of C-14 during the early phase of the repository is high according to the results obtained in the First Nuclides and the CAST projects.

The highest priority to reduce the uncertainty on the release behaviour of C-14 is mainly related to three questions:

1. Which is percentage of C-14 which can be released into volatile form?
2. Which is the temporal behaviour of the release?
3. Is water necessary to transfer C-14 into volatile form or does this occur also without the presence of humidity?

References

BMU (Federal Ministry for the Environment, Nature Conservation and Nuclear Safety): Safety Requirements Governing the Final Disposal of Heat-Generating Radioactive Waste. Version of Sept., 30. 2010.

BOLLINGERFEHR, W.; FILBERT, W.; LERCH, C.; THOLEN, M. 2012: Endlagerkonzepte. Bericht zum Arbeitspaket 5. Vorläufige Sicherheitsanalyse für den Standort Gorleben. GRS-272, Gesellschaft für Anlagen- und Reaktorsicherheit, Köln.

BOLLINGERFEHR, W.; FILBERT, W.; DÖRR, S.; HEROLD, P.; LERCH, C.; BURGWINKEL, P.; CHARLIER, F.; THOMAUSKE, B.; BRACKE, G.; KILGER, R. 2012: Endlagerauslegung und –optimierung. Bericht zum Arbeitspaket 6. Vorläufige Sicherheitsanalyse für den Standort Gorleben. GRS-281, Gesellschaft für Anlagen- und Reaktorsicherheit, Köln.

HUMMELSHEIM, K., HESSE, U. 2001: Abbrand und Aktivierungsrechnungen von UO2- und MOX-Brennelementen für DWR unter Berücksichtigung der Verunreinigungen in Brennstoff und Strukturmaterial. GRS-A-2924, Gesellschaft für Anlagen und Reaktorsicherheit (GRS) mbH: Garching.

KIENZLER, B.; METZ, V.; VALLS, A. 2014: Fast / Instant Release of Safety Relevant Radionuclides from Spent Nuclear Fuel; FIRST-Nuclides Final scientific report, Deliverable No: 5.13, European Commission, Luxemburg.

LARUE, J.; BALTES, B.; FISCHER, H.; FRIELING, G.; KOCK, I.; NAVARRO, M.; SEHER, H. 2013: Radiologische Konsequenzenanalyse. Bericht zum Arbeitspaket 10. Vorläufige Sicherheitsanalyse für den Standort Gorleben. GRS-289, Gesellschaft für Anlagen- und Reaktorsicherheit, Köln.

MELESHYN, A.; NOSECK, U. 2012: Radionuclide Inventory of Vitrified Waste after Spent Nuclear Fuel Reprocessing at La Hague - Basic Issues and Current State in Germany. GRS-294, Gesellschaft für Anlagen- und Reaktorsicherheit, Braunschweig.

MÖNIG, J.; BUHMANN, D.; RÜBEL, A.; WOLF, J.; BALTES, B.; FISCHER-APPELT, K. 2012: Sicherheits- und Nachweiskonzept. Bericht zum Arbeitspaket 4. Vorläufige Sicherheitsanalyse für den Standort Gorleben. GRS-277, Gesellschaft für Anlagen- und Reaktorsicherheit, Köln.

PEIFFER, F., MCSTOCKER, B., GRÜNDLER, D., EWIG, F., THOMAUSKE, B., HAVENITH, A., KETTLER, J. 2011: Abfallspezifikation und Mengengerüst. Basis Ausstieg aus der Kernenergienutzung (Juli 2011). Bericht zum Arbeitspaket 3, Vorläufige Sicherheitsanalyse für den Standort Gorleben, GRS-278, Gesellschaft für Anlagen- und Reaktorsicherheit, Köln.

SMITH, H. D., BALDWIN, D. L. 1993: An investigation of thermal release of carbon-14 from PWR Zircaloy spent fuel cladding. *Journal of Nuclear Materials* 200, pp.128-137.

PART 4 – Generic host rock

CArbon-14 Source Term

CAST

Integration of CAST results to safety assessment: Contribution from RWM to D6.3

C-14 UK Summary Report

Lucia Gray and Alex Carter

Date of issue of this report: 15/12/2017

Executive Summary

This note summarises Radioactive Waste Management Limited (RWM)'s current position on C-14, detailing updates to the Disposal System Safety Case, in particular the Environmental Safety Case (ESC), including the Post-closure Safety Assessment (PCSA) and Operational Environmental Safety Assessment (OESA), and summarising the key messages and conclusions of Phase 2 of the Carbon-14 Integrated Project in the context of RWM's safety case studies.

Understanding from the Carbon-14 Integrated Project has led to:

- improved understanding of C-14 distribution in the UK inventory and behaviour in the Gas Status Report;
- improved off-site gas release rates for C-14-bearing gases in RWM's ESC, including the OESA and PCSA; and
- improved understanding of C-14 behaviour in the biosphere, leading to more realistic dose per unit release factors being used the OESA.

The conclusions drawn from the Gas Status Report and PCSA have informed the radiological assessment of radionuclides in gas, presented in the ESC to show how various lines of argument will be constructed to demonstrate that geological disposal of the UK's higher activity radioactive wastes will meet environmental safety requirements as set out in the Environment Agency's Guidance on Requirements for Authorisation (GRA) when a GDF site is available.

Scope for further work on C-14 has been identified in:

- updating the assumed effective release height for C-14-bearing gases during the operational period (from 15 to 30 m) in the OESA; and
- carrying out further research to better understand the effect of gas pressurisation within the facility and its potential implications for C-14 release.

List of Contents

1 UK Context

Radioactive Waste Management Limited (RWM) has been established as the delivery organisation responsible for the implementation of a safe, sustainable and publicly acceptable programme for the geological disposal of the higher activity radioactive wastes in the UK. As a pioneer of nuclear technology, the UK has accumulated a legacy of higher activity wastes and material from electricity generation, defence activities and other industrial, medical and research activities. Most of this radioactive waste has already arisen and is being stored on an interim basis at nuclear sites across the UK. More will arise in the future from the continued operation and decommissioning of existing facilities and the operation and subsequent decommissioning of future nuclear power stations.

Geological disposal is the UK Government's policy for higher activity radioactive wastes. The principle of geological disposal is to isolate these wastes deep underground inside a suitable rock formation, to ensure that no harmful quantities of radioactivity will reach the surface environment. To achieve this, the wastes will be placed in an engineered underground facility – a geological disposal facility (GDF). The facility design will be based on a multi-barrier concept where natural and man-made barriers work together to isolate and contain the radioactive wastes.

To identify potentially suitable sites where the GDF could be located, the Government has developed a consent-based approach, based on working with interested communities that are willing to participate in the siting process. The siting process is on-going and no site has yet been identified for the GDF.

Prior to site identification, RWM is undertaking preparatory studies which consider a number of generic geological host environments and a range of illustrative disposal concepts. As part of this work, RWM maintains a generic Disposal System Safety Case (DSSC). The generic DSSC is an integrated suite of documents which together give confidence that geological disposal can be implemented safely in the UK. The most recent update to the DSSC was published in August 2017.

C-14 is a key radionuclide in the assessment of the safety of a geological disposal facility for radioactive waste because of the potential radiological impact of gaseous C-14-bearing species during the operational and post-closure periods. This is discussed within the generic Environmental Safety Case (ESC) [RWM, 2016a] in the DSSC, which in turn is supported by the generic Operational Environmental Safety Assessment (OESA) [RWM, 2016b] and the Post-closure Safety Assessment (PCSA) [RWM, 2016c].

This note summarises RWM's current understanding of C-14 as described in the 2016 generic ESC and generic OESA. These, in turn, reflect understanding gained during RWM's Integrated Project on C-14, which ran from 2012 to 2016, and which is described in the next section.

2 DSSC

The ESC considers the environmental safety of a GDF during the operational period and after closure of the facility. It is supported by the PCSA, itself supported by the Gas Status Report, and OESA, which present an assessment of discharges (operational and post-closure, respectively) associated with all wastes and materials covered by the 2013 DI [RWM, 2016d]. The improved understanding and modelling results from phase two of the Carbon-14 Integrated Project have informed the 2016 generic ESC, and in particular section 10.4 'Radiological assessment: radionuclides in gas', which discusses the assessment of gas for each generic geological host environment, illustrative disposal concept and waste category in the UK inventory.

The generic geological host environments are each based on a host rock typical of UK geologies, namely a higher strength rock (HSR), a lower strength sedimentary rock (LSSR) and halite (rock salt, an evaporitic rock). For each of these, illustrative disposal concepts for both Low Heat Generating Waste (LHGW) and High Heat Generating Waste (HHGW) were selected and used as the basis for the illustrative designs.

RWM's analysis of gas generation and migration is discussed in detail in the generic PCSA [RWM, 2016c][§6] and is based on the consideration of gas behaviour in different geological environments reported in the Gas Status Report [RWM, 2016e][§6] together with RWM's recent supporting research on C-14 behaviour [NDA, 2012] [RWM, 2016f] from the IPT, as discussed in the previous section. Key findings with regard to the assessment of the radiological impacts of gas for different waste groups and disposal concepts are discussed below.

The assessment and analysis presented in the ESC show how various lines of argument will be constructed to demonstrate that geological disposal of the UK's higher activity radioactive wastes will meet environmental safety requirements as set out in the GRA [Environment Agency and Northern Ireland Environment Agency, 2009] when a GDF site is available.

The OESA presents an assessment of operational discharges associated with all wastes and materials covered by the 2013 DI [RWM, 2016d]. The improved understanding and modelling results from phase two of the Carbon-14 Integrated Project have informed the 2016 generic OESA [RWM, 2016b], in particular sections 4.4.3, which drew on the improved understanding of gas generation routes to identify key sources of C-14 in the 2013 Derived Inventory, and 4.5.1, which drew on the improved understanding of gas generation routes to derive off-site gas release rates for C-14-bearing gases.

3 The Carbon-14 Integrated Project

In 2012 RWM established an Integrated Project Team (IPT) to develop an holistic approach to C-14 management in a geological disposal system. The overall aim of the project was:

"To support geological disposal of UK wastes containing C-14, by integrating our evolving understanding from current and pre-existing projects, in order to develop an holistic approach to C-14 management in the disposal system."

The Carbon-14 Integrated Project phase two[7] overview report [RWM, 2016f] provides an overview of the work completed during the final phase of the project. The report presents an updated understanding of the key generation and migration processes for C-14, including knowledge gaps that were filled. This improved understanding, together with improvements to underlying data, were used to develop and update models which were used to provide a revised assessment of the implications of C-14-bearing gases that may be released from intermediate-level waste. Alternative treatment, packaging or design options are also discussed.

3.1 Modelling Methodology

A key task of the Phase 2 work was to update the previously performed assessment calculations in light of the improvements to data and understanding made through the IPT. Calculations were made of both the generation rates of bulk and C-14-containing gases and the associated consequences of these gases by applying appropriate conversions to the gas generation results to produce: a dose rate from off-site discharge in the operational period, and a risk from release to the biosphere in the post-closure period (as presented in the Phase 1 report [NDA, 2012]). The modelling basis adopted in this project is discussed in more detail in the Carbon-14 Integrated Project phase two modelling report [Swift and Leung, 2016b][§1.5].

To keep the number of gas generation calculations manageable, calculations were carried out only to represent the case of a GDF in a higher strength host rock. This will only affect the gas generation results calculated for the post-closure period because the flow of groundwater into the GDF will be greater than in other environments. This will maximise the rate of gas generation over the time scales relevant to the release of C-14 as gas generating reactions will not be restricted by the supply of water [Hoch et al., 2016]. Therefore, the results provide an upper bound to the gas generation results expected for other geological environments. In

[7] The IPT was formed of two phases. Phase 1 [NDA, 2012] and then recommended work for Phase 2 [RWM, 2016f].

addition the calculations have focused on waste in those parts of the GDF from which the vast majority of the gaseous C-14 is expected to be generated (namely Legacy ILW and some nuclear new build ILW).

The consequences from off-site discharge in the operational period were assessed by calculating doses from C-14-containing methane and carbon monoxide released from waste packages and then discharged through a stack. Updated dose per unit release factors for each gaseous species were used. C-14-containing carbon dioxide is also expected to be generated. However, the cementitious materials present in a GDF react with carbon dioxide. There is a substantial body of evidence supporting the view that this carbonation will occur [Hoch et al., 2016]. The wastes that will contain significant amounts of C-14 (i.e. graphite, steels and reactive metals) are expected to generate only small amounts of carbon dioxide compared with the carbonation capacities of the cement materials that will be present in a GDF [Hoch et al., 2016]. Therefore, it is reasonable to assume that the carbonation reactions will occur, and any C-14-bearing carbon dioxide that is generated will be immobilised as solid carbonate minerals.

There are uncertainties associated with C-14 in metal wastes. In this assessment, the C-14 in metal wastes was all cautiously assumed to be released as gas as the metal corrodes, whereas only a fraction may be gas in practice. It was also assumed to be evenly distributed throughout the metal, whereas the true distribution is unknown. This therefore my not be a conservative assumption. Furthermore, the resulting dose will depend on the gaseous species formed, and there is considerable uncertainty about the form in which C-14 will be released from corrosion of metals.

Consideration was given to effects of uncertainties in the C-14-containing gases that may be generated. The consequences in the post-closure period were assessed by calculating risks based on release via migration through the geosphere. The risks were calculated for a number of generic geosphere cases and assuming different fractions of the C-14 are released as gas from ILW vaults and tunnels to account for uncertainties in the C-14-containing gases that may be generated. An updated biosphere dose conversion factor was used.

A number of assessment calculations were performed. First, a set of calculations were performed for a Reference Case gas generation scenario. Although this scenario is only one of several possible scenarios, it is expected to provide a reasonable – and conservative - generic representation of most aspects of the likely gas generation behaviour. In addition, calculations were performed for a number of variant gas generation scenarios. These examined the sensitivity of the results to key parameters and considered potential alternative options for the disposal of some wastes. The results from this modelling are presented in [RWM, 2016f][§13.1] and section 4 of this report.

4 Outcomes

4.1 Total System Model

In addition to the assessment calculations, a further modelling task was undertaken as part of Phase 2. To complement the modelling using SMOGG (RWM's Simplified Model of Gas Generation from Radioactive Wastes) [Swift, 2016], a preliminary version of a total system model for the gas pathway for C-14 was developed and some initial calculations performed [Swift and Leung, 2016b][§1.5]. A Total System Model is a probabilistic Monte Carlo simulation which covers the entire process from gas generation to receptors, taking simplified information from component models and process models in order to calculate overall performance measures of the GDF system, such as radiological dose and risk. The model allows uncertainty to be included explicitly in calculations, and so avoids the need to perform separate sensitivity calculations. This potentially has significant advantages given the number of uncertain parameters in gas generation calculations. At this stage the total system model developed is intended to be a 'demonstration of capability' only, but this work is intended to be the initial phase of a much longer cycle of development and may be revisited as the siting process progresses.

4.2 The integrated technical approach (the 'AND' approach)

As part of phase 1 of the Carbon-14 Integrated Project [NDA, 2012], the project team developed an integrated technical approach to the work [RWM, 2016f][§13.2], based on an understanding of the key processes affecting the fate of C-14. The approach is known as the 'AND' approach and is described below. The project team used this approach as a way of considering the problem comprehensively and to underpin the prioritisation of the work across phase 1 and phase 2 of the project.

For the radiological impact of gaseous C-14 to be an issue:

- There must be a significant inventory of C-14; AND
- That waste has to generate C-14-bearing gas; AND
- A bulk gas has to entrain the C-14-bearing gas; AND
- These gases must migrate through the engineered barriers in significant quantities; AND
- These gases must migrate through the overlying geological environment (either as a distinct gas phase or as dissolved gas); AND
- These gases must interact with materials in the biosphere (i.e. plants) in a manner that leads to significant doses and risks to exposed groups or potentially exposed groups.

The conclusions to the phase 2 work of the Integrated Carbon-14 Project were presented as answers to questions derived from the 'AND' approach, discussed in [RWM, 2016f][§13.3] and section 3.1 of this report, and the final outcome for the major waste groups in the UK inventory for disposal in a GDF is presented in Table 1.

Table 1: Conclusion from applying the 'AND' approach to the main waste groups

'AND' Question	Do these gases lead to significant risks to potentially exposed groups in the post-closure phase?	
Graphite	Impact is site specific.	Risks are assessed to be below the risk guidance level provided that the release is not focused over a small area.
Irradiated steel		The radiological risk is expected to be tolerable in most environments.
Irradiated Magnox		Risks are expected to be tolerable provided releases are to an area comparable to the GDF footprint and the proportion of the C-14 released as $^{14}CH_4$ or ^{14}CO is limited, or there is a significant hold-up of gas in the geosphere.
Irradiated uranium	Provided uranium corrodes anaerobically after emplacement, it will all have corroded before closure.	

4.3 Inventory

Although many of the changes to C-14 in RWM's safety cases are due to the improved understanding and modelling results from the Carbon-14 Integrated project, some are attributable to changes in the DI [RWM, 2016d].

The major changes in the C-14 inventory are as follows:

- An overall increase of 422 TBq in Magnox ILW core graphite due to the remodelling of activities and volumes. The following stations show the largest changes:
- Wylfa - waste stream 9H311 (+501 TBq);
- Trawsfynydd - waste stream 9G311 (+40.6 TBq); and
- Oldbury - waste stream 9E319 (-124 TBq).
- An overall increase of 639 TBq in AGR ILW core graphite based on station life extensions coupled with more up-to-date information regarding fuel burn-up and neutron flux levels in the cores. Increases at individual stations are in the range 100 to 111 TBq with the exception of Hinkley Point B where the increase is 211 TBq.
- An overall decrease of 74.1 TBq in ILW steels, principally as a result of the following factors:

  - For ILW other ferrous metal decommissioning wastes, a lower volume estimate from Steam Generating Heavy Water Reactor (SGHWR) decommissioning (waste stream 5G302); and
  - For ILW stainless steel reactor decommissioning wastes, a lower volume estimate from the decommissioning of submarines (waste stream 7G104).
- A decrease of 352 TBq in organic ILW from GE Healthcare due to the closure of the Cardiff site and waste incineration. The company plans to continue incineration of C-14 contaminated wastes, and if this can be achieved there would be further reductions in the C-14 activity requiring disposal in a GDF.

4.3.1 C-14 gaseous discharges - inventory

Sources of C-14 in the inventory for disposal are dominated by irradiated metals, irradiated graphite, spent ion-exchange resins and organic materials [RWM, 2016b][§4.4.3]. These may act as sources of C-14-bearing gases, as discussed in the Gas Status Report [RWM, 2016e].

The proportion of the total C-14 inventory present in each relevant waste material group is provided in the report on inventory for the Carbon-14 Integrated Project [Adeogun, 2016] and is summarised in Table 2. Activities at 2040 are shown, as this is the assumed start of GDF operations. These data were back-decayed to the assumed emplacement start date to provide the input data required for release rate calculations.

Table 2: Effective assignment of C-14 activity by material type [Swift and Leung, 2016]

Material type	C-14 activity (TBq)		
	Legacy ULLW/ UILW at 2040 AD	**Legacy SLLW/ SILW at 2040 AD**	**NNB UILW at 2100 AD**
Stainless steel: 2F03/C	3.00×10^{1}	–	–
Stainless steel: 2F08	3.91×10^{1}	–	–
Stainless steel: AP301	–	–	1.20×10^{3}
Stainless steel: EP302, EP303	–	–	5.55×10^{3}
Stainless steel: Other waste streams	8.52×10^{1}	6.01×10^{1}	6.70×10^{-2}
Mild steel	4.28×10^{1}	1.40×10^{2}	1.15×10^{0}
Zircaloy	2.85×10^{1}	7.85×10^{-1}	–
Nimonic	2.79×10^{1}	5.13×10^{0}	–
Magnox (uncorroded): Plates	6.76×10^{1}	–	–
Magnox (uncorroded): Spheres	–	–	–
Uranium (uncorroded): Plates	9.26×10^{0}	–	–
Uranium (uncorroded): Spheres	8.76×10^{0}	–	–
Graphite	7.50×10^{2}	6.31×10^{3}	–
GE Healthcare waste[1]	*2.08×10^{2}*	–	–
Other[2]	*7.62×10^{1}*	*4.48×10^{0}*	*3.14×10^{0}*
Total considered in gas release rate calculations	**1.09×10^{3}**	**6.52×10^{3}**	**6.75×10^{3}**

Notes:

1. GE Healthcare waste is expected to be incinerated (and so assumed not to be disposed of in the GDF), as discussed in [RWM, 2016f][§12.2] and earlier in section 3 of this report. Therefore it is excluded from calculations of release rates of C-14 in the 2016 OESA. This is a significant update to the OESA as it makes up a large proportion of the C-14 activity, and was included in the C-14 inventory considered in the 2010 OESA.

2. In the case of other wastes, as discussed in [RWM, 2016f][§12.5] and below, there is not expected to be any release of C-14, therefore they are excluded from calculations of release rates of C-14 in the 2016 OESA.

From this data set it is clear that the highest activity for C-14 is contained within the graphite present in SLLW/SILW, and NNB stainless steel waste streams.

4.3.2 Other Wastes

There are a number of other waste streams that contain a modest quantity of C-14. These are discussed briefly in turn, and the reasons are presented as to why they are not a significant source [RWM, 2016f][§12].

Other legacy ILW waste streams that contain C-14 include:

- Encapsulated Enhanced Actinide Removal Plant (EARP) floc, arising from reprocessing at Sellafield. This is a high volume waste stream, with a low inventory of C-14 and the C-14 is likely to be in the form of carbonate (either dissolved or precipitated). It is unlikely to be a source term for gaseous C-14 release.

- Spalled oxide and dust, which may include spalled metal oxide and graphite dust. This is a small volume waste stream, where the C-14 content is likely to be an estimate and may be associated with corroded metal (and therefore unlikely to be a source term for gaseous C-14 release) or with graphite (where it would contribute a small additional source of gaseous C-14 release).

- Spent resins arising from reactor coolant purification. C-14 in the coolant may have been associated with dissolved or spalled corrosion product and would be absorbed on the resin beads in trace quantities. The C-14 in this waste stream is unlikely to be a source term for gaseous C-14 release. A state-of-the-art review on releases from spent ion-exchange resins has been prepared as part of the CAST project [Rizzato et al., 2015].

Also listed in this category is a small amount of C-14 (5 TBq) associated with ‘other ILW from nuclear new build’. As discussed in [RWM, 2016f][§9], the inventory of C-14 associated with nuclear new build will be better defined in the future; the dominant contribution to the

C-14 inventory from these wastes is in spent fuel and in the decommissioning wastes and this small amount in 'other ILW' has not been considered further in this project, but would be considered as part of future disposability assessments for these wastes.

There are a number of other ILW waste streams in [Adeogun, 2016] with a total inventory of C-14 of 0.58 TBq and a packaged volume of 31.5 m^3. These are streams 9A52, 9A53, 9A55, 9A56, 9C47, 9D44, 9E40, 9E41, 9E43, 9F43, 9G41. They are declared as being primarily Zircaloy or Nimonic. As the inventory is so small they are not considered further in this study.

4.4 Operational Period

4.4.1 Methodology

The modelling approach for the operational period is discussed in [Swift and Leung, 2016b][§4.1.1]. The main pathway for aerial discharges from the underground facilities during operations will be through the GDF ventilation system and into the atmosphere through a discharge stack. In Phase 2 of the project, a methodology was developed to calculate the effective dose rates arising from a continuous discharge of C-14-containing gases from a 15 m high stack to a local resident family receptor group [Thorne and Kelly, 2015], which was cautiously assumed:

- To be located 100 m from a discharge point of a GDF;
- To consume food grown at 500 m from a GDF.

These values were chosen to be consistent with the Environment Agency guidance [Environment Agency, 2006] [Environment Agency, 2006b] and the 2010 generic Operational Environmental Safety Assessment (OESA) [NDA RWMD, 2010].

The methodology for assessing operational discharges was applied to the pre-backfilling period. For releases following backfilling but before GDF sealing and closure, there was some uncertainty as to whether they would be discharged through the ventilation system or whether they would be retained within the engineered system until after closure (when the post-closure

methodology would be applicable). Given the uncertainties for this stage, it was considered appropriate to apply both the OESA and post-closure methodologies.

4.4.2 Dose per unit release factors

The relationship between a radionuclide emission or discharge rate and the resultant dose received by a receptor can be expressed by a dose per unit release (DPUR) factor. DPUR factors are discussed in [RWM, 2016b][§5.1.2]. DPUR values have been calculated by the Environment Agency for 100 different radionuclides. The value of a DPUR depends on the radionuclide; the exposure pathway; and the location, habits and age of the representative person. The exposure pathways themselves also depend on the location and habits of the representative person. The exposure pathways considered by the Environment Agency [Environment Agency et al., 2006a] for discharges to air for the local resident family are:

- Inhalation of radionuclides in the effluent plume;
- External irradiation from radionuclides in the effluent plume and/or which have been deposited to the ground; and
- Consumption of terrestrial food incorporating radionuclides which have been deposited to the ground.

The Environment Agency methodology report [Environment Agency et al., 2006b] describes how the DPUR values were calculated using the 1998 version of the software PC-CREAM, developed by the National Radiological Protection Board (now Public Health England) [Mayall et al., 1997]. PC-CREAM is based on an EC methodology for assessing the radiological consequences of routine releases to the environment [Mayall et al., 1995]. It contains modules that are used to calculate the transfer of radionuclides through different environments and the food chain; the module PLUME is used for atmospheric environments. PC-CREAM and its underlying dispersion models are robust, fit for purpose, and have been verified against environmental data [Simmonds, 1998] [Jones, 1986].

The Environment Agency DPUR values for C-14 have been superseded by more recent work [Thorne and Kelly, 2015], which uses a more realistic representation of the discharge pathway for releases of C-14-bearing gases from the GDF during operations. In particular, different C-14-bearing gases are considered separately; methane and carbon monoxide being those relevant to this assessment, and an effective release height of 15 m is included in the factors calculated. In the Environment Agency methodology, the default DPUR values assume releases at ground level but can be scaled for different effective release heights; [RWM, 2016b][§5.1.3]. The Carbon-14 Integrated Project 'Operational Impacts from Aerial Discharges of C-14-Bearing Gases' [Thorne and Kelly, 2015] calculated updated DPUR values for C-14 for three age groups: infant, child and adult.

The DPUR values used in this assessment are presented in Table 3 (C-14-bearing methane and carbon monoxide). These are discussed in the 2016 DSSC Data Report [RWM, 2016h][§3.10.3].

Table 3: Dose per unit release values for a local resident family for C-14-bearing methane and carbon monoxide [Environment Agency et al., 2006b][Table 6]

Radioactive gas	**DPUR accounting for all pathways (µSv/year per Bq/year of discharge to the atmosphere, for an effective release height of 15 m)**		
	Infant	**Child**	**Adult**
C-14-bearing methane	1.5×10^{-14}	8.7×10^{-15}	9.0×10^{-15}
C-14-bearing carbon monoxide	1.2×10^{-10}	7.1×10^{-11}	7.2×10^{-11}

There are uncertainties in the DPUR values for C-14-bearing gases, particularly for carbon monoxide, which are explained in detail in [Thorne and Kelly, 2015]. The uncertainty in the carbon monoxide DPUR arises largely because the uptake of carbon monoxide by plants (relevant to the ingestion pathway) is poorly constrained, and conservative assumptions have therefore been applied. Further work to reduce this uncertainty could be beneficial, as this assessment has shown that carbon monoxide releases are potentially significant contributors to dose.

4.4.3 Effective Release Height

Effective Release height is discussed in [RWM, 2016b][§7.1.1]. Doses are strongly dependent on the effective release height, which is a function of both design-specific factors, including stack height and efflux parameters, and site-specific factors such as topography and weather.

Weather conditions appropriate for a yearly average have to be used. For a site-specific assessment weather parameters appropriate for the local climate would be chosen. This is discussed further in [Lambers et al., 2014], which used inputs typical for the UK. Until a specific site and detailed GDF design are available, there is uncertainty regarding the effective release height. This assessment has assumed an effective release height of 15 m for consistency with previous operational environmental safety assessments [NDA RWMD, 2010] [Saleh, 2011], but parallel operational safety work [Lambers et al., 2014] supports changing the assumed effective release height to 30 m, a value that has been robustly underpinned [Schofield and Lambers, 2014][Appendix B]. Aspects of the design could be tailored in order to increase effective release height and mitigate doses if required, and a scoping calculation assessing the effect on doses of assuming an effective release height of 30 m is presented in the OESA [RWM, 2016b][§7.1.2].

4.4.4 Derivation of offsite gas release rates for C-14-bearing gases

A base scenario and variant scenarios were chosen to bound the range of possibilities in parameters where there were significant uncertainties. These are described below and discussed further in [RWM, 2016b][§4.5]:

- **Base scenario**: The base scenario was chosen to provide a reasonable generic representation of most aspects of the likely gas generation behaviour. The strategy used in defining this scenario was to use the best estimate case where one is available, and the conservative case otherwise. Hence, it uses the best estimate GDF temperature, the pessimistic assumption that uranium corrodes anaerobically, and the baseline backfilling schedule. Hence, although it is considered likely, the base scenario does include some conservatisms.

- **Higher temperature variant:** These calculations assumed an upper bound temperature profile rather than the best estimate profile used in the base scenario. For the main operational period, there was insufficient information on how the temperature in a vault might increase above the best estimate value, so this was not varied in this scenario. For the backfilling period, the temperature will depend on the ambient rock temperature at the depth of the GDF. Based on the potential range of rock temperatures, it was assumed that the upper bound temperature for the waste during backfilling, which is used in the variant calculations, was 60°C.
- **Aerobic uranium corrosion variant:** This scenario assumed that uranium corrodes under aerobic conditions rather than anaerobic conditions as assumed in the base scenario. In the base scenario calculations, it was assumed that conditions in packages containing uranium were anaerobic at all times after emplacement in the GDF. However, it is not certain that conditions for uranium waste will be anaerobic during the operational period (particularly if the grout does not contain blast furnace slag). The rate of uranium corrosion is substantially lower for aerobic conditions than for anaerobic conditions, which could have a substantial effect on the overall C-14 and tritium release rates. Variant calculations were performed assuming that the uranium corrodes under aerobic conditions during the operational period. The base scenario and variant calculations are intended to bound the range of possible uranium corrosion behaviours.
- **Staged backfilling variant:** In the base scenario calculations, backfilling is assumed to occur during the final 10 years of the operational period, after waste has been emplaced in all vaults. Staged backfilling is an alternative strategy in which a vault is backfilled as soon as it has been filled with waste. Backfilling occurs at a separate time for each vault rather than over a single period as in the base scenario calculations. A key consideration in interpreting the gas release results for the staged backfilling variant calculations is whether the gases released from waste packages are released into the GDF ventilation system, as it is this release that is relevant to this assessment. This was uncertain for these variant calculations as it is not clear whether a vault will be ventilated once backfilling has been completed. Given this, two cases were presented based on

two alternative assumptions that bound the releases via the GDF ventilation system. In staged backfilling variant A, it was assumed that gases were released into the GDF ventilation system from all vaults throughout the operational period. In staged backfilling variant B, it was assumed that gases were released into the GDF ventilation system only from vaults for which backfilling has not been completed.

It was noted that these variant scenarios explore the sensitivity of gas releases to operational and host rock-related factors, rather than potential changes in the inventory for disposal.

Offsite releases for C-14-bearing gases are described in [RWM, 2016b][§4.5.1]. There are a number of uncertainties regarding the release of C-14 from corrosion of metals, as discussed in section 2.1 of this report. Release as methane and carbon monoxide is considered in [Swift and Leung, 2016]; as discussed in section 2.1 of this report, carbon dioxide is assumed not to be released as a gas, as it is expected to react with cementitious materials present within waste packages to form carbonate [RWM, 2016f].

The dose per unit release is several orders of magnitude higher for carbon monoxide than methane, so in the subsequent discussion and quantitative dose assessments, it is cautiously assumed that all C-14 released from corrosion of metals is in the form of carbon monoxide. The implications of these uncertainties and assumptions, most of which are conservative, are discussed further in the OESA [RWM, 2016b][§7.1.1].

The release of C-14 from graphite can be rapid (acute), slow (chronic) or zero. The acute period of relatively rapid C-14 release is not relevant to calculations for the GDF, as this release will occur when the graphite is initially packaged. Only the subsequent chronic release of C-14 from irradiated graphite is of potential interest during the operational period. A parameterisation exercise for the graphite model was undertaken as part of the Carbon-14 Integrated Project [Swift et al., 2016]. The values for the fraction of C-14 available for slow release, and the rate constant of slow release, as well as the speciation of the released C-14 (all used in the calculation of release rates) are taken from this. Figure 1 shows the release of C-14-bearing carbon monoxide over the operational period for the base scenario. The main component is from the legacy ULLW/UILW throughout the operational period. The peak

release rate is 0.43 TBq per year and occurs at 2064 AD (the end of the 24-year rapid emplacement period for legacy ULLW/UILW). At around 2100 AD, the release rate decreases by a factor of ~4 to ~0.1 TBq per year until the start of the backfilling period, when it rises again to close to initial levels. The key process contributing to this release is corrosion of uranium and Magnox wastes.

Figure 2 shows the release of C-14-bearing methane over the operational period for the base scenario. The main component is from the legacy SLLW/SILW throughout the operational period. The peak release rate is 0.012 TBq per year and occurs at 2112 AD (the end of the first emplacement period for legacy SLLW/SILW). The key process contributing to this release is the degradation of graphite.

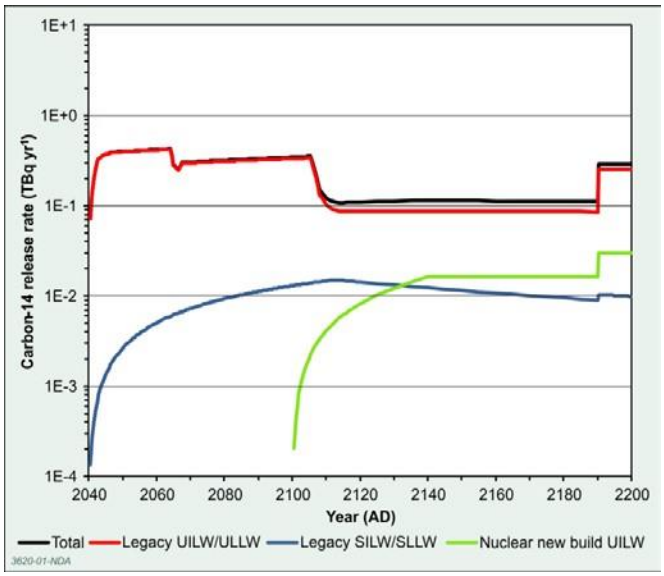

Figure 1 Summary of calculated release rates for C-14-bearing carbon monoxide during the GDF operational period base scenario, assuming all C-14 released from metals takes the form of carbon monoxide

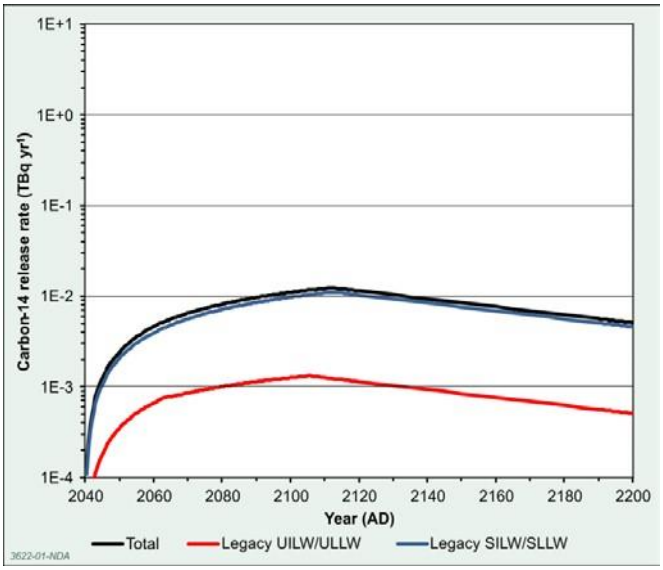

Figure 2 Summary of calculated release rates for C-14-bearing methane during the GDF operational period base scenario, assuming all C-14 released from metals takes the form of carbon monoxide

In the higher temperature variant, the results only differ after 2190 AD. The effects of the higher temperature between 2190 and 2200 AD are to increase the release rate from corrosion of Magnox by about a factor of five, from corrosion of stainless steels by about a factor of two, and from corrosion of mild steels by about 40%. This means that, in this scenario, the peak release rate of C-14-bearing carbon monoxide now occurs at 2190 AD and is 1.3 TBq per year. The magnitude and timing of the peak release rate of C-14-bearing methane are unchanged. Plots of the release rates over time for the variant scenarios can be found in [Swift and Leung, 2016].

In the aerobic uranium corrosion variant scenario, uranium corrosion is less rapid and continues throughout the operational period, rather than the uranium in each package completely corroding shortly after emplacement. As a result the C-14-bearing carbon monoxide release rate from uranium corrosion increases gradually during emplacement, then reduces gradually, and the peak rate from this source is only about half of the peak rate in the base scenario. This means that the peak release rate in this scenario occurs at the start of the backfilling period (2190 AD), and is lower than the peak in the base scenario at 0.37 TBq per

year. The magnitude and timing of the peak release rate of C-14-bearing methane are unchanged.

There are two variant scenarios for staged backfilling, A and B, depending on whether it is assumed that gases are released into the GDF ventilation system from all vaults throughout the operational period or only from vaults for which backfilling has not been completed. In both staged backfilling variant scenarios, the peak release rate of C-14-bearing carbon monoxide is slightly higher than in the base scenario. The rapid corrosion of uranium means that most of the peak release occurs from a single vault and the temperature is slightly higher (due to earlier backfilling) at the time of peak release rate. The peak release rate of

C-14-bearing carbon monoxide is therefore relatively insensitive to which of variants A and B is assumed (0.51 TBq per year at 2061 AD and 0.48 TBq per year at 2052 AD respectively). For C-14-bearing methane, the peak release rate is 0.016 TBq per year at 2116 AD for staged backfilling variant A, and 0.0031 TBq per year at 2055 AD for staged backfilling variant B.

4.4.5 Consequences

The calculated gas generation rates described above were converted to doses using the methodology described in [RWM, 2016b][§5, 6], allowing doses to members of the public from gaseous emissions to be calculated [RWM, 2016b][§9].

A gas release base scenario (expected to provide a reasonable generic representation of most likely aspects of the gas generation behaviour) and a bounding case scenario (taking the highest peak release rate for each radionuclide across three variant scenarios) were considered in a quantitative assessment of dose. In the base scenario, backfilling of the vaults was assumed to occur after all emplacement operations had ceased, as currently scheduled for the GDF in a Higher Strength Rock. In the bounding case scenario, the highest peak release rate for C-14 arises from a higher temperature variant.

Illustrative, conservative calculations of dose to members of the public were undertaken. The annual dose to members of the public from peak gas release rates during the operational period according to the base scenario, based on conservative assumptions appropriate to this generic

stage, was calculated to be 0.17 mSv per year. The majority of this dose arises from Rn-222 (0.11 mSv per year, almost all via the inhalation pathway), with minor contributions from C-14-bearing gases (0.052 mSv per year) and tritium (0.0098 mSv per year).

The annual dose to members of the public from peak gas release rates during the operational period according to the bounding case, again based on conservative assumptions, was calculated to be 0.28 mSv per year. The contribution from Rn-222 was unchanged from the base scenario at 0.11 mSv; the additional dose arising from C-14-bearing carbon monoxide (0.16 mSv per year) and tritium (0.015 mSv per year).

The calculated doses to members of the public from gaseous emissions are below the legal dose limit for members of the public of 1 mSv per year but above the source-related dose constraint of 0.15 mSv per year and the BSO of 0.02 mSv per year. Therefore more work is needed before it can be demonstrated that the dose will be below the identified constraints.

4.5 Post-closure Period

4.5.1 Gas generation and migration processes

The assessment of the impacts of gaseous radionuclides released from degrading waste packages has focused on the consideration of gas generation and migration processes for the illustrative concepts for HHGW and LHGW disposal in different geological environments [RWM, 2016a][§10.10.2]. The main radioactive gas requiring consideration in a GDF post-closure safety assessment is C-14. If long-lived radionuclides in the uranium series migrate to and accumulate in the near-surface environment, then Rn-222 in-growth may also be significant in terms of potential radiological risk, depending on exposure pathways. The generation of radioactive gases is less of a concern for HHGW than LHGW, although small amounts of radioactive gases may be generated from defective or degrading spent fuel pins after container breach. This is discussed further in sections 3.5.3-3.5.7 of this report. As the gas phase migrates through the geological environment, it will come into contact with groundwater and some or all of the gas will dissolve into the groundwater, thereby entering the groundwater pathway. Gas transfer through the geological environment around a disposal

facility will be specific to the characteristics of the disposal site, surrounding geosphere and design of the GDF, including, for example, whether faults or fractures are present, and the overall rate of groundwater flow through the facility. Calculations of radiological risk have shown that the risk guidance level is not exceeded provided the proportion of C-14 released from reactive metals is limited and any gas that does migrate to the biosphere is released over an area roughly equivalent to the GDF footprint or larger.

The methodology developed as part of RWM's research into C-14 behaviour has enhanced RWM's knowledge base on gas generation and its impacts and is also used to support RWM's assessment of the suitability of waste packaging proposals for geological disposal.

A summary of the maximum generation rates in the different periods is presented in Table 4 (based on calculations using the SMOGG software). The assumed date of closure is taken to be 2200. The generation rates presented are for the total quantity of C-14 generated, excepting $^{14}CO_2$, which is excluded, as it is expected to react with cementitious materials present in the GDF as discussed in section 2.1. The two major contributors are also shown. This table shows the UK waste streams that are potentially most important in the various periods. Each of the major waste streams appears in at least one of the time periods.

Table 4: Summary of the maximum generation rates of C-14-bearing gases (TBq yr^{-1}) in the different time periods for the GDF

Period	Maximum Generation Rate (TBq yr^{-1})	Major Contributor	%age of Max[1,2]	Next Contributor	%age of Max[1,2]
Emplacement period (2040-2190 AD)	4.32×10^{-1}	Uranium (Legacy UILW)	85%	Magnox (Legacy UILW)	19%
Backfilling and early post-closure period (2190-2230 AD)	2.96×10^{-1}	Magnox (Legacy UILW)	75%	Various Steels (Legacy UILW & SILW, NNB)	21%

Period	Maximum Generation Rate (TBq yr^{-1})	Major Contributor	%age of Max[1,2]	Next Contributor	%age of Max[1,2]
Medium-term post-closure period (2230- 3000 AD)	1.25×10^{-1}	Magnox (Legacy UILW)	96%	Graphite (Legacy UILW & SILW)	65%
Long-term post-closure period (From 3000 AD)	8.39×10^{-4}	Various Steels (Legacy UILW & SILW, NNB)	90%	Zircaloy (Legacy UILW)	10%

Notes:

1 The percentage of the maximum generation rate given in the second column.

2 The percentages can add up to more than 100% if the maxima occur at different times in the period.

To illustrate the results, Figure 3 shows the generation rates from legacy UILW/ULLW during the operational and early post-closure periods; Figure 4 shows the same generation rates during the late post-closure period.

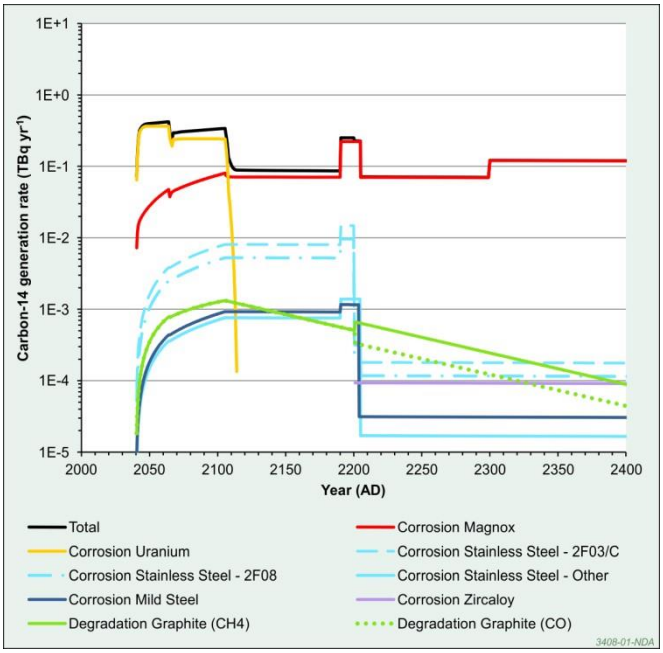

Figure 3: Breakdown by waste group of calculated generation rates for C-14-containing gases from Legacy UILW / ULLW during GDF operations and early post-closure

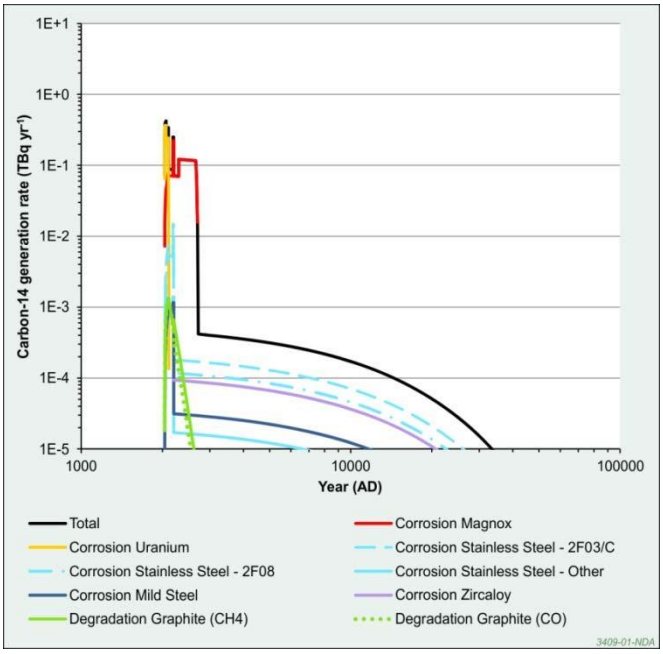

Figure 4: Breakdown by waste group of calculated generation rates for C-14-containing gases from Legacy UILW / ULLW in the long term

4.5.2 HHGW disposal in HSR

The illustrative concept for HHGW disposal in higher strength rock involves packaging the wastes within cast iron inserts inside copper containers and placing the containers in vertical deposition holes lined with a bentonite buffer [RWM, 2016a][§4].

The chemical form of the spent fuel (apart from metallic fuel) and its dryness means that the wasteform will produce negligible volumes of gas; small amounts of radioactive gases could leak from any defective fuel pins, but the gas would be retained within the high integrity containers [RWM, 2016e][§4.4]. Likewise, vitrified HLW and the stainless steel canister within which it is contained will not generate gas when dry within the intact disposal container.

Under anaerobic conditions in the disposal facility, the corrosion of the copper containers is expected to be negligible and no gas will be generated. Hydrogen may be generated from radiolysis of groundwater in contact with the outer surface of disposal containers [RWM, 2016e][§6.1.4] [RWM, 2016g][§9.2.1; §11.2.1], although the presence of the bentonite will limit the availability of water in contact with the container.

Copper corrosion is only likely to proceed in the presence of sulphide, but this reaction is not expected to generate gas. If sulphide attack, or some other disruptive event, were to result in container breach and groundwater ingress, then gas could be generated from the corrosion of metals in the container, especially the iron insert, and from radiolysis of water [RWM, 2016e][§6.1.4]. Small amounts of radioactive gases could leak from any defective or degrading fuel pins. These gases are likely to dissolve in groundwater as they migrate from the EBS, although this depends on the properties of the geological environment, as discussed in Section 10.4.2 for LHGW disposal.

4.5.3 HHGW disposal in LSSR

The illustrative concept for the disposal of HHGW in lower strength sedimentary rock involves packaging the wastes within thick-walled carbon steel containers. The waste packages will be placed on bentonite plinths in tunnels and the tunnels will be backfilled with pelleted bentonite [RWM, 2016a][§6].

The main source of gas (hydrogen) after GDF closure will be corrosion of the carbon steel containers, although the slow movement of water through the host rock and bentonite backfill will limit water availability for corrosion reactions [RWM, 2016c][§6.1.3]. Similar to the concept for HHGW disposal in higher strength rock, the chemical forms of spent fuel (apart from metallic fuel) and vitrified HLW are such that they will produce negligible volumes of gas following water ingress after container breach. Small amounts of radioactive gases could leak from defective or degraded fuel pins, although this is unlikely to have a significant impact on disposal system performance.

4.5.4 HHGW disposal in Evaporite

The illustrative concept for the disposal of HHGW in evaporite involves packaging the wastes within thick-walled carbon steel containers. The waste packages will be placed on the floor of tunnels, which will be backfilled with crushed host rock [RWM, 2016a][§8].

Gas generation will be limited because evaporites are dry and so there will be little water available for gas generation reactions after GDF closure. The water content of the waste packages will constrain the amount of gas that could be generated [RWM, 2016e][§6.1.3], although the granular salt backfill may provide a source of water if it is wetted to facilitate compaction [RWM, 2016c][§6.1.5]. As discussed in Section 10.4.1, the form of the packaged HHGW is such that there is not expected to be any water available for gas generation reactions. Therefore, in this illustrative concept, it is very unlikely that there will be significant amounts of gas generated.

4.5.5 LHGW in HSR

The understanding of gas generation and migration processes for LHGW in HSR that informed the ESC are presented in [RWM, 2016a][§10.4.2]. Carbon dioxide (CO_2) (and any C-14 it contains) was assumed to react with cementitious materials in the EBS and, thus, not to be released into the host rock as a free gas. Methane (including $^{14}CH_4$) was estimated to be generated mainly from the microbial degradation of organic molecules over a period of about 10,000 years (although the major waste stream contributing to $^{14}CH_4$ generation in the long term may now not be disposed of in the GDF [RWM, 2016f][§6.1.2]). In addition, C-14 in the gas phase could be generated from the corrosion of stainless steel, carbon steel and Zircaloy wastes, radiolysis of organic molecules and releases from irradiated graphite. Recent calculations of C-14 gas generation undertaken as part of RWM's research on C-14 behaviour [NDA, 2012] [RWM, 2016f] found that the corrosion of Magnox metal, irradiated stainless steel Advanced Gas-cooled Reactor fuel cladding, fuel assembly components and Zircaloy fuel cladding are the main contributors to the generation of C-14-bearing gas.

Illustrative calculations of gas migration through HSR are discussed in the Gas Status Report [RWM, 2016e][§6.3.2] and are summarised in the generic PCSA [RWM, 2016c][§6.2.1]. The calculations indicate that, on a timescale of a few tens of years, the gas pressure will become comparable to hydrostatic pressure and the gas may begin to move out of the facility into the surrounding rock.

Fractured rocks typically do not form a significant barrier to gas migration. As the gas phase migrates through the geological environment, it will come into contact with groundwater. Some of the gas will dissolve into, and will be transported by, the groundwater. The amount of gas that dissolves will depend on the volume of groundwater contacted and the gas solubility. If, as the gas migrates, it encounters a large flow of groundwater in permeable rocks [RWM, 2016c][§6.2.1], it may dissolve to the extent that a free gas phase ceases to exist. Gas transfer through the geological environment of a disposal facility will therefore be complex and specific to the characteristics of the disposal site and the design of the GDF.

If a free gas phase does reach the biosphere, calculations from the Carbon-14 Integrated Project show that the presence of methane that includes C-14 presents the most significant potential concern with regard to radiological risk to exposed groups. Calculations of risk depend on the assumptions made about the area over which the gas is released and potential human exposure pathways. Such issues were considered as part of RWM's research on C-14 behaviour [NDA, 2012] [RWM, 2016f]. The C-14 research included a number of illustrative calculations of risk associated with exposure to C-14 based on different assumptions about how the gas will migrate through fractures in the host rock and about features in the overlying geological environment that could delay or prevent gas reaching the biosphere and affect the area over which any gas would be released.

Analysis of the calculated radiological impact from gaseous C-14 shows that risks are dominated over the first thousand years following GDF closure by the release of C-14 from irradiated reactive metals as they corrode [RWM, 2016f][§13.1-§13.2]. In this period, the calculated risk from gaseous C-14 is below the risk guidance level provided the proportion of C-14 released from reactive metals as methane or carbon monoxide is limited (to less than about 30% of the inventory) and any gas that does migrate to the biosphere is released over an area roughly equivalent to the GDF footprint or larger. A more focused release of gaseous C-14 results in the calculated risk exceeding the risk guidance level for the conservative assumptions used.

In the longer term, calculated risks are dominated by the generation of methane from steel wastes [RWM, 2016f][§13.1-§13.2]. Calculated risks are below the risk guidance level if no more than 10% of the C-14 inventory is released as gas, irrespective of the assumed release area. The risk guidance level is exceeded only if release to the biosphere is assumed to occur over a focused area and the proportion of C-14 released in the gas phase as a result of steel corrosion is greater than about 30%.

4.5.6 LHGW in LSSR

The understanding of gas generation and migration processes for LHGW in LSSR that informed the ESC are presented in [RWM, 2016a][§10.4.4]. Gas generation reactions will be similar to those described for LHGW disposal in HSR [RWM, 2016c][§10.4.2], although the slow movement of groundwater through the host rock and backfill will limit the availability of water for gas generation reactions and a complex coupling between water inflow and gas generation and flow could then develop [RWM, 2016c][§6.1.4] [Public Health England, 2009][§6.1.2].

The hydraulic conductivity of a LSSR, such as a clay, could be too low, and the pressure for the gas to enter the host rock could be too high, for all the gas that is generated in the disposal facility to be dissolved. Furthermore, a free gas phase that enters the undisturbed host rock may migrate so slowly that the gas pressure becomes sufficient for micro-fissures to be created [RWM, 2016c][§6.2.2]; [NDA, 2012][§6.3.3].

The gas will migrate through such micro-fissures, which may then close as the gas pressure falls, depending on the properties of the host rock. Eventually, self-sealing of fractures may occur, as is observed in laboratory experiments for LSSR such as the Boom Clay in Belgium and the Opalinus Clay in Switzerland [Bernier et al., 2007]. Any significant gas generation could result in displacement of contaminated groundwater from the GDF [Public Health England, 2009][§6.4]. A more detailed understanding of gas generation and its effects will be developed as necessary for a disposal concept in LSSR as relevant site-specific and GDF design-specific information becomes available.

Whether the free gas phase (including radioactive gas such as C-14) reaches the biosphere will depend on the specific characteristics of the geological environment, including the cover rocks. The generic PCSA includes discussion of illustrative calculations of gas migration from a GDF in clay, calculated using full 3D models, which show how free gas dissolves as it migrates through the rock, but the free gas phase eventually reaches the top of the host rock [RWM, 2016c][§6.2.2].

RWM's research on C-14 behaviour included illustrative calculations of radiological risk from gaseous C-14 migration for a LSSR disposal concept [NDA, 2012] [RWM, 2016f]. No releases of gaseous C-14 were calculated to occur in the first thousand years following GDF closure [RWM, 2016f][§13.1§13.2]. In the longer term, calculated risks are below the risk guidance level irrespective of assumptions about the release area and the fraction of C-14 that is released in the gas phase. For details on the assumptions made see section 2.1.

4.5.7 LHGW in Evaporite

The illustrative concept for the disposal of LHGW in evaporite involves stacking waste packages in unlined vaults. Sacks of magnesium oxide will be placed on top of each waste package stack, but the vaults will not be backfilled. Rock creep will reduce void space and close the vaults naturally over a period of decades.

Again, gas generation after GDF closure will be limited because of the lack of water to drive gas generation reactions. The water content of the waste packages at closure will constrain the amount of gas that could be generated [RWM, 2016e][§6.1.3]. It is likely that there will only be a small volume of gas generated from the degradation of LHGW in the evaporite disposal concept under expected conditions.

Undisturbed evaporite rock is virtually impermeable to gas. If gas is generated, it would only migrate if sufficient gas pressures are generated to result in fracturing of the rock. The fractures would self-heal by creep on subsequent pressure reduction. Assumptions about the performance of the shaft seals and their prevention of water movement into the disposal region are important to assessments of the environmental safety of this disposal concept with regard to the potential impacts gas generation [RWM, 2016e][§6.3.4].

5 Implications

The project Formation and Migration Report [Hoch et al., 2016] considers in detail the migration of C-14 released from a GDF as gas. The three potential generic host rock environments have been considered, along with relevant features that may be found in the overlying rocks.

The calculated post-closure consequences are dependent on the initial migration time relative to the half-life of C-14 and the area over which the C-14 is released to the deep soil.

Six illustrative cases have been developed to enable the implications of the release of C-14 to be assessed; they include a case where there is no release of C-14. These cases are not exhaustive, but they span the geological environments that may be considered in the future to host a GDF in the UK. The development of the cases is discussed in the project Formation and Migration Report [Hoch et al., 2016]. They are listed in Table 5. Given that there is no specific site currently being investigated, none of these cases is given more weight than any other. The corresponding conversion factors from C-14 generation rate to flux at the surface for each geosphere case are summarised in Table 6.

Any C-14-bearing gases that reach the biosphere following closure would be released to the deep soil. Recently a combined experimental and modelling programme has been completed, which focused on whether methane would be oxidised to carbon dioxide in the soil [Hoch et al., 2014]. This has been complemented by a wider review of the understanding of methane oxidation in soils from other fields [Shaw and Thorne, 2016]. This work shows that the bulk of the methane will be oxidised. In the light of the results of this programme, a revised assessment model has been developed [Bernier et al., 2007]. This model is consistent with those used by the Low Level Waste Repository (LLWR).

Table 5: Post-closure geosphere cases considered

ID	Description	Delay time (14C ½-lives)	Release area (m^2)
A	Higher-strength host rock where gas is released over an area similar to the footprint of the GDF ILW / LLW vaults	0	10^6
B	Environments where there is a low permeability formation limiting gas migration	No release	
C	Higher-strength host rock where there are features that focus the release of gas to an area much less than the footprint of the GDF ILW / LLW vaults	0	10^4
D	Higher-strength host rock where there are features that distribute the release of gas to an area greater than the footprint of the GDF, e.g. as a result of dissolution	0	10^7
E	Lower-strength sedimentary host rock where gas migrates slowly across the host rock and is released over the footprint of the GDF ILW / LLW vaults	1	10^6
F	Lower-strength sedimentary host rock where gas migrates slowly across the host rock and there are features that distribute the release of gas to an area greater than the footprint of the GDF, e.g. as a result of dissolution	1	10^7

This revised model provides a single multiplying factor to be used to convert the flux of C-14-containing gases at the surface to the dose rate received by a local family receptor group. The conversion factor is given in Table 7; it is slightly higher than the value used in Phase 1 of the C-14 project [NDA, 2012]. The value for C-14-containing methane has been applied to the sum of the release rates of C-14 as methane and carbon monoxide; this is expected to be cautious.

Table 6: C-14 generation rate to flux at the surface conversion factors for different geosphere cases during the GDF post-closure period

ID	Delay time (14C ½-lives)	Release area (m^2)	Conversion factor (($Bq\ m^{-2}s^{-1}$) per $TBq\ yr^{-1}$)
A	0	10^6	3.17×10^{-2}
B	No release		–
C	0	10^4	3.17×10^{0}
D	0	10^7	3.17×10^{-3}
E	1	10^6	3.17×10^{-2} (zero until 7930 AD)
F	1	10^7	3.17×10^{-3} (zero until 7930 AD)

Table 7: C-14 flux at the surface to dose rate conversion factor for off-site discharge to the local resident family receptor group during the GDF post-closure period

C-14-containing gas	Conversion factor ($Sv\ yr^{-1}$ per ($Bq\ m^{-2}s^{-1}$))
Methane	0.0225

5.1 UK Regulatory Context

The UK Regulator, the Environment Agency, issues Guidance on Requirements for Authorisation (GRA) [Environment Agency and Northern Ireland Environment Agency, 2009] for a GDF. This contains two requirements that are particularly relevant to the post-closure period [RWM, 2016f][§4.3]:

If there is a period of institutional control after closure, then the source-related dose constraint[8] for members of the public for a new facility of 0.15 $mSv\ yr^{-1}$ applies (Requirement R5 [Environment Agency and Northern Ireland Environment Agency, 2009]). This stems

[8] ICRP has established a dose limit for members of the public that is intended to limit the risk to any individual for all sources of radiation exposure. The Commission recommends the use of an individual source related criterion called a dose constraint, set at a level of dose below the dose limit. The purpose is to ensure that no individual exceeds the dose limit from exposures due to all sources and to reduce the inequity between members of the public due to the detriment from the source. In this case, the source would be the Geological Disposal Facility.

from the Health Protection Agency's[9] recommendation that, for the operational and active institutional control phases, a dose constraint of 0.15 mSv (annual dose) should apply to exposure to the public from a new disposal facility for radioactive waste [Public Health England, 2009].

After any period of institutional control, risks should be consistent with the risk guidance level of 10^{-6} (Requirement R6 [Environment Agency and Northern Ireland Environment Agency, 2009]), using the dose to risk conversion factor of 0.06 Sv^{-1}. A risk guidance level of 10^{-6} means that the assessed radiological risk from a disposal facility to a person representative of those at greatest risk should be consistent with a risk guidance level of 10^{-6} per year (i.e. 1 in a million per year) [Environment Agency and Northern Ireland Environment Agency, 2009].

At this generic stage of the programme, there is uncertainty over the period of institutional control, and so for simplicity the risk guidance level is applied at all times; this is more stringent than the source-related dose constraint.

5.2 Emplacement period

The pathway considered for release from the GDF is for the gases to be ventilated out of a 15m high stack. The highest release rates from waste packages during the emplacement period are those for uranium wastes.

The contribution to effective dose rate from C-14 during the emplacement period is below the maximum effective dose rate constraint to members of the public from a new facility of 0.15 mSv yr^{-1}.

[9] An organisation whose role was to provide an integrated approach to protecting UK public health through the provision of support and advice to the NHS, local authorities, emergency services, other Arms Length Bodies, the Department of Health and the others. The HPA became part of Public Health England in 2013.

5.3 Backfilling and early post-closure period

The highest generation rate arises from Magnox wastes, but they are lower than the generation rates in the emplacement period (see Table 4). Releases during this period could be either through a stack or through the rock.

For releases up a stack, the contribution to effective dose rate from C-14 is below the maximum effective dose rate constraint to members of the public from a new facility of 0.15 mSv yr^{-1}.

In the early post-closure period the risks in a number of the migration cases are above the risk guidance level. However, this release is over a very short period and the release to the biosphere may be spread in time as the gas migrates through the EBS or through the geosphere, which would reduce the maximum release rate to no more than that in the medium-term post-closure period.

5.3.1 Medium term post closure period

The medium term post closure period corresponds to the period over which Magnox corrodes (about 1000 years). The highest generation rate arises from Magnox wastes (see Table 4).

Post-closure risks arising from the release of C-14-bearing gases are given in Table 8 (medium-term post-closure period). These are obtained by combining the reference-case generation rate given in for example in Figure 3 (and summarised in Table 4), the migration cases, the biosphere factors given, and the cases for the proportion of C-14 released as methane or carbon monoxide discussed in the respective sections.

The Environment Agencies' risk guidance level is 10^{-6} per year [Environment Agency and Northern Ireland Environment Agency, 2009], and risks above this guidance level are shown in Bold. The reference case for the values proportion of C-14 released as methane or carbon monoxide are in Black – other values are shaded Grey. As the risks are dominated by Magnox, the reference case corresponds to a release of 30% as methane or carbon monoxide.

Table 8: Calculated peak risks from C-14-containing gas for the medium-term post-closure period for a range of scenarios

Geosphere case	Fraction of C-14 released as gas from metals[1,2,3]			
	100%	**30%**	**10%**	**1%**
A	**5.36×10^{-6}**	**1.72×10^{-6}**	6.78×10^{-7}	3.46×10^{-7}
B	0	0	0	0
C	**5.36×10^{-4}**	**1.72×10^{-4}**	**6.78×10^{-5}**	**3.46×10^{-5}**
D	5.36×10^{-7}	1.72×10^{-7}	6.78×10^{-8}	3.46×10^{-8}
E	0	0	0	0
F	0	0	0	0

Notes:

1 The fractions for graphite are taken from the parameterisation of the revised graphite model. In this Table the same value is used for the fraction released as gas for each metal. In practice the fraction from the various metals will be different.

2 The reference case values are in black (dominated by Magnox) – other values are shaded grey.

3 Values below the risk guidance level of 10^{-6} are in plain text. Values above the risk guidance level are in Bold.

The risks in a number of the migration cases are above the risk guidance level. It is seen that:

- For a release area of 10^6 m^2 and no delay (Case A), provided the proportion released as methane or carbon monoxide is less than around 30% the risks will be below the risk guidance level;
- For a focused release to an area of 10^4 m^2 (Case C), neither the reference case nor the variants considered are below the risk guidance level;
- For Cases B, D and F, there is no release.

In environments where resaturation is slow, gas generation may be reduced because of a lack of water availability.

The results will be updated once there is more information on the release of C-14-bearing methane and carbon monoxide from Magnox as it corrodes. Once specific sites are identified and are being investigated, it will be important to understand the gas migration characteristics and whether a focused release may occur.

5.4 Long-term post-closure period

The long-term post-closure period corresponds to the period after the reactive metals have corroded. The highest generation rate arises from the anaerobic corrosion of steel wastes (see Table 4). The generation rates during the long-term post-closure period are expected to be lower than in the medium-term post-closure period, and there may not be a gas phase present by that time if sufficient groundwater is available that allows total gas dissolution.

Post-closure risks arising from the release of C-14-bearing gases are given in Table 9 (long-term post-closure period). These are obtained by combining the reference-case generation rate given in for example in Figure 3 (and summarised in Table 4), the migration cases, the biosphere factors, and the cases for the proportion of C-14 released as methane or carbon monoxide.

The Environment Agencies' Risk Guidance Level is 10^{-6} per year [Environment Agency and Northern Ireland Environment Agency, 2009], and risks above this guidance level are shown in Bold. The reference case for the values proportion of C-14 released as methane or carbon monoxide are in Black – other values are shaded Grey. As the risks are dominated by steel wastes, the reference case corresponds to a release of 10% as methane or carbon monoxide.

Table 9 Calculated peak risks from C-14-containing gas for the long-term post-closure period for a range of scenarios

Geosphere case	Fraction of C-14 released as gas from metals[1,2,3]			
	100%	**30%**	**10%**	**1%**
A	3.59×10^{-8}	1.08×10^{-8}	3.63×10^{-9}	4.06×10^{-10}
B	0	0	0	0
C	**3.59×10^{-6}**	**1.08×10^{-6}**	3.63×10^{-7}	4.06×10^{-8}
D	3.59×10^{-9}	1.08×10^{-9}	3.63×10^{-10}	4.06×10^{-11}
E	1.98×10^{-8}	5.95×10^{-9}	1.98×10^{-9}	1.98×10^{-10}
F	1.98×10^{-9}	5.95×10^{-10}	1.98×10^{-10}	1.98×10^{-11}

Notes:

1 The fractions for graphite are taken from the parameterisation of the revised graphite model. In this Table the same value is used for the fraction released as gas for each metal. In practice the fraction from the various metals will be different.

2 The reference case values are in black (dominated by steels) – other values are shaded grey.

3 Values below the risk guidance level of 10^{-6} are in plain text. Values above the risk guidance level are in Bold.

In the long-term post-closure period, only two of the cases are above the risk guidance level. These are for a focused release to an area of 10^4 m^2 (Case C) where most of the C-14 is released as methane. Even with a focused release, the two variants, where 10% or 1% is released as C-14-bearing methane are below the risk guidance level.

In environments where resaturation is slow, there may not be a bulk gas phase in the long term.

The results will be updated once there is more information on the release of C-14-bearing methane and carbon monoxide from the anaerobic corrosion of steel wastes. Once specific

sites are identified and are being investigated, it will be important to understand the gas migration characteristics and whether a focused release may occur.

6 Summary

6.1 Position

A summary of the position on C-14, arrived at by the Carbon-14 Integrated Project, is presented in [RWM, 2016f][§13.2]. The integrated approach has covered a wide range of technical areas, gathering evidence to improve the knowledge base that supports our approach to the management of these wastes.

A large number of knowledge gaps have been filled and the improved knowledge base has been captured in updated and new models. The calculated impact is site specific and is dominated over the first thousand years following closure by the release of carbon-14 from irradiated reactive metals as they corrode.

In the first thousand years following closure, the calculated impact from gaseous carbon-14 will be below the risk guidance level, provided that:

- the proportion of carbon-14 released from reactive metals as methane or carbon monoxide is limited; and
- any gas that is released to the biosphere is released over an area roughly equivalent to the repository footprint or larger.

If there were a focused release of gas to a small area, risks may be above the risk guidance level. Therefore it will be important to understand the gas migration characteristics of any site proposed for the disposal of these wastes.

The inventory is based on the 2013 DI [RWM, 2016d]. There are a number of waste streams where the inventory may be overestimated. The inventory is updated every three years.

The results presented here will be updated once experimental measurements on the speciation of carbon-14 released from irradiated Magnox and irradiated stainless steels become available.

Consideration should be given to developing a better understanding of the rate and extent of corrosion of reactive metal wastes prior to closure of a GDF. Sellafield is working towards measuring gas release form active waste packages, but these data will take several years to obtain. Such data would be valuable for comparison with the assessed releases.

Our improved understanding also has implications for the assessment of the groundwater pathway in terms of the inventory available for release and the speciation of carbon-14 in the aqueous phase. Account could be taken of the significant proportion of carbon-14 in graphite that would not be released on relevant timescales and the long timescales over which carbon-14 would be released from steels.

Carbon-14 remains a key radionuclide in the assessment of the safety of a GDF for radioactive waste because of the potential radiological impact of gaseous carbon-14-bearing species. As a result of this focused programme of work, we now have the knowledge base required to support packaging decisions for specific wastes and understand the envelope of conditions within which disposal of the UK's wastes containing carbon-14 can be managed.

6.2 Updates to the 2016 DSSC

The improved understanding of gas generation routes from the Carbon-14 Integrated Project, developed through the integrated technical approach (AND approach), has contributed to identifying key sources of C-14 in the DI [RWM, 2016d], informing the OESA and PCSA.

The improved understanding of gas migration routes, through the modelling results from phase two of the Carbon-14 Integrated Project, has contributed to the derivation of off-site gas release rates for C-14-bearing gases in the OESA and PCSA.

The Carbon-14 Integrated Project calculated updated DPUR values for C-14, which superseded the Environment Agency values, using a more realistic representation of the

discharge pathway for releases of C-14-bearing gases from the GDF during operations. These updated values were used in the OESA.

The conclusions drawn from the PCSA have informed the radiological assessment of radionuclides in gas, presented in the ESA to show how various lines of argument will be constructed to demonstrate that geological disposal of the UK's higher activity radioactive wastes will meet environmental safety requirements as set out in the GRA [Environment Agency and Northern Ireland Environment Agency, 2009], when a GDF site is available.

6.3 Scope for further work

Operational safety work [Lambers et al., 2014] carried out in parallel to the 2016 OESA supports changing the current assumed effective release height of 15 m (chosen for consistency with previous operational environmental safety assessments) to 30 m, a value that has been robustly underpinned [Schofield and Lambers, 2014][Appendix B]. It is expected that the future issues of the OESA will use this revised height.

Gas generation associated with waste and container degradation reactions could result in the development of high pressures that could disrupt an engineered and natural barrier system through induced fracturing. This is of particular relevance in lower strength sedimentary rocks and possibly, under circumstances where brine enters the disposal facility, evaporite rocks. Also, radionuclides such as C-14 could be generated in the gas phase, which could affect the radiological risk associated with disposal. Research is necessary, building on the results of RWM's recent integrated project on C-14 behaviour [NDA, 2012] [RWM, 2016f], to understand these processes further [RWM, 2016a][§11.2].

References

Adeogun A., "Carbon-14 Project Phase 2: Inventory," March 2016.

Bernier F., X. Li, W. Bastiaens, L. Ortiz, M. V. Geet, L. Wouters, B. Frieg, P. Blümling, J. Desrues, G. Viaggiani, C. Coll, S. Chanchole, V. D. Greef, R. Hamza, L. Malinsky, A. Vervoort, Y. Vanbrabant, B. Debecker, J. Verstraelen, A. Govaerts, M. Wevers, V. Labiouse, S. Escoffier, J. F. Mathier, L. Gastaldo and C. Bühler, 2007, "Fractures and Self-sealing within the Excavation Disturbed Zone in Clays (SELFRAC) – Final Report,"

Environment Agency, 2006, "Initial radiological assessment methodology – part 1 user report", May 2006

Environment Agency, 2006, "Initial radiological assessment methodology – part 2 methods and input data", May 2006

Environment Agency; Scottish Environment Protection Agency, Department of Environment in Northern Ireland, Food Standards Agency, Health Protection Agency, 2006, "Initial Radiological Assessment Methodology – Part 1 User Report"

Environment Agency; Scottish Environment Protection Agency, Department of Environment in Northern Ireland, Food Standards Agency, Health Protection Agency, 2006b, "Initial Radiological Assessment Methodology – Part 2 Methods and Input Data,"

Environment Agency; Northern Ireland Environment Agency, February 2009, "Geological Disposal Facilities on Land for Solid Radioactive Wastes: Guidance on Requirements for Authorisation"

Hoch A., D. Lever and G. Shaw, 2014, "Uptake of Carbon-14 in the Biosphere: Summary Report"

Hoch A., C. Rochelle, P. Humphreys, J. Lloyd, T. Heath and K. Thatcher, 2016, "Carbon-14 Project Phase 2: Formation of a Gas Phase and its Migration"

Jones J., 1986, "The Seventh Report of a Working Group on Atmospheric Dispersion: the Uncertainty in Dispersion Estimates Obtained from the Working Group Models"

Lambers B., J. Williams and J. Schofield, 2014 "Methodology, Input Data and DRRs for Operation of a GDF"

Mayall A., T. Cabianca, C. Atwood, C. Fayers, J. Smith, J. Penfold, D. Steadman, G. Martin, T. Morris and J. Simmonds, 1995, "Methodology for Assessing the Radiological Consequences of Routine Releases of Radionuclides to the Environment", European Commission, Luxembourg

Mayall A., T. Cabianca, C. Atwood, C. Fayers, J. Smith, J. Penfold, D. Steadman, G. Martin, T. Morris and J. Simmonds, 1997, "PC-CREAM Installing and Using the PC System for Assessing the Radiological Impact of Routine Releases"

NDA, 2012, "Geological Disposal: Carbon-14 Project – Phase 1 Report", December 2012

NDA RWMD, 2010, "Geological Disposal: Generic Operational Environmental Safety Assessment", December 2010

Public Health England, 2009, "ICRP 2007 recommendations: UK application", July 2009

Rizzato C., A. Rizzo, G. Heisbourg, P. Večerník, C. Bucur, J. Comte, D. Lebeau and P. Reiller, 2015, "State of the Art review on Sample Choice, Analytical Techniques and Current Knowledge of Release from Spent Ion-exchange Resins (D4.1),", January 2015

RWM (Radioactive Waste Management), 2016a, "Geological Disposal: Generic Environmental Safety Case Main Report," December 2016

RWM (Radioactive Waste Management), 2016b, "Geological Disposal: Generic Operational Environmental Safety Assessment," December 2016

RWM (Radioactive Waste Management), 2016c, "Geological Disposal: Generic Post-closure Safety Assessment," December 2016

RWM (Radioactive Waste Management), 2016d, "Geological Disposal: The 2013 Derived Inventory," December 2016

RWM (Radioactive Waste Management), 2016e, "Geological Disposal: Gas Status Report," December 2016

RWM (Radioactive Waste Management), 2016f, "Geological Disposal: Carbon-14 Project Phase 2: Overview Report," May 2016

RWM (Radioactive Waste Management), 2016g, "Geological Disposal: Waste Package Evolution Status Report," December 2016

RWM (Radioactive Waste Management), 2016h, "Disposal System Safety Case: Data Report," December 2016

Saleh S., 2011, "Illustrative assessment of impacts on non-human biota from operational radioactive releases from a generic geological disposal facility: Input to the operational environmental safety assessment," January 2011

Schofield J. and B. Lambers, 2014, "Identification of a finalised set of parameters for calculation of DRRs," 2014

Shaw G. and M. Thorne, 2016, "The Oxidation of Methane in Soil as a Factor in Determining the Radiological Impact of a Geological Disposal Facility"

Simmonds J.R. (ed.), 1998, "NRPB Models for Calculating the Transfer of Radionuclides Through the Environment: Verification and Validation"

Swift B., 2016, "Specification for SMOGG Version 7.0: A Simplified Model of Gas Generation from Radioactive Wastes"

Swift B. and C. Leung, 2016, "Gas Generation Data to Support the 2016 Generic Operational Environmental Safety Assessment," March 2016

Swift B. and C. Leung, 2016b, “Carbon-14 Project Phase 2: Modelling, AMEC Report,” 2016

Swift B., S. Swanton, W. Miller and G. Towler, 2016, “Carbon-14 Project Phase 2: Irradiated Graphite Wastes,” March 2016

Thorne M. and M. Kelly, 2015, “Operational impacts from aerial discharges of carbon-14-bearing gases,” March 2015